

AES/RE & PE/ Development of a reserve reconciliation tool for the Hengelo Brine Field

7/8/2015 Jasper Schootstra



Development of a reserve reconciliation tool for the Hengelo Brine Field

by

J. Schootstra

to obtain the degree of Master of Science
at the Delft University of Technology
to be defended publicly on Friday August 28, 2015 at 15:00

Student nr. : 4034740

Thesis committee : Dr. M.W.N. Buxton TU Delft, supervisor
Prof. Dr. P.L.J. Zitha TU Delft
A.M. den Hartogh, MSc. AkzoNobel Industrial Chemicals B.V.

Postal Address : Department of Applied Earth Sciences

Delft University of Technology

P.O. Box 5028

The Netherlands

Telephone : (31) 15 2781328 (secretary)

Telefax : (31) 15 2781189

This thesis is confidential and cannot be made public until July 31, 2017

i. Abstract

Reserve reconciliation is widely applied in the petroleum and mining industry. By updating the reserves throughout the operation, the remaining reserves can be better quantified and the extraction scheduling optimized. The goal of this study is to develop a reserve reconciliation tool for the Hengelo Brine Field, operated by AkzoNobel Industrial Chemicals B.V. in the Netherlands, in order to improve the long-term development and production planning for the field.

The study follows the principles of the LeanSixSigma methodology for problem solving in five phases: define, measure, analyze, improve and control (DMAIC cycle). The study consists of 4 parts. The first part provides background information on the production process, the Hengelo Leaching Technique and the geological situation. The second part measures and analyzes the mass balances in the field, magnitude of fluid losses, Solling Fm., sonar measurements and insoluble material. The report continues with the reserve reconciliation in which an accounting tool is implemented on an area with 23 caverns. In the fourth part the discussion, conclusion and recommendations are discussed.

The aim of this study was to determine if it is feasible to develop a predictive methodology able to accurately quantify the properly and if this methodology can be utilized in the long-term planning of the production and development of the Hengelo Brine Field. The extraction process is affected by geological and mining related uncertainties. The most important uncertainties are:

- Fluid losses from caverns
- Cavern shape & geometry
- Insoluble material & bulking factor

Salt is produced from the Röt Fm. (Middle Triassic age) in the Hengelo Brine Field. The layer located below the Röt Fm. is the Solling Fm. (Lower Triassic age). It was believed that the caverns are closely connected to the Solling Fm., but no clear proof was found yet.

Fluid losses were identified and quantified, using mass balances and pressure tests. By accounting for material entering and leaving the caverns, on both a field- as an individual cavern scale, it was found that the brine out/water in ratio varies throughout the field. For the majority of caverns this ratio is lower than the theoretical ratio. An average loss of 30 m³/day per cavern is expected. For the entire field the losses add up to thousands of cubic meters per year. The pressure tests indicate that the caverns are sometimes connected to neighbouring caverns. It was noticed that flows in the field either tend to follow isopachs to other caverns or pathways towards caverns which shallower, probably due to the pressure gradient.

The mass balance- and pressure tests indicate that the Solling Fm. has significant influence on fluid flow. Core observations showed that the Solling Fm. is heavily fractured. This in combination with favorable permeable interlayers (sand accumulations lead to three possible flow paths which are responsible for the losses/connections:

1. Connection between caverns through the Solling Fm.
2. Fluid loss to the Solling Fm.
3. Direct connection between caverns.

Calculations indicate that both the pressure gradient and capacity are present to accommodate the observed losses within the Solling Fm. An in/outflow test was developed. This test can be utilized to predict in- or outflow of fluids from a cavern, by comparing a geological-, sonar- and brine out/water in ratio. The majority of tested caverns showed fluid outflow.

Sonar measurements are used to determine the shapes and volumes of the caverns. Comparing the production- and sonar volumes, major deviations were observed. These are partly caused by the limitation of the sonar tool, specifically the inability to measure behind irregularities in the walls and the resolution of the tool. These limitations result in neglected volumes in the sump, roof and wall of caverns. Detailed analysis using 3-dimensional modelling software indicate that large volumes are neglected.

Detailed analyses of the insoluble content of the salt indicates that the content is lower than the previously assumed value currently used to calculate reserves. An average value of 7.1% is expected, instead of the current 10%. The salt in the lowest part of the Röt Fm. is purer, whereas the higher part of the salt contains twice as much insolubles.

Other uncertainties (gamma-ray logs, seasonal effects and salt creep) were investigated. No relationship between the gamma-ray log and the amount of insolubles (anhydrite and claystones) was indicated. The accuracy of the gamma-ray tool is affected by the resolution (in combination with the background noise) and the inclination of the borehole. However, correlation between neighbouring gamma-ray logs was possible. The influence of seasonal effects and salt creep on the extraction process, were found to be negligible.

Analysis of the current production profile shows that the production can be predicted accurately. The reserves can however be calculated more precisely using the new data. A reconciliation tool was developed and validated on 23 caverns.

The production controlled handling of the caverns results in a loss of reserves. This loss is caused by the outflow of fluids from a cavern. The average recovery factor for the first leaching phase is estimated to be 75%, versus the 80% which is used in the current reserve estimates. However, due to the conservative initial estimate of the reserves based on the insoluble content, the caverns still show a small surplus. The implementation of this tool for the entire field and incrementally improving it will assist future long term planning of the Hengelo Brine Field.

ii. Acknowledgements

First of all I would like to thank my daily supervisor Marinus den Hartogh. He helped me understand the problem and provided valuable input. Marinus introduced me to the different persons which I needed to cooperate with during the project, this was very helpful. I also would like to thank my second supervisor Tobias Pinkse for his critical notes and support.

From the Delft University of Technology I would like to thank Mike Buxton for his supporting role during this thesis, in which I combine two master tracks (i.e. Petroleum- and Resource Engineering). I appreciated the time he made for me to listen to my progress presentations and discuss the thesis in detail.

Furthermore I would like to thank the entire Mining Development & Compliance team of AkzoNobel for their hospitality and treating me like one of their colleagues. The professional environment was very beneficial for me. I received valuable input from the team during the weekly meetings and my progress presentations. Special thanks to Henk Leusink who taught me a lot about solution mining, familiarized me with the databases and was always available for questions, whether relevant or not. Thank you Sebastiaan Robertus and Tjeerd Koopmans for discussing my thesis during the dinners we had.

A special thanks to the field crew for giving me the opportunity to assist at various operations, such as drilling, well logging, performing workovers and one of the highlights of the graduation internship; the coring job. I also appreciated the assistance they gave me when I was conducting the different experiments in the field.

Prof. Dr. P.L.J. Zitha, representing the petroleum department, thank you for your time.

Delft, University of Technology
August 7th, 2015

J. Schootstra

iii. Table of contents

i.	Abstract.....	1
ii.	Acknowledgements.....	3
iii.	Table of contents	4
iv.	List of figures.....	9
v.	List of tables	13
1.	Introduction	15
1.1	AkzoNobel.....	15
1.2	Hengelo Brine field	16
1.3	Problem definition.....	18
1.4	Aim & Objectives	18
1.5	Research questions.....	19
1.6	Approach	20
1.7	Scope & Limitations	21
1.8	Thesis outline.....	22
1.9	Database	23
2.	Background information	25
2.1	History of salt.....	25
2.2	Production of salt at the Hengelo Brine Field.....	25
2.2.1	Hengelo Leaching Technique	25
2.2.2	Explanation of the leaching process.....	26
2.2.3	Leaching phases	27
2.2.4	Good Salt Mining Practice	27
2.2.5	Processing plant	28
2.3	Previous research	28
2.3.1	Specific research for the brine field of AkzoNobel in Hengelo.....	28
2.3.2	General research on salt	30
2.3.3	Fluid pathways	30
2.4	Reconciliation of reserves.....	31
2.4.1	Petroleum vs. Mining industry	31
2.4.2	Reserves & Data reconciliation	32
3.	Geology	33
3.1	Geological setting & Stratigraphy.....	33
3.1.1	Regional geology	33
3.1.2	Local geology & stratigraphy.....	37
3.2	Structural setting	39

3.2.1	Regional structural setting	39
3.2.2	Local structural setting	41
3.3	Cavern shape & geometry	44
3.4	Hydrogeology.....	45
4.	Mass balance.....	47
4.1	Theoretical mass balance	47
4.1.1	Mass balance equation	47
4.1.2	Theoretical results for the HBF	49
4.1.3	Mass balance hypothesis	49
4.2	Mass balance according to plant and field data	50
4.2.1	Flow data	53
4.2.2	Discussion.....	55
4.3	Mass data	58
4.3.1	Calculating the masses	58
4.3.2	Comparing the three masses	59
4.4	Mass balance for individual caverns.....	60
4.4.1	Method.....	60
4.4.2	Field test setup.....	61
4.4.3	Test results	62
4.5	Summary of the mass balance.....	67
5.	Pressure tests	69
5.1	Methodology	69
5.2	Test results	69
5.3	Cavern compressibility	70
5.4	Fluid inflow & distance of influence	71
5.5	Pressure test to check connectivity	73
5.6	Summary pressure tests	74
6.	Solling Formation	75
6.1	Core observations.....	75
6.2	Possibilities of fluid loss from a cavern.....	77
6.2.1	Connection between caverns through the Solling Fm.	77
6.2.2	Fluid loss to the Solling Fm.....	77
6.2.3	Direct connection between caverns.....	77
6.2.4	Possible explanations for establishing connections	79
6.3	Interaction between caverns and the Solling Fm.	81
6.3.1	Pressure phases in the field	81
6.4	In-/Outflow test	84
6.4.1	Production vs. Geology	84

6.4.2	Production vs. Sonar	84
6.4.3	Brine out / Water in (Mass/Volume balance on individual caverns)	85
6.4.3	Possible combinations.....	85
6.4.4	Discussion.....	85
6.5	Where do the fluids go?	87
6.6	Summary of key findings	88
7.	Sonar measurements	89
7.1	Methodology	89
7.2	Limitations & Neglected volumes.....	90
7.2.1	Sump	91
7.2.2	Roof.....	91
7.2.3	Wall	92
7.2.4	Combined neglected volumes.....	92
7.3	Sonar-/Production volume relationship	93
7.3.1	Relationship without taking loss of fluids into account	93
7.3.2	Relationship when taking fluid losses in consideration	95
7.4	Summary sonar measurements.....	95
8.	Insoluble material & Bulking factor.....	97
8.1	Bulking factor.....	97
8.1.1	Bulking factor insoluble material in the halite	97
8.1.2	Bulking factor rock layers in between salt layers	97
8.1.3	Current bulking factor	98
8.1.4	Bulking factor vs. Void ratio	98
8.2	Insoluble content background.....	99
8.2.1	Insoluble content HBF	99
8.3	Insoluble content determination.....	100
8.3.1	Method.....	100
8.3.2	Hypothesis.....	101
8.3.3	Insoluble content from modified cavern volumes	101
8.4	Summary insoluble content.....	103
9.	Other uncertainties	104
9.1	Gamma Ray log.....	104
9.1.1	Interpretation of Gamma Ray logs.....	104
9.1.2	Correlating GR-logs	107
9.2	Seasonal effects.....	108
9.2.1	Effect on the leaching process	108
9.2.2	Thermal expansion	108
9.3	Salt Creep.....	109

9.4	Summary of uncertainties in the field	109
10.	Reserve reconciliation tool & implementation	111
10.1	Current LT-plan	111
10.2	Analyzing predicted versus actual production data	112
10.3	Recovery factor analysis	115
10.4	Reserve reconciliation tool	117
10.5	Validating the reserve reconciliation tool	119
	Analyzing the reserve development during MLS-1	120
11.	Discussion	121
12.	Conclusions	122
12.1	Geology & Cavern shape	122
12.2	Mass balance	122
	Plant and field data	122
	Individual caverns	122
12.3	Pressure tests	123
12.4	Solling Formation	123
12.5	Sonar measurements	124
12.6	Insoluble material & Bulking Factor	124
12.7	Other uncertainties	125
	Gamma-Ray logs	125
	Seasonal effects	125
	Salt creep	125
12.8	Reconciliation of reserves	125
12.9	Answer to the research questions	126
13.	Recommendation	127
13.1	General	127
13.2	Mass balance	127
13.3	Pressure test	127
13.3	Ganzebos expansion	127
13.4	Real time monitoring	128
13.5	Reserve reconciliation	128
	References	129
	Bibliography	129
	Appendix A – Salt mining cavern types AkzoNobel	133
	Appendix B – Caverns	134
	Appendix C – Cavern interior	135
	Appendix D – Resource Reporting (AkzoNobel)	136
	Appendix E – Deviation in flow data caused by flow meter inaccuracies	137

Appendix F – Graphs from pressure tests.....	138
Appendix G – Average temperatures and related water density	140
Appendix H – Ratios for individual mass balance tests.....	141
Appendix J – Map of the caverns in the Usseleres area.....	144
Appendix K – Additonal stratigraphic information	145

iv. List of figures

Figure 1 – AkzoNobel’s integrated supply chain for salt. The integrated supply chain includes the production-, processing- and marketing & sales to various industries of salt, as shown in the figure.	15
Figure 2 – Location of the Hengelo Brine Field. Left: map of the Netherlands. Right: the HBF, the map shows all caverns which have been developed until April 2015. Usseleres is located in southwest of the HBF, whereas the new expansion area Ganzebos is located in the south.....	16
Figure 3 – Illustration of caverns developed at the HBF. Left: Multiple Completion Cavern (MCC). Right: Single Completion Cavern (SCC).....	17
Figure 4 - Natural and artificial components play a role during the development of a cavern	20
Figure 5 – Components of the DMAIC cycle (Creative Safety Supply, 2015)	22
Figure 6 – Map showing the locations of the caverns (table 1) used in chapters 7, 8 & 10.	22
Figure 7 – Illustration of a Single Completion Cavern. The well includes 3 casings; 1: 9 5/8”-casing, 2: 7”-casing, 3: 4 1/2”-casing, 4: Blanket control system	25
Figure 8 – Schematic leaching process including the concentration curve of a single completion cavern	26
Figure 9 – Overview of the purification installation. In the pictures the basins are shown where the brine is pumped into after it arrives from the field. Left: (1) 1 st reaction basin where brine, sodium hydroxide and lime are mixed. (2) basin where the brine mixture from basin 1 is able to settle (3) 2 nd reaction basin where soda is added to the brine. Right: one of the three 2 nd reaction basins at the processing plant site.....	28
Figure 10 – Schematic overview of the different fluid pathways. The following fluxes are identified, through the: 1. cavern wall, 2. roof, 3. Well (casing and shoe) & 4. the cavern floor. The well is illustrated with the different annular spaces (centre is brine, middle is water and the outer is oil).	30
Figure 11 – Extent of the Southern Permian Basin (SPB). The red circle indicates the location of the Hengelo Brine Field (Doornenbal & Stevenson, 2010)	33
Figure 12 – a) Triassic correlation chart. The red lines indicate from top to bottom the base of the Lower Jurassic, the base of the Upper Triassic, the base of the Middle Triassic and the base of the Buntsandstein Group and equivalents (Doornenbal & Stevenson, 2010) b) Enlarged section of the Triassic correlation chart which shows the relevant formations for the HBF.....	34
Figure 13 - Conceptual model of the geology and hydrogeology of the subsurface of the HBF (AkzoNobel).....	37
Figure 14 – Early Triassic tectonic evolution, indicating the basins and grabens present at that time (Doornenbal & Stevenson, 2010).	40
Figure 15 - Overview of the main structural elements in the HBF (NITG-TNO, 1998)	41
Figure 16 – The HBF has been divided in multiple areas. As indicated in the figure, the Boekelo fault zone is NW-SE oriented.	42
Figure 17 – Pictures from the visual inspection of caverns 382 (left) and 383 (right). The stalactites, consisting of insolubles, are clearly visible.....	44
Figure 18 – Representation of an actual cavern; based on multiple sonar measurements.	44
Figure 19 – Mass balances in the field. 1&2 are the balances which can be established between the processing plant and the pump station and/or field data, whereas 3 indicates the mass balance for individual caverns.....	47
Figure 20 – Cavern showing all important variables for the theoretical mass balance equation	48
Figure 21 – Overview of the measuring points in the field and processing plant. The yellow measuring points indicate main flow meters, used for the brine out/water in ratios (1: Flow from the pump station, 2: Flow at producing caverns, 3: Flow measured at the raw brine tanks). The green measuring points indicate the flow meters in the processing plant, these flows are mainly waste flows. At the orange measuring point the salt is weighted. The slurry to caverns and recycle brine flow are excluded.....	51
Figure 22 - Overview of the field and processing plant. Different flows with water are pumped to the field, brine comes back to the plant through the raw brine tanks. From the tanks it continues into the processing facility.	52
Figure 23 - This graph shows the average water and brine flow (m ³ /h) per month.....	53
Figure 24 - The graph is showing the total amount of flow measured per year.....	53
Figure 25 – Relationship between brine and water based on data from the main pump station and raw brine tanks.	54
Figure 26 – Distribution of the brine/water ratios based on pump station- and raw brine tank data	54
Figure 27 – Relationship between the flows measured at producing caverns and the brine in the brine tanks.....	54
Figure 28 – Explaining pressures in a cavern	55
Figure 29 – Brine/water density ratio vs. the ratio between brine out/water in.	56

Figure 30 – Comparing the total amount of salt measured/calculated from 3 sources (caverns, brine tank & final product).	59
Figure 31 – Deviation between weighed salt and salt calculated at the caverns and in the brine.	59
Figure 32 - Diagram showing the main issues of the flow meter which is placed on the outflowing brine side.	60
Figure 33 – Test setup in the field including a illustrative representation of the rock catcher, which ‘catches’ the insoluble rock particles by means of gravitational forces.	61
Figure 34 – Insoluble material from the caverns which causes the clogging of the flow meters. As indicated in the pictures, relatively large particles are produced. Left: material recovered from 505. Right: Clogged material found in the meter from cavern 487.	61
Figure 35 – Data from flow measurements on individual caverns. The ratio of brine out / water in of the test are shown in the graph.	62
Figure 36 – Diagram showing calculation of gain or loss of fluids from a cavern during the individual mass balance test	63
Figure 37 – Accuracy of the flow meters. Left: Range of the ratios plus average for the measured caverns (dotted line is theoretical brine out/water in ratio. Right: Flow meter error; blue columns indicate manufacturer error, orange indicate measured error.	64
Figure 38 – Results of the mass balance tests at caverns 487 and 488. The red dotted line indicates the flow meter switch.	65
Figure 39 – Map with location of caverns 490 and 491.	66
Figure 40 – Pressure responses monitored at neighbouring caverns. The numbers in the boxes below the bars indicate in which cavern the pressure was increased, whereas the number on top of individual bars indicate the specific cavern where the pressure increase was measured.	69
Figure 41 – Cavern system compressibility values for the different tests, the results are sorted according to cavern volume. The orange dotted trendline shows the average value for the SCC’s, whereas the blue dotted trendline shows the average compressibility value for the MCC’s.	70
Figure 42 – Inflow in caverns during the pressure tests of KBB and Deep. The numbers in the boxes below the bars indicate in which cavern the pressure was increased, whereas the number on top of individual bars indicate the specific cavern where the pressure increase was measured. The data has been scaled to 100 hours.	71
Figure 43 – Inflow in caverns during pressure tests of AkzoNobel.	71
Figure 44 - Relationship between the amount of inflow and the horizontal distance between the test cavern and neighbouring caverns (note: distances are measured from borehole to borehole).	71
Figure 45 – Topographic elevation map of the top of the Solling Fm. The blue lines indicate faults. The green arrows indicate main flow directions to higher elevations (i.e. less deep than the tested cavern) or main flows along isopachs. The black arrows indicate main flow directions towards caverns which are located deeper than the tested cavern.	72
Figure 46 – Installed pressure gauges. Left: cavern 503, right: cavern 479.	73
Figure 47 – Pressure monitoring test on caverns 479 and 503 during idle time	73
Figure 48 – Pictures from the coring operation. Left: Solling Fm. core fresh out the coring tool. Middle: Core handling from the rig to the work floor. Right: Kremco K400 rig during the coring operation	75
Figure 49 – Pictures of core samples from the Solling formation, core are from different drilled holes (Borne, Cavern 534 or BKM-02)	76
Figure 50 – Schematic illustration of the Solling formation.	78
Figure 51 – Schematic illustration of the development of the sump. Top: Normal development. Bottom: Possible situation when the sump is developed too deep.	79
Figure 52 – Schematic illustration of the Solling Fm. Left: the initial situation. Right: Situation after the formation gets in contact with fluids, the veins and faults act as fluid pathways, the leaching process starts in the Solling Fm. Permeability’s are taken from tests in the lab (de Vlieg, 2015).	81
Figure 53 – Different pressure situations during production of a cavern. The situations are explained accordingly in the different boxes.	82
Figure 54 – Theoretical outflows for situation 1, as described in Figure 53. Min = 250 mD, average = 1000 mD and max. = 2000 mD	83
Figure 55 – Map showing the caverns of the analytical in-/outflow test, including two possible locations where faults might be located.	86
Figure 56 – Graph showing all possible available volumes in the Solling Fm. using different parameters, based on different scenarios (from minimum to maximum.	87

Figure 57 – Sonar measurement. Left: Sonar tool hanging in the top part of the well. Middle: Rotatable head of the sonar tool which holds the sound transmitter and receiver. Right: Logging vehicle.	89
Figure 58 – Illustration of the sonar device when emitting acoustic pulses and the reflection from the wall.	89
Figure 59 – Left: Illustration of the edge of the roof, the distance between the measuring points is 6.31m at 60m and 6°. Right: Illustration of the roof of the cavern; the grey marked areas indicate the areas which are neglected due to stalactites hanging from the roof.	90
Figure 60 – Distribution of the neglected sump volumes	91
Figure 61 – Neglected roof volumes (i.e. neglected volumes due to stalactites and measuring inaccuracies of the edge of the roof) sorted on leaching phase.	91
Figure 62 – Total neglected volumes for the measured caverns (i.e. the sum of the neglected volumes of the sump, roof and wall). The neglected volumes are clearly normal distributed.	92
Figure 63 – Relationship between the leached volume and the sonar volume.....	93
Figure 64 – Leached volume vs. sonar volume relationships. Left: Relationship for MLS-1 caverns. Right: Relationship for MLS-2 caverns.	94
Figure 65 – Error when using the relationships to determine the cavern volume	94
Figure 66 – Relationships between the leached volumes (calculated from the corrected production data) and volume from the sonar measurements (corrected for the neglected volumes) are shown in the three graphs. Top left: Relationship for MLS-1 caverns. Right top: Relationship for MLS-2 caverns. Bottom: relationship for the combined types of caverns.	95
Figure 67 – Representation of the two bulking factors, the length of fragments is given by b. Left: Insoluble material present in the halite falls to the bottom of the cavern, the void space is quite high resulting in a high bulking factor. Right: When the cavern is leached out to the roof, i.e. the rock bench separating the salt layers, the roof can collapse, large fragments will float to the bottom and tend to pile up as layers, resulting in a low bulking factor.....	97
Figure 68 – Drilled core in salt A; showing insolubles in the clear salt. B; insoluble nodule present in the salt.....	99
Figure 69 – Pictures from the fractions (Drost, 2012). A is the fraction with the smallest particles (< 2mm) and A+ shows the particles when zoomed in with an electron microscope, the particles of B range from 2mm to 6cm and C shows the particle fraction larger than 6 cm.	99
Figure 70 – Steps involved when determining the insoluble content	100
Figure 71 – Insoluble content analysis of cavern 487. The green part indicates the volumes measured during the first sonar measurements, whereas the white part is the volume measured during the most recent measurement. Subtracting the white volume from the total volume gives the amount of insoluble material which lies currently at the bottom of the cavern.	101
Figure 72 – Results of the insoluble content determination.	101
Figure 73 – Results of insoluble content determination for multiple completion caverns (MCC's), a bulking factor of 1.2 is used for the rock benches and salt B, as explained in Figure 67.	102
Figure 74 – Frequency distributions of the insoluble contents. Left: Distribution of MLS-1 caverns. Right: Distribution of MLS-2 caverns. The generated data shows the distribution of 2000 random numbers, determined with the average and standard deviation of the actual data.....	102
Figure 75 – Distribution of radiation levels (Russell, 1944).	104
Figure 76 – GR-log data from well 484. Left: raw data. Middle: smoothed data. Right: Smoothed data, the orange coloured surface indicates the AUC (i.e. Area under Curve).....	105
Figure 77 – Surfaces of the GR-logs plotted vs. the insoluble contents of the corresponding caverns. Left: showing the data from the first leaching phase (MLS-1). Right: data corresponding to the second leaching phases of salt A.	106
Figure 78 – Correlation between the gamma ray log and the actual core.	106
Figure 79 – Correlation between two adjacent caverns, indicated by the red line.	107
Figure 80 – Correlation of the GR-logs of wells 532 & 531. The 4 salt layers can easily be correlated, but the continuation of the individual smaller peaks are difficult to match on both GR-logs.	107
Figure 81 – Maximum, minimum and average temperatures of the mixing water.	108
Figure 82 – Summary of the uncertainties in the HBF and the ability to be quantify each of them.	109
Figure 83 – Determining the capacity utilization factor	111
Figure 84 – LT production profile, showing the production for the next 10 years.	112
Figure 85 – Showing the average flow per hour for 23 of the 28 caverns in the Usseleres area. Top: Predicted flow for the different groups of caverns. Middle: Actual flow of the caverns. Bottom: Plotting the actual flow on top of the predicted in order to indicate deviations.....	113

Figure 86 – Showing the raw data. Left: predicted and actual salt production in ton/month for the Usseleres caverns. Right: predicted and actual average flow per hour.....	114
Figure 87 – The predicted/actual ratios are shown in the graphs for the period from 2008 until 2015. Left: the predicted/actual for the entire period, including the time during which the sumps are developed. Right: the ratio for the period in which all caverns are either in MLS-1 or 2.	114
Figure 88 – Comparing the total amount of predicted and actual salt on a yearly basis.	114
Figure 89 – Shape of the theoretical cavern at the far left (1) and a representation of an actual cavern at the far right (3). The shape in the middle (2) provides a better predicted shape.	115
Figure 90 – Relationship between the radii from sonar measurements and production data.....	116
Figure 91 – Recovery factors as function of the measured radius.....	116
Figure 92 – Principle of the 2 recovery factors explained: (i) is based on the actual measured radius, whereas (ii) is based on the theoretical radius (i.e. 60 m)	117
Figure 93 – Reserve reconciliation tool for the Hengelo Brine Field.	118
Figure 94 – The development of the reserves in the Usseleres area, showing 23 caverns. RF = recovery factor.	119
Figure 95 – The results of the different reserve estimations combined in 1 graph.....	119
Figure 96 – Reserve development. The initial reserve (A), recalculated reserve based on the new insoluble contents (B) and reserves based on the sonar measurement after MLS-1 has finished are shown.....	114
Figure 97 – Summary of the conclusions which are drawn with respect to the Solling Fm.	124
Figure 98 – Comparing the 3 salt mining operations of AkzoNobel. The typical shapes of the caverns and characteristics are given in the figure. Note that the cavern shape in Hengelo (i.e. the Hengelo Brine Field) is significantly different than the caverns at the other locations.	133
Figure 99 – Caverns used for determination of the insoluble content	134
Figure 100 – Detailed representation of caverns 490, 491 and 492. The shape of the caverns is clearly visible. The general shape is circular with. It can be noticed that the top (i.e. roof) of the cavern is uneven, indicating that the roof is not flat. The emitted sonar pulses are reflected back from solid objects, insolubles hanging from the roof cause this uneven surface.....	134
Figure 101 – The pictures above provide an inside look in the salt caverns around Hengelo. It is clearly visible how irregular the walls are and how big the rock fragments hanging from the roof are.	135
Figure 102 – Difference between volumes measured at the cavern and the volume at the pump station	137
Figure 103 – Ratio between brine outflow and water inflow measured at the caverns.	137
Figure 104 – Ratio between brine outflow and water inflow measured at the pumpstation	137
Figure 105 – Pressure test at cavern 367. The sharp increases to 20 bar indicate the moments of brine injection during the pressure test.	138
Figure 106 – Pressure test at cavern 372.....	138
Figure 107 – Pressure test at cavern 381.....	138
Figure 108 – Pressure test 472	139
Figure 109 – Pressure test 441	139
Figure 110 – Pressure test 487	139
Figure 111 – Pressure test 488. The pressure in cavern 487 follows the trend of 488 closely, indicating a direct contact between both caverns.....	140
Figure 112 – Pressure test 505	140
Figure 113 – Left: Average temperatures in Hengelo (Klimaatinfo.nl). Right: Density of water as function of temperature	140
Figure 114 – Brine out / water in ratios of cavern 487 during tests 1 and 2.	141
Figure 115 – Brine out / water in ratios of cavern 490 during tests 1 and 2.	141
Figure 116 – Brine out / water in ratios of cavern 488 during tests 1 and 2.	141
Figure 117 – Brine out / water in ratios of cavern 491 during tests 1 and 2.	142
Figure 118 – Brine out / water in ratios of cavern 504 during tests 1 and 2.	142
Figure 119 – Brine out / water in ratios of cavern 506 during tests 1 and 2. A large increase in ratio was noticed.	142
Figure 120 – Map of Usseleres area.....	144

v. List of tables

Table 1 – Caverns used in chapter 7, 8 & 10.....	23
Table 3 – Typical dimensions of AkzoNobel caverns (S. Robertus, personal communication, April 30, 2015).....	30
Table 3 – Thickness of stratigraphical units in the HBF.....	39
Table 4 – Brine water ratios according to inflow and outflow densities	56
Table 5 – Ratios brine inflow vs. water outflow (measured at the caverns and pump station)	57
Table 6 – Yearly amounts of salt in Mton	59
Table 7 – Results of the 1 st individual mass balance test.....	63
Table 8 – Results of the 2 nd individual mass balance test	63
Table 9 – Combined results of the individual mass balance tests (the ratio indicates brine out / water in).....	64
Table 10 – Observations & measurements during workover (cavern 490)	66
Table 11 – Unaccounted (i.e. lost) volumes during the pressure tests of KBB and Deep	72
Table 12 – Average leaching speeds during the sump phase	80
Table 13 – Expected in-/outflows for the different pressure situations. The chosen cavern pressures are based on a depth of 450 m, whereas the pressures for the Solling Fm. have been chosen according to realistic values.....	83
Table 14 – Possible combinations and conclusions	85
Table 15 – Summary of the results of the analytical in-/outflow test.	86
Table 16 – Properties of the surfaces, calculated for the 23 wells from the dataset.	105
Table 17 – BKM-02 core description; core was drilled in the Solling Fm.	143

1. Introduction

1.1 AkzoNobel

AkzoNobel is a world-leading producer of coatings and specialty chemicals. Products range from decorative paints to salt. AkzoNobel had an annual revenue of €14.3 billion in 2014, is the 11th largest company in the Netherlands and belongs to the Global Fortune 500.

AkzoNobel mines salt at three different locations. In 2014 AkzoNobel produced the following amounts of salt from these locations (M. den Hartogh, personal communication, March 17, 2015):

- Hengelo (The Netherlands); 2,5 Mton/yr
- Delfzijl (The Netherlands); 2,8 Mton/yr
- Mariager (Denmark); 0,5 Mton/yr



In 1918 the Koninklijke Nederlandse Zoutindustrie (i.e. KNZ) started producing salt in Boekelo, the Netherlands. The salt was dissolved in the underground salt layers and obtained by means of evaporation in open pans. In 1926, AkzoNobel adopted the more energy efficient method of vacuum evaporation. The vacuum evaporation method will be explained in chapter 2.2.5. Since 1933, when the construction of the Twente-Rijn canal was finished, AkzoNobel has been producing high quality salt from deposits close to Hengelo.

The discovery of salt in the Zechstein Fm. and the construction of facilities for loading seagoing ships in the Northern part of the Netherlands in 1951, led to the construction of a salt-producing plant in Delfzijl. This facility started producing in 1959. In 1963 AkzoNobel developed a third production site, which is located in Denmark, in order to serve the Scandinavian markets.

The division which deals with the salt production and sales is called Salt Specialties. Since AkzoNobel is involved from production until the distribution of salt, the division can be described as an integrated supply chain (Figure 1). AkzoNobel is one of the world's leading salt specialists, supplying high-quality products for all different kinds of applications. Salt Specialties exports salt products throughout the world. These products cover a broad spectrum of grain sizes, ranging from extra fine, to coarse salt, to compacted products. Some well-known brand names under which the products are sold, include Jozo®, KNZ®, Sanal®, Suprasel®, Broxo® and Broxomatic®. Salt Specialties distinguishes six market segments: Retail (road salt), Food, Pharmaceutical, Agriculture, Industrial and Water Treatment.

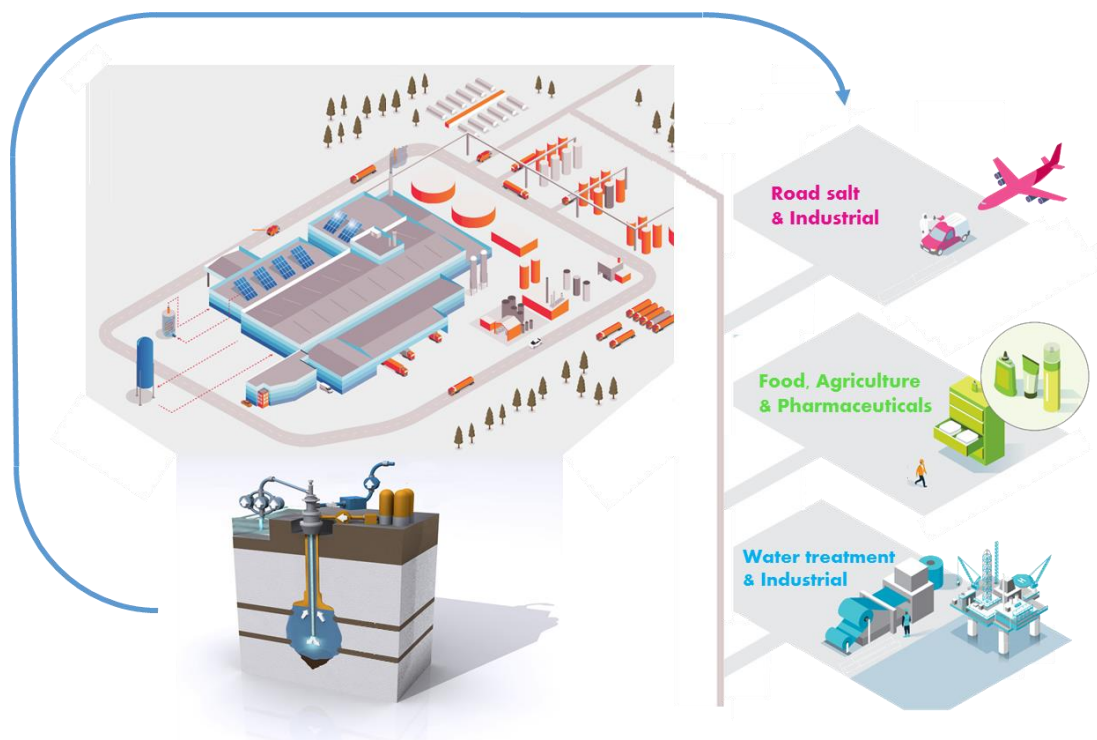


Figure 1 – AkzoNobel's integrated supply chain for salt. The integrated supply chain includes the production-, processing- and marketing & sales to various industries of salt, as shown in the figure.

1.2 Hengelo Brine field

In 1933, after completion of the Twente-Rijn canal, AkzoNobel started producing salt in the area around Hengelo in the eastern part of the Netherlands. This part of the Netherlands is commonly referred to as Twente. The concession from which salt is produced is called the Hengelo Brine Field (HBF). Figure 2 shows the exact location of the HBF. The mining of salt in this area started in the early days to the processing facility. During the following decades the development of the field moved in a southeastern direction. Currently most salt is produced in the Usseleres & Usseleres South areas. In the future (2015 to 2019) development of the HBF will be focused on the area called Ganzebos, which is located approximately 3.5 km south of the processing facility.

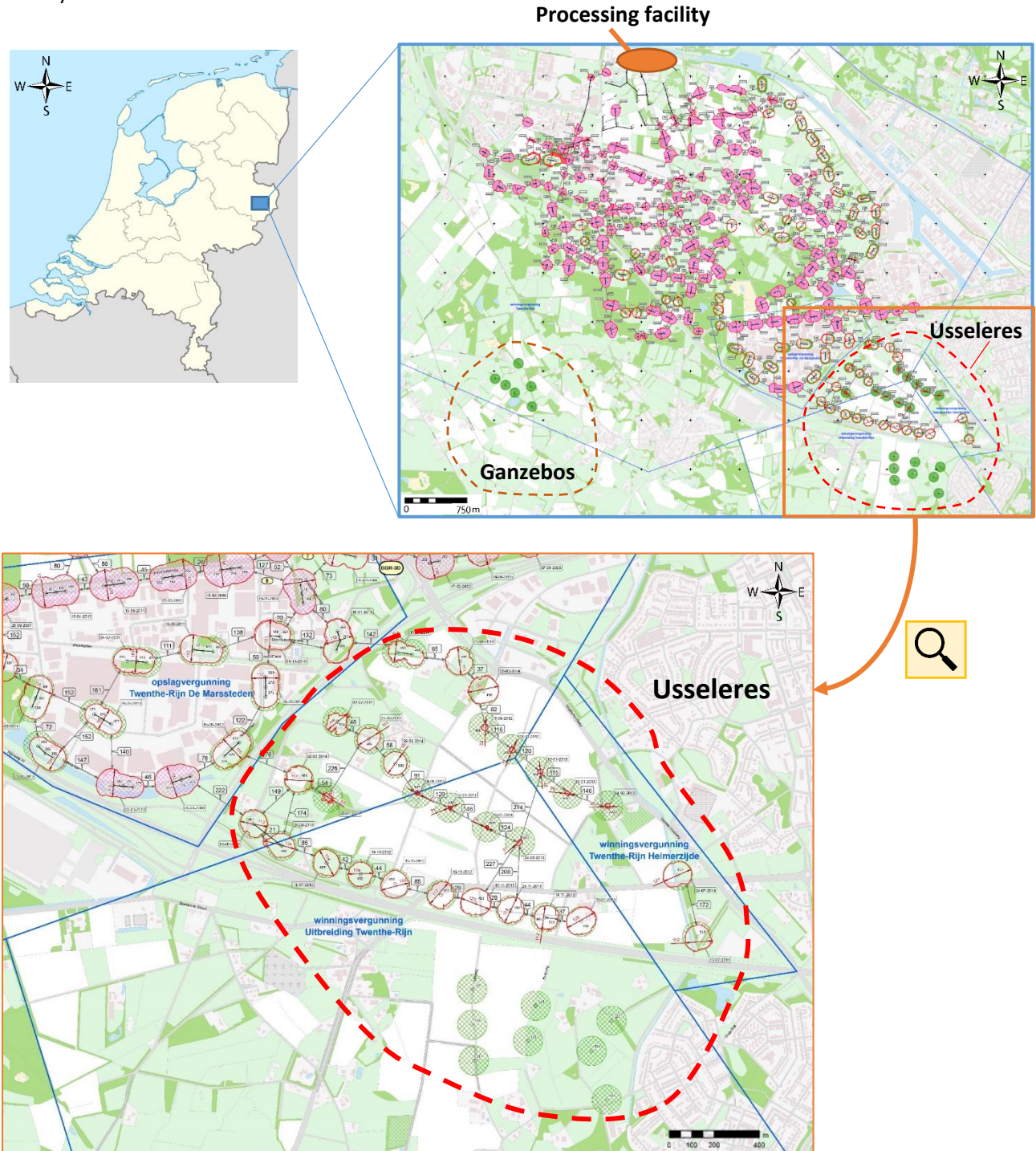


Figure 2 – Location of the Hengelo Brine Field. Left: map of the Netherlands. Right: the HBF, the map shows all caverns which have been developed until April 2015. Usseleres is located in southwest of the HBF, whereas the new expansion area Ganzebos is located in the south

There are two types of caverns in the HBF that both have the general shape of a pancake (the width is much larger than the thickness) and they have a more or less circular shape. The older type of cavern is called a *Multiple Completion Cavern* (MCC), because it is developed by drilling three wells. The caverns created by these wells are connected during the development phase and form a large cavern with an elongated geometry. The new type, which was introduced in 2005 and is the only one still being developed, uses only a single well and is called a *Single Completion Cavern* (SCC). Figure 3 shows an illustration of both types of caverns. The caverns are developed in different three phases; the initial development is the so-called sump, the second phase is the first main leaching stage (MLS-1) and the third is the second main leaching stage (MLS-2)

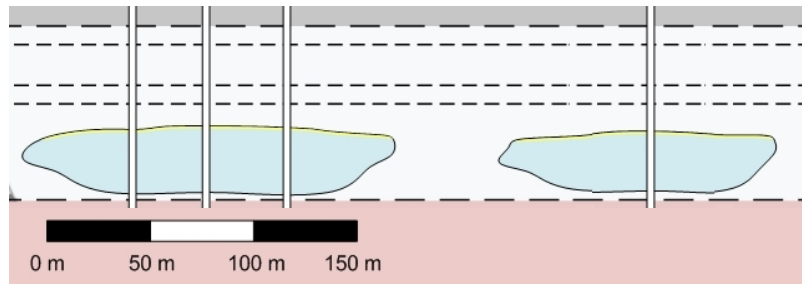


Figure 3 – Illustration of caverns developed at the HBF. Left: *Multiple Completion Cavern* (MCC). Right: *Single Completion Cavern* (SCC)

1.3 Problem definition

AkzoNobel currently has over 60 active caverns in the HBF, from which 45 are producing brine (the other 15 are waiting for a scheduled sonar measurement or maintenance). During the next 8 years 50 more caverns are scheduled to be developed. In order to optimize the long term planning for the field and to supply the processing plant with enough brine, it is important to find the correct balance between capacity and reserves. However, a proper methodology or accounting tool is not available at present.

Determining the volume of a cavern is an important part of the production process. The volume of a cavern is measured using two different methods:

- Amount of inflowing water
- Sonar measurements

Each cavern has a flow meter installed on the water inflow at the wellhead. The amount of inflowing water is used to estimate the size of the cavern. The caverns are also monitored with a sonar tool after each leaching phase and after a certain amount of produced salt (every ~150.000 ton produced). The main purpose of this measurement is to determine the volume of the cavern in order to update and validate the remaining reserves. The estimated cavern volume from wellhead data should theoretically match one to one with the estimated volume using the sonar method. However, a comparison between these volumes shows a lot of variation, causing uncertainties with respect to the actual subsurface volumes. The discrepancy is partly caused by errors in measurements and interpretation of both the sonar and wellhead data. Unknown amounts of insoluble material, connection between caverns and other geological features result in even larger discrepancies.

At the moment the results from previous calculations are not compared with the updated calculations nor are the differences explained. Observed variations in the field are not fully quantified. A better prediction of the reserves will improve the planning of future investments. Over the years, hundreds of wells (>500) have been drilled in the HBF in an area close to 50 km², creating a huge database of production and sonar measurements. Combining this data with the new insights regarding the remaining reserves will be the driving factor for the reserve reconciliation (i.e. a reserves accounting tool).

1.4 Aim & Objectives

The aim of this MSc. thesis is to quantify the uncertainties and give more insight in the mass balances of the salt production in order to create a systematic reserve reconciliation tool, for the Hengelo Brine Field, in order to achieve an optimal utilization of the caverns and to act as the main input for the Long Term development plan (i.e. LT-plan).

Five objectives were established for this project. Currently the predicted production from each cavern based on drilling data is estimated. However, the results are not checked with the actual data nor are they compared to results from sonar measurements. The prediction capability of the reserves calculation formula should be improved. With this improved knowledge of estimating the reserves and predicting the production, the LT-plan will be more accurate. This improved accuracy can potentially save €150k to €250k per year (M. den Hartogh, personal communication, November 17, 2014), due to informed decisions for future investments in new wells and pipelines and preventing mismatches between the produced amount of salt and the demand of the plant. However before such a tool can be developed it is important to fully understand the mass balances in the HBF. Therefore more research has to be done on factors that influence the recovery.

The objectives of this thesis are:

- Identifying the uncertainties related to the quantification of the production of salt at the HBF
- Quantifying the impact of the insoluble contents on reserves estimation
- Study the connection between caverns by field tests
- To relate and compare volume measurements to improve the mass balance
- To develop a reserve reconciliation tool

1.5 Research questions

The need for a reconciliation tool was described in section 1.4. Hence, the main research question for this study is defined as: *Is it feasible to develop a predictive methodology which is able to quantify the uncertainties properly, and can be utilized in the long-term planning of the production and development of the Hengelo Brine Field?*

Being able to predict the recovery of the caverns is an important part of this thesis. Most of the following research questions have influence on the recovery and utilization of the concession. To gain deeper insight into the different aspects, the research questions are subdivided into different subjects. The subjects with the accompanying questions are:

1. Uncertainties related to the production of salt at the HBF
 - What are the most important factors & parameters that cause uncertainty during the production of salt from the Hengelo Brine Field?*
2. Influence of the insoluble content in the salt formation
 - a. What the internal structure/geology of a cavern look like?*
 - b. What is the accurate value of the bulking factor for the salt layers?*
 - c. What is the insoluble content, and is there variation within the salt?*
 - d. Can the amount of insolubles be determined with a Gamma Ray log?*
3. Mass balance equation
 - a. What is the relationship and ratio between injected water and produced brine?*
 - b. Are the caverns closed systems?*
 - c. If not closed, what kind of connections are present between caverns? (i.e. direct, indirect or only with the Solling Fm.)*
 - d. Can pressure tests be used to analyze connections in the field?*
 - e. What is the role of the local geology (in particular the Solling Fm.)?*
 - f. What is the influence on the recovery and development of caverns?*
4. Volume measurements
 - a. What are the limitations of the sonar tool?*
 - b. How do the different (production data, sonar & geological) volume measurements differ?*
5. Developing a reserve prediction and accounting tool
 - a. How can the predicted, current and future salt reserves be combined to create an accurate production profile?*
 - b. What is the expected capacity of the caverns for the coming years and can this be achieved?*

1.6 Approach

Multiple aspects are combined during the salt production process. The entire production process can be divided into natural- and artificial components (Figure 4). Although there is a large distinction between the natural and artificial component of the process, an understanding of both components is needed in order to produce the salt optimally. Without proper knowledge of the geology, the mining process can't be executed. While excellent knowledge of only the geology is not sufficient to produce the salt.

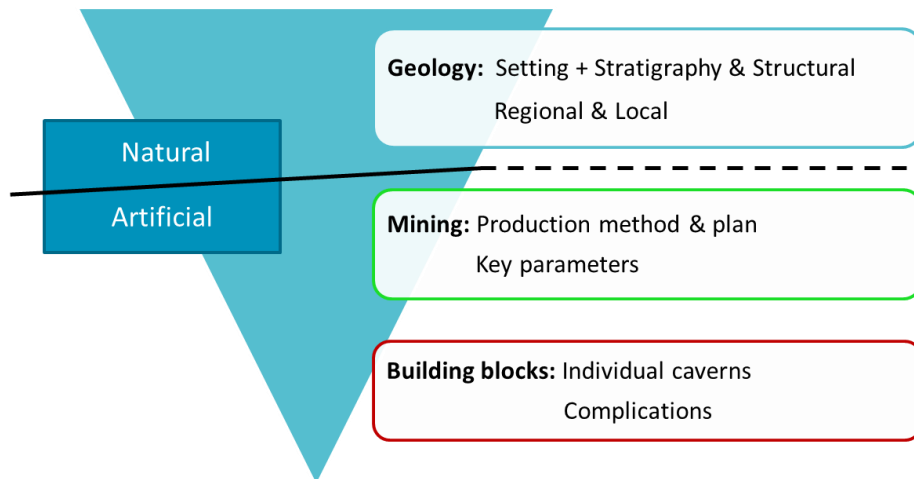


Figure 4 - Natural and artificial components play a role during the development of a cavern

The two components can be described as follows:

- The natural component refers to the geology of the field. It includes both stratigraphy and the geological structural setting on a regional and local scale, as discussed in chapter 3. The hydrological properties (e.g. permeability and porosity) and salt specific properties (e.g. halite density) are also part of this component.
- The artificial component refers to the mining & production process and can be subdivided into two parts. The 'mining' part describes the production method which is used (i.e. solution mining) and the long term planning for the field. The production process is determined by different overlying key parameters, such as the Hengelo Leaching Technique (section 2.2.1). The field is however a combination of multiple caverns which can be seen as the field's building blocks. Each building block comprises an individual cavern. These caverns have their own characteristics and production planning.

Previous research has only focused on individual parts (section 2.3). In order to apply correct reserve reconciliation for the entire field it is essential to link the natural and artificial components. The mass balance of the caverns has an important role in the reserve reconciliation process. Using the amount of fluids pumped into the field the produced amount of salt is estimated per cavern. When fluids are lost during the process this produced amount of salt is difficult to determine for individual caverns.

The mass balance depends on the mining process and the geology. The goal is to combine the following 3 different topics:

- geology of the field,
- hydrological properties,
- and the mass balance of the field,

in order to determine the causes of the volume discrepancies of the different methods and to fully understand the mass balances in the HBF. In chapter 4 it becomes clear that there is a systematic fluid loss in the system. Combining these topics will provide an explanation regarding the mass balance of the field, which will provide additional information for the reserve reconciliation model.

1.7 Scope & Limitations

This study considers the applicability of a reserve reconciliation tool. However, in order to do so many underlying topics are also investigated. The tool will be tailored for the HBF, although the basic principles are also applicable to the other AkzoNobel locations (i.e. Delfzijl in The Netherlands and Mariager in Denmark). The scope of this research is limited to the HBF.

Included in this study are:

- Literature review of the geological setting & stratigraphy of the HBF
- Only single completion caverns are included.
- Mass balance for the HBF including data from the plant, field and tests on individual caverns
- Review of the conducted pressure tests including an analysis of the fluid inflow. A different type of pressure test is proposed and verified as well.
- Comprehensive study regarding the sonar measurements including neglected volumes and a relationship between the production data and sonar volumes.
- Analysis of the insoluble content in a number of caverns.
- Review of the Gamma Ray log and whether it can be utilized to estimate the amount of insolubles material.
- Quantification of seasonal effects for the leaching process and salt creep for pressure built up.
- Analysis of the Solling Fm. by using the mass balance & pressure test results and combining it with the core and field observations.
- In-/Outflow test to determine whether fluids are flowing in or out a cavern.
- Reserve reconciliation tool based on 23 of the 60 producing caverns including detailed analysis of the first main leaching phase.

Excluded in this study are:

- Data from the plant from before 2009 (new meters were installed in 2009).
- Cavern data from before 2008 (the single completion caverns used in this study are drilled in 2008 and later).
- Multiple completion caverns
- Geostatistical methods to determine the distribution of geological features in the Solling Fm. (e.g. the number and density of halite filled fractures and veins and the salt/clay ratio).
- Measurement of pressure increase at caverns in active regions of the HBF. Tests were only performed at 2 caverns at the outskirts of the HBF.

Limitations of this study are:

- For every field test/calculation only a certain number of caverns are used: Data may be biased.
- Due to the limited number of flow meters and insoluble material which causes the flow meters to clog, only 6 caverns were measured extensively.

1.8 Thesis outline

The main goal of the project is to create a reserve reconciliation tool as described in section 1.4. The development of this tool is approached using the *Lean Six Sigma* (L6S) methodology (George & Lawrence, 2002). L6S projects are built on a DMAIC framework. DMAIC (an abbreviation for Define, Measure, Analyze, Improve and Control, (Figure 5)) refers to a data-driven improvement cycle used for improving, optimizing and stabilizing business processes and designs. The DMAIC improvement cycle is the core tool used to drive Six Sigma projects.

The author of this report has completed the Yellow Belt training.

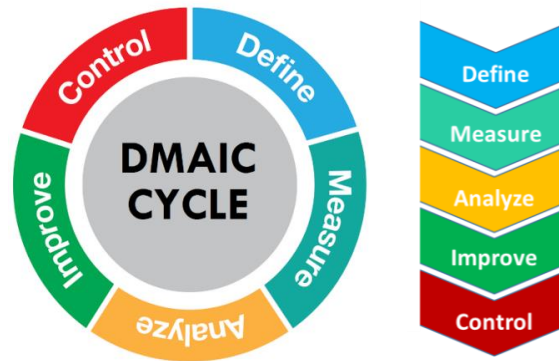


Figure 5 – Components of the DMAIC cycle
(Creative Safety Supply, 2015)

- D** This report follows the principles of the DMAIC methodology. The report starts with a general introduction of the project, including the aim & objectives, the research questions, the hypothesis and the scope and limitations. Chapter 2 provides background information of AkzoNobel and includes a brief explanation of the salt production at the HBF. The Hengelo Leaching Technique (HUT, 2012) and Good Salt Mining Practice are explained. Chapter 3 provides a thorough background on the geology of the field, furthermore the shape and geometry of the salt caverns are discussed in this chapter. These first three chapters are all part of the *Define*-phase.
- M** The *Measure*- and *Analyze* phase are closely related. The volume- and mass balances of the field and individual caverns are discussed in chapter 4. Chapter 5 includes the performed pressure tests, which provide additional information regarding the hydrological connections between caverns. Chapter 6 presents a theory for the behaviour of the Solling Fm., as part of the *Analyze*-phase. The observed fluid losses are further discussed and related to the Solling Fm. A conceptual model is presented of the underground environment.
- &**
- A** The sonar measurements, which are used to determine the volumes of caverns, are explained in chapter 7. After defining the uncertainty of the sonar tool, a relationship is determined which provides the real volume of a cavern, based on the sonar volume measurement. The error of this relationship is also discussed. Chapter 8 continues with the bulking factor and insoluble content determination. Other uncertainties such as the Gamma Ray logs and influence of the temperature are discussed in chapter 9.
- I** In chapter 10 the actual reserve reconciliation is developed for 23 caverns located in the southeastern part of the HBF. Developing the reconciliation tool is part of the *Improve*-phase of the DMAIC cycle. Chapter 10 also discusses the current development plan by comparing the predicted with the actual development.
- Finally the report concludes with the discussion, conclusions and recommendations of the study (chapters 11, 12 and 13).
- C** It may be noticed that the *Control*-phase is not part of this thesis. The responsibility for the *Control*-phase lies with AkzoNobel. AkzoNobel can improve the extraction process when the recommendations are implemented.

1.9 Database

The Mining Development & Compliance department within AkzoNobel is responsible for the data of the HBF. The database used in this department is called the *Borehole Management-database* (BPB-database). This database contains all information regarding the developed caverns of AkzoNobel in Hengelo (e.g. production volumes & sonar measurements). Another database used within the AkzoNobel's Hengelo-site is the process history database (PHD-database). The PHD-database contains all data of the processing plant including volumes of water pumped to the field and brine entering the raw brine tanks.

Data in this report is used from both the BPB- as the PHD-database. In chapters 6, 7 & 8 data from 23 specific caverns is used to analyze the neglected volumes when measuring the cavern by sonar, the insoluble content and to perform the in-/outflow test (section 6.4). The caverns used are listed in Table 1. Thirteen caverns which just finished the 1st main leaching stage (MLS-1) were selected, whereas 10 other caverns were chosen for which 1 or more sonar measurements in the 2nd main leaching stage (MLS-2) have been made. These different leaching stages will be described in section 2.2.3. Appendix B shows the 3D visualizations of these caverns.

Table 1 – Caverns used in chapter 7, 8 & 10

MLS-1 Caverns		MLS 2-Caverns	
# in dataset	Cavern #	# in dataset	Cavern #
1	487	1	482
2	512	2	479
3	492	3	440
4	497	4	484
5	490	5	493
6	504	6	485
7	498	7	441
8	488	8	483
9	491	9	442
10	505	10	446
11	494		
12	486		
13	506		

Chapter 10 will discuss the reserve reconciliation tool and implementation. This tool is developed using data from 23 SCC caverns (Caverns 486 to 506, excluding 500, 507, 508, 509 and 510), which are located in the Usseleres area (Figure 6 & Figure 120 in Appendix J).

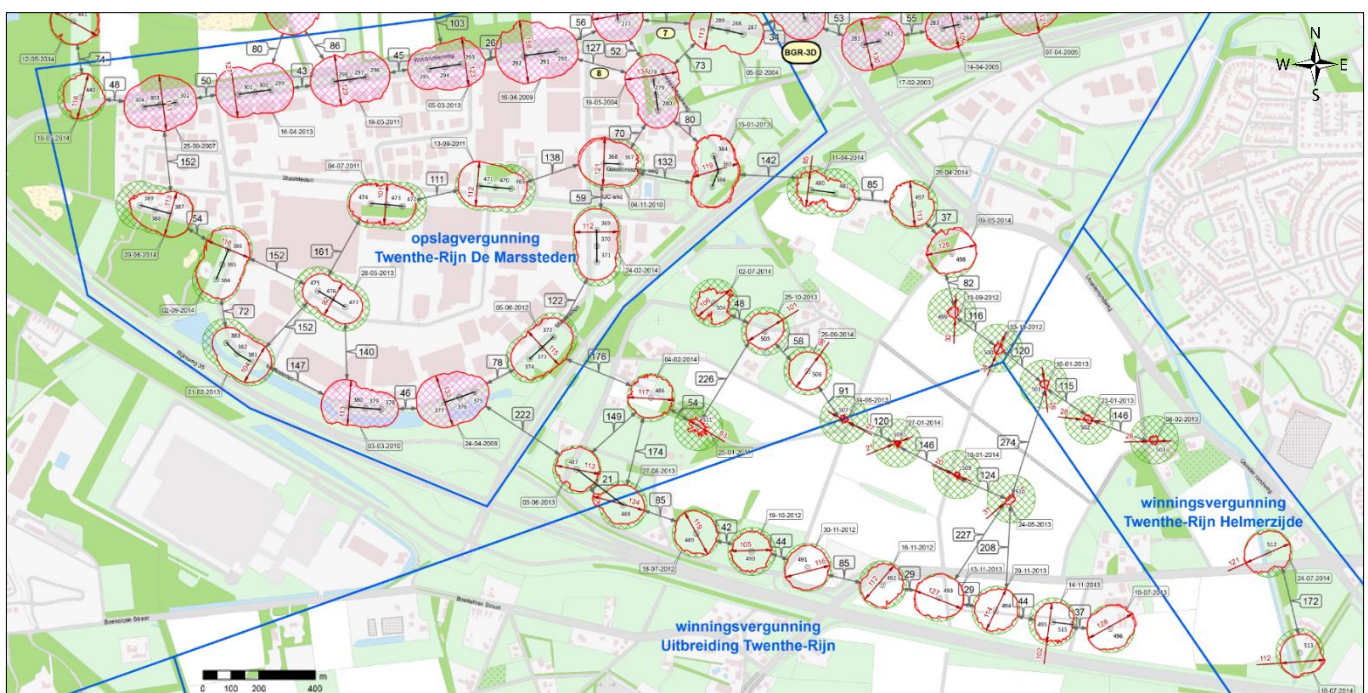


Figure 6 – Map showing the locations of the caverns (table 1) used in chapters 7, 8 & 10.

2. Background information

2.1 History of salt

Salt has been exceptionally important to humans for thousands of years. As far back as 6050 BC, salt has been an important and integral part of society. Historically it was difficult to mine and obtain the salt. It was therefore a highly valued trade item to the point of being considered a form of currency by certain civilizations (the word 'salary' is derived from the Latin word *salārium*, possibly referring to money given to soldiers so they could buy salt). Salt routes criss-crossed the globe. One of the most traveled routes led from Morocco across the Sahara to Timbuktu. Another example is that Venice's glittering wealth was not so much attributable to exotic spices as it was to commonplace salt, which Venetians exchanged in Constantinople for the spices of Asia (TIME Magazine, 1982)



Since ancient times there have been two main sources for salt: sea water and rock salt. Rock salt occurs in vast beds of sedimentary evaporite minerals that result from the evaporation of enclosed lakes, playas, seas and other salt water bodies. Extensive thick beds of salt are present all over the world. The salt is extracted from underground beds either by mining or by in-situ leaching (i.e. solution mining).

Halite is commonly known as rock salt. Halite is the mineral form of sodium chloride (NaCl). Its structure contains isometric crystals. The color is typically colorless or white, but can have many other colors depending on impurities.

2.2 Production of salt at the Hengelo Brine Field

AkzoNobel produces salt using the solution mining method at all of its sites. This means that water is pumped through a borehole into the salt formations to dissolve/leach the salt, forming a saturated brine. This brine is then pumped back up to the surface and transported to the processing plant

The salt is produced from the Main Röt Evaporite. This part of the stratigraphy will be discussed in section 3.1.2. The leaching of the salt creates caverns in the salt formation. These caverns can 'grow' large when the optimal production conditions are met. The following subchapters describe the leaching process in more detail. The shape of the cavern will be explained in section 3.3.

2.2.1 Hengelo Leaching Technique

After many years of experience, AkzoNobel has created its own leaching technique method, the so-called Hengelo Leaching Technique (HUT, 2012). This method was first applied to the multiple completion caverns (i.e. MCC's), with which elongated spherical caverns were created through the use of 3 boreholes. AkzoNobel switched to single completion caverns (SCC's) in 2005 (Figure 7). The HUT (2012) provides standard leaching rates and lifetime stages of the cavern as well as instructions on salt reserve calculation and timing of sonar measurements. It also provides information on the equipment and materials used for the development of the caverns. The blanket oil is also described. This is the oil which separates the under-saturated brine in the cavern from the roof. This prevents uncontrolled leaching of the roof and allows the cavern to grow in width, rather than in height. The blanket control system (i.e. BCS) is installed on the 7"-casing (a standard casing size in the oil and gas industry, 7" is 17.8 cm) and is used to control the blanket oil.

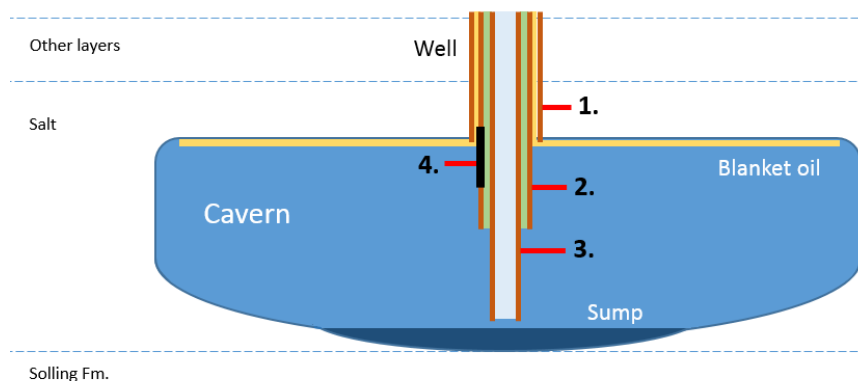


Figure 7 – Illustration of a Single Completion Cavern. The well includes 3 casings; 1: 9 5/8"-casing, 2: 7"-casing, 3: 4 1/2"-casing, 4: Blanket control system

Since the switch to these SCC's, with only one borehole and a diameter of 120m, the 'Good Salt Mining Practice guidelines (hereinafter referred to GSMP) have been utilized. This had led to a simplification of the brine extraction and development of the caverns. The most important outcome of the GSMP is that the development time of a cavern has been reduced and the flow per borehole has been increased. Flexibility of the operation has been increased as well since only one borehole is needed to develop a cavern, therefore less space at the surface is required. From a risk management point of view, the development of the SCC's has also reduced the possibility of significant subsidence.

2.2.2 Explanation of the leaching process

There are some basic theoretical principles included in the HUT which have to be followed during the leaching process. By doing this, the results of sonar measurements can be explained according to the leaching process. If needed mitigation actions can be implemented to leach the remaining salt according to the HUT.

The following is entirely based on the 7th edition of the HUT (2012). The following basic principles are followed:

- The amount of water injected in the cavern can be compared to injecting water through a garden hose in an Olympic swimming pool. The cavern is assumed to be at rest, since the effect of inflow can be neglected. This assumption implies that the concentration of the dissolved salt is constant for each location taken on a random horizontal slice in the cavern.
- The concentration differs in the vertical direction. This is illustrated in Figure 8.
 - In the area between the water injection and cavern roof the concentration is constant. This results in an equal enlargement of the cavern at every location along the cavern wall, regardless of the radius of the cavern.
 - In the area between the water inlet and the brine outlet the concentration increases with depth. The concentration increase shows a parabolic curve, meaning that the concentration increase rapidly in the first couple of meters, whereas it slows down towards the brine outlet.
 - Below the brine outlet the concentration is completely saturated, no further dissolving/leaching takes place.
- Horizontal parts of the wall are leached more slowly than those parts which are inclined. This is caused by the relatively heavy, saturated, brine which slowly flows downwards along the wall. Therefore no unsaturated brine can reach these horizontal parts. The same takes place in an opposite manner at inclined parts of the wall. Heavy saturated brine flows down, clearing the way for less saturated brine.
- Insoluble material sinks to the floor of the cavern, it is possible that undissolved fractions of the salt sink down as well, when insolubles break off in the cavern. This salt is considered lost, since no leaching takes places below the brine outlet.
- Gas-oil prevents leaching of the roof. Since the oil is lighter than the water/brine present at the top of the cavern, it forms a so-called blanket. This blanket separates the water/brine from the cavern roof.

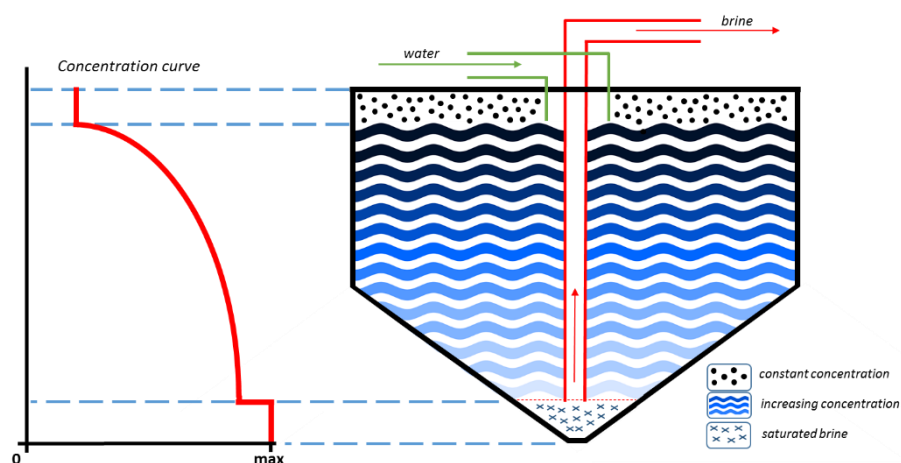


Figure 8 – Schematic leaching process including the concentration curve of a single completion cavern

2.2.3 Leaching phases

The SCC caverns have a lifespan of approximately 10 to 15 years. During this lifespan different leaching phases are active. Each phase has its own characteristics such as the height, minimum and maximum allowable flow (m^3/h) and the duration of the specific phase. The actual flow lies somewhere, according to the desired concentration, in between the minimum and maximum flow.

In between the leaching phases workovers take place. A workover is the process of performing major maintenance or other activities on a well. During a workover in the HBF the 4 1/2"-casing and 7"-casing* are usually removed, cleaned and reinstalled at different depths than before, in order to develop the cavern in height.

During the development of the cavern the following 4 phases/stages are used:

- The sump-phase: An inverted cone with a diameter of 80m is created by maintaining a flow of 15 m^3/h for approximately 14 months. The goal is to leach as much space in the shortest possible time. After 14 months a height of 2,5m is achieved and approximately 6000 m^3 of volume is created. Creating this sump allows AkzoNobel to achieve high production when starting with the 1st main leaching stage. During this phase brine is pumped through multiple caverns with the use of a third pipe, in order to achieve a higher concentration.
- After the sump-phase is completed a workover takes place, during which the tubing is positioned 5 meters above the top of the sump. This phase is called the 1st main leaching stage (MLS-1). The flow has to be maintained at least at 15 m^3/h . The maximum allowable flow is however 30 m^3/h . After the production of 139.000 tons of salt (which corresponds to approximately 80.000 m^3 of cavern space) a work over is carried out to continue with the 2nd main leaching stage.
- During the 2nd main leaching stage (MLS-2) the production tubing is repositioned with increments of a few meters during a couple of years, until the inherently safe height is reached. The minimum flow is still 15 m^3/h . The maximum flow is however increased with 10 m^3/h (i.e. 40 m^3/h), compared to the previous phase.

2.2.4 Good Salt Mining Practice

Since 2005 the GSMP has been utilized for all new caverns which are developed. The GSMP contains a number of rules which have to be followed. These rules describe how to deal with the caverns and surrounding environment. The implementation of the GSMP has resulted in a standardized procedure and complies with the Dutch Mining Law (Mijnbouwwet, 2002).

The following list contains the most important elements of the GSMP (HUT, 2012):

- Caverns are developed in parallel lines. This is clearly visible in the southeastern part of Figure 16. The diameter of the caverns is 120m and the pillar width between adjacent caverns is based on geotechnical calculations.
- The maximum allowable cavern height should be inherently safe. This implies that only minor subsidence will occur straight above the cavern in case the cavern collapses. This height is estimated on the basis of the depth of the Base Tertiary, the depth of the cavern roof and the bulking factor. Every cavern has therefore its unique maximum allowable cavern height. This height is not fixed. When insolubles sink to the bottom, the cavern floor will rise slowly, the inherently safe height will rise therefore as well.
- In order to control the development of the cavern height the blanket-oil (i.e. the oil situated on top of the brine in the cavern) is fixed at a certain depth during the leaching phases. The depth of the brine-oil contact is constantly monitored by the electronic Blanket Control System (i.e. BCS). The height of the cavern can easily be adjusted and controlled with the BCS.
- Subsidence forecasts are made for new drilling locations. The subsidence rate should stay below 50mm / 100 years.

** In the early 1860's oil production started in the USA. Therefore all dimensions related to the oil and gas are given in imperial units. The size of the casings in the HBF are also given in inches (1 inch = 2.54 cm).*

2.2.5 Processing plant

In the plant the brine is purified through a complicated process. This is done to remove most of the minerals other than NaCl. The brine is then evaporated in vacuum evaporators. In this installation the brine is heated and the pressure is lowered, allowing the water to evaporate in an efficient manner. After this entire process the salt contains less than 2% water. Figure 9 shows the purification installation.



Figure 9 – Overview of the purification installation. In the pictures the basins are shown where the brine is pumped into after it arrives from the field. Left: (1) 1st reaction basin where brine, sodium hydroxide and lime are mixed. (2) basin where the brine mixture from basin 1 is able to settle (3) 2nd reaction basin where soda is added to the brine. Right: one of the three 2nd reaction basins at the processing plant site.

2.3 Previous research

This subchapter has been divided into a specific- and general research section. In the specific research section three reports are discussed which have focused on three different topics. These reports are all related to the reserve reconciliation. The mass balance, geology of the field and properties of the Solling Fm. are discussed. The general research section will discuss some general findings.

2.3.1 Specific research for the brine field of AkzoNobel in Hengelo

Three different reports have been made regarding different types of research conducted for the brine field of AkzoNobel. This subchapter summarizes the reports and provides the main conclusions of these reports.

Mass balance (van Berkel, 2014)

Research was conducted at AkzoNobel regarding the mass balance and reserve reconciliation (van Berkel, 2014). The project combined both topics and analyzed three possible reasons for the observed differences regarding the reserve reconciliation and mass balance. The following reasons were discussed:

- Assumed parameters are incorrect: various parameters (e.g. brine concentration, salt density, etc...) were analyzed and a sensitivity analysis of the parameters was performed in order to check the impact on the volume and reserve calculations. Some basic assumptions were made regarding the insoluble content. The insoluble content should and can be determined with more detail.
- Measurements in the field are incorrect:
 - Brine flow and brine concentration: The brine flow and concentration of produced brine from the cavern was analyzed and tested for errors. For the caverns it is however impossible to measure the brine flow correctly due to the fact that only in the inflowing water is measured. A link with the processing plant could give more insight regarding the total amount of brine flow in the field.
 - Sonar measurements: the sonar device was described and the main limitation (i.e. the wavelength/amplitude which limits the correct measurement of pockets smaller than 1 m) was described. No emphasis was placed on the general capability of the sonar device to measure the caverns correctly, nor were neglected volumes discussed.

- Inflow or outflow of fluids from the cavern system: two tests were performed on a select number of caverns. The first test was a mass balance test during which the inflowing water and outflowing brine was monitored. This test was however only performed on two caverns (i.e. 441 & 442). These caverns were one of the first single completion caverns in the field, and are located outside the Usseleres area (i.e. the area where the majority of the current SCC's are located) and were surrounded by multiple completion caverns. The main lesson learned from this test was to switch the meters, in order to reduce the measurement error. Furthermore it showed that cavern 441 was leaking fluids, whereas an inflow of fluids was observed at cavern 442.
The second type of test which was performed was a pressure test. During this test, which was performed on different 4 caverns, water was pumped into the cavern, whereas the brine valve was closed. The pressure responses in the cavern and neighbouring cavern were monitored. These tests showed that the caverns were either directly and/or indirectly connected to each other. Further research on the nature of the connections was recommended.

The main conclusion regarding the reserve reconciliation was that the recovery factor, as expected, is the most influential parameter regarding the calculation of the salt reserves in caverns. The assumed recovery factor was 79.8%. This value was taken from another AkzoNobel/TU Delft report (Ensing, 2012). A comprehensive analysis whether the real recovery is in the same order of magnitude was not performed.

Geology of the field (van der Kroef, 2012)

In 2012 research regarding the fault patterns which are present in the HBF was conducted. In this study a reconstruction of the fault population of the field was made to assess the consequences for sustainable underground storage (i.e. SUS) activities of AkzoNobel. Cross sections were created from well data and were used as a tool to generate a fault displacement data set for several key geological horizons. The structural methodology which was applied led to two new interpretations for the fault population, both with a minimum and maximum fault length scenario. The first interpretation had a WNW-ESE fault trend throughout the brine field whereas the second trend shows a deviating WSW-ENE fault system in the north/northwest compared to a WNW-ESE trend in the south/southeast. This second interpretation was believed to give the best representation of the fault population. This research, together with reports from Geowulf Laboratories (2011) & (2014), indicated the presence of many faults, especially below the Rot Salt (i.e. in the Solling Fm.), in the area. These faults can possibly act as fluid pathways when in contact with the caverns.

Properties of the Solling Fm. (de Vlieg, 2015)

The Solling Fm. is located directly under the Rot Salt. De Vlieg (2015) showed that the upper part of the Solling Fm. consists of one type of sedimentary facies in the HBF, known as a "playa and mud flat" sedimentary facies. Different lab tests performed on 5 samples taken from a small piece of core indicated that the matrix of the Solling Fm. has a very low permeability. A fault has a much higher permeability, and when filled with halite cement, can act as fluid pathway. The lab tests also showed that the matrix of the Solling Fm. contains a high percentage of halite cement in the pores, which, when in contact with fresh fluids or unsaturated brine, can be leached. This leaching of the Solling Fm. can create extra volume in addition to the cavern, which can be filled with extra fluids.

Synthesis

Two main components play a role when producing the salt from the caverns close to Hengelo. These are the natural (i.e. the geology) and artificial (i.e. the production method) components in order to conduct proper reserve reconciliation both components should be taken into account. Previous research showed that the mass balances for the caverns do not correspond to the theoretical values. Furthermore it was concluded that caverns showed connectivity, probably created during the development of the caverns. These caverns can only be connected if the geology allows it to. Research regarding the fault patterns showed the presence of multiple faults in the field. It can be assumed that an abundant network of faults is present. Research regarding the hydrological parameters (e.g. permeability and porosity) showed that fluid pathways can be created. Further research should focus on the coherence between geological and mining related factors leading to mass balance deviations, different volume measurements and large variations in reserve estimates during the lifetime of caverns.

2.3.2 General research on salt

There is a lack of scientific articles on solution mining, specifically as it is conducted in Hengelo. Most research has been done for storage caverns (i.e. dedicated caverns for the storage of hydrocarbons). The mining process applied at the caverns of AkzoNobel in Hengelo is a very specific type of solution mining. The main difference, compared to other caverns around the world, is the depth of the deposit. Whereas the salt is generally produced from salt deposits deeper than 600m, creating narrow caverns with heights higher than 100 m, the caverns in Hengelo are developed at depths between 400 and 500 m, with heights up to 40 meters. The main reason is the thickness of the Rot salt, whereas other companies produced from other formations (e.g. the Zechstein salt). The width/height ratio of the caverns in Hengelo is therefore much higher than the ratio of other caverns around the world. In Table 2 the dimensions are shown for the caverns of AkzoNobel. A schematic overview of the different caverns is shown in appendix A.

Table 2 – Typical dimensions of AkzoNobel caverns (S. Robertus, personal communication, April 30, 2015)

	Hengelo (SCC's)	Delfzijl	Mariager
Cavern diameter (m)	max. 120	max. 120	max. 110
Cavern height (m)	30	1000	1100
Average salt production (tons)	$400 \cdot 10^3$	$15 \cdot 10^6$	$14 \cdot 10^6$

There is however an interesting paper on the effect of insoluble layers present in the salt. This phenomena can be one of the reasons for fluids to leave the cavern. Rock salt is seldom free from mechanical anisotropy. There are layers of anhydrite or layers of other insolubles which are significantly stronger than halite. This results in an inhomogeneous strain distribution in the salt. The laminated rock salt can exhibit considerable different mechanical properties compared to pure salt (Li et al., 2007). The interfaces between the intercalated competent layers and salt are particularly important because at these locations the stress, strain and deformation mechanics change. It has also been stated that the contacts between the salt and the insoluble layers (e.g. anhydrite) could act as pathways for migrating fluids (Zulauf et al., 2010).

2.3.3 Fluid pathways

A study conducted by TNO & Deltares (van Duijne, 2012) regarding the risk assessment of gas oil storage in salt caverns in the Twente region highlighted possible fluid paths (or so-called fluxes). The possible leakage paths were identified by a literature study in combination with interviews and a workshop with experts. An overview of the identified leakage fluxes is given in Figure 10.

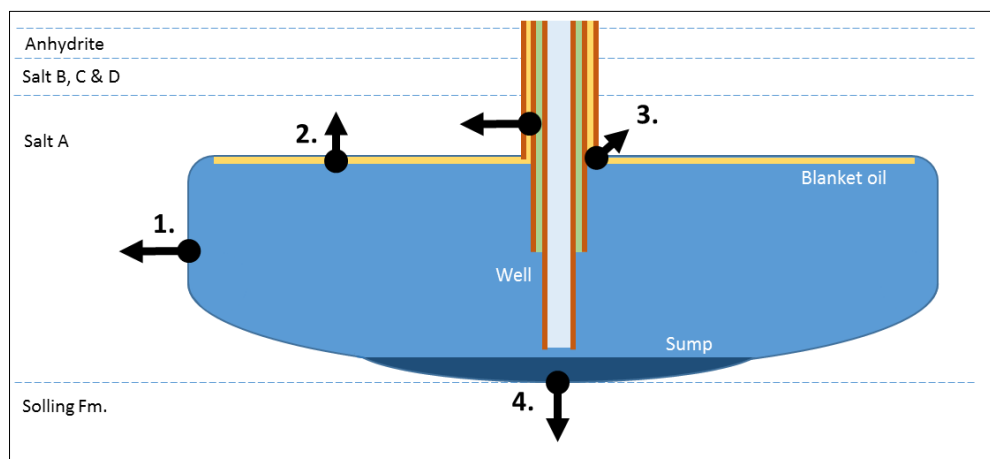


Figure 10 – Schematic overview of the different fluid pathways. The following fluxes are identified, through the: 1. cavern wall, 2. roof, 3. Well (casing and shoe) & 4. the cavern floor. The well is illustrated with the different annular spaces (centre is brine, middle is water and the outer is oil).

1. Cavern walls

Flux through the cavern wall includes paths created in the salt and/or possible permeable interlayers. As described in section 2.4.2 the presence of insoluble interlayers can possibly cause fluid pathways. It is difficult to detect these pathways since the shape of the caverns is generally irregular and the sonar device cannot measure voids smaller than 1 m (section 7.2). A narrow pathway in-between two caverns may exist without the sonar being able to see it, connecting both caverns. Such direct connections can be indicated by pressure tests, as described in section 10.2.3.

2. Cavern roof

Flux through the cavern roof could also occur. The presence of cracks and/or permeable faults can result in fluid pathways. The formation of cracks in the roof is possible due to tensile or shear fracturing. Tensile fractures can occur due to extensional stresses, whereas shear fractures are caused by compressional stresses. These type of cracks can occur when the cavern is unstable. Cavern stability depends on the thickness of the salt roof above the cavern, the thickness of the competent anhydrite layer which forms the top of the Main Rot Evaporite and the halmostatic pressure which is present in the cavern. Leakage through the roof is however very unlikely. When developing a cavern, a layer of salt (minimum of 5 m) is left between the roof of the cavern and the anhydrite that is located on top of the halite. Leakage is therefore unlikely to occur due to this impermeable layer of salt. Furthermore the oil blanket acts as a boundary between the brine and roof.

3. Well (casing and shoe)

Leakage can also occur in the wellbore. Three different migration pathways through a well can be distinguished: leakage at the surface as surface casing vent flow, flow along the annulus, fluid penetration out of the well into the adjacent rocks (Watson & Bachu, 2009). However, it is easy to notice such leakages, since the pressures (i.e. the brine, water and oil pressure are monitored) at the wellhead will change.

4. Cavern floor

Another possible pathway is through the floor of the cavern. Two contacts can occur: the sump of the cavern can be in contact with the underlying Solling Fm. and/or there can be an open connection through the drilled hole, which is drilled approximately 3 m into the Solling Fm. There are observations that point to possible fluid flux into and from the Solling Fm. This water influx is only possible when the internal pressure in the cavern, which is halmostatic, is smaller than the effective pore pressure outside the cavern, which may be assumed to be hydrostatic in the absence of compartmentalizing faults. Outflow can also occur, when the pressure in the cavern is much higher than the pressure in the Solling Fm.

Although all possible fluid pathways are possible, the most likely pathway is through the cavern floor. From tests in the field this connection between the cavern and the Solling Fm. is demonstrated. In chapters 4 & 5 the tests will be discussed, indicating possible fluids losses from the cavern, whereas chapter 6 will focus on the Solling Fm. and its capabilities to accommodate fluid losses and allow connections between caverns.

2.4 Reconciliation of reserves

This section addresses the basic principles of reserve reconciliation. There are different types of reserve reconciliation; data and reserves. The difference between the mining- and petroleum industry regarding the terms resources and reserves is discussed.

2.4.1 Petroleum vs. Mining industry

Reserve estimation methods differ between the petroleum and mining industry. Although both industries recover 'resources', the mining industry recovers solids whereas the petroleum industry recovers fluids. Both industries have their own classification:

- The mineral resource classification is used in the mining industry and is the classification system of mineral deposits based on their geologic certainty and economic value. A 'Mineral Resource' is a concentration or occurrence of material of intrinsic economic interest in or on the earth's crust in such form, quality and quantity that there are reasonable prospects for eventual economic extraction. Mineral Resources are sub-divided, in order of increasing geological confidence into the following categories: inferred, indicated and measured (JORC Code, 2012).

- The oil industry uses a different classification. The term *resources* is replaced by *reserves*. The relative degree of uncertainty can be expressed by dividing reserves into two principal classifications: proven and unproven. Unproven reserves can further be divided into two subcategories: probable and possible. This is done in order to indicate the relative degree of uncertainty about their existence (SPE, 2007).

In essence the classification systems are similar. There is a high degree of convergence between resources and reserves as defined.

Although the salt produced in the HBF can be considered a mineral resource, the production is undertaken using petroleum industry related techniques. AkzoNobel refers to the entire exploration license as its mineral resource, whereas it uses the term salt reserves for the sum of estimates on a cavern-by cavern basis taking into account cavern-specific considerations such as e.g. the technical guidelines for stability as set by the good salt mining practice, restrictions to mining due to surface infrastructure and environment, and economical considerations. Once more, this shows the interrelations. In appendix D the JORC code is formulated and explained as it is applied for the HBF of AkzoNobel (this is based on the JORC code from 2004).

2.4.2 Reserves & Data reconciliation

There is a difference between reserves and data reconciliation. Data reconciliation is widely applied in different industries (e.g. in mineral & metal processing plants) to improve information quality. Imprecision, unreliability and incompleteness of measurements are common problems motivating the implementation of the technique (Vasebi et al., 2014). The use of statistics is an important part of this type of reconciliation. Reserve reconciliation is however an accounting tool for the petroleum and mining industry, in order to properly update their total reserves and/or resources periodically.

In both the petroleum and the mining industry reserve reconciliation is applied. Because of the uncertainty in estimating oil & gas and ore reserves, the exact quantity of resources/hydrocarbons to be recovered will never be known until production reaches the economic limit and the site is abandoned. It is however necessary from time to time to estimate the reserves to be recovered throughout the producing life of a field. This is done in order to verify that the reserves are properly estimated and classified according to the definitions and guidelines specified in the code which is used (according to the industry and country). The testing procedure that is used is referred to as a “Reserves Reconciliation” and should be performed at least annually or more often if there are material changes to reserves estimates (Robinson & Elliott, 2004). In case of solution mining this testing procedure can be performed after every sonar measurement.

A reserve reconciliation is a powerful tool in tracking changes in reserve estimates. The process tracks the inventory. For the HBF the following situations can occur:

- Reserves can be added to the total inventory by:
 - Discovery of new suitable locations for the development of caverns
 - Extensions of existing caverns
 - Installation of improved recovery schemes
- Reserves can be deducted from the inventory by:
 - Production of salt from the caverns
 - Write-offs (e.g. when a cavern has a sub-optimal shape, salt is left during the development)
- Reserves can fluctuate within the inventory because of:
 - Economic effects (e.g. salt price, issues with competitors)
 - Technical revisions

Although the salt price is relatively constant (T. Pinkse, personal communication, April 3rd, 2015), changes in economic conditions may cause either additions or reductions to the reserves in the future. Technical reviews occur due to estimation procedures, resulting in moving reserves from one classification to another. This might happen after obtaining new information or due to poor geological- and engineering reserves estimation practices.

3. Geology

This section gives an overview of the geology of the Hengelo Brine Field. The HBF is located close to Hengelo, in the Eastern part of the Netherlands. The chapter will describe the regional and local geological and structural development and stratigraphic units which are present at the HBF. It will focus on the period starting at early Triassic until present day (i.e. the Holocene). The regional geologic- and regional structural setting are based on Doornenbal & Stevenson (2010). The local setting is based on studies done by Geowulf Laboratories (2011) & (2014). Furthermore information was used from the report written by van der Kroef (2012).



3.1 Geological setting & Stratigraphy

3.1.1 Regional geology

The HBF is located in the Southern Permian Basin (SPB). The SPB covers an area from England to Poland and Denmark to Belgium. Geologically the SPB extends in a west-east direction across the Paleozoic Platform of western and central Europe and intrudes east- and north-eastwards onto the Precambrian east European Craton (EEC). The present-day topography and bathymetry of the SPB is largely shaped by the pattern of uplift and subsidence established during the Cenozoic. Figure 11 shows the extent of the SPB.



Figure 11 – Extent of the Southern Permian Basin (SPB). The red circle indicates the location of the Hengelo Brine Field (Doornenbal & Stevenson, 2010)

Triassic

Triassic rocks extend across the SPB area from England to Poland and Lithuania. They also extend beyond the area, northwards into northern Denmark and the central and northern North Sea, and southwards into southern Germany, northern Switzerland and eastern France. During the Triassic continental conditions prevailed, interrupted by a marine incursion from the East during the middle of this period. The thickness development in The Netherlands is related to the structural pattern of the Northwestern part of the SPB. The relevant rocks of the HBF (i.e. the Buntsandstein-, Röt- and Muschelkalk formations) were deposited during the Triassic. The entire succession of the Triassic, as found in section from the Netherlands towards Denmark, is shown in Figure 12. In the enlarged section of the figure the succession of the relevant part is shown more clearly.

Buntsandstein group & equivalents

Whereas the uppermost Zechstein (Upper Permian) was predominantly characterized by evaporitic sabkha sedimentation, a shift towards predominantly fluvial, lacustrine and playa deposits is noticed in the

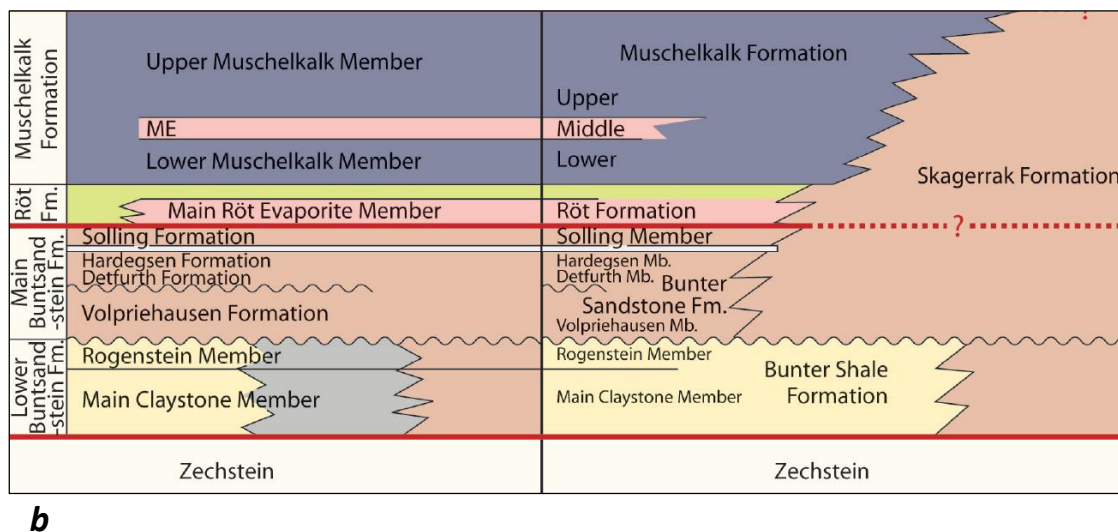
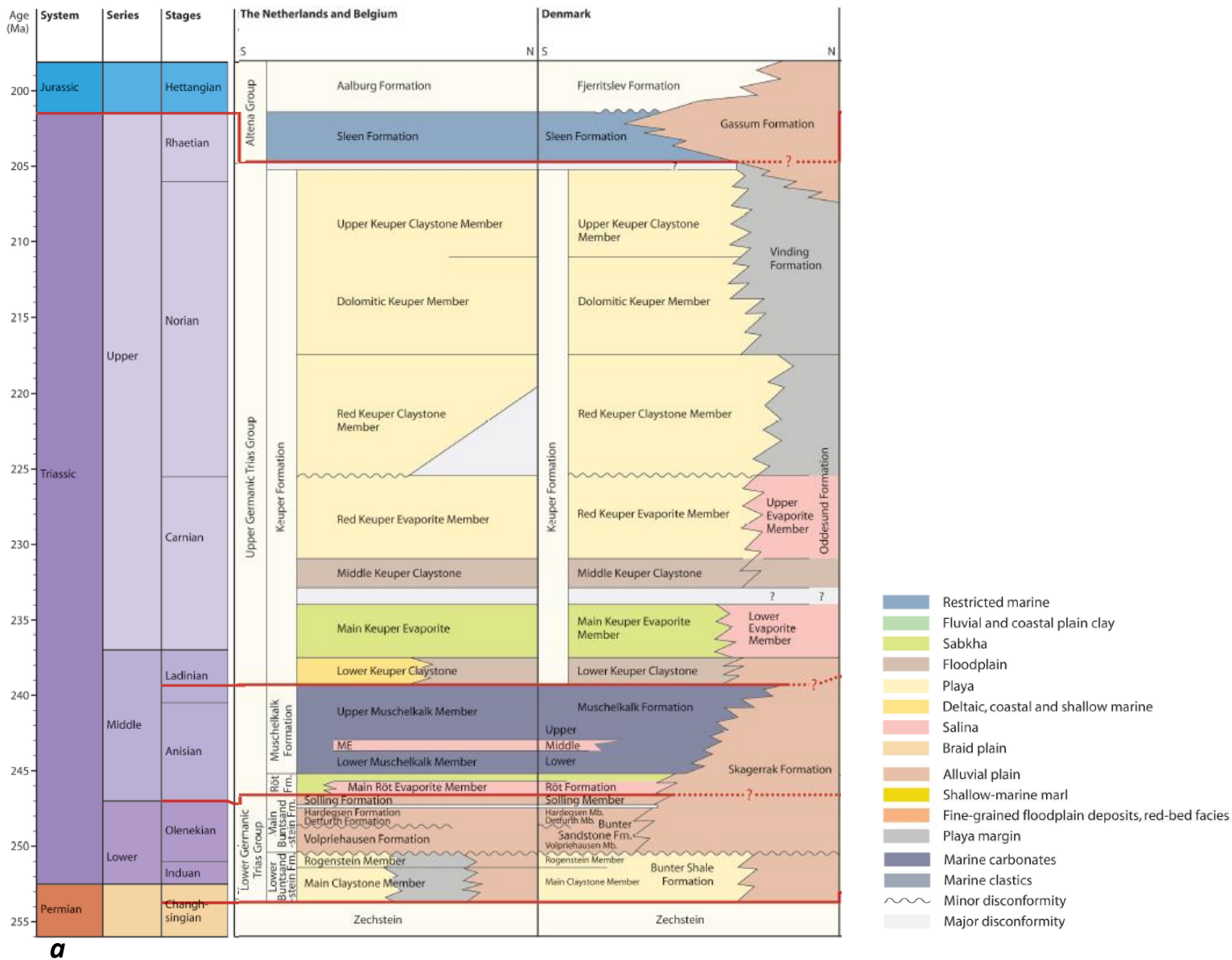


Figure 12 – a) Triassic correlation chart. The red lines indicate from top to bottom the base of the Lower Jurassic, the base of the Upper Triassic, the base of the Middle Triassic and the base of the Buntsandstein Group and equivalents (Doornenbal & Stevenson, 2010)
b) Enlarged section of the Triassic correlation chart which shows the relevant formations for the HBF

Buntsandstein Group (Bachmann & Kozur, 2004). The group contains three subgroups; the Lower Buntsandstein, Main/Middle Buntsandstein and Upper Buntsandstein. This multilateral subdivision is recognizable throughout large parts of the SPB.

Lower Buntsandstein

The Lower Buntsandstein succession reflects a gradual subsidence of the entire SPB area. During Induan times, the SPB area was not connected to the Tethys Ocean. Alluvial and fluvial deposits derived from the surrounding Variscan and older massifs (the London-Brabant, Rhenish and Bohemian massifs and the Fennoscandian Shield) were accumulated in marginal areas. The sediments consist mainly of fine-grained clastics with prominent oolitic carbonate beds (Doornenbal & Stevenson, 2010).

Main Buntsandstein

An important restructuring phase took place at the end of Lower Buntsandstein, which formed the transition to the Main Buntsandstein (Kozur 1999). Tensional and trans-tensional stresses created north-north-east and west-north-westerly trending highs and lows that dissected the Lower Buntsandstein depositional areas. This resulted in very variable amounts of subsidence. Throughout the SPB the sediment thickness reflects a combination of subsidence in the grabens and uplift and erosion elsewhere (Geluk & Röhling, 1997).

At the end of the Main Buntsandstein the Solling formation was deposited. The Solling Fm. rests unconformably on Lower and Middle Buntsandstein formations throughout the SPB, separated by the pre-Solling Hardegsen unconformity. In north-western part of Germany and the eastern part of the Netherlands, aeolian sands (resp. the Salzwedel and Dotlingen sandstones) occur in the lower part of the Solling Formation (Schulz & Röhling, 2000). The dune areas were separated by an extensive playa-lake system that extended from the central SPB area into the present-day eastern Netherlands and southern Germany (Röhling, 1991). The upper units of the formation are more closely related to the overlying Rot Formation than to older Main Buntsandstein formations.

Upper Buntsandstein

The transition from the Solling to the Rot Formation is in general marked by an increase in marine sediments. The facies pattern of the lower Rot Formation is typical for a semi-closed evaporitic basin. Most of the Netherlands and the southern North Sea were also situated in this salt basin. **Error! Reference source not found.** provides an illustration of the facies distribution during the Upper Buntsandstein. A large brackish-water lagoon developed, which resulted in evaporite deposition. The deposits consist of fine-grained predominantly red clastics, from which the name 'Rot' is derived (Doornenbal & Stevenson, 2010). The Formation can be sub-divided into four stratigraphic members, existing of evaporitic sequences, formed by an alternation of marine influxes and periods in which arid conditions prevailed. These four members will be explained in detail in section 3.1.2.

Muschelkalk

The Röt Formation is overlain by the Muschelkalk Formation. The carbonate-dominated Muschelkalk Group marks a fundamental change in paleogeography. The sedimentary environment of the Muschelkalk deposits is associated with a general sea-level rise. This sea-level rise was established by the opening of the gateways in the south-east and south-west, which resulted in connections between the Tethys Ocean and the SPB (Doornenbal & Stevenson, 2010).

Jurassic

The Jurassic rocks of western and central Europe, which form the core of the SPB area, were deposited in a shallow epicontinental basin that extended from the present-day UK area through the Netherlands, eastwards into Poland, and from southern Germany to Denmark in the north. Throughout the Jurassic connections through the North Sea to a northern Boreal Ocean and via gateways in the south to the Tethys Ocean were present. The waxing and waning of these two oceanic areas had a profound influence not only upon sedimentation and facies in the Jurassic, but also for biostratigraphic correlation across the basin (Callomon, 2003). A major phase of tectonic inversion and erosion took place during the Late Cretaceous to Early Cenozoic. As a result, Jurassic sediments have not only been uplifted and exposed at outcrop across much of the SPB area, but are also now preserved on the north-west European continental shelf as a series of disconnected basin remnants subcropping variable thicknesses of Cretaceous and Cenozoic sediments.

Cretaceous

The transition from the Jurassic to the Cretaceous Period took place against a background of abating rifting and a gradual change to a period of regional tectonic subsidence controlled by lithospheric cooling following the Jurassic rifting events. The transition is defined by a main unconformity of early Berriasian age (Late Cimmerian Unconformity = Base Cretaceous Unconformity), which may truncate Jurassic or even older sediments. Different periods followed each other; first there was a main phase of sedimentation, then there was emergence and erosion, subsequent non-marine 'Wealden'-type sedimentation and finally a period of continuous transgression (Mutterlose & Bornemann, 2000).

Cenozoic

Until the late Quaternary, the Cenozoic strata of the SPBA area were deposited within a single depositional area referred to as the Tertiary North-west European Basin (Vinken, 1988). Neotectonic restructuring in the Late Quaternary led to the present-day configuration in which the North Sea Basin is separated from a shallow basin to the south-east, known as the East German – Polish Basin. The Cenozoic fill of the North Sea Basin has been the subject of especially intense investigation during the last 40 years due to the discovery of major oil and gas reserves in the Paleocene and Eocene rocks of the central and northern North Sea. There are no significant hydrocarbon reserves in the Cenozoic of the SPBA area, but the changing patterns of Cenozoic subsidence and sedimentation have exerted an important control on the generation of hydrocarbons in older parts of the stratigraphic column (Rasmussen et al., 2005).

3.1.2 Local geology & stratigraphy

The HBF has been tectonically active, resulting in various fault zones in the region. The concession can be subdivided in several areas based on the presence of these tectonic elements. The geology has been described in detail by the following companies; Geowulf Laboratories (2011) & (2014), MWH (2010) & (2011), Deltares (van Duijne, 2012). Detailed lithological and stratigraphic studies of cutting samples from various wells combined with gamma-ray logs have created a geological framework for the HBF.

Figure 13 shows a schematic representation of the stratigraphic succession of the HBF. The salt caverns, which are located in the Main Röt Evaporite layer, are shown in the figure as well. The stratigraphy in the Twente area is formed by the following stratigraphical units, from old to young:

- Solling Fm. (RNRO: RNSOC)
- Röt Fm. (RNRO: RNSOC, RNRO1, RNROM, RNRO2 & RNROU)
- Muschelkalk Formation (RNMU: RNMUL, RNMUM & RNMUU)
- Altena Group (AT: ATRT & ATAL)
- Niedersachsen Group (SK: SKWF & SKCF)
- North Sea Group (N: N1 & N2)

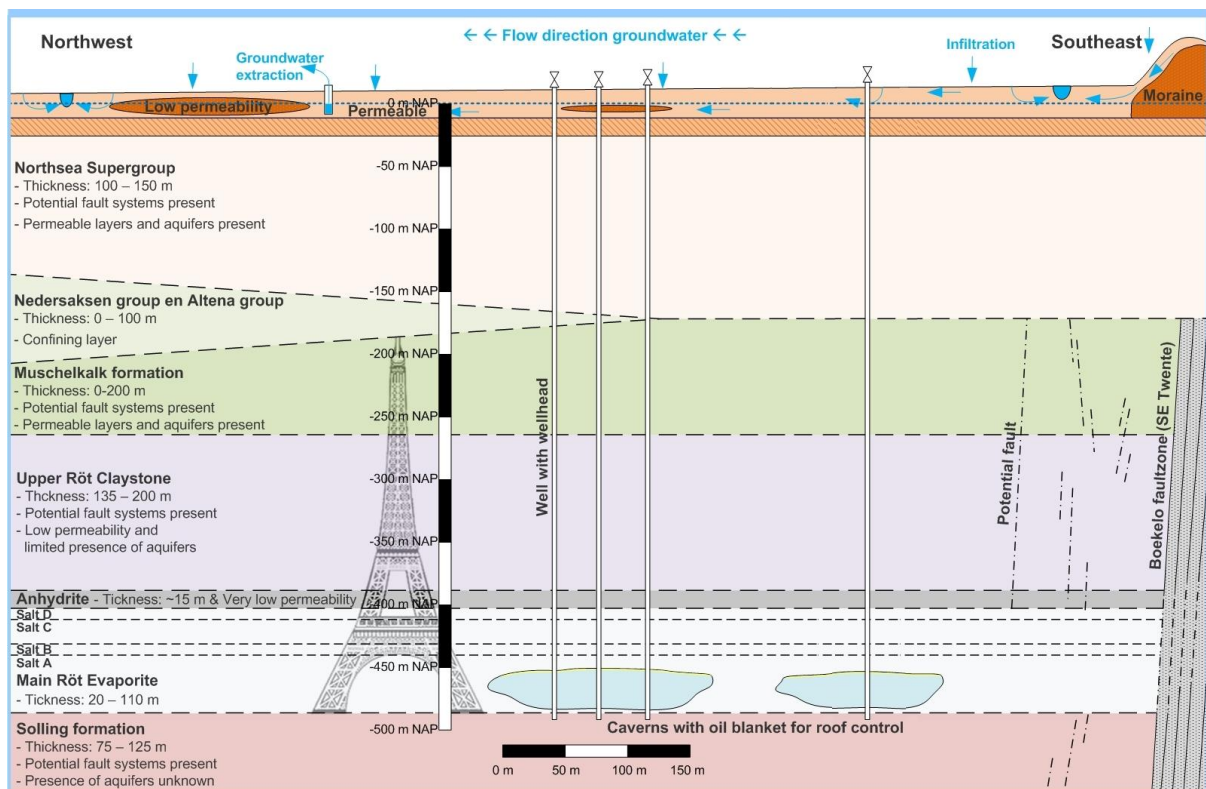


Figure 13 - Conceptual model of the geology and hydrogeology of the subsurface of the HBF (AkzoNobel).

The Upper Germanic Trias Group

Within the Triassic rocks, two major groups of sediments are recognized, i.e. the Lower Germanic Trias Group, a mainly clastic succession and the Upper Germanic Trias Group, comprising an alternation of clastics, carbonates and evaporites. The Upper Germanic Trias Group comprises the Solling (RNSO), Röt (RNRO), Muschelkalk (RNMU) and Keuper (RNKP) Formations. The Keuper will not be described as it is absent in the HBF.

Solling Formation

The Solling Formation is subdivided into the Basal Solling Sandstone Member and the Solling Claystone Member. The formation lies unconformably on top of the Lower Germanic Trias Group and is conformably overlain by the Röt Formation. The Basal Solling Sandstone Member has a thickness of a few meters at most and consists of red fine-grained calcareous sandstone. The Solling Claystone Member consists of red or red-brown dolomitic silty claystone. Characteristic for this geological layer is the appearance of green stains, which

are probably caused by reduction processes around radioactive minerals (halo's). Towards the south the sand fraction of the geological unit increases. The unit is thickest in the Ems Low (over 120 m) and decreases in thickness to approximately 70 m towards the west. Sand content of this layer increases towards the south and sand lenses may occur (van der Kroef, 2012). Locally, not much information is available as wells were drilled only a couple of meters into the Solling Formation.

Röt Formation

The depositional setting of the Röt and Muschelkalk formations was in a coastal plain to coastal sebkha environment (**Error! Reference source not found.**). The Röt Formation is subdivided into the Main Röt vaporite Member, the Middle Röt Claystone Member, the Upper Röt Evaporite Member and the Upper Röt Claystone Member. At locations where the Upper Röt Evaporite Member cannot be distinguished, the Röt Formation is subdivided in the Main Röt Evaporite Member and the Röt Claystone Member. The formation lies conformably on the Solling Formation and is conformably overlain by the Muschelkalk Formation. The thickness of the Röt Formation varies between 225 m in the north and 300 m in the central part of the area and decreases in southern direction to slightly less than 200 m (Geowulf Laboratories, 2011).

Main Röt Evaporite

The Main Röt Evaporite Member (RNRO1) consists primarily of halite, with a thick anhydrite layer at the base, and with intercalated clay/anhydrite layers of 10 to 15 m thickness at the top. The largest thickness of the Main Röt Evaporite Member is 110 m in the Ems Low. Southeast of the Gronau Fault zone, located north of the HBF, thicknesses of more than 100 m have been encountered. The salt member of the Main Röt Evaporite (in which the salt caverns are located) is subdivided into four salt layers by the presence of four claystone intervals (with additives of dolomite and anhydrite) that can be very well correlated over the area. These layers were created due to several cycles of regression and transgression. In the HBF, the four salt layers have been named A, B, C and D from bottom to top. Salt layers A, B, and C consist mainly of light grey or transparent rock salt, while layer D consists of red colored rock salt (additives of poly-halite en red colored claystone). Salt layer A has a thickness that varies between 10 and 60 m, while layer C has a more constant thickness of 15 to 20 m. The thickness of salt layers B and D is generally only several meters.

Middle Röt Claystone

The Middle Röt Claystone Member (RNROM) consists of red-brown colored claystone beds and locally gypsum nodules and anhydrite laminae. It has regionally a relatively constant thickness of 25 to 35 m (van Duijne, 2012). This layer can be easily recognized on well logs due to its high gamma-ray values that contrast with the low values of the under- and overlying evaporate layers. In the HBF this layer has a thickness of 19 to 28 m, with the thickest parts in the north-eastern and eastern part of the area.

Upper Röt Evaporite

The Upper Röt Evaporite (RNRO2) comprises crystalline anhydrite which is locally silty and dolomitic. The Upper Röt Evaporite Member has developed in the anhydrite facies and consists of an alternation of anhydrite and claystone layers. The thickness of the Upper Röt Evaporite Member varies between 1 and 15 m. In the HBF it has a thickness of approximately 1 to 2 m (van der Kroef, 2012).

Upper Röt Claystone

The Upper Röt Claystone Member (RNROU) consists of purple, orange, red brown and green claystone, with intercalated siltstone beds and beds with concentrations of gypsum nodules. With dolomite cement and/or gypsum/anhydrite cement and mica are found most frequently in the upper and lower parts of the member. Thickness ranges from 125 to 144 m within the Twente-Rijn area and its thickness distribution shows an increase from south-west to north-east. Regionally in the Ems Low it can reach a thickness of up to 200m (Dufour, 1998).

Muschelkalk Formation

The Muschelkalk Formation (RNMU) is subdivided into different geological units: the Lower Muschelkalk Member, the Muschelkalk Evaporite Member, the Middle Muschelkalk Marl Member and the Upper Muschelkalk Member, these units are described in Appendix K. The Muschelkalk Evaporite Member and the Middle Muschelkalk Marl member are often combined, and called the Middle Muschelkalk. This results in three

units. The distribution of these layers has been influenced by tectonic activity, resulting in erosion. Only the Lower Muschelkalk is present in the entire HBF (Geowulf Laboratories 2011). The contact between the Muschelkalk Formation and the underlying Röt Formation is conformable, whereas the contact with the overlying Altena Group, the Niedersachsen Group or North Sea Group is unconformable. Regionally the total thickness of the Muschelkalk Formation ranges from 0 to 200m. In the HBF its thickness is found to be up to 120m (van der Kroef, 2012).

Other stratigraphical units

The other 3 stratigraphical units, as shown in Figure 13 (i.e. the Niedersachsen group, Altena group and Northsea Supergroup), are less relevant for the HBF. These groups are described in Appendix K.

Stratigraphical thicknesses in the HBF

Geowulf Laboratories has determined all thicknesses of the different stratigraphical units (Geowulf Laboratories, 2011). A summary can be found in Table 3.

Table 3 – Thickness of stratigraphical units in the HBF

Formation/Group	Unit	Abbreviation	Min (m)	Max (m)	Average (m)
Solling Formation	Solling Claystone	RNSOC	-	-	>100,0
Röt Formation	Main Röt Evaporite	RNRO1	22,0	113,0	72,0
	Middle Röt Claystone	RNROM	19,5	27,5	25,5
	Upper Röt Evaporite	RNRO2	0,2	1,8	0,7
	Upper Röt Claystone	RNROU	122,0	147,0	138,0
Muschelkalk Formation	Lower Muschelkalk	RNMUL	32,3	37,7	63,2
	Middle Muschelkalk	RNMUM	25,0	30,0	27,5
	Upper Muschelkalk	RNMUU	*	*	-
Altena Group	Sleen Formation	ATRT	0,0	19,0	8,0
	Aalburg Formation	ATAL	*	*	-
Niedersachsen Group	Weiteveen Formation	SKWF	18,8	32,5	24,5
	Coevorden Formation	SKCF	47,8	94,9	67,9
North Sea Group	Lower North Sea Group	N1	12,1	22,2	16,3
	Upper North Sea Group	N2	52,0	135,0	93,0

3.2 Structural setting

This subchapter is divided into two parts. In the first part an overview will be given of the regional structural setting whereas the second part will focus on the local setting.

3.2.1 Regional structural setting

The structural geological history of the SPB plays an important role in the occurrence of fault- and fracture patterns in this area. Two major phases can be described that have shaped the basin as it is today;

- i. The Mesozoic rifting and breakup of Pangaea (260 to 220 million years ago)
- ii. Cenozoic subsidence and presence/absence of the Zechstein salt (65 million year ago until present day)

Mesozoic rifting and breakup of Pangaea

During Late Permian to Mid-Triassic times, the development of the Northern and Southern Permian basins was controlled by thermal subsidence. Development of the Arctic-North Atlantic rift system between Greenland and Scandinavia had commenced in the Late Carboniferous. This rift system propagated southwards during Late Permian and Early Triassic times as rifting intensified. This resulted in the development of the Viking and Central grabens that propagated into the North Sea as well as the North Atlantic domain (Ziegler, 1990). The different grabens and basins during the Early Triassic are shown in Figure 14.

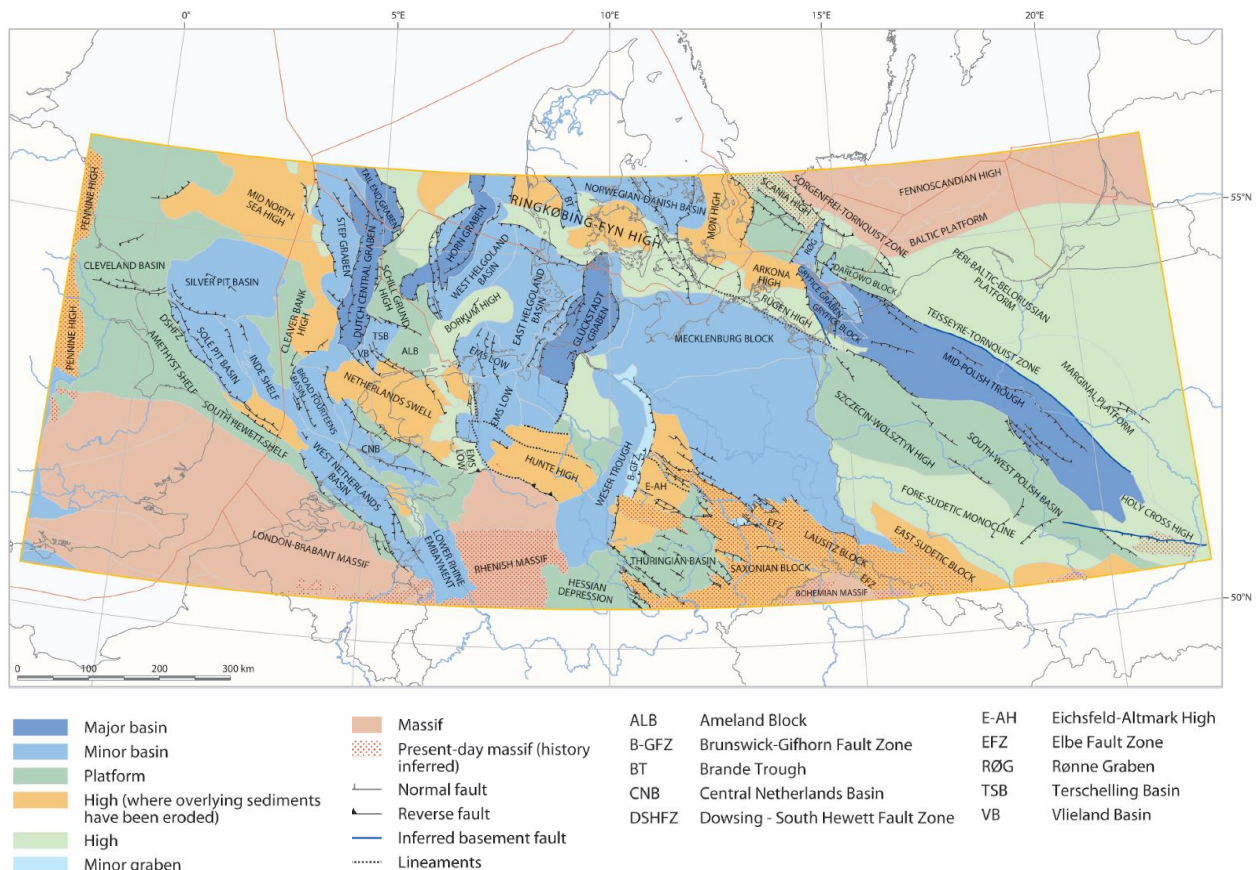


Figure 14 – Early Triassic tectonic evolution, indicating the basins and grabens present at that time (Doornenbal & Stevenson, 2010)

From Middle to Late-Triassic, the marine depositional environment of the SPB became shallower, resulting in a transition from marine into continental, fluvial and lacustrine deposits. This shallowing upward sequence was the result of far-field compressional stresses resulting in a lower subsidence rate, due to a collision between Pangaea (N) and the Cimmerian terranes (S), caused by north-ward subduction and eventually disappearing of the Paleo-Tethys Ocean (Stampfli et al., 2002). During the Late Triassic, the Arctic-North Atlantic rift propagated southwards into the Central Atlantic domain where crustal separation was achieved towards the end of the Early Jurassic. This resulted in activity in the underlying Zechstein salt deposits, resulting in salt movement along the faults in the grabens (Maystrenko et al., 2006). Mid-Jurassic crustal separation and opening of the Alpine Tethys Ocean entailed a reorientation of the stress field of north-west Europe. The Horn and Glückstadt grabens became inactive during Mid-Jurassic uplift of a large thermal dome straddling the Central Graben (Ziegler 1990). For the Netherlands this change in regimes meant that the structural outline progressively started to change from the single, extensive Southern Permian Basin (SPB), into a more complicated pattern of smaller, fault-bounded basins and highs. During the Late Jurassic to Early Cretaceous, accelerated crustal extension across the North Sea rift system caused north-west-trending trans-tensional basins to develop along the southern margin of the SPB, large areas of which became exposed and subjected to erosion (Herngreen et al., 2003). Three interactive structural provinces could be distinguished by the end of the Jurassic (Wong, 2007):

1. NW-SE block-faulted basin system through the Netherlands connecting the Roer Valley Graben, West Netherlands Basin, Central Netherlands Basin and Broad Fourteens Basin,
2. the E-W oriented, Lower Saxony Basin system (previous N-S oriented, Ems Low) extending into Germany, and
3. the N-S oriented Dutch Central Graben-Vlieland Basin system.

Following a period of intense Early Cretaceous rifting, the North Atlantic Ocean started to open during mid-Cretaceous times, whereas the North Sea rift system became inactive and rifting activity concentrated on areas between Europe and Greenland (Ziegler, 1990). Due to this rifting the Zechstein salt was mobilized again causing local subsidence. Meanwhile, the Tethys Ocean was opening to the south of Europe.

Cenozoic subsidence and influences of the Zechstein salt

During the Cenozoic, the Netherlands was incorporated into a large epicontinental, continuously subsiding, basin of north-south orientation (Wong, 2007), that developed in response to the gradual cooling of the impinged Aalenian mantle plume. At the onset of the Paleocene (Early Tertiary), a second, more intense, phase of inversion tectonics took place, the Laramide pulse. It marked the end of a carbonate dominated depositional regime that was initiated during the Late Cretaceous and gave way to siliclastic deposition (Pharaoh 2010). The inversion resulted in significant erosion down to Jurassic deposits of the West Netherlands, Central Netherlands and Broad Fourteens basins as well as the Dutch Central Graben (de Jager, 2007). A third inversion pulse, the Pyrenean pulse, took place at the end of the Eocene resulting in uplift of the West and Central Netherlands basins. In the Broad Fourteens Basin towards the north-west, the amplitude of uplift decreased sharply (de Jager, 2007). The inversion caused uplift was without fault reactivation. However, relaxation of the stress regime at the end of the Pyrenean pulse resulted in localized normal reactivation of faults (Pharaoh 2010). At the end of the Oligocene a last pulse of inversion tectonics occurred (Savani) affecting mainly the Sole Pit Basin. No significant inversion has been demonstrated at that time in the Netherlands (de Jager, 2007).

The presence or absence of Zechstein salt played an important role in the development and final architecture of the inverted basins (Doornenbal & Stevenson, 2010). Basins with no or little Zechstein salt occurrence were dominated by reverse reactivated faults in Jurassic and Cretaceous strata forming prominent ridges of flower structures (e.g. West Netherlands Basin), whereas basins with thick Zechstein salt occurrence (e.g. Dutch Central Graben), faults were entirely detached along the top of the Zechstein, resulting in a detachment plane along which broad uplift of post-salt strata could occur (Pharaoh et al., 2010).

At the onset of the Miocene inversion had ceased and gave way to a period of relative low tectonic activity, with regional subsidence lasting till recent times. Much of the North Sea area still subsides, however the south-eastern part of the Netherlands rises in conjunction with uplift of the Rhenish Massif (de Jager, 2007).

3.2.2 Local structural setting

The thickness of the layers vary throughout the HBF. These variations are related to tectonics because the changes in thickness distribution are abrupt and extensive, a sedimentary origin is therefore excluded (Geowulf Laboratories, 2011). By means of evaluating the gamma ray logs and correlating the stratigraphic boundaries of all lithological units, Geowulf Laboratories has constructed a geological model which includes the locations of the major faults.

The main structural elements are shown in Figure 15. The main fault zones are NW-SE oriented. This orientation is also valid for the Boekelo fault zone, which is located in the HBF.

In 2012 a subsequent study has been conducted (van der Kroef, 2012) in which the locations of the faults have been further researched. The field has been divided into four characteristic sub-areas in which different structural geological events have occurred:

- Area 1: The northern and north-western part of the HBF
- Area 2: The central and eastern part of the HBF
- Area 3: The southern and south-eastern part of the HBF
- Area 4: Ganzebos section in the south-western part of the HBF

A map is shown in Figure 16 in which the areas are indicated. It can be noticed that the 4 areas have been divided further into 7 sub-areas in total. There are also two major fault zones present close to the HBF. The Gronau fault zone is located approximately 15km NE of the HBF. The Boekelo fault zone divides area 4 (i.e. Ganzebos) from the other areas.

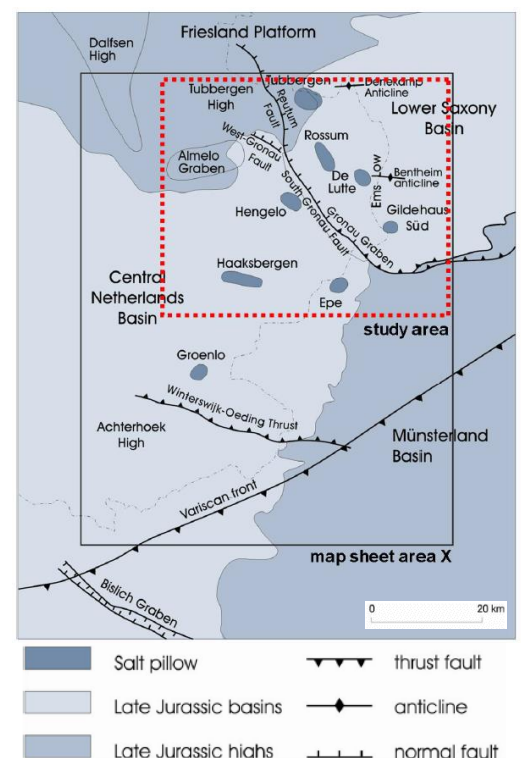


Figure 15 - Overview of the main structural elements in the HBF (NITG-TNO, 1998)

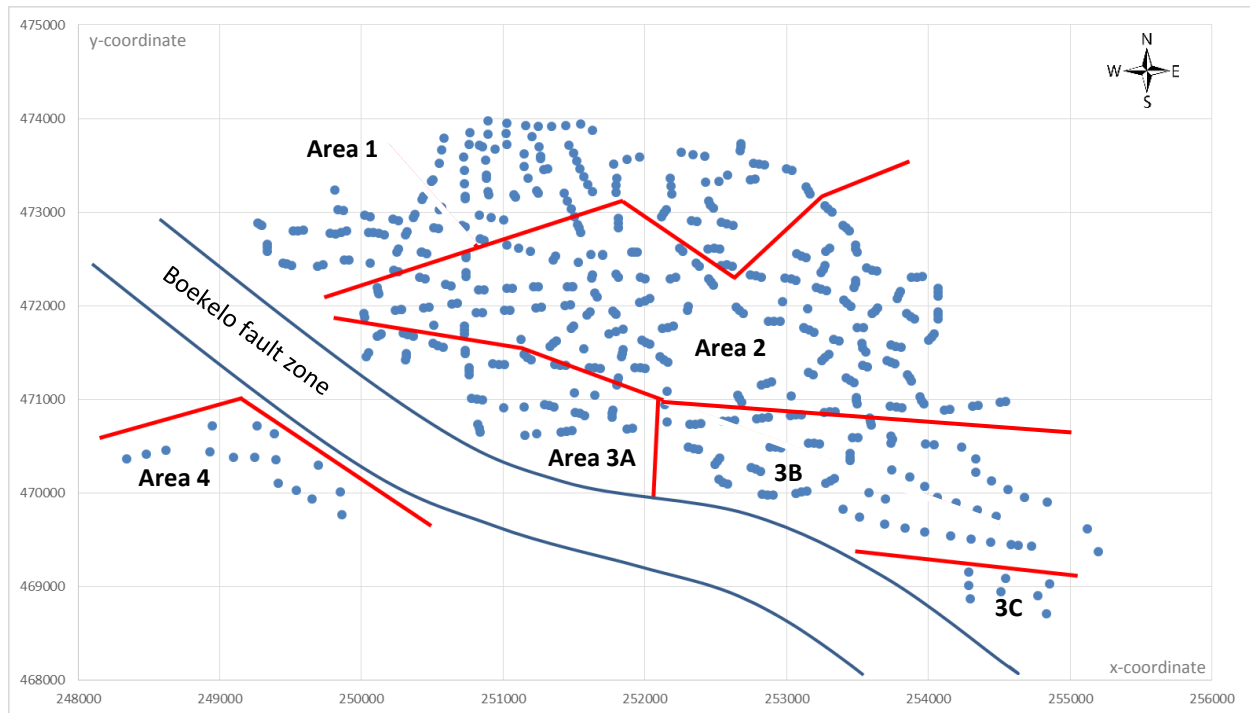


Figure 16 – The HBF has been divided in multiple areas. As indicated in the figure, the Boekelo fault zone is NW-SE oriented.

Gronau fault system

In the eastern part of the Netherlands a system of WNW-ESE trending faults was active during Triassic times, of which the major Gronau fault system is one of the largest faults. This zone consists of three separate branches of which the so-called South Gronau Fault is located just a few km's north of the HBF. During the Early Kimmerian phase, this fault was reactivated under influence of an extensional regime, during which many new individual faults were formed. Salt accumulation occurred, especially along this South Gronau Fault. During the Late Kimmerian tectonic phases the main tectonic elements in the Dutch subsurface, mainly former NW-SE faults, were reactivated. Also the Gronau Fault Zone, located at the transition from the Central Netherlands Basin in the West and the Lower Saxony Basin in the East was reactivated. This fault zone mainly showed normal faulting, but also dextral strike-slip faulting and growth-faulting took place (syn-sedimentary faulting). During Late Cretaceous and Early Tertiary the Gronau Fault Zone was reactivated again by extensional tectonic phases. Inversion led to thrust faulting. Which type of structural style was active in the Gronau fault zone is difficult to say and may differ strongly from place to place, depending on the local presence and thickness Zechstein salt deposits (MWH, 2010)

Boekelo fault zone

The WNW-ESE orientated Boekelo Fault Zone is a major geological structure which crosses the HBF and separates Area 4 from the other areas (see Figure 16). It is believed that this fault zone formed a separate branch of the Gronau fault system. This implies that the same fault processes may have been active in the Boekelo fault zone. The fault has been analyzed in detail by MWH (2011). The following four tectonic situations have probably influenced the Boekelo fault zone:

- During Early and Late Kimmerian two extensional regimes were active, both during and after the deposition of the Röt salt. Possibly dextral strike slip-, normal- and growth-faulting in combination with the movement of the Zechstein salt occurred.
- A switch from the extensional to compressional regime during Late Cretaceous ensured the reactivation and inversion of faults, causing thrust faulting and the formation of some flower structures.
- The last tectonic situation included an extensional regime once again, during which subsidence occurred throughout the area.

Area 1: The northern and north-western part of the HBF

This area is characterized by a depression and complex system of faults. According to van der Kroef (2012), the minor and abrupt thickness changes in the formations of interest in the downthrown blocks are caused by these faults. Therefore these faults must have been active during sedimentary deposition in the form of growth faults. The strike of the faults in area 1 is WSW – ENE in general, but locally, small NW – SE and NNW – SSE faults are found (Geowulf Laboratories, 2011). The structural dip is 0.7 – 0.8m / 10m towards the SW for the Triassic strata. Furthermore the differences in thickness of the lithological bodies in the up- and downthrown blocks suggest that the faults have originated as growth faults as well, but that they were later on inverted due to the compressional tectonic event which occurred from Late Cretaceous until Early Tertiary (van der Kroef, 2012).

Area 2: The central and eastern part of the HBF

The central part of the HBF is largely tectonically undisturbed. The offset is relatively low compared to the other areas, whereas no relative movement between the northeastern and southwestern sides is observed at the Röt level (MWH, 2010). Due to this low disturbance the thickness of the salt in this area is likely to be the original stratigraphic thickness, with an average of around 70m (Geowulf Laboratories, 2011). The dip of the lithological Triassic units is rather uniform, approximately 0.6m / 10m towards the SW.

Area 3: The southern and south-eastern part of the HBF

This area is characterized by severe faulting which is related to the Boekelo fault zone. Salt thicknesses vary considerably as a result of flow across faults, both towards high ranges as towards low ranges. The area is subdivided into three parts; 3A, 3B & 3C. The two parts are separated by a N-S fault, situated just west of the wells B440, B441 & B442. The Boekelo fault zone has a WNW-ESE orientation and forms the southern boundary for both areas. This fault zone is a system of multiple parallel WNW-ESE faults with throws towards the SW. This has resulted in multiple N-S oriented faults as well. In area 3A the dip of the Triassic strata is estimated to be in the order of 0.6 - 0.8m / 10m towards the southwest. In area 3B Early Kimmerian faults are recognized by the occurrence of differentially preserved sections of the Muschelkalk Fm. below sections of the Sleen Fm., located between wells B346 and B348. In area 3B the strata is sub-horizontal to convex shaped, in the southwest a dip of approximately 0.6m / 10m is measured (Geowulf Laboratories, 2011). Area 3C is the so-called Usseleres area. In the southern part of this area three faults have been found with the same WNW-ESE orientation as mentioned above. The structural dip of this area is 0.5m / 10m towards the southwest (Geowulf Laboratories, 2014). The Main Röt Evaporite becomes significantly thinner across this area towards the Boekelo fault zone (i.e. the SSW direction).

Area 4: Ganzebos

Area 4 is located in the south-western part of the HBF. This area is called Ganzebos. The Boekelo Fault zone separates Ganzebos from the other areas. Ganzebos will be developed in the next 8 years. It is expected that many faults are present in this area, since significant displacement is observed between the Boekelo Fault zone and area 4 (M. den Hartogh, personal communication, April 2nd, 2015).

3.3 Cavern shape & geometry

As mentioned earlier (section 2.2.1.) the caverns are created in the Main Rot Evaporite (MRE). The MRE consists mostly of halite, but also contains anhydrite and anhydritic claystone. The optimal shape for SCC's, which would result in the maximal possible salt production, is a theoretical flat cylinder. This is however never the case for the caverns in the HBF due to multiple reasons:

- The sump is not cylindrical; the shape of the sump is to some extent responsible for the shape which can develop during the 1st main leaching stage.
- Speed of the leaching process; it is important to stay within certain minimum and maximum flow speeds, as described in subchapter 2.2.2.3. A lower or higher flow speed can cause interruptions in the leaching process, resulting in uneven leaching of the salt.
- The presence of insolubles; there is a certain amount of insolubles present in the salt. As the word already implies, these insolubles do not dissolve when water is injected into the cavern. When salt from the center of the cavern is leached, the insolubles present in this part of the cavern will sink to the bottom, and fill up the sump. At the walls this process is more complicated. The insolubles can occur in layers, which form strong components. It is therefore possible that pieces consisting of insoluble material are sticking into the cavern from the walls. This results in an irregular cavern wall. These insolubles can also form stalactites. This phenomena is clearly visible in Figure 17. This figure shows screenshots from a visual inspection which was carried out in December 2014. When the stalactites break off and sink to the bottom, 'stalagmites' can be formed. This was also observed when the camera was lowered to the bottom of the cavern. Appendix C has more images of the cavern.

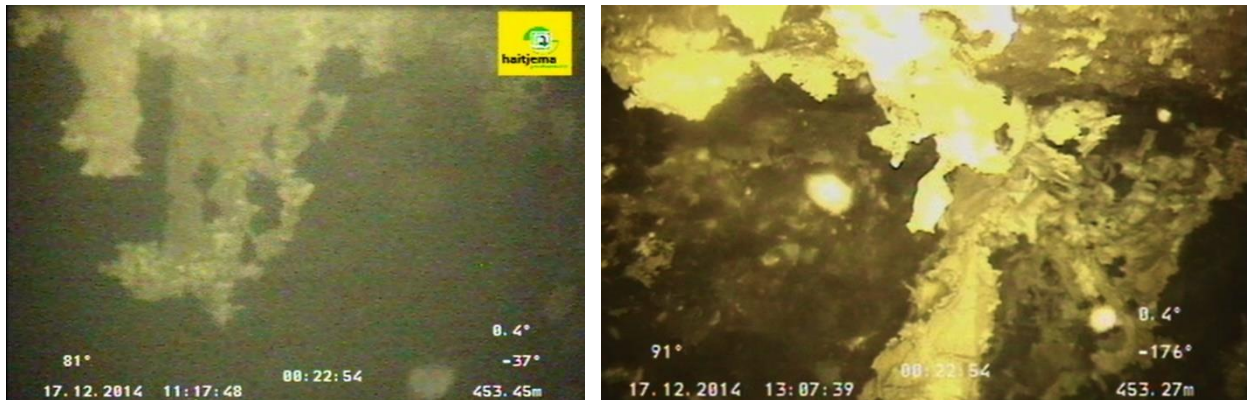


Figure 17 – Pictures from the visual inspection of caverns 382 (left) and 383 (right). The stalactites, consisting of insolubles, are clearly visible.

Figure 18 shows an actual cavern. The model is based on combined sonar measurements. The different stages are clearly visible. Whereas MLS-1 has been completed for this cavern, MLS-2 is currently developed in this cavern. From both the side- and top view many irregularities can be noticed. These are caused by the insolubles and capability of the sonar tool, which is discussed in chapter 7.

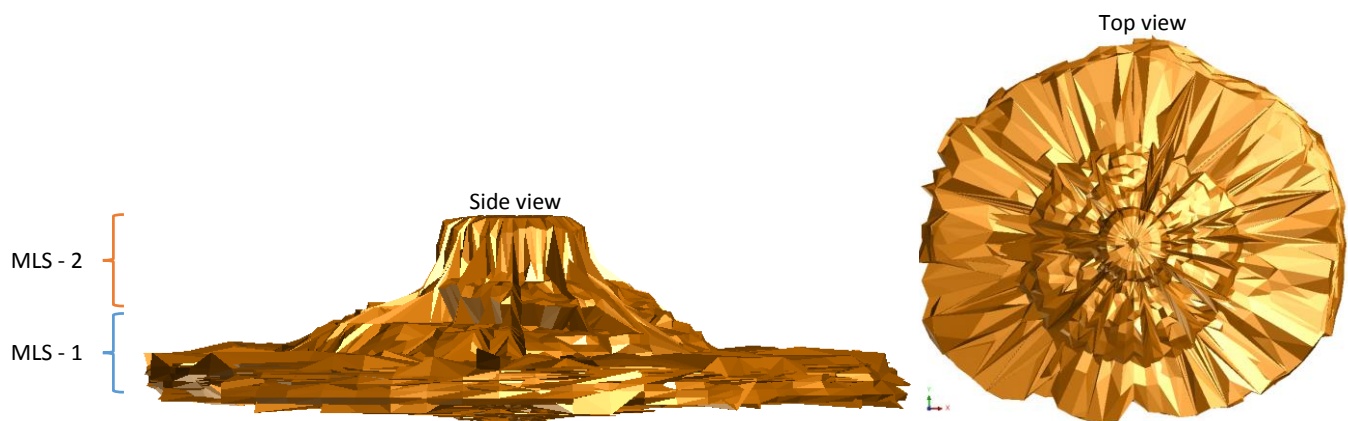


Figure 18 – Representation of an actual cavern; based on multiple sonar measurements.

3.4 Hydrogeology

The subsurface of the Twente area can be subdivided in two domains from a hydrogeological perspective: the permeable aquifers in the sandy deposits above the hydrogeological base and the generally less permeable deposits below the hydrogeological base. This chapter describes the hydraulic properties and the relation between hydrogeology and faults.

The main parameters are the porosity and permeability. The total porosity is the sum of the total connected and unconnected pore volumes and is defined as the part of rock that contains void space, expressed as a percentage or fraction. Most important properties that affect the porosity of a specific rock or sediment type are the particle shape and arrangement of the particles (Domenico & Schwartz, 2008). However, the porosity also depends on a host of diagenetic features that have affected the rock since deposition. Compaction of rocks and sediments due to the weight of the overburden contributes to reduction of the porosity from some initial higher value.

The permeability is the main parameter for possible fluid transport through the subsurface. As a rule of thumb, the permeability of sandy deposits and sandstone is higher than that of silt, followed by limestone, clay and claystone, and finally evaporites like salt and anhydrite (Bear, 1972). This means that liquids flow faster through sandstone than through the other types of deposits.

No general assumption can be made on the porosity and permeability of fault zones. It is assumed that the permeability of permeable faults is several orders in magnitude higher than that of the surrounding host rock. Faults can form preferential pathways between aquifers at different depths over vertical distances of several hundreds of meters (that are otherwise separated by confining units) when fault permeability is strongly anisotropic. This has important implications for the assessment of the connection between caverns through the Solling Fm. and/or for fluid loss into the Solling Fm.

4. Mass balance

The mass balance is important for solution mining. By accounting for material entering and leaving a system (i.e. a cavern), mass flows can be identified and quantified. The exact conservation law used in the analysis of the system depends on the context of the problem, but mass conservation is always applicable, material cannot just disappear or be created. Figure 19 indicates the mass balances present in the field. This chapter will focus on both the balances of the entire brine field and the mass balance for individual caverns.

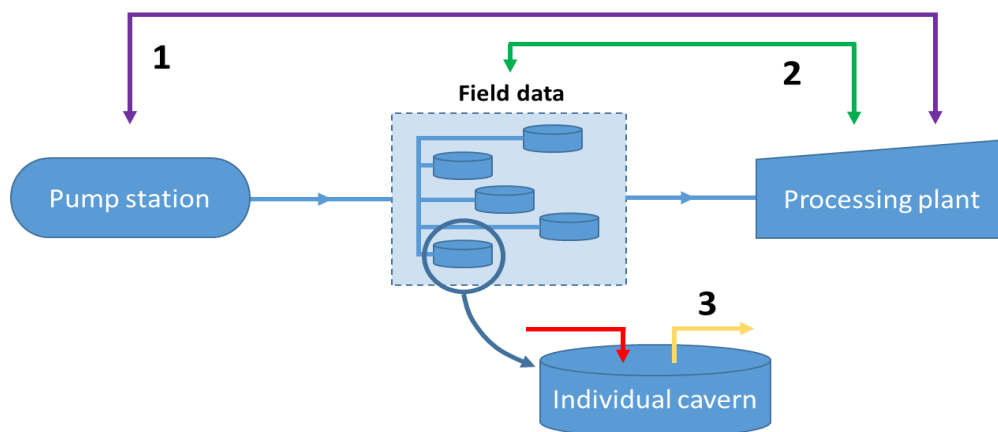


Figure 19 – Mass balances in the field. 1&2 are the balances which can be established between the processing plant and the pump station and/or field data, whereas 3 indicates the mass balance for individual caverns.

4.1 Theoretical mass balance

First of all a theoretical mass balance can be determined for the solution mining process. In order to regulate the efficiency of the production process a few parameters are of importance:

- Water is used as the solvent for the salt
- A certain mining/flow rate is in place
- Dissolved salt and water stay behind in the cavern

The water that stays behind in the cavern is referred to as “accumulation water”. In order to establish the amount of accumulation water, the flow rate into the cavern should be known, this is in turn a function of the amount of accumulation of water. This circular reasoning can be solved by the derivation of a system of algebraic equations (McEwan & Ramey, 2010) which results in the theoretical mass balance. This mass balance can then be compared with a mass balance determined from measurements at individual caverns, but also with measurements covering the entire field. This will provide the uncertainty of the mass balance closure. When the physical theoretical value deviates more than expected from the field observations, the caverns are either gaining or losing fluids.

4.1.1 Mass balance equation

In order to write the equations, the in- and outlet variables should be established first:

Well inlet

M_1 = Mass flow rate (kg/hr)

V_1 = Volume flow rate (m^3/hr)

ρ_1 = Density (kg/m^3)

C_1 = Mineral concentration wt%/100 (this is usually zero when there is no mining solvent recycle, however in this case there might be a brackish water flow towards the field with a certain concentration higher than zero).

Well outlet

ρ_2 = Density outflowing brine (kg/m^3)

C_2 = Mineral concentration wt%/100

Unknown variables required to establish a theoretical mass balance are:

M_2 = Mass flow rate (kg/hr)

V_2 = theoretical outlet volume flow rate (m³/hr)

Z = product mining rate (kg/h)

As the salt being mined goes into solution in the cavern, the volume left by the salt is replaced by the accumulation water. This amount of accumulation corresponds to the mining rate as follows:

$$W_a = (Z / \rho_m) \cdot \rho_w \quad (1)$$

where W_a is the accumulation water mass and is normally given in kg/h, ρ_m is the density of the salt being mined, and ρ_w is the density of the accumulation water, these densities are given in kg/m³.

The described variables above are shown in Figure 20.

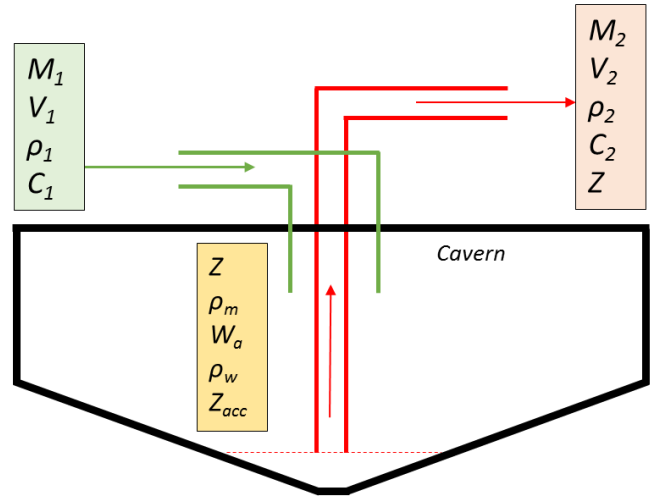


Figure 20 – Cavern showing all important variables for the theoretical mass balance equation

The total mass balance can be written as follows:

Mass out = Mass in + Mass mined – Accumulation water mass, or in equation form:

$$M_2 = M_1 + Z - (Z / \rho_m) \rho_w \quad (2)$$

The final salt production mass balance for the cavern is:

$$C_2 M_2 = C_1 M_1 + Z - C_2 (Z / \rho_m) \rho_w \quad (3)$$

In this formula (3) it is assumed that the salt concentration in the accumulated water is equal to the concentration in the outlet stream, C_2 . Furthermore the formula can only be used when only 1 mineral is being produced, which is for this case true. The formula could be expanded to solve for multiple minerals as well, but this will not be explained as it is not the case.

The mass flow rates (4 & 5) can be written in terms of volumetric flow rates:

$$M_1 = V_1 \cdot \rho_1 \quad (4)$$

$$M_2 = V_2 \cdot \rho_2 \quad (5)$$

Combining equations (4) and (5) with equations (1) and (2) gives the following:

$$V_2 \rho_2 = V_1 \rho_1 + Z - (Z / \rho_m) \rho_w \quad (6)$$

$$C_2 V_2 \rho_2 = C_1 V_1 \rho_1 + Z - C_2 (Z / \rho_m) \rho_w \quad (7)$$

Since V_2 is unknown, the equations are solved to make it independent of V_2 , first equation (6) is rewritten:

$$V_2 = (V_1 \rho_1 + Z - (Z / \rho_m) \rho_w) / \rho_2 \quad (8)$$

Equation (8) is subsequently substituted in equation (7) which results in equation (9):

$$C_2 (V_1 \rho_1 + Z - (Z / \rho_m) \rho_w) = C_1 V_1 \rho_1 + Z - C_2 (Z / \rho_m) \rho_w \quad (9)$$

When solving for the mining rate (i.e. Z), it becomes clear that Z is only dependent on ingoing mass and the in- and outgoing concentrations of the flows:

$$C_2 V_1 \rho_1 + C_2 Z - C_2 (Z / \rho_m) \rho_w = C_1 V_1 \rho_1 + Z - C_2 (Z / \rho_m) \rho_w \rightarrow C_2 V_1 \rho_1 + C_2 Z = C_1 V_1 \rho_1 + Z \quad (10)$$

$$(C_2 - 1) Z = (C_1 - C_2) V_1 \rho_1 \quad (11)$$

which results in:

$$Z = [(C_1 - C_2) / (C_2 - 1)] V_1 \rho_1 \quad \text{or} \quad Z = [(C_1 - C_2) / (C_2 - 1)] M_1 \quad (12)$$

The theoretical outflow rate can be determined after combining equations (8) and (12)

$$V_2 = (V_1 \rho_1 + [(C_1 - C_2) / (C_2 - 1)] V_1 \rho_1 - [(C_1 - C_2) / (C_2 - 1) \rho_m] V_1 \rho_1 / \rho_w) / \rho_2$$

$$\rightarrow V_2 = V_1 \cdot \frac{\rho_1}{\rho_2} \left[1 + (C_1 - C_2) / (C_2 - 1) - (C_1 - C_2) / (C_2 - 1) \rho_w / \rho_m \right] \quad (13)$$

When assuming that the density of the accumulation water left in the well, ρ_w , is equal to the density at the outlet, ρ_2 , equation (13) can be rewritten to:

$$V_2 = V_1 \cdot \frac{\rho_1}{\rho_2} \left[1 + \frac{(C_1 - C_2)}{(C_2 - 1)} (1 - \rho_2 / \rho_m) \right] \quad (14)$$

Since all parameters in equation (14) are known, the theoretical outlet flow rate can be determined.

At last, the net mining/production rate, defined as the total mineral mass (i.e. salt) leaving the well minus the mass going in (which is practically zero), can be determined using equation (15) below:

$$Z_{net} = C_2 V_2 \rho_2 - C_1 V_1 \rho_1 \quad (15)$$

The accumulated mineral in the cavern is the difference between the mining/production rate and the net mining/production rate, which can be written as:

$$Z_{acc.} = Z - Z_{net} \quad (16)$$

4.1.2 Theoretical results for the HBF

The formulas derived can be used to determine the theoretical values for the HBF. For the solution mining process at the HBF the following parameters are known (H. Leusink, personal communication, April 16, 2015):

$$V_1 = 15-40 \text{ m}^3/\text{hr}$$

$$\rho_1 = \pm 998 \text{ kg/m}^3$$

$$C_1 = 0$$

$$\rho_2 = \pm 1201 \text{ kg/m}^3$$

$$C_2 = \pm 26\% \quad (312 \text{ kg/m}^3 \text{ salt in } 1201 \text{ kg/m}^3 \text{ brine})$$

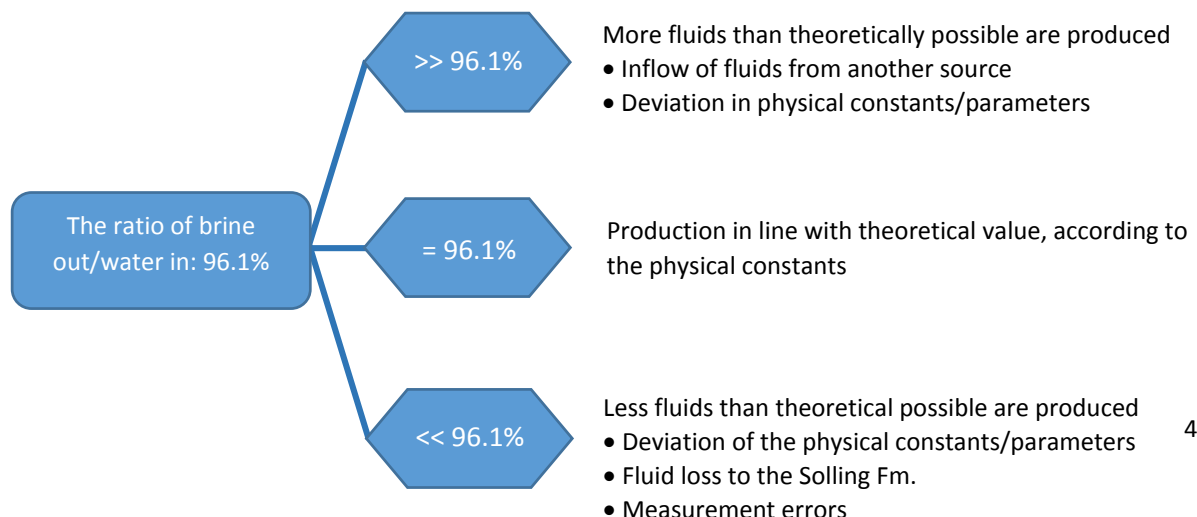
From these parameters the theoretical outflow rate can be calculated:

$$V_1 = 20 \text{ m}^3/\text{h}, \quad V_2 = 20 \cdot \frac{998}{1201} \left[1 + \frac{(0 - 0,26)}{(0,26 - 1)} (1 - 1201 / 2165) \right] = 19.2 \text{ m}^3/\text{h}$$

This results in a theoretical inflow/outflow ratio of: 96.1%

4.1.3 Mass balance hypothesis

With the theoretical value known, it is expected that when 1 m³ of water is injected, 0.96 m³ of brine is expected to be produced from a certain cavern. Over the whole field it can be stated that for every m³ of water sent to the field, 0.96 m³ brine should be measured at the raw brine tanks in the processing plant.



4.2 *Mass balance according to plant and field data*

Flow is measured at different locations in the system. These are indicated in Figure 21. The main pump station is the first measuring point, flow is continuously measured. The pump station pumps water from 4 flows to the field (2 flows with mixing water, 1 brackish water flow and 1 concentrate purge flow).

The second point where flow is measured is in the field. Each individual cavern has an analog flow meter installed on the water inlet. These are monitored on a weekly basis. From the outlet flow, only the concentration is measured, the total amount of brine is not being measured. After leaving the cavern the brine is redirected back to the processing plant and enters it at the 2 raw brine tanks. The incoming brine flow is measured on a continuous basis. As indicated by the numbers 1 and 2 in Figure 19, a mass balance can be established between the pump station and the 'processing plant' (i.e. the flow measured at both raw brine tanks) and between the caverns and the 'processing plant'.

From the raw brine tanks the brine is pumped with a continuous flow into the processing plant where it is processed to salt. In the plant different waste flows are monitored (Figure 22). The final salt product is weighed and used for different product purposes. The mass balances can therefore be determined for both flow as well as for the total amount of salt, since the concentration is measured and the final salt production is weighed.

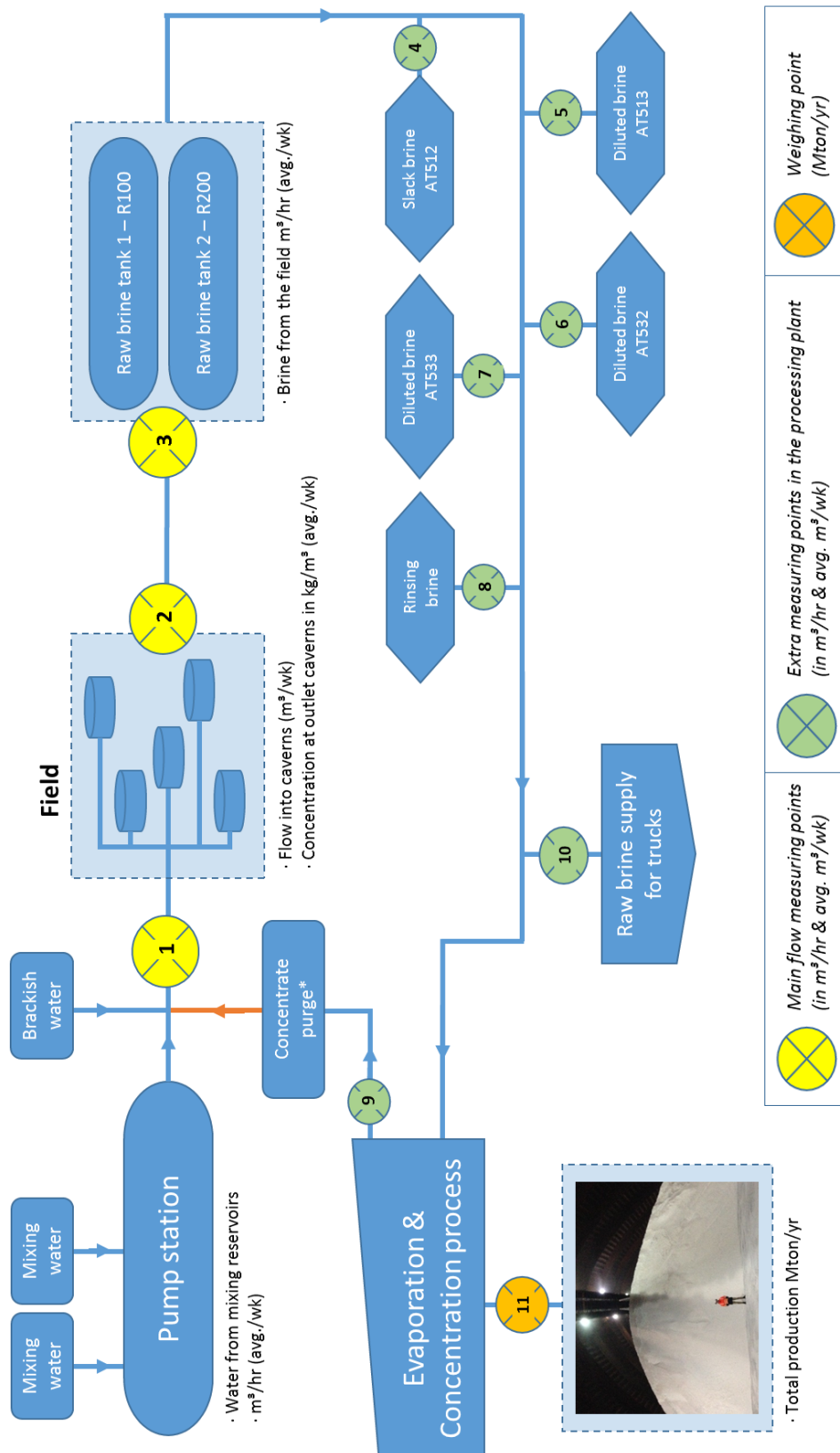


Figure 21 – Overview of the measuring points in the field and processing plant. The yellow measuring points indicate main flow meters, used for the brine out/water in ratios (1: Flow from the pump station, 2: Flow at producing caverns, 3: Flow measured at the raw brine tanks). The green measuring points indicate the flow meters in the processing plant, these flows are mainly waste flows. At the orange measuring point the salt is weighted. The slurry to caverns and recycle brine flow are excluded.

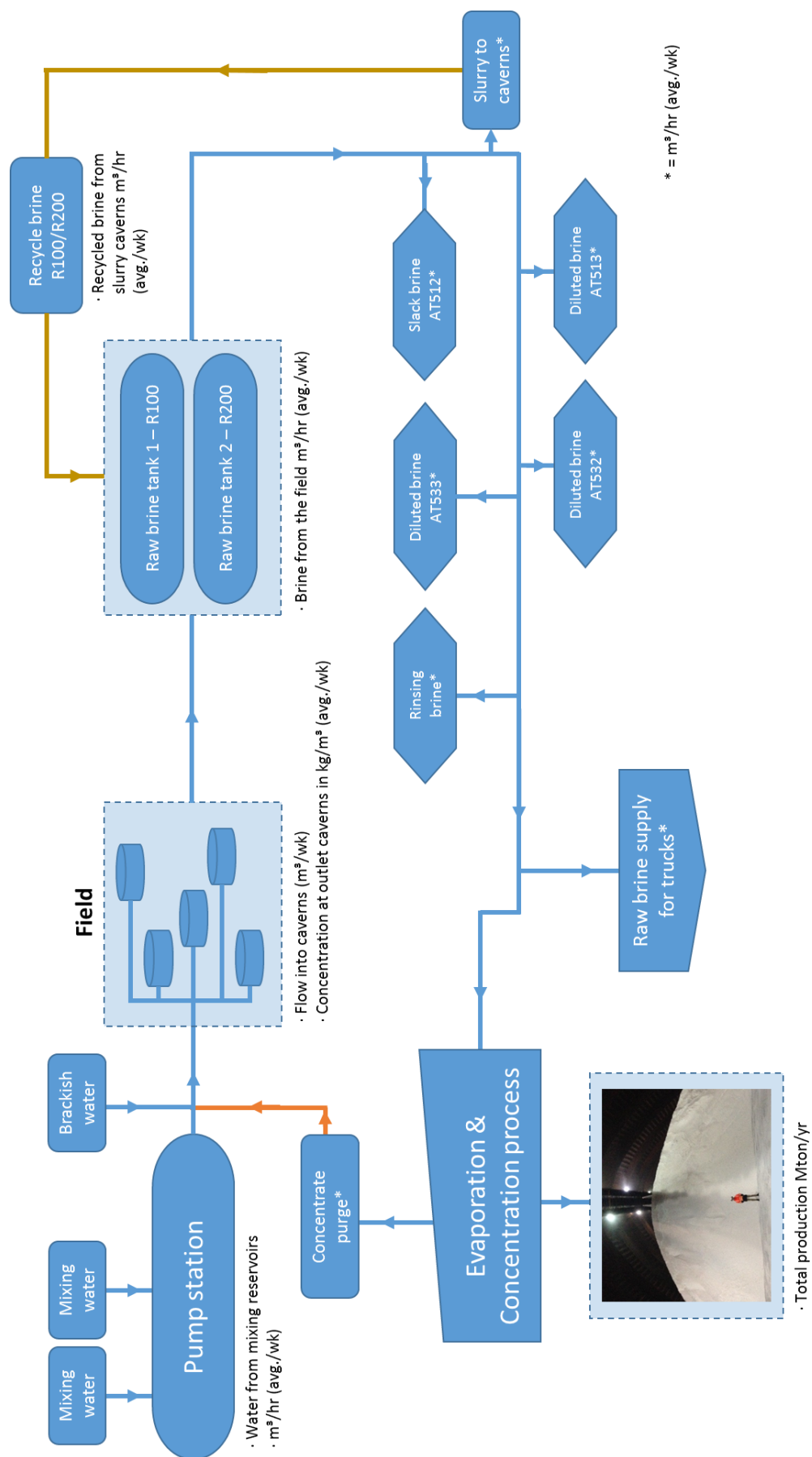


Figure 22 - Overview of the field and processing plant. Different flows with water are pumped to the field, brine comes back to the plant through the raw brine tanks. From the tanks it continues into the processing facility.

4.2.1 Flow data

The flow at the pump station and raw brine tanks is monitored and stored in the PHD-database. Data from the PHD-database is available from 2006. Figure 23 shows average flows for the flow to the field and brine to the processing plant. When analyzing the data, which is averaged in m^3/h per month, it becomes clear that something happened in November 2009 (indicated by the red line). Before this date considerably more brine was measured than water which was sent to the field. This is impossible. It is assumed that new meters were installed or recalibrated in 2009, after which the data shows a plausible relationship. Therefore only data from November 2009 and later is used (indicated by the red dotted line in Figure 23).

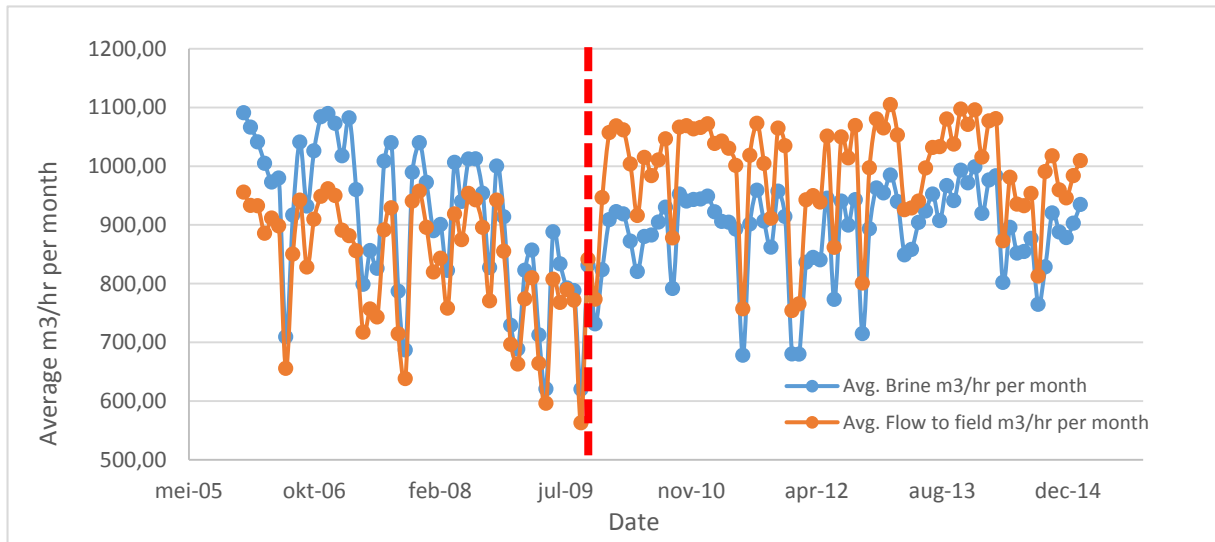


Figure 23 - This graph shows the average water and brine flow (m^3/h) per month.

Figure 24 shows the flow data after recalculating the data from Figure 23 to yearly volumes and combining it with the flow measured at producing caverns. It is important to note that only producing caverns are taken into account. Caverns which are in the saturation phase are not added to the total.

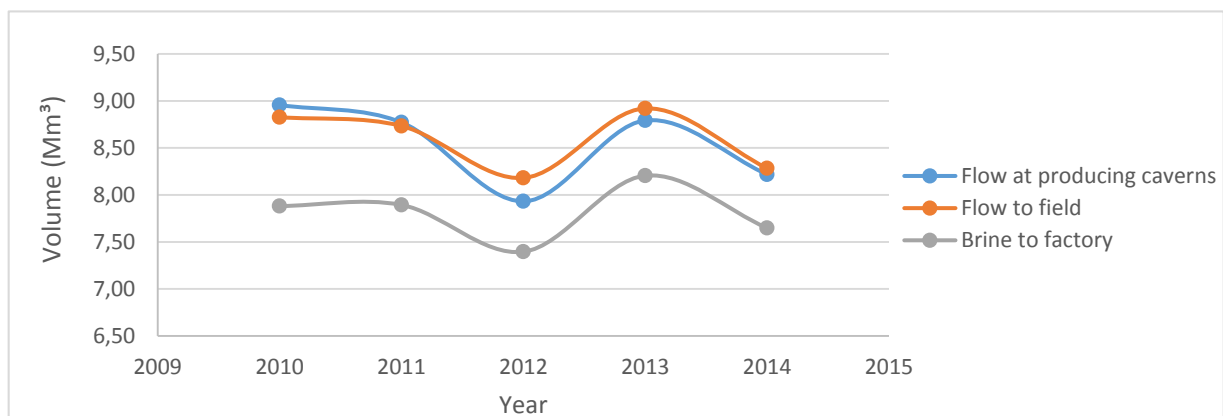


Figure 24 - The graph is showing the total amount of flow measured per year.

As expected the volumes from the water to the field and water measured at the caverns are reasonably close to each other (Figure 24), whereas the brine which is measured in the raw brine tanks shows a lower volume.

When comparing the total amount of water pumped to the field with amount of brine which enters the processing plant, a relationship can be established. From the theoretical mass balance it is known that 0.96m^3 of brine can be recovered when injecting 1 m^3 of water. Figure 25 shows the ratios between the brine and water per month and per year.

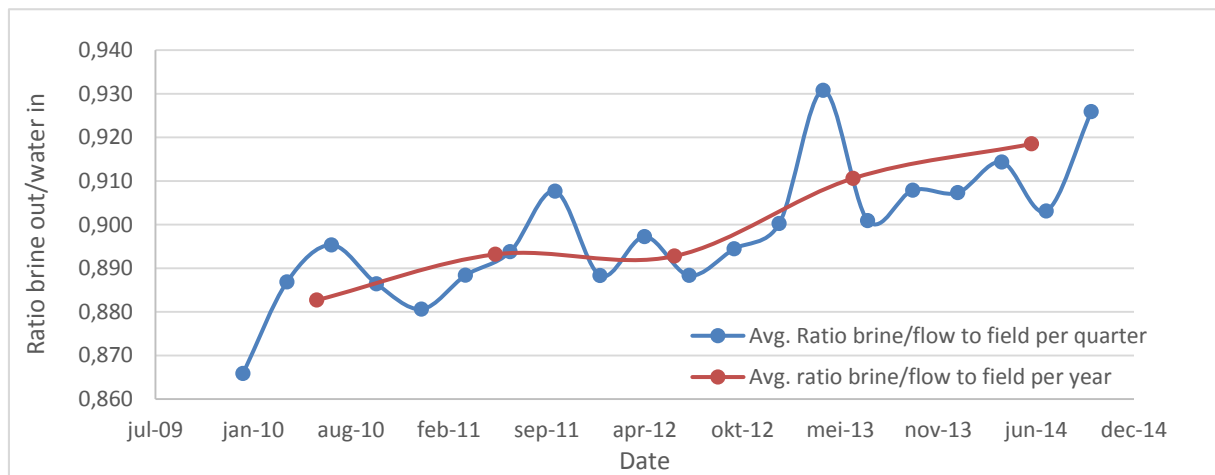


Figure 25 – Relationship between brine and water based on data from the main pump station and raw brine tanks.

From these relationships it is clearly visible that the ratio brine/water is considerably lower than the theoretical 0.96. When analyzing the data averaged per month it can be noticed that the ratio varies between a minimum of 0.87 and maximum of 0.93. The data is more or less normal distributed, as indicated by Figure 26. The average value is approximately 0.90. The yearly averages show a clear linear increase from 2010 to 2013, whereas from 2013 to 2014 it levels off to a constant ratio of about 0.915. Comparing this value with the theoretical value gives a deviation of 4.5%. For 2014 this indicates that $3.7 \cdot 10^5 \text{ m}^3$ is not accounted for.

When comparing the flow measured at the producing caverns with the recovered brine, the ratio is slightly higher with an average ratio of 0.93. This would suggest a deviation of 3%, which translates into an unaccounted volume of $2.5 \cdot 10^5 \text{ m}^3$.

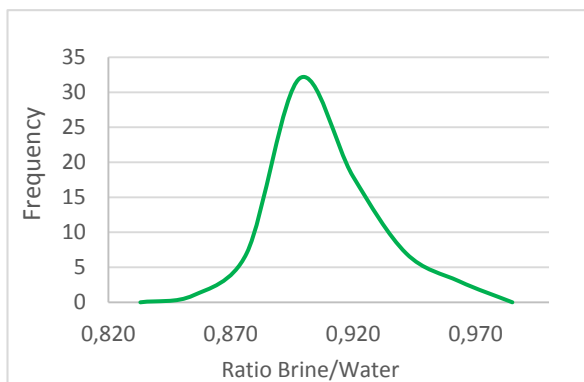


Figure 26 – Distribution of the brine/water ratios based on pump station- and raw brine tank data

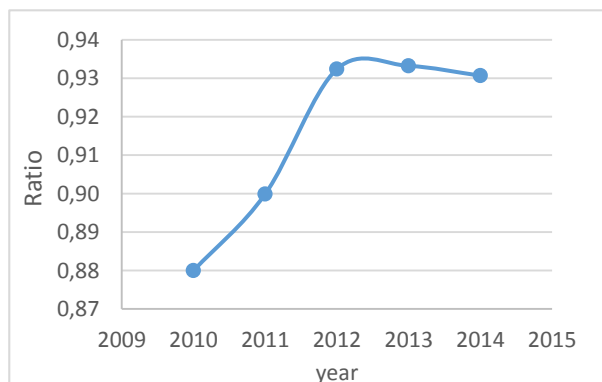


Figure 27 – Relationship between the flows measured at producing caverns and the brine in the brine tanks

From Figure 25 & 25, it can be concluded that the brine/water ratios have been improved over the past few years. This could be attributed to the fact that the multiple completion caverns (MCC's) have been gradually replaced by SCC's which are more reliable in estimated production volumes than the older MCC's.

4.2.2 Discussion

The indicated volume loss in the system can be explained by the following factors:

- Pressure built up in the caverns
- Brine concentration
- Infrastructure & Operations in the field
- Measurement errors in the flow meters
- Loss to Soling & Connection between caverns

Pressure built up in the caverns

The caverns are operated at a certain overpressure. The pressure at the water inflow is approximately 17 bar, whereas the pressure at the brine outlet is approximately 5 bar (Figure 28). This results in an overpressure of about 5 bar in the cavern.

$$A: p_{water} = \rho_{water} \cdot h_{water\ outlet} \cdot g + p_{water\ at\ surface} \quad (17)$$

$$B: p_{brine} = \rho_{brine} \cdot h_{brine\ inlet} \cdot g \quad (18)$$

with $\rho_{water} = 1000\text{ kg/m}^3$, $\rho_{brine} = 1203\text{ kg/m}^3$ results in:

$$p_{water} = 63.1\text{ bar}$$

$$p_{brine} = 56.5\text{ bar}$$

A difference of 6.6 bar is observed ($p_{water} - p_{brine}$), since the brine has an overpressure of 5 bar when leaving the cavern at the surface, the pressure at the brine inlet should at least be 61.5 bar. This results in a difference of +1.6 bar in the system, which could possibly be attributed to frictional losses

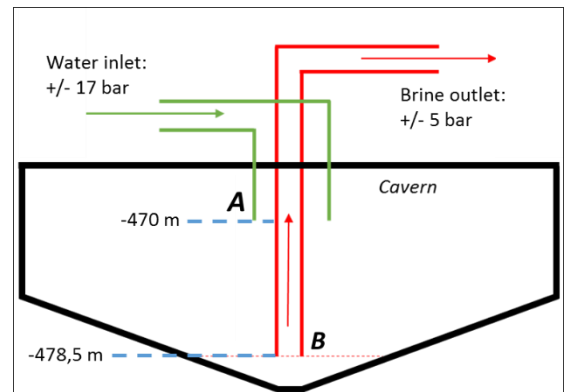


Figure 28 – Explaining pressures in a cavern

Using the compressibility factor the amount of extra fluid can be calculated to in order to create the overpressure in the cavern.

$$\Delta V = \beta_s \cdot \Delta P \cdot V_{cavern} \quad (19)$$

$$\text{with } \beta_s = \beta_c + \beta_{fluid} \quad (20)$$

Water in the liquid state is only compressible to a very small degree with a compressibility factor is $4.6 \cdot 10^{-5}\text{ bar}^{-1}$. The compressibility factor of saturated brine is even smaller, approximately $2.7 \cdot 10^{-5}\text{ bar}^{-1}$. The cavern also has however its own compressibility factor, which should be added to the water and brine factors. More information on the compressibility factors will be given in chapter 6. From field data the cavern compressibility varies between $1.6 \cdot 10^{-5}$ to $6.3 \cdot 10^{-5}\text{ bar}^{-1}$ (measured at caverns larger than $190,000\text{ m}^3$).

There is no overpressure in the cavern during a workover or other operation. When the workover is completed the water inflow is opened again. The overpressure is therefore reinstated. From the information above the volumes of water can be determined which are needed to increase the pressure in the cavern by 5 bar:

- When only water would be present in the cavern, the volume needed varies between: 62 to 109 m^3 .
- In the case only brine is present in the cavern, the volume needed varies between: 43 to 90 m^3 .

Although both cases are incorrect, since there is always a mixture of unsaturated brine present, the minimum and maximum volumes can be taken as a benchmark; only 43 to 109 m^3 is needed to increase the pressure in the cavern by 5 bar. These 'small' volumes can be neglected when comparing it with the total amount of losses on a yearly basis.

Brine concentration

The theoretical mass balance ratio of 96.1% is calculated when water (998 kg/m³) is flowing into the cavern and saturated brine (1201 kg/m³; i.e. 314 kg/m³ salt) is flowing out. When these densities are altered, the ratio changes as well. Table 4 gives the theoretical ratios which correspond to the different densities.

Table 4 – Brine water ratios according to inflow and outflow densities

ρ_1 (kg/m ³)	C_1	ρ_2 (kg/m ³)	C_2	ρ_m (kg/m ³)	In- /outflow
998	-	1201	26,1%	2165	0,962
1023	2,4%	1201	26,1%	2165	0,973
1048	4,8%	1201	26,1%	2165	0,985
998	-	1206	26,4%	2165	0,959
998	-	1196	25,9%	2165	0,965
998	-	1191	25,7%	2165	0,968
998	-	1201	26,1%	2160	0,962
998	-	1201	26,1%	2155	0,961

ρ_1 (kg/m³) = Density inflowing fluid

C_1 = mineral concentration dissolved in inflowing fluid

ρ_2 (kg/m³) = Density outflowing fluid

C_2 = mineral concentration in outflowing fluid

ρ_m (kg/m³) = density of the matrix

In- /outflow = ratio

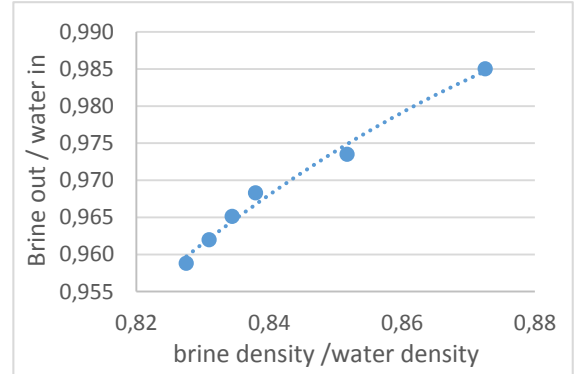


Figure 29 – Brine/water density ratio vs. the ratio between brine out/water in.

As can be noticed from the table, the theoretical ratios vary very little when the densities are changed. A 5% increase in density of the inflowing fluid, C_1 (as stated in formula 14), which is possible when the concentration of the brackish water flow increases, with normal outflowing brine, increases the ratio to 0.985. For the other cases the ratio varies around 0.96. The water, brine or halite density/concentration is therefore not responsible for the systematic lower value determined from field and plant data. This can also be concluded from Figure 29, which shows a linear relationship between the brine out / water in ratio and the ratio determined from dividing the brine density by the water density. A lower brine density, results in a lower brine out / water in ratio.

Infrastructure & Operations in the field

A large network of pipes is present in the HBF. It is estimated that the total length is more than 150 km (H. Leusink, personal communication, April 2, 2015). The network includes main pipes, which transport water to the field and brine back to the processing facility, and many branches to different groups of caverns. Pipes have not been recovered after production had ceased. A large portion of the network is therefore not active anymore. It is however possible that fluids were still present in these sections at the time of their shut off. The total volume of this particular loss is very small on a yearly average.

During different operations water is used for cleaning or other purposes. This is tapped of the main network. This water can also be seen as a loss to the system. The percentage of this loss is however very small related to the entire flow towards the field.

The main volume loss in the system, and therefore the deviation between the theoretical ratio and ratio determined from field data, should therefore be ascribed to the measurement errors in the flow meters and/or fluid loss to the Solling and connection between caverns.

Measurement errors in the flow meters

The uncertainty of the flow meters is unknown. The manufacturer indicates a maximum error of 0.25%. According to employees of AkzoNobel the uncertainty should be higher than that, especially for the flow meters at the caverns in the field. Meters in the field are likely to deviate more than the flow meters at the pump station or raw brine tanks (M. den Hartogh, personal communication, April 13, 2015). It is however remarkable to see that the raw flow data measured at the pump station is reasonably close to the flow measured at producing caverns (Figure 24).

Based on observations during tests in the field, the deviation of the flow meters could be measured. This will be explained in section 4.4.3. According to measurements the error deviates between 0.5 to 2.5% (when using the same type of flow meters at the water inlet and brine outlet). Using a conservative 5%, a study can be done for the whole field.

Figures 102, 103 and 104 in Appendix E show the results when assuming that the flow meters measure 5% less or more flow. The difference in volumes measured at the caverns and the pump station would be -0.9 to +0.8 Mm³. When the same uncertainty is applied to the ratio brine outflow over water inflow, the ratio would be reduced dramatically when 5% more water and 5% less brine is measured, whereas it would exceed 1 when the opposite is the case. These results can be found in Table 5.

Table 5 – Ratios brine inflow vs. water outflow (measured at the caverns and pump station)

Year	Ratio brine / water measured at caverns			Ratio brine / water measured at pump station		
	Average	min	max	Average	min	max
2010	0,88	0,80	0,97	0,89	0,81	0,99
2011	0,90	0,81	0,99	0,90	0,82	1,00
2012	0,93	0,84	1,03	0,90	0,82	1,00
2013	0,93	0,84	1,03	0,92	0,83	1,02
2014	0,93	0,84	1,03	0,92	0,84	1,02

It is very unlikely that the ratio exceeds 1. This would imply that more volume is coming back to the processing plant than being sent to the field. It can therefore be ruled out that the flow meters in the raw brine tank measure 5% less flow, whereas the flow meters at the caverns and pump station would give 5% higher readings. The minimum cases are unlikely as well, because the loss to in the field would be too high. To get more confidence in the values measured at the flow meters, the numbers should be compared to the mass measurements in the processing plant. The total amount of salt can be compared to the volumes of brine and related salt concentrations. This comparison will be made in section 4.3.2.

Loss to Solling & Connection between caverns

Wells are drilled into the Solling formation, in order to guarantee that the borehole covers the entire salt interval. These drilled sections into the Solling formation form a link between the salt cavern and permeable layers in the Solling. This link can cause fluid loss to the Solling. The presence of hydrological connections between salt caverns has also been determined. During pressure tests, performed on different caverns, a pressure response was measured at surrounding caverns, indicating connections between caverns. This will be further explained in chapter 5.

It is important to differentiate between a fluid loss and a fluid connection. When a connection exists between two caverns, the mass balance over the two caverns should be more or less correct. The only loss in this case is the amount of volume that fills the fluid path between the two caverns. Fluid loss is also possible if a path is created between multiple permeable rock accumulations.

It is difficult to calculate the total volume of fluid loss since the amount and distribution of permeable rock accumulations is unknown. However when assuming that the flow meters measure the correct amount of flow and the entire deviation is ascribed to flow into the Solling, 2.5 to 3.7·10⁵ m³ is lost each year (when the theoretical value of 96% is assumed to be correct). With approximately 50 active caverns, the loss per cavern would be 5·10³ to 7.4·10³ m³ per year, which is 14 to 20 m³ per day. This number is quite high. Comparing the fluid inflow data with the actual brine production might give a better estimation. This comparison can be found in section 4.4.

4.3 Mass data

The total mass of the produced salt can be estimated at different locations in the system. These masses can be compared with each other. The only actual mass weighing measurement, as indicated in Figure 24, is performed at the conveyor belts, through which the salt (i.e. the final product of the processing plant) leaves the processing plant. At the other measuring points the mass of the salt can be estimated using the amount of brine flow and the concentration of the salt in the brine.

Three masses can be estimated:

- Mass of salt at the caverns, based on water inflow and concentration of the outflowing brine (measuring point 2 in Figure 21).
- Mass of salt in the brine which arrives at the raw brine tanks (measuring point 3).
- Mass of salt at the conveyor belt (measuring point 11)

In the next sections (4.3.1 – 4.3.2) the three masses listed above will be further explained and described.

There are different flows present in the processing plant through which salt is lost (measuring points 4-10). The total amount of this salt can be calculated and either subtracted from the mass measured at the caverns and the brine flow, or added to the total amount of salt which is measured at the conveyor belt. The amount of salt which is lost in these different flows is on average 2.2% of the total salt measured in the processing plant (data from 2010 to 2014).

4.3.1 Calculating the masses

At the caverns (estimated)

As mentioned earlier two main parameters are determined at every cavern; the rate of inflowing water (m^3/h) and the concentration of the outflowing brine. Using this information the total amount of salt, which is produced from every 'producing cavern', can be estimated. There is a distinction between *producing caverns* and *saturation caverns*. Producing caverns supply brine directly to the processing plant, whereas saturation caverns don't. Caverns in their initial phase of development are called *saturation caverns*. These caverns do not have the required brine concentration yet, fluids from these caverns are therefore pumped into producing caverns.

To calculate the total amount of salt per week, data from the database was used (BPB). The amount of inflowing water (i.e. the average flow in m^3/h averaged per week for each particular cavern) is multiplied by the theoretical value of 96% (section 4.1.2) in order to calculate the total amount of brine which was theoretically produced. This amount was subsequently multiplied by the average concentration which is measured at the cavern on a weekly basis. The uncertainty regarding loss to the Solling and connection between caverns will be discussed later.

At the raw brine tank (estimated)

The total amount of salt in the brine which arrives at the processing plant (Figure 21, measuring point 3) is calculated by multiplying the total amount of flow with the standard amount of salt present in the brine (i.e. $314 \text{ kg}/\text{m}^3$). Data from the PHD-database were used.

At the conveyor belt (weighed)

Salt is produced from the brine which enters the processing plant. The final product is weighed on conveyor belts. This is a direct measurement of the total amount of salt. The uncertainty of the weighing devices is however unknown. In order to compare it with the other two estimated masses the total amount of salt in the waste- and other flows (present in the processing plant) are added to the total amount of weighed salt.

The results from the calculations are shown in Table 6.

Table 6 – Yearly amounts of salt in Mton

Year	Weighed salt (Mton)	Cavern data (Mton)	Brine data (Mton)
2010	2,55	2,69	2,48
2011	2,62	2,72	2,48
2012	2,45	2,47	2,32
2013	2,64	2,69	2,58
2014	2,48	2,55	2,40

4.3.2 Comparing the three masses

When plotting the data a clear deviation between the 3 masses is visible. This is shown in Figure 30. When assuming that the salt which is measured in the processing plant (i.e. the sum of the weighed salt at the conveyor belt plus the other flows in the plant) is the base case; it can be concluded that the salt measured at the caverns overestimates the total amount of salt, whereas the salt present in the arriving brine from the field underestimates. The salt calculated from the caverns overestimate the weighed salt on average by 3%, whereas the salt calculated from the brine in the raw brine tanks underestimates the total amount on average by 4%. It is however difficult to compare this data, since 3 different datasets/methods are used. Each method has its own uncertainties and inaccuracies.

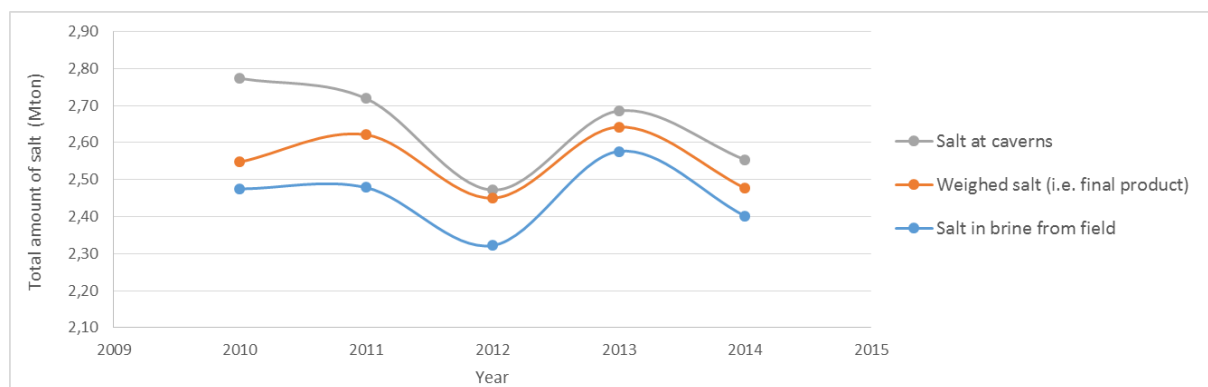


Figure 30 - Comparing the total amount of salt measured/calculated from 3 sources (caverns, brine tank & final product).

The salt calculated from the caverns is based on the theoretical value of 96% to convert the amount of inflowing water to outflowing brine. However, as indicated in chapter 5.2.1, this ratio doesn't include uncertainties such as loss to the Solling or measurement errors in the flow meters. When using the ratio which is determined in chapter 4.2.1, which is based on flow data measured at caverns and states that only 0.93m³ is recovered for every m³ of water, the deviation between the salt measured at the caverns and the weighed salt is on average only 0.3%. This can be considered as equal to each other. The deviations from the weighed amount of salt are plotted in Figure 31. In this case one can argue that this is just a coincidence, but when plotting the data the deviation seems quite constant. When neglecting the inaccuracies of the measuring devices, one can conclude that the ratio of 0.93 seems reasonably valid. Indicating a total volume loss in the order of 3% to the Solling. This will be discussed in detail in chapter 10.

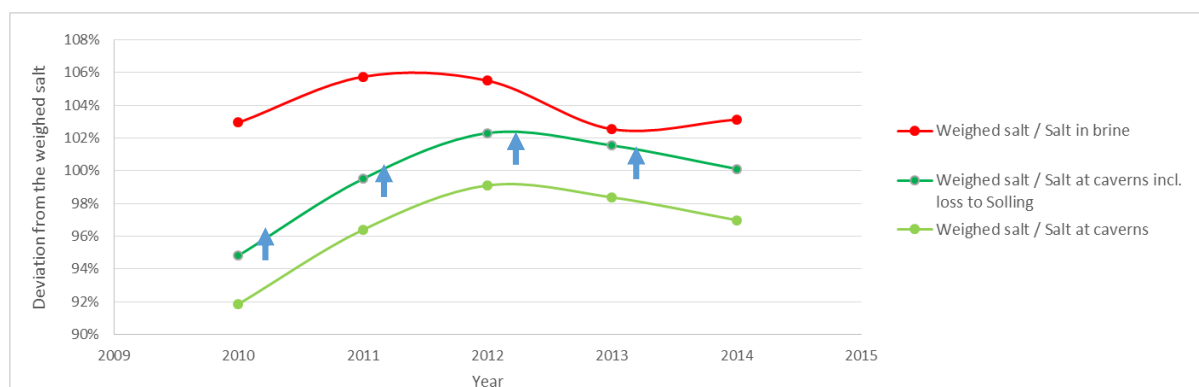


Figure 31 – Deviation between weighed salt and salt calculated at the caverns and in the brine.

4.4 Mass balance for individual caverns

The main issue with the data from the caverns is that the amount of outflowing brine is unknown since this is not measured. All data is based on the inflowing amount of water and the theoretical value for dissolving salt (i.e. halite in this case). It would therefore be interesting to conduct some tests on individual caverns, in order to measure some actual outflowing brine volumes. When measuring the flow on both the in- as outflowing pipes not only a real mass balance for individual caverns can be determined but a loss to the Solling or connection between caverns can be demonstrated as well. This subchapter will focus on the mass balance for individual caverns, the loss to the Solling and connection between caverns will be discussed in chapter 10.

4.4.1 Method

The method for determining the individual mass balance for caverns is relatively simple, as illustrated in Figure 32. Every cavern has a mechanical flow meter installed on the inflowing water pipe. During the testing period the same type of flow meter is installed on the outflowing brine side in order to measure the amounts of flow on both the inflowing and outflowing pipes. Whereas the flow meters on the inflowing side (i.e. water) are usually measuring correctly, some problems can occur regarding the flow meter which measures the outflowing brine. Due to the presence of insolubles in the cavern, small particles are produced. Particles larger than 8mm can cause clogging of the flow meter. This issue can however be solved by installing a filter or rock catcher between the wellhead and flow meter. Another minor issue is the calibration of the flow meters. The flow meters used during this test were brand new. The meters are calibrated for water by the manufacturer, which states that the meters have a maximum error of only 0.25% (this is almost negligible). Brine has a slightly higher viscosity, which can cause a minor error as well.

Once installed in the field, the meters are not calibrated again. One should therefore take into account that the meters on the water side are installed a few years ago and have already measured many of cubic meters. Therefore due to wear and tear these flow meters may have developed a measuring inaccuracy.

During the test both the total amount of flow and flow speed were monitored daily. In order to eliminate inaccuracies, such as a varying pressure regime of the pipe network and varying flow speeds, it was decided that the test should last for more than 1 month. In the next subchapter the field test setup will be described.

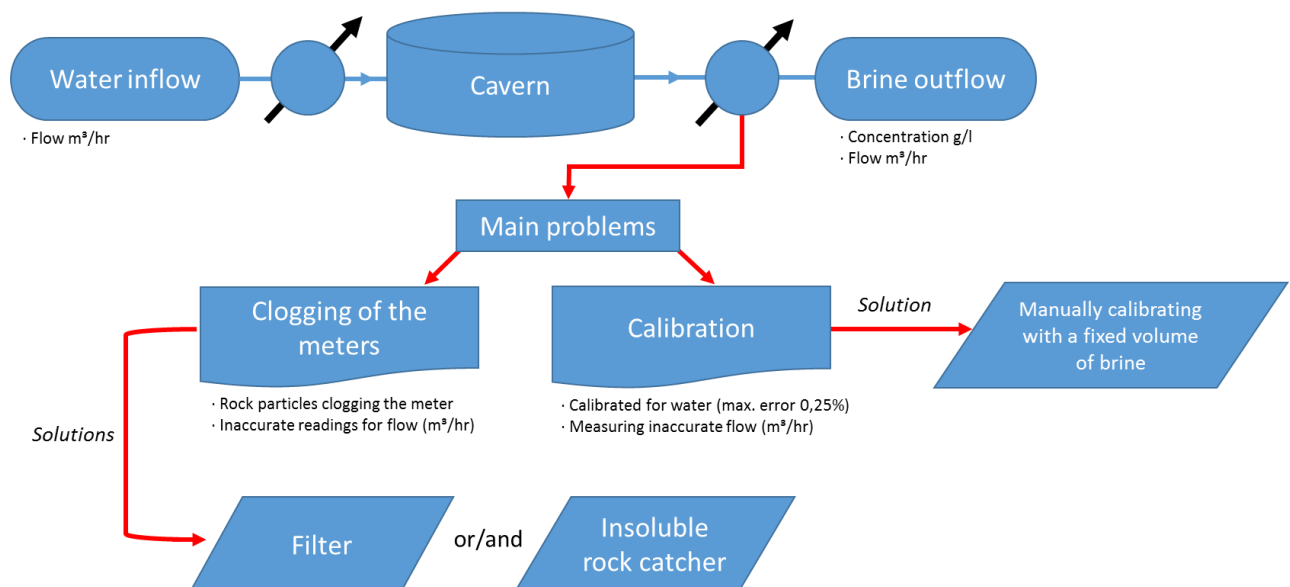


Figure 32 - Diagram showing the main issues of the flow meter which is placed on the outflowing brine side.

4.4.2 Field test setup

Two tests were carried out:

- Test 1: from the 16th of March until the 4th of May 2015, including caverns 487, 488, 490, 491, 504, 505 & 506.
- Test 2: from the 7th of May until the 23rd of June 2015, including caverns 486, 487, 488, 490, 491 & 492.

In total 6 flow meters were installed on the selected caverns during the test period. Two of these meters were installed in combination with a stone catcher, whereas the other meters were installed on caverns which had a lower possibility for clogging due to the production phase and/or depth of the pipes in the cavern. The setup including the rock catcher is illustrated in Figure 33.

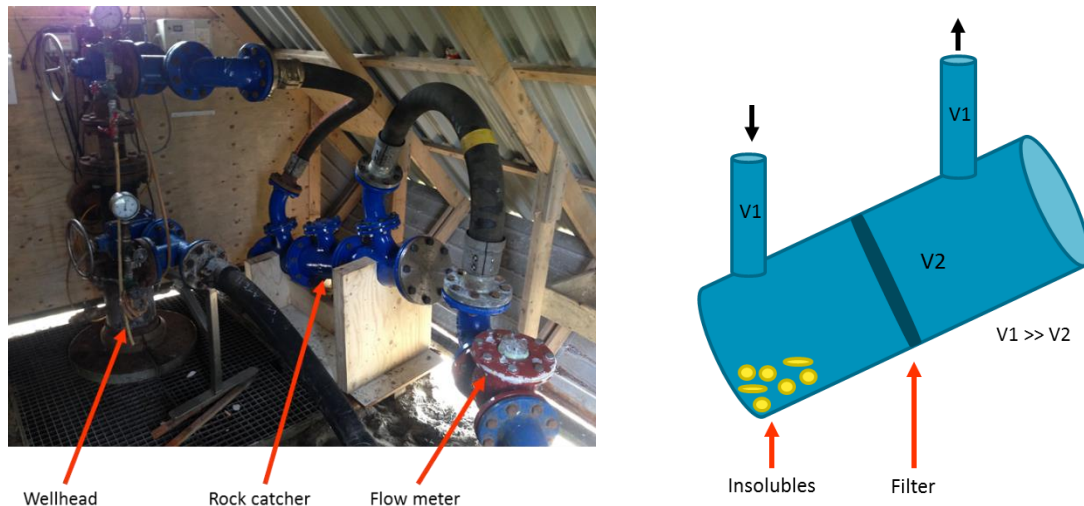


Figure 33 – Test setup in the field including a illustrative representation of the rock catcher, which ‘catches’ the insoluble rock particles by means of gravitational forces.

Initially flow meters were installed on the following caverns: 487, 488, 491, 504, 505 & 506. The flow meter in 505 clogged however after 16m³ of brine. After cleaning the meter it clogged again after an additional 6m³ of brine flowing through it. The meter was removed and reinstalled at cavern 490. Although rock catchers were installed the meters at 487 & 488 also clogged a couple of times. After installing a filter in the rock catcher, the clogging stopped. In Figure 34 two pictures are shown of insoluble rock particles which caused clogging of the meters. The particles were relatively large. The material retrieved from 505 smelled like oil, indicating fresh material from the roof, since this part of the cavern is in contact with the oil blanket.

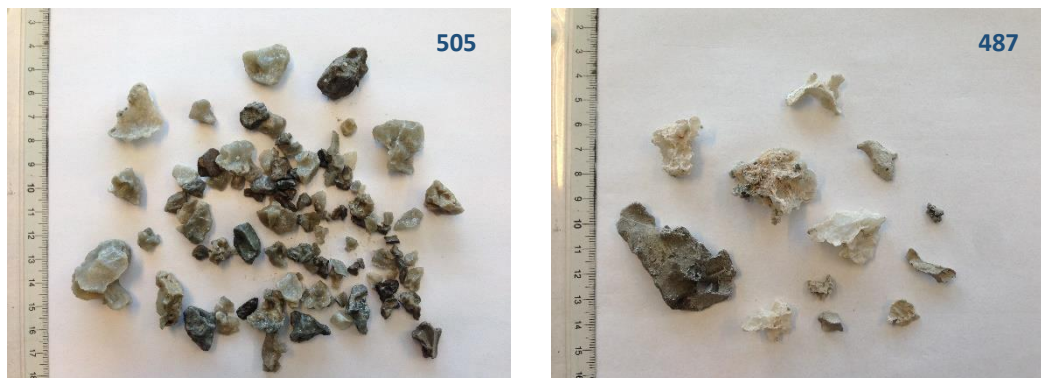


Figure 34 – Insoluble material from the caverns which causes the clogging of the flow meters. As indicated in the pictures, relatively large particles are produced. Left: material recovered from 505. Right: Clogged material found in the meter from cavern 487.

Normally this material flows unnoticed into the pipe network. Until now this has never caused problems, however looking at the size and distribution, at some point in the future one of the main brine production pipes may clog. This is however not discussed further in this report.

4.4.3 Test results

During the test period the pressure of the entire system fluctuated between 12 and 19 bars. This fluctuation is a direct effect of the capacity of the processing plant. Less flow results in less pressure in the system. The caverns are subjected to pressure changes on a daily basis. It is therefore important to measure the in-/outflow for at least 1 month, in order to find a general trend for the individual caverns. During the testing period some caverns were stopped from production for different reasons. Some were stopped because extra oil needed to be pumped into the cavern (for the oil blanket), 491 was stopped due to workover which took place at 490, and 487 & 488 were stopped due to clogging and a filter which needed to be installed. These downtimes have been accounted for.

Test 1

The testing period started at the 16th of March (2015) with cavern 488. One week later the other flow meters were installed at 487, 491, 504, 505 & 506. Due to continuous clogging of the meter at cavern 505, this meter was moved to cavern 490, since this cavern seemed to be influenced by cavern 491 during a workover which took place at 490 during the first weeks of testing. This connection between 490 & 491 will be discussed in the next subchapter.

The data which was acquired during the 1st test period is shown in Figure 35. When plotting the data, spikes can be noticed, however when adding trendlines, the ratios seem quite constant. The graphs with the ratios throughout both tests can be found in appendix F.

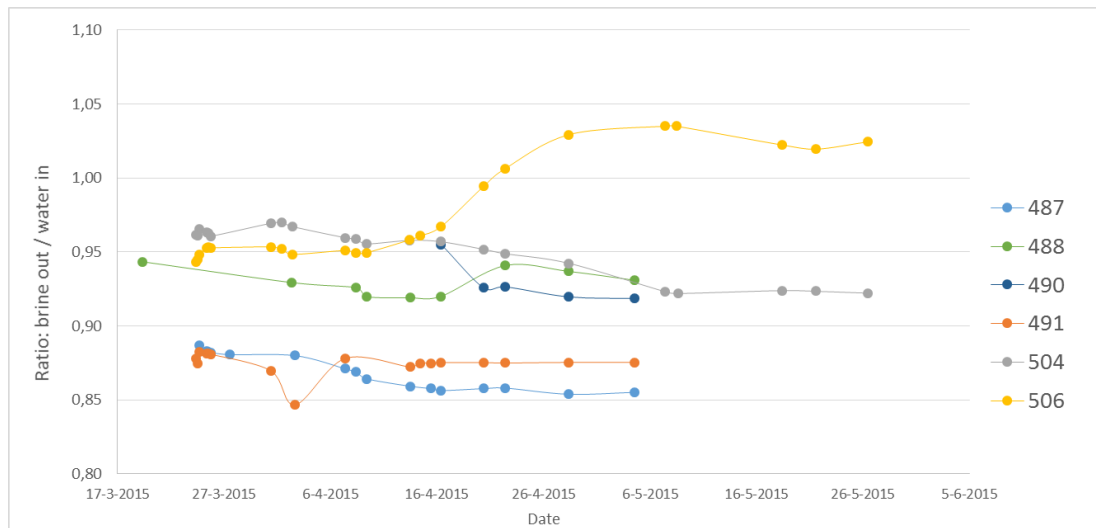


Figure 35 - Data from flow measurements on individual caverns. The ratio of brine out / water in of the test are shown in the graph.

It is interesting to note that the ratios are either lower or higher than the theoretical 0.96 as described in section 4.1.3. For these relatively small volumes the discrepancies cannot be attributed to measuring errors of the flow meters. The most obvious assumption would be that there are connections between caverns and/or that there is a loss of fluids to the underlying Solling Fm. This will be further discussed in chapter 10.

Observation in test data

A clear increase in ratio can be observed at cavern 506. Before the 13th of April the ratio was on average 0.95, however after the 13th a steady increase was observed (starting at 1.01 to 1.32 at the 22nd of April). At the same time cavern 505 was stopped for maintenance. A change in the pressure regime could have been induced when production was stopped at cavern 505, resulting in an increase of produced brine in cavern 506.

Analyzing data from Test 1

From the test results the amount of outflow per day can be determined, since the water inflow and brine outflow and time is monitored. The diagram in Figure 36 shows the principle behind this calculation.

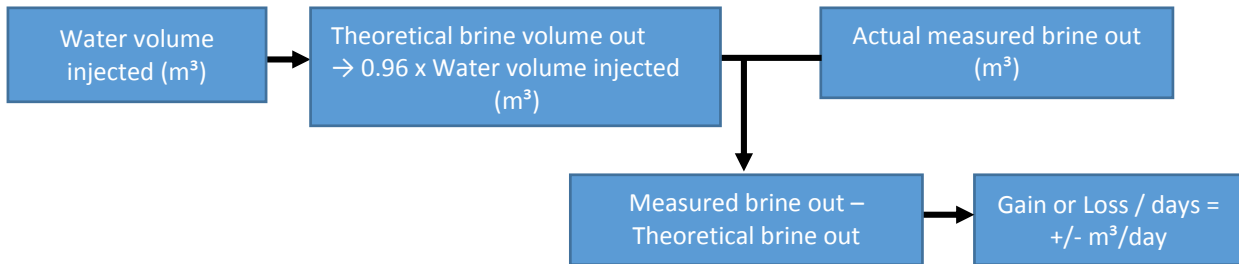


Figure 36 – Diagram showing calculation of gain or loss of fluids from a cavern during the individual mass balance test

The results are shown in Table 7. In Figure 35 the ratios of brine out/water in already showed large discrepancies between both fluid flows. Whereas the losses per cavern were estimated at 14 to 20 m³/day, which was believed to be higher than expected (section 4.2.1 & T. Pinkse, personal communication, 5 March, 2015), the actual losses are bigger. Caverns 487 and 491 lose an amount of respectively 74 and 71 m³/day. Whereas the neighbouring caverns 488 (i.e. located next to 487) and 490 (i.e. located next to 491) lose respectively 24 and 15 m³/day. Together, both pairs of caverns lose approximately 90 m³/day. The main question is where do these fluids go? These losses imply that there has to be loss of fluids to the underlying Solling Fm. The capacity of the Solling Fm. is discussed in section 6.5.

Although unlikely, possible measuring inaccuracies can be caused by temporary clogging of the flow meters measuring the brine. For the water flow meter this is however ruled out. Other inaccuracies can be caused by wear and tear on the flow meters. This can happen on both the water as brine flow meter. The meters might also give wrong readings due to the higher viscosity of brine, because the meters are calibrated for water by the manufacturer.

Table 7 – Results of the 1st individual mass balance test

Cavern	Water volume m ³	Theoretical brine m ³	Brine volume m ³	Loss/Gain m ³	Total time days	Loss/Gain m ³ /day
487	2,6E+04	2,5E+04	2,2E+04	-2,7E+03	37	-74
488	2,0E+04	2,0E+04	1,9E+04	-5,9E+02	26	-23
490	1,2E+04	1,2E+04	1,1E+04	-5,2E+02	17	-31
491	3,0E+04	2,8E+04	2,6E+04	-2,5E+03	36	-71
504	2,1E+04	2,0E+04	1,9E+04	-7,9E+02	60	-13
506	1,5E+04	1,4E+04	1,5E+04	9,4E+02	61	15

Test 2

The 2nd testing period started on the 7th of May. In order to rule out the measurement error caused by calibration settings, the meters were switched. During the second test phase, the meters from 504 and 506 were moved to caverns 486 and 492. These caverns are located closer to 487, 488, 490 and 491. The results for the 2nd test are shown in Table 8.

Table 8 – Results of the 2nd individual mass balance test

Cavern	Water volume m ³	Theoretical brine m ³	Brine volume m ³	Loss/Gain m ³	Total time days	Loss/Gain m ³ /day
486	not enough data yet					
487	2,8E+04	2,9E+04	3,0E+04	7,9E+02	46	17
488	2,8E+04	2,9E+04	2,7E+04	-2,2E+03	46	-48
490	3,2E+04	3,1E+04	2,8E+04	-2,7E+03	32	-86
491	1,7E+04	1,6E+04	1,5E+04	-7,6E+02	21	-36
492	not enough data yet					

During the 2nd test there is still a loss noticed for all caverns. However the magnitudes of the losses differ from the 1st test. This is also clearly visible in the figures in appendix H, a clear shift in ratios can be observed when comparing both testing periods. This implies that the flow meters are not measuring the same volumes. The results of both tests will be combined in order to estimate the total amount of losses/gains for the tested caverns.

Combined results

The results after the switch have been combined with the results from before the switch and are shown in Table 9. The losses/gains have been averaged using the cumulative data from both testing periods (applying the weighted average method). It can be noticed that the results from both tests differ. However after combining the results an average loss or gain can be determined. The results indicate that the caverns are losing substantial amounts of fluids.

Table 9 – Combined results of the individual mass balance tests (the ratio indicates brine out / water in).

Cavern	Ratio test 1	Ratio test 2	Combined (cum. data)	Average loss/gain (m ³ /day)
487	0,86	0,98	0,89	-24
488	0,93	0,89	0,93	-41
490	0,92	0,87	0,90	-66
491	0,87	0,91	0,89	-58
486	not enough data yet			
492	not enough data yet			
504	0,92			-13
506	1,02			17

Loss over the whole field

What do these results mean for the whole field? Assuming that, based on the results, an average cavern loses 25 - 35 m³/day. Given 40 producing caverns, which are producing 11 months per year, the total loss per year adds up to approximately 3.3 - 4.7·10⁵ m³. This is a considerable amount of fluid loss. In section 6.5 the capacity of the Solling Fm. will be discussed. These values for the fluids losses are in line with the values determined in section 4.2.1, in which the losses are estimated to be in the range of 2.5 to 3.7·10⁵ m³.

Accuracy of the flow meters

In the graphs in Appendix H and in Table 9 it can be observed that the ratios differ when switching the flow meters. The flow meters are therefore not measuring the same amount of fluids. The test was conducted using 2 flow meters, so either the brine is under-/overestimated or the water is under-/overestimated. By switching the meters the error of the flow meters can be determined, assuming that one of the 2 meters is correct. The results from cavern 487 show a large deviation. A possible explanation for the difference of cavern 487 is the fact that two different types of meters are used for measuring the flow. The old meter has probably a deviation of about 7%, which results in a higher water flow reading during test 1 (i.e. lower brine/water ratio) and a higher brine reading during test 2 (i.e. higher brine/water ratio). The plot shown in Figure 37 gives an indication of the range of the ratios for the different caverns.

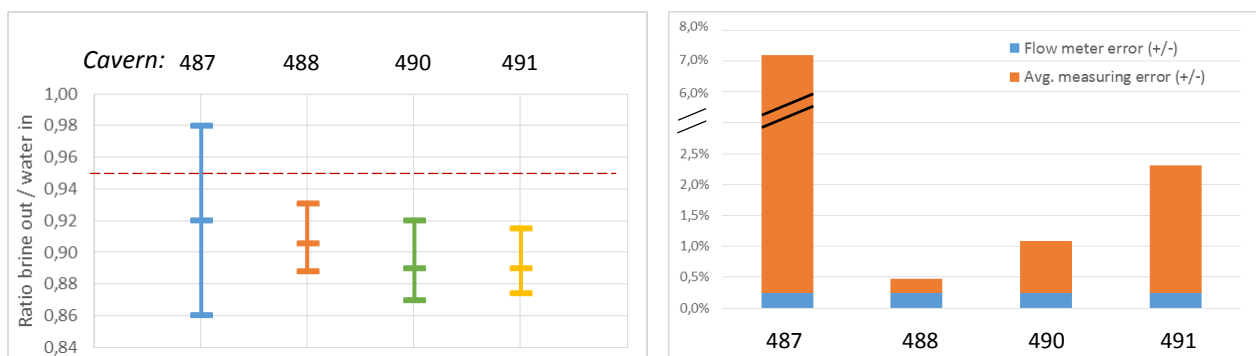


Figure 37 – Accuracy of the flow meters. Left: Range of the ratios plus average for the measured caverns (dotted line is theoretical brine out/water in ratio). Right: Flow meter error; blue columns indicate manufacturer error, orange indicate measured error.

Observations at caverns 487 & 488

Figure 38 shows the measured ratios (i.e. the ratios between 2 measurements and the average ratio, before and after the flow meter switch). Just after the flow meter switch the ratios measured at cavern 488 seem to be quite constant, this is indicated in Figure 37 as well, where the very low measurement error for this cavern is given. For cavern 487 a big jump can be noticed (these 3 caverns are located close to each other, Figure 39). Another remarkable event happened at the 1st of June (2015), when the brine out/water in ratio of cavern 487 increased by almost 0.1, whereas the same ratio dropped by almost 0.1 at cavern 488. Looking closer to the measured values, this drop is caused by the measured brine. A possible explanation is that the pressure regime in both caverns changed to the upcoming workover at cavern 489. It is known from the pressure tests that 487 and 488 are directly connected due to instantaneous pressure measured at both caverns. The 'loss' of brine at 488 is therefore most likely produced at cavern 487.

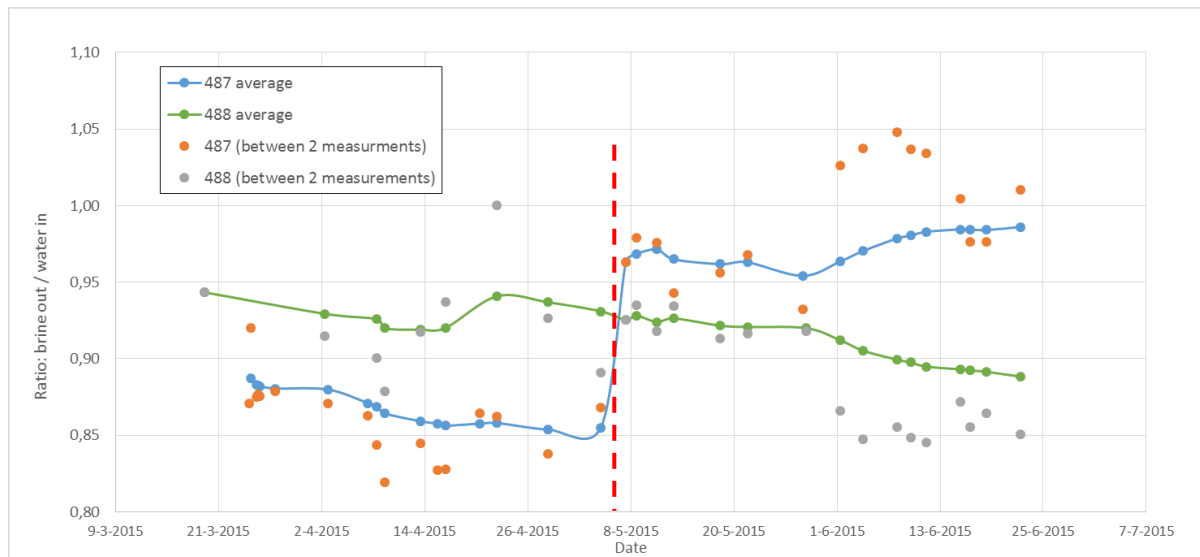


Figure 38 – Results of the mass balance tests at caverns 487 and 488. The red dotted line indicates the flow meter switch.

Field observation during workover at cavern 490

At the 23rd of March flow measurements started at cavern 491. During the initial phase of this experiment a workover was started at cavern 490 at the 26th of April. During this workover problems were encountered with the pressure in the cavern. Figure 39 shows the location of these caverns. Calculations indicate that to release 5 bar overpressure: ~50 m³ must be pumped from the cavern theoretically. This was here however not the case. Table 10 shows the procedures which were conducted during the workover.

Table 10 – Observations & measurements during workover (cavern 490)

Date	Pumping (hrs):	Description
26-3-2015	6	Before the start of the workover
27-3-2015	4	After these 4 hours, 4" pipe could be removed, cavern 491 was stopped
30-3-2015	5	Remaining pipes removed, vacuum tank was used
31-3-2015	2	Pressure built-up again, 2 more hours of pumping before sonar measurement could be done
7-4-2015	4	After these 4 hours, start of installing pipes
7-4-2015	2	Another pressure built-up, 491 was stopped again after which the pressure could be released
8-4-2015	2	Last phase of pipe installation, pressure too high again, cavern 491 was stopped again
Total:	25	

When assuming that the pump pumps 20 m³/h (J. Keizer, personal communication, April 8, 2015), a total of 500m³ was pumped from the cavern. This is more than the theoretical volume which should be pumped from the cavern. Only when production was stopped at cavern 491, cavern 490 could get an allowable pressure to continue with the work over. This implies a connection between the two caverns. This will be further discussed in chapter 10.

Field observation during workover at cavern 489

In week 24 and 25, 2015, a workover took place at cavern 489. During this workover it was difficult to depressurize the cavern. The crew had to stop to production at caverns 490 and 491 and had to depressurize the cavern 9 times (pumping on average for 3 hours). In total 28 hours was pumped which results in approximately 560 m³.

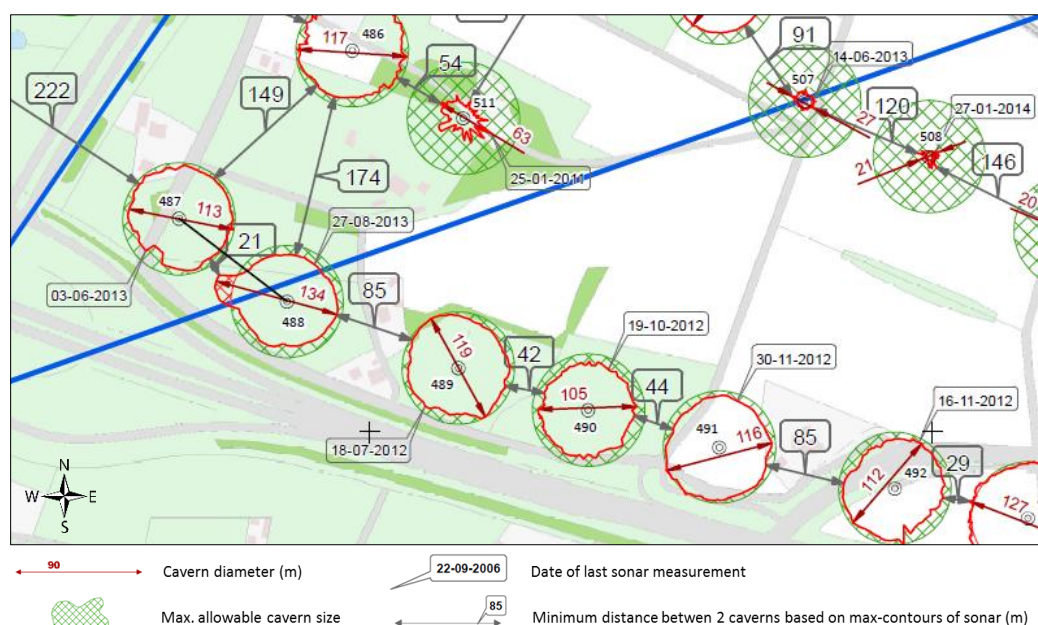


Figure 39 – Map with location of caverns 490 and 491

4.5 *Summary of the mass balance*

Measuring the material entering and leaving the caverns and comparing this to the theoretical value when dissolving halite, provides an important indicator whether caverns are closed or not. Hence three different balances were discussed in detail:

1. The mass balance based on flow data, based on the whole field
2. The mass balance based on masses, based on the whole field
3. Mass balances for individual caverns.

According to the theoretical calculation (section 4.1.2) for every injected m^3 water, 0.96 m^3 brine should be produced. After analyzing the data from the plant and field it is clearly indicated that fluids are 'missing' (section 4.2.1). Different possibilities, which might explain the unaccounted amount of fluids, are discussed:

- Pressure built up in the caverns
- Brine concentration
- Infrastructure & Operations in the field
- Measurement errors in the flow meters
- Loss to Solling & Connection between caverns

Due to the magnitude of the losses the Solling Fm. and connection between caverns were considered to be the main reason for the observed fluids losses.

In order to increase the understanding at cavern-level, individual mass balance tests were performed as discussed in section 4.4. It proved to be difficult to measure the outflowing brine due to insoluble particles clogging the flow meters. Installing 'stone-catchers' solved this issue.

From the individual caverns it becomes clear that some caverns are losing significant amounts of fluids. The average loss measured was approximately $30 \text{ m}^3/\text{day}$, which results in 3.0 to $4.0 \cdot 10^5 \text{ m}^3$ of losses each year. This value is in accordance with the results from the plant and field.

The only logical explanation would therefore be that the fluids have flowed from the caverns into the underlying Solling Fm. This will be further discussed in chapter 6.

5. Pressure tests

In 2013/2014 a series of pressure tests were performed in the field. Four tests were carried out by the companies KBB and DEEP and four were executed by AkzoNobel. The main purpose of the tests done by KBB and Deep was to check the general pressure integrity of the caverns which were selected for gasoil storage, by injecting brine and increasing the pressure to a level, which would be required to ensure the tightness of the caverns. The other tests were done as part of a MSc. thesis (van Berkel 2014) which gave an initial insight in the mass balance of the field.



5.1 Methodology

Two series of tests were performed. The general methodology is the same for both series. During the test three phases can be distinguished: the injection phase, observation phase & withdrawal phase. During the injection phases the pressure is increased in one cavern. The pressure in the cavern is increased in steps to approximately 20 bar (this is an increase of approximately 15 bar). In between these steps, the pressure was monitored during the observation phases. At the end of the test, the overpressure was released by pumping brine from the cavern. By monitoring the pressure in both the cavern where the pressure is increased and the neighbouring caverns possible connections between caverns could be established. Gradual delayed increases in the neighbouring caverns suggests that the brine has found a pathway through the underlying formation (i.e. the Solling Fm.) This is however only possible when the underlying formation contains permeable rock layers which allow flow. From the pressure increase, in combination with the compressibility factor, the amount of fluid in- and outflow can be calculated. An instantaneous pressure increase was also observed. This indicates a direct contact/connection between caverns. There is a fundamental difference between the two series of tests. KBB and Deep have tested MCC's, whereas AkzoNobel has tested SCC's.

During the test the following influencing phenomena are not taken into account (Holenstein et al., 2014):

- Brine heating and brine expansion due to heat flux from the salt formation
- Transient creep
- Micro-permeability through the cavern walls (percolation)
- Cavern reaction as a response of the pressurization and depressurization
- Discontinuities due to the operating of the pressurization equipment

5.2 Test results

The graphs with the pressure responses of the different tests are summarized in appendix F (Figures 105 – 112). The direct and delayed pressure responses/increases are clearly visible in these graphs. A summary of the pressure tests is shown in Figure 40. It can be noticed that the total testing time of the pressure tests vary.

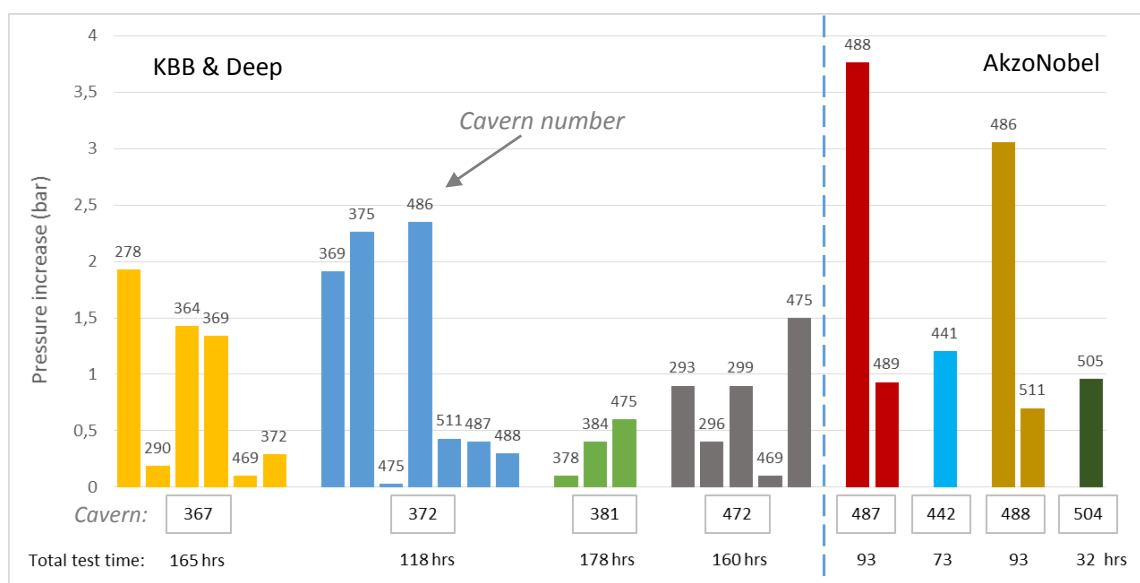


Figure 40 – Pressure responses monitored at neighbouring caverns. The numbers in the boxes below the bars indicate in which cavern the pressure was increased, whereas the number on top of individual bars indicate the specific cavern where the pressure increase was measured.

It is clearly visible that some caverns show a large pressure increase response when the pressure is increased in the test caverns. These responses clearly indicate the possibility of connections between caverns. As indicated in appendix F all but one test show delayed increases. The test which shows an instantaneous increase is the test performed on cavern 487 (Figure 110). The response was measured at caverns 488 & 489. Whereas 489 shows a gradual increase, 488 shows exactly the same trend as 487, indicating a direct connection between both caverns. There are however also caverns in which the pressure doesn't increase much. Increases lower than 0.2 bar are neglected.

5.3 Cavern compressibility

With the pressure increases from previous subchapter the total amount of inflow can be calculated. This can be done when the cavern compressibility factor is known. The relation between the amount of injected brine and the wellhead pressure shows linear behaviour and represents the cavern system compressibility (Bérest et al., 2006). The following formula is used to determine the cavern system compressibility factor of the caverns:

$$\Delta V = \beta_s \cdot \Delta P \cdot V_{cavern} \quad (1)$$

where ΔV is the relative volume increase in m^3 , β_s is the cavern system compressibility in bar^{-1} , ΔP is the pressure increase in bar and V_{cavern} is the volume of the cavern in m^3 . Since the $\Delta V/\Delta P$ gradient is known from the tests and the volume of the cavern is known (to some degree) as well, the system compressibility can be determined using the following simplification:

$$\frac{\Delta V}{\Delta P} \cdot (V_{cavern})^{-1} = \beta_s \quad (2)$$

The cavern system compressibility is the sum of the cavern compressibility factor β_c and the brine compressibility factor β_b . Whereas the brine compressibility can be considered constant (i.e. approximately $2.7 \cdot 10^{-5} bar^{-1}$), the cavern compressibility can vary due to the cavern shape and the rock-salt properties (Holenstein et al., 2014). For each test the minimum and maximum system cavern compressibility value has been calculated since multiple $\Delta V/\Delta P$ gradients were available for the individual tests due to the step-wise testing method. This variation in system cavern compressibility values exists due to brine losses. Figure 41 shows the cavern system compressibility values for the different tests.

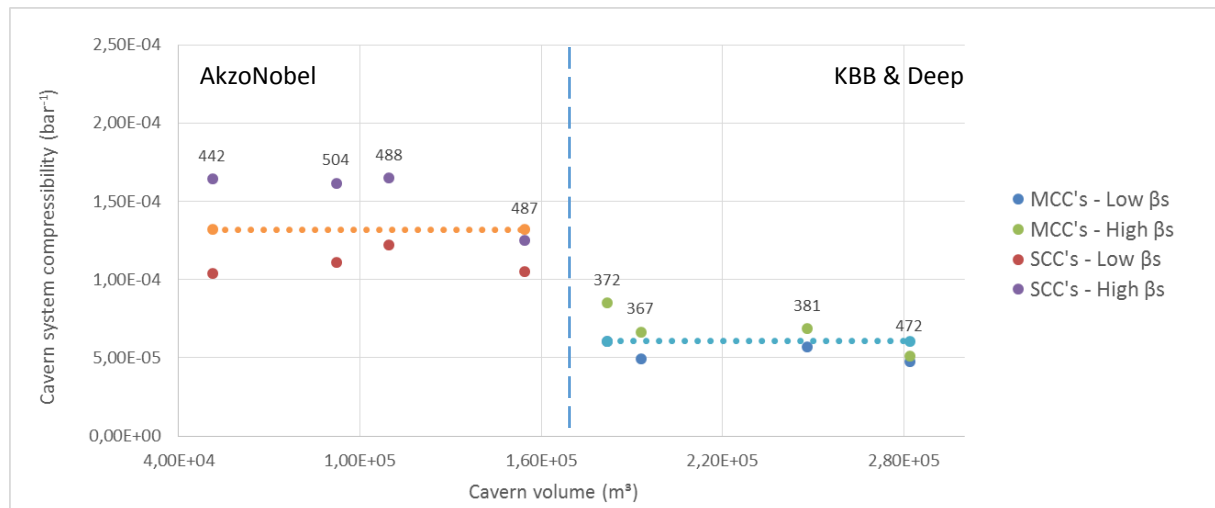


Figure 41 - Cavern system compressibility values for the different tests, the results are sorted according to cavern volume. The orange dotted trendline shows the average value for the SCC's, whereas the blue dotted trendline shows the average compressibility value for the MCC's.

A clear difference can be noticed between the two series of tests (Figure 41). The average compressibility value determined from the tests performed by AkzoNobel is $1.32 \cdot 10^{-4} bar^{-1}$, while the tests carried out by KBB and Deep show an average value of $6.07 \cdot 10^{-5} bar^{-1}$. This is a difference of factor 2. A possible explanation could be the type of caverns used during the tests. Therefore it was decided that the value determined from the AkzoNobel tests would be used to calculate the inflow for SCC's whereas the KBB & Deep results were used for MCC's.

5.4 Fluid inflow & distance of influence

Combining the test results with the cavern compressibility, the total amount of in-/outflow can be determined. From this data two things can be determined: By combining the data with a topographic map of the top of the Solling Fm. preferred pathways can be indicated between certain caverns whereas combining the amount of in-/outflow with the distance between caverns results in a distance of influence plot.

The measured amount of inflow for both series of tests are shown in the figures below. The inflow data has been scaled to 100 hours, this enables the tests to be compared properly.

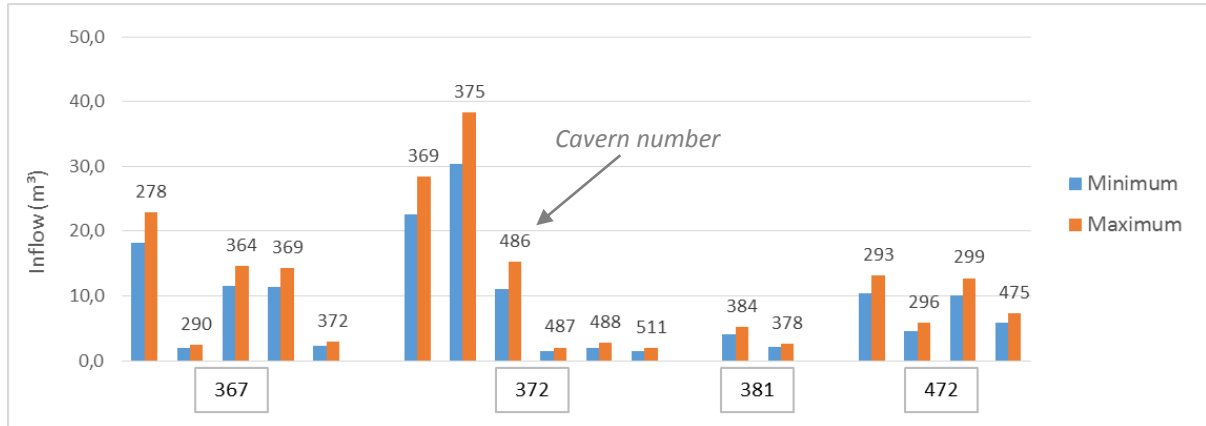


Figure 42 – Inflow in caverns during the pressure tests of KBB and Deep. The numbers in the boxes below the bars indicate in which cavern the pressure was increased, whereas the number on top of individual bars indicate the specific cavern where the pressure increase was measured. The data has been scaled to 100 hours.

In these figures only inflow amounts larger than 1m^3 are taken into account. As expected, when comparing these figures to Figure 40, clear similarities can be noticed. The highest inflow is measured at cavern 488, i.e. the cavern which is directly connected to cavern 487. When plotting this data vs. the distance between the caverns an interesting trend is shown, the amount of inflow decreases drastically with an increasing distance between caverns. This is shown in Figure 44.

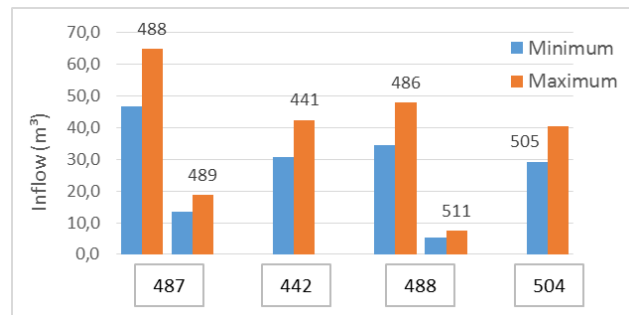


Figure 43 – Inflow in caverns during pressure tests of AkzoNobel

The reason why no data points are shown between 0 and 145 meters is due to the regulated minimum distance between two caverns. The decreasing trend could be explained by the fact that the test only lasted for a certain amount of time. Since the fluids have to find a path towards the neighbouring caverns, a large portion of the fluids fill the open voids in the Solling Fm. The greater the distance the more void space is encountered. Therefore smaller portions of fluids enter the neighbouring caverns eventually. Another explanation is that the pressure gradient decreases with distance.

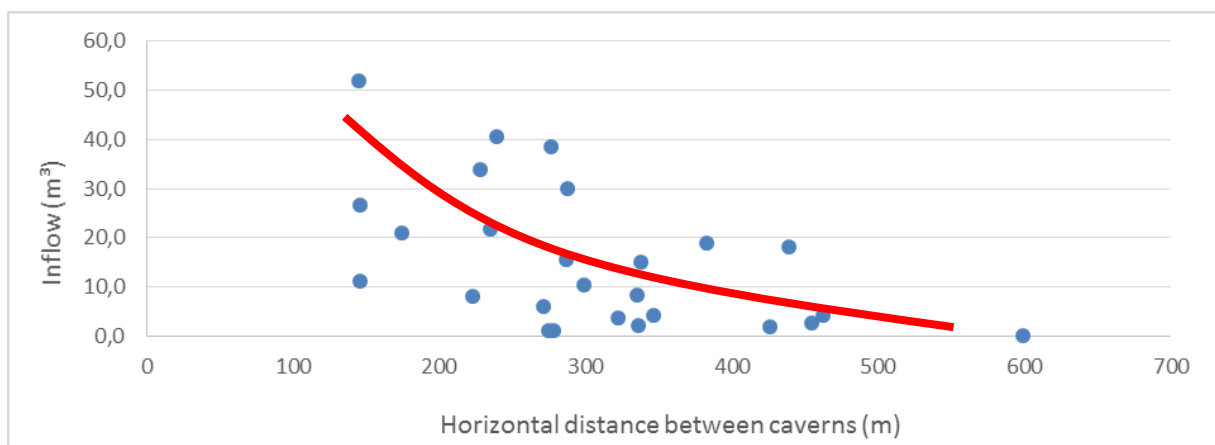


Figure 44 - Relationship between the amount of inflow and the horizontal distance between the test cavern and neighbouring caverns (note: distances are measured from borehole to borehole).

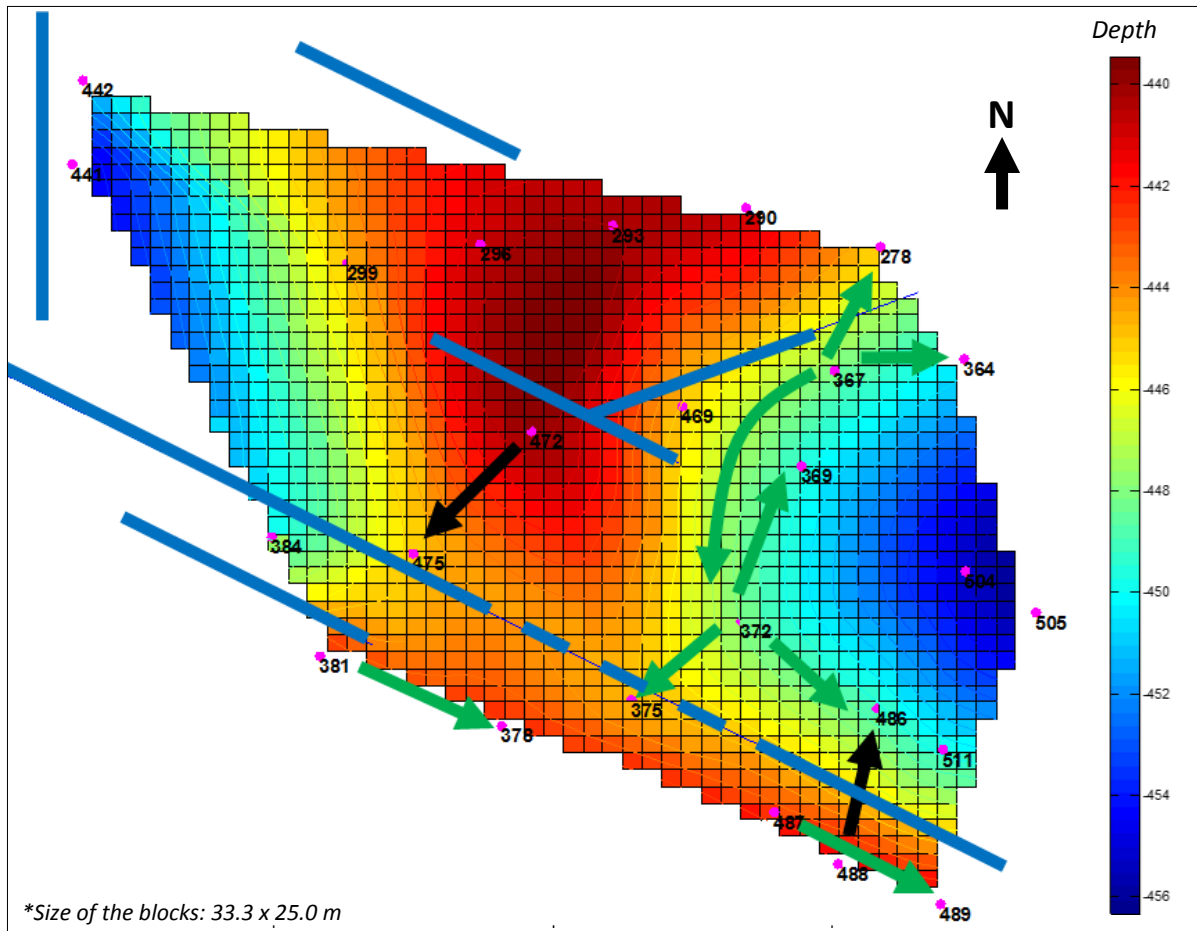


Figure 45 – Topographic elevation map of the top of the Solling Fm. The blue lines indicate faults. The green arrows indicate main flow directions to higher elevations (i.e. less deep than the tested cavern) or main flows along isopachs. The black arrows indicate main flow directions towards caverns which are located deeper than the tested cavern.

Figure 45 indicates the main flow directions of the brine during the tests. It can be noticed that the flows tend to follow isopachs, or flowpaths to caverns which are located less deep than the tested cavern. However the black lines also indicate flows towards deeper caverns. This is normally not possible due to the natural pressure gradient, but in case of a high overpressure (i.e. resulting in a large pressure gradient between caverns) the fluids can also flow downwards.

From the pressure test data it is also possible to determine the amount of brine that is lost, since the amounts of injected and retrieved brine and the amounts of brine inflow at neighbouring caverns are known:

$$\text{Volume lost brine} = \text{Injected brine} - \text{Retrieved brine} - \text{Inflow neighboring caverns} \quad (1)$$

The results from this calculation are shown Table 11. The main problem with calculating the amount of brine that has been lost is that only a number of neighbouring caverns were monitored during the test. It is also possible that the fluids have found paths towards other caverns. The amount gives therefore only an estimate of the amount of brine that can't be accounted for, and is either located in the underlying Solling Fm. or other caverns.

Table 11 - Unaccounted (i.e. lost) volumes during the pressure tests of KBB and Deep

Cavern	Injected (m ³)	Retrieved (m ³)	Total inflow other caverns		Unaccounted volume
			Low (m ³)	High (m ³)	Range of volume (m ³)
367	404	105	74,8	94,3	204,7 ~ 224,2
372	421	71	81,1	104,6	245,4 ~ 268,9
381	271	161	11,0	13,8	96,2 ~ 99,0
472	270	171	49,5	62,4	36,6 ~ 49,5

In caverns 367 and 372 considerably more brine was injected than in caverns 381 and 472. The percentage of retrieved brine in these caverns was however much lower, approximately 20% vs. 60%. During the tests of 367 and 372 more neighbouring caverns were measured than during 381 and 472. This, including the amount of injected brine, might explain the fact that the amounts of unaccounted volumes vary.

5.5 Pressure test to check connectivity

One method to check connectivity in the future is to install pressure gauges on a cavern which is stopped from production due to maintenance activities, for example during workovers. Caverns are generally stopped a month prior to the actual workover. By installing a pressure gauge on the brine pipe during this idle time, pressure changes can be measured in the cavern.

The hypothesis of such a test is that the pressure decreases during the first days because of ongoing leaching of the salt due to unsaturated fluids which are still present in the cavern shortly after production has ceased. During this ongoing leaching extra volume will be created in the cavern, causing the pressure to drop. When connections with neighbouring caverns exist it is however possible that the pressure finds an equilibrium at a certain moment or that the pressure even starts to increase. When a pressure increase occurs the amount of inflowing fluids can be calculated using the compressibility factor, as explained before.

Field test

It was difficult to find suitable caverns to perform the test. Many caverns were already stopped, the only two caverns which were available were caverns 479 and 503. Both caverns are of the SCC type. Whereas cavern 479 is located at approximately 4km northwest of Usseleres and surrounded by old MCC's. Cavern 503 is located at the north-eastern edge of Usseleres. A minimum inflow was therefore expected at these two cavern. The installed pressure gauges are shown in Figure 46.



Figure 46 – Installed pressure gauges. Left: cavern 503, right: cavern 479

The results of the field tests are shown in Figure 47. The steady pressure decrease during the first couple of days is clearly visible. After 12 days the pressure remains constant and in the subsequent weeks no pressure increase is monitored, possibly implying that an equilibrium with the underlying Solling Fm. was reached. From the pressure drop it is calculated that in cavern 479 ~96m³ was created, whereas in 503 ~42m³ was created. At the end of the testing period, the pressure increased slightly in cavern 479 (increase of 0.06 bar), possibly because of a measuring error in the pressure gauge. The calculation shows only an inflow of 1m³, this can therefore be neglected. This test shows that the pressure can be monitored properly. It is however recommended to repeat this test on caverns which are surrounded by active caverns, in order to observe steady pressure increases over time.

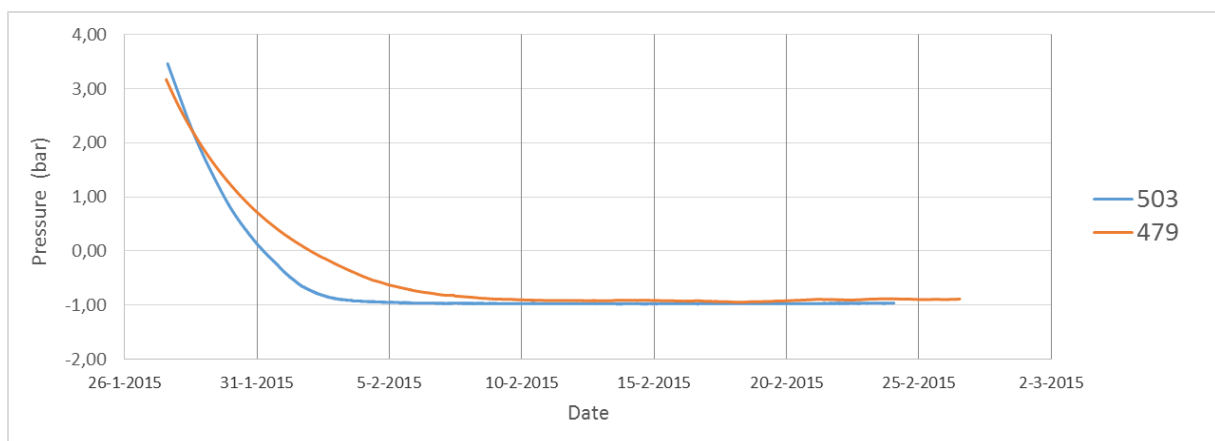


Figure 47 – Pressure monitoring test on caverns 479 and 503 during idle time

5.6 *Summary pressure tests*

Pressure tests provide a good indicator whether a connection is present with the Solling Fm. and if fluid pathways exist between caverns. Two series of tests were performed. During the test three phases can be distinguished: the injection phase, observation phase & withdrawal phase. KBB and Deep have tested MCC's, whereas AkzoNobel has tested SCC's.

By monitoring the pressure in both the cavern where the pressure is increased as well as in the neighbouring caverns, possible connections between caverns could be established. Gradual delayed increases in the neighbouring caverns suggests that the brine has found a pathway through the underlying formation (i.e. the Solling Fm.). From the pressure increase, in combination with the compressibility factor, the amount of fluid in- and outflow can be determined.

Results show that the amount of inflow decreases with an increasing distance between caverns. It can be assumed that this decreasing trend between distance and inflow is caused by the decline of the pressure gradient and the increasing volume of the fluid pathways. By converting the pressure increases to brine volumes and plotting these on a topographical map, the major directions of fluid flow can be analyzed. In general it can be noticed that the flows tend to follow isopachs or paths towards shallower caverns.

A pressure test is described to easily measure inflow at stationary caverns (e.g. caverns which need a workover). The methodology was tested on 2 caverns. This test can be used in the near future to create a detailed map of caverns which show inflow.

6. Solling Formation

From chapter 5 it is clear that there is a systematic fluid loss in the system. The most obvious explanation for this fluid loss and/or connection between caverns, is to link the caverns through the underlying Solling Fm. As described in chapter 3, the Solling formation consists of fine sand-, silt-, and claystone layers/accumulations, interspersed by fractures, due to the structural history. This chapter will combine the information and data from the known geology, calculated volume & mass balances, performed sonar measurements and observations from different cores. It will furthermore describe an in-/outflow test, based on different ratios.



6.1 Core observations

Various cores have been retrieved from the Röt salt and layers above. Cores from the Solling are however scarce. However during the last exploration drilling campaign (BKM-02), +/- 9m was drilled in the Solling Fm. The coring operation was carried out with the Kremco K400 rig. Figure 48 shows some pictures from the coring operation. Three cores were drilled in total:

- Salt C (612 m to 621 m)
- Salt A (636.66 m to 645.66 m)
- Solling Fm. (645.66 m to 653.61 m)

The actual observations of the Solling formation are shown in Appendix I. Observations from the core which was drilled in combination with information gathered during a visit to the national core house show some interesting insights regarding this formation. The national core house is managed by the Netherlands Organisation for Applied Scientific Research (in Dutch: Centraal Kernhuis TNO)

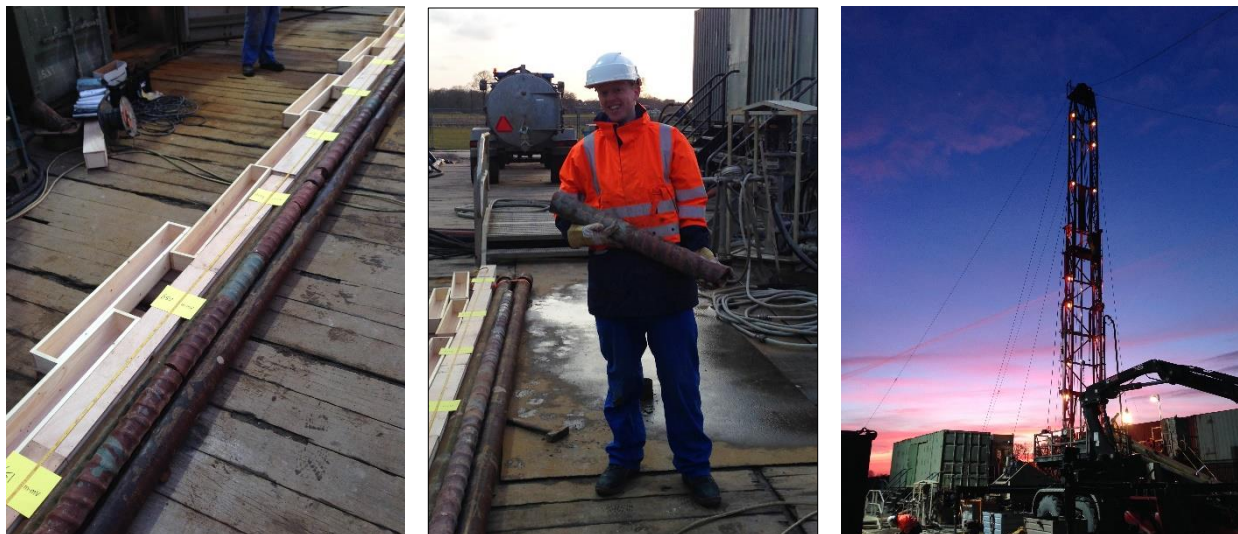


Figure 48 – Pictures from the coring operation. Left: Solling Fm. core fresh out the coring tool. Middle: Core handling from the rig to the work floor. Right: Kremco K400 rig during the coring operation

Figure 49 shows pictures from the observed. Pictures were taken from three different cores: (A) Borne, which is located just north of the HBF, (B) B534, which is drilled in the Northern part of Ganzebos and (C) BKM-02, located in the Southern part of the Ganzebos area. Fractures and veins, both filled with halite and anhydrite are clearly visible. Normally the boundary between the Röt salt and Solling Fm. is formed by an anhydrite layer. However pictures 5a and 5b (in Figure 49) show a clear halite layer underneath the anhydrite layer. Furthermore sand and clay accumulations were observed. These sand formations are of great importance when suggesting that there is a fluid loss from the caverns.

These observations not only confirmed the presence of permeable sand stone and impermeable claystone, but also the presence of fractures, which were created due to the structural history, and halite veins, which were formed during the burial phase of the Solling Fm.



Figure 49 – Pictures of core samples from the Solling formation, core are from different drilled holes (Borne, Cavern 534 or BKM-02)

- 1a: Core from exploration in Borne, large fracture filled with salt visible (Borne).
- 1a+: Same core as 1a, but in more detail. 1b: Top view from the fracture (Borne).
- 2: Fracture filled with salt observed in core from Borne as well (Borne).
- 3: Core taken from cavern 534, part of salt filled fracture visible (Cavern 534)
- 4: Core from BKM-02 exploration drilling, fracture filled with salt (BKM-02).
- 5a: BKM-02, relatively thick salt underneath the anhydrite layer which normally forms the boundary between bottom salt and the Solling Fm. (BKM-02).
- 5b: Another view of core from 5a. (BKM-02).
- 6: Clay and sand layers are visible in the Solling Fm. (BKM-02).
- 7: Halite salt vein in the Solling Fm. (BKM-02).
- 8: Halite salt veins in combination with anhydrite (BKM-02).

6.2 Possibilities of fluid loss from a cavern

When drilling a well for the development of a new cavern, the hole is drilled a couple of meters into the Solling Fm. as explained in section 4.2.2. This is the moment when the main connection between the Röt salt and Solling formation is created. The hole is not plugged after drilling has been completed. It therefore remains an open hole. After installing the pipes in the cavern in order to create the sump, water is injected to start the leaching process. The water will however also flow into the open hole which is still present in the Solling Fm. When this initial fresh water comes into contact with halite filled fractures and/or halite filled veins, the halite can easily dissolve from these geological features, and create flow paths into the Solling Fm. Another problem that can occur is that the sump is developed too deep (i.e. too close to the underlying Solling Fm.), this can result in a large contact area between the sump and the top part of the Solling Fm., instead of having a protective layer of Röt Salt between the sump and the Solling Fm.

With this information a simple geological model has been constructed, indicating the possible flow paths between caverns. This model is shown in Figure 50. As illustrated in the figure a distinction can be made between three different situations:

1. Connection between caverns through the Solling Fm.
2. Fluid loss to the Solling Fm.
3. Direct connection between caverns.

The underlying principle of fluid outflow from the initial cavern where the fluid is injected is that there needs to be a pressure gradient. Without a pressure gradient connections and/or losses will most likely not occur. The Röt formation is not situated at the same depth throughout the HBF, caverns are therefore located at different depths. Different depths imply different pressures, a pressure gradient is therefore present in the HBF. Furthermore the caverns are operated at a certain overpressure. When a workover takes place at a certain cavern, the overpressure is released, the neighbouring caverns are however still operating at their overpressure, creating pressure gradients between different locations.

6.2.1 Connection between caverns through the Solling Fm.

The main issue in of the caverns in the HBF is that only inflowing water is measured. Therefore a clear distinction between connections and/or losses can't be made directly. However during the pressure tests performed in the field (chapter 6) and the mass balance tests on individual caverns (chapter 5) indications for connections were noticed. The results from these tests showed the existence of these connections. From the radius of influence plot (shown in Figure 44) it could be seen that caverns within 500 meters of each other showed connections.

Results from the individual mass balance tests showed in- and outflow from caverns as well. A clear connection was observed between 490 and 491, as described in section 4.4.3.

6.2.2 Fluid loss to the Solling Fm.

It is also possible that the fluids which are injected are lost to the Solling Fm. As described before open connections can exist between the cavern and the Solling Fm. As indicated in Figure 49 (picture 6) and observed in other parts of the core, sand accumulations occur. The sand observed has generally a high porosity and permeability and can therefore be seen as a reservoir in the Solling Fm. Fluids can therefore find their way directly to these sand accumulations when a direct contact exists, or they can find their way through the network of halite filled fractures and veins to this sand.

It is likely that the greater faults in the area also play a role in the loss of fluids. When the faults are not smeared by, for example, clay, they can act as flow paths through which the fluids can leave the HBF. This has however not been proven yet.

6.2.3 Direct connection between caverns

A direct connection can also exist. This is the result of uncontrolled leaching of the cavern, due to the composition of the salt in a particular cavern. The composition can cause preferred leaching directions. When one is not monitoring (for example measuring in-/outflow ratios) such caverns for a longer period of time, a connection can occur between caverns.

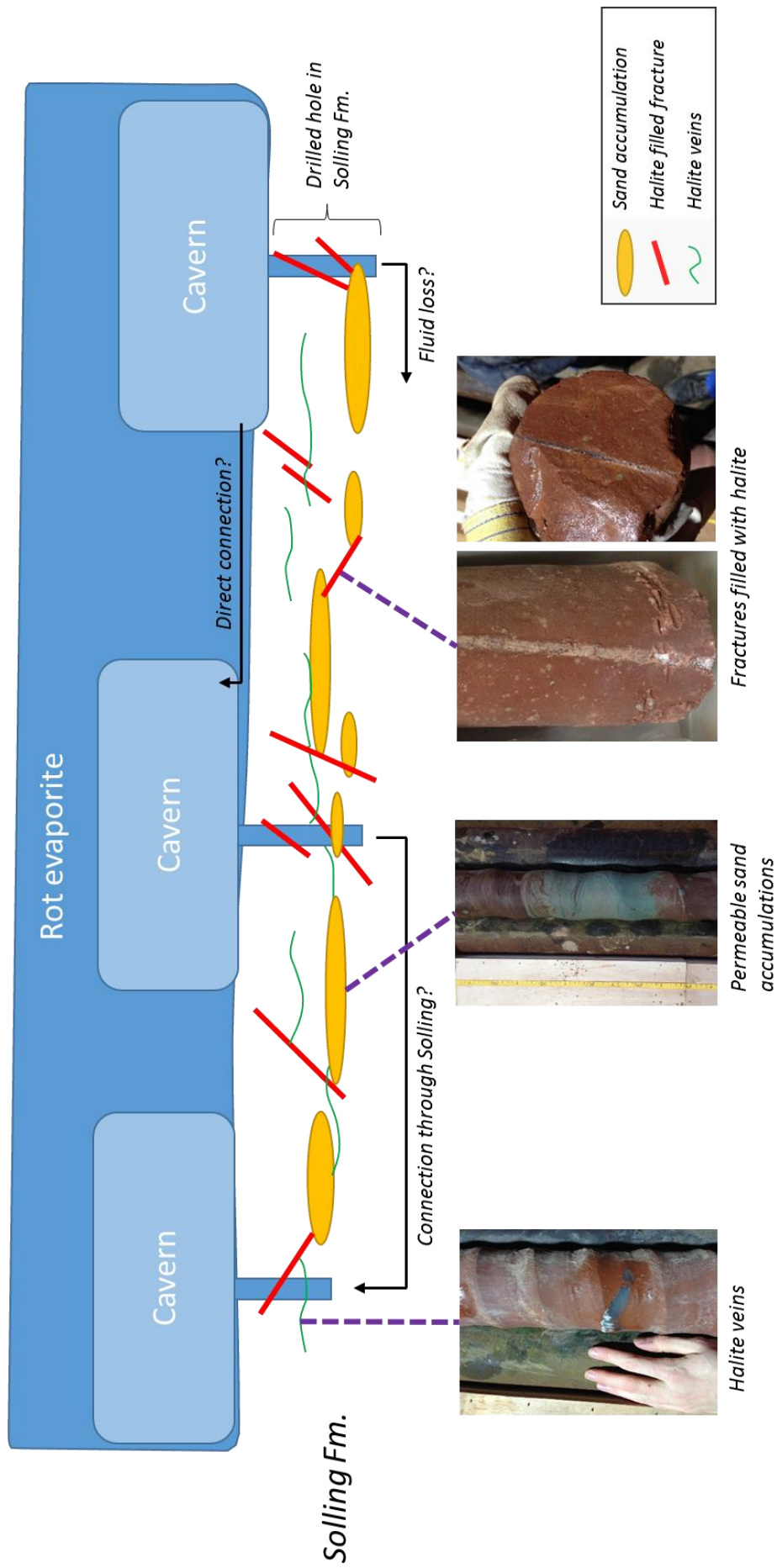


** Illustration is not to scale!*

Figure 50 - Schematic illustration of the Solling formation

This is for example the case between caverns 487 and 488. During pressure tests on cavern 487, pressure variations were noticed instantly at cavern 488. This is only possible when both caverns are directly connected to each other. Otherwise a delay would have been noticed, as described in chapter 6.

6.2.4 Possible explanations for establishing connections

It is clear that connections between caverns and/or Solling Fm. exist. As described in sections 6.2.1-3, three different situations can occur in the field. The connection between the cavern and the Solling Fm. is either established during drilling of the hole or during the development of the sump. Direct connections between caverns can also occur during the development of the sump, but it might also occur during the 1st main leaching stage.

Connection during drilling

As explained earlier the hole is drilled into the Solling Fm. during the drilling operation to ensure that the Rot salt is completely covered. After drilling has completed, the hole is left open. The casings and tubings are installed subsequently, after which the leaching process starts. Fresh water is pumped into the hole to start leaching the salt. This water will however flow into the hole as well, starting to leach fractures in the Solling Fm. and create flow paths into the Solling Fm. This is illustrated in Figure 50.

Development of the sump

The connection can also occur during the development of the sump. This connection can be caused due to two reasons: (i) the sump is developed too close to the top of the Solling Fm., or (ii) the sump is leached with a leaching rate which deviates from the proposed rate.

- i. When the sump is developed too close to the Solling Fm., a large contact area is created between the cavern and the Solling Fm. Both the Rot salt and the Solling Fm. have a dip. The degree of this dip differs throughout the field. Contacts can therefore be established. Although the top of the Solling Fm. is formed by a thin impermeable anhydrite layer, this layer is also influenced by the geological events (section 3.2). Fracturing could have caused the anhydrite layer to break and allowing halite filled fractures or permeable accumulations to reach the top of the Solling Fm. This is illustrated in Figure 51.

In the bottom part of the figure the situation is shown when the sump is developed too deep. The green line indicates the contact between the sump (i.e. cavern) and the Solling Fm. The red circle (A) illustrates the situation when the top part of the Solling Fm. is fractured and permeable rock accumulations can get in direct contact with the sump.

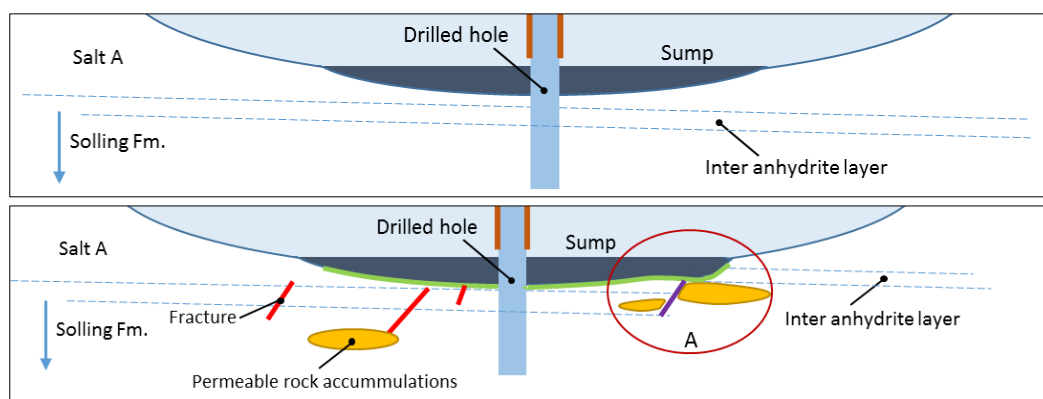


Figure 51 – Schematic illustration of the development of the sump. Top: Normal development. Bottom: Possible situation when the sump is developed too deep.

- ii. According to the HUT (section 2.2.1) the sump is created by maintaining a flow of 15 m³/h for approximately 14 months. In the field these values deviate drastically from cavern to cavern. Some caverns are leached by *slow* leaching whereas others are leached with *fast* leaching. The difference between these two is the difference in flow speed. An analysis was done on caverns at which, during workovers, a steady increase in pressure was noticed. The leaching speed of a select number of caverns was determined. The results are shown in Table 12. The caverns have been chosen according to observations during workovers (H. Leusink & J. Keizer, personal communication, April 22-24, 2015).

Table 12 – Average leaching speeds during the sump phase

Cavern #	Flow (m ³ /h)	Time of sump (months)
Pressure increase noticed during workover		
487	5.9	15.4
488	3.9	22.4
490	3.9	23.8
491	4.9	19.1
504	14.1	10.9
441	15.6	18.4
442	15.1	19.3
505	11.7	11.9
511	8.2	11.7
No pressure increase observed		
482	5.9	15.7

In the table a distinction has been made between the caverns from the individual mass balance tests (section 4.4) and other caverns. Although the flow speeds deviate a lot from the theoretical 15 m³/h, and the time of the sump is in most cases longer than the proposed 14 months, it is clearly visible that there is no relationship between the leaching speed and the connection with the Solling Fm.

6.3 Interaction between caverns and the Solling Fm.

It is clear that there is a certain interaction between the caverns and the Solling Fm. due to the observed fluid losses. These losses can only occur when:

- the permeability is high enough to allow fluids to flow,
- a certain porosity is present, to provide the capacity to hold fluids,
- a pressure gradient exists.

The permeability of the claystone, which forms a large portion of the matrix of the Solling Fm. is believed to be quite low, in the order of micro-Darcy's. During the core observations the presence of sand accumulations was also demonstrated. Lab tests indicated that the pores of the matrix were filled with salt, with, when leached, pore space in the order of 30% (de Vlieg 2015). However to get fluids into these pores in order to leach the salt and create volume for extra fluids, there have to be fluid pathways in place. The fluids pathways are most likely created by the presence of fractures filled with halite and halite veins, as observed in the cores. The fractures and veins, if not filled with anhydrite, can provide excellent pathways for fluids to move through or into the surrounding Solling Fm. The combination of these fluid pathways with the sand accumulations, as shown in Figure 50, can be a possible explanation for the fluid losses. When the fresh water gets in contact with the sand accumulations, which are filled with halite cement, the halite will start to leach and volume will be created. This process is illustrated in Figure 52.

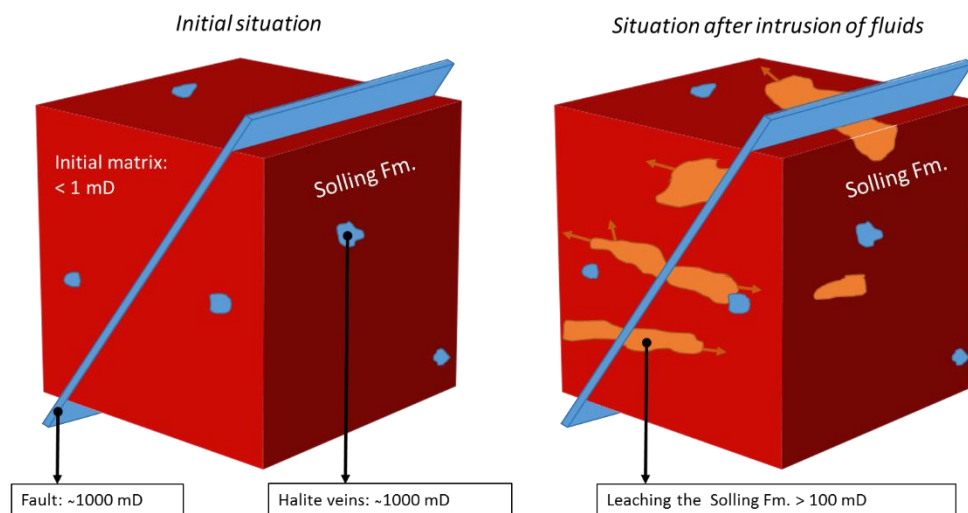


Figure 52 - Schematic illustration of the Solling Fm. Left: the initial situation. Right: Situation after the formation gets in contact with fluids, the veins and faults act as fluid pathways, the leaching process starts in the Solling Fm. Permeability's are taken from tests in the lab (de Vlieg, 2015).

A gradient is also needed in order to allow fluids to flow. In this case the pressure difference is assumed to cause the gradient between the cavern and the underlying Solling Fm. As described earlier the base of the Rot Fm. varies throughout the field, causing pressure gradients between caverns. However the biggest pressure gradient exists between the caverns and the Solling Fm. The cavern pressure is believed to be 'halmostatic'. A cavern is assumed to be halmostatic when a well is filled with saturated brine and no pressure is applied on the well at the wellhead (Bérest 2006). This is the case for the caverns operated in the HBF. The pressure gradient of the brine is approximately 0.12 bar/m. Besides this the cavern is operated with 5 bar overpressure during production. The Solling Fm. is initially at 'hydrostatic' pressure. The gradient of the pressure in the Solling Fm. is assumed to be approximately 0.1 bar/m. At the given depths of the caverns, the difference in these pressure gradients creates large pressure gradients.

6.3.1 Pressure phases in the field

Five different pressure phases/situations can be distinguished during the production of a cavern (Figure 53). During these situations the outflow from a cavern into the Solling Fm., and vice versa, varies. Assuming that the cavern is at 'halmostatic' pressure, the Solling Fm. is initially at 'hydrostatic' pressure and the viscosity of the

brine is constant (i.e. 2 cP), the in-/outflow volumes from a cavern can be estimated using Darcy's law. Darcy's law is given by:

$$Q = \frac{-k \cdot A}{\mu} \cdot \frac{\Delta P}{L} \quad (1)$$

where Q gives the flow in volume per time (e.g. m³/day), k is the permeability (in m², i.e. 1 Darcy = 10⁻¹² m²), A is the area through which the fluid flows (in m²), μ is the viscosity of the fluid (Pa·s, i.e. 1 cP = 10⁻³ Pa·s), ΔP is the pressure drop $P_b - P_a$ (in Pa) and L is the length over which the pressure drop takes place (in m).

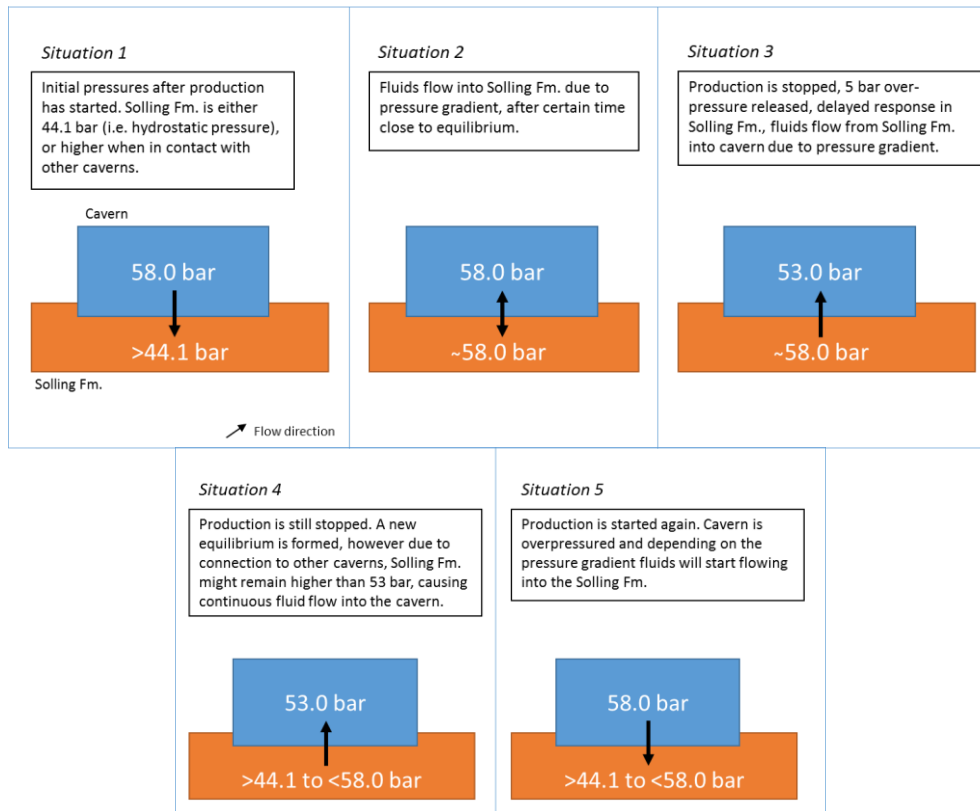


Figure 53 – Different pressure situations during production of a cavern. The situations are explained accordingly in the different boxes.

- Situation 1: Initially the Solling Fm. is at hydrostatic pressure, whereas the cavern (i.e. filled with brine) is at halmostatic pressure plus 5 bar overpressure. This creates the largest pressure gradient of all 5 situations. Fluids can easily flow into the Solling Fm. during this phase.
- Situation 2: After a while the pressure will rise in the Solling Fm. in order to find a certain equilibrium. The pressure gradient will be reduced to a minimum, resulting in less outflow.
- Situation 3: During a workover the overpressure will be released from the cavern. The Solling Fm., which acts like a sponge, will have a higher pressure than the pressure in the cavern. This will start a reverse reaction, fluids will flow from the Solling Fm. into the cavern. This is also the reason why the drilling crew often has to pump considerably more brine from the cavern than theoretically calculated (J. Keizer, personal communication, April 8, 2015).
- Situation 4: During a workover the production is normally stopped for a couple of weeks. Due to the inflow of fluids the pressure will decrease in the Solling Fm. However, due to connections with other caverns, the pressure might remain at a certain level. This might result in a small, but constant, flow of fluids into the cavern.
- Situation 5: After the workover is completed, production will be started again. The cavern will be brought back to 58 bar. Fluids will start to flow into the Solling Fm. again due to the reversed pressure gradient.

For each situation (Figure 53) an estimation can be made of the amount of in- or outflow. These estimations have been made for 3 different permeability's (i.e. 250, 1000 and 2000 mD) with a varying distance. In order to

calculate the volume flow, also the surface (i.e. A) through which the fluids flow needs to be known. A 9 5/8" (approximately 24.5 cm) drill bit is used when drilling the hole. The hole is drilled approximately 1 to 3 meters into the Solling Fm. Assuming that the hole is in contact with permeable fluid pathways, the average surface is 1,15m². The graphs with the flow for each situation can be found in appendix (will be added later). The expected outflows for situation 1 are shown in Figure 54.

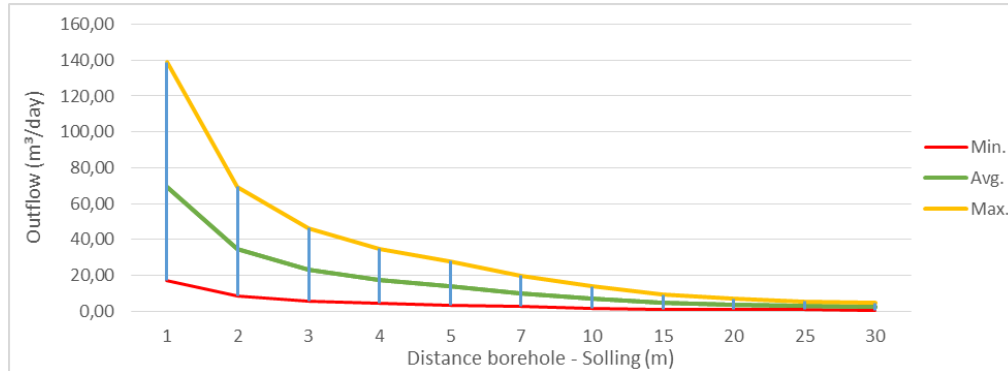


Figure 54 – Theoretical outflows for situation 1, as described in Figure 53. Min = 250 mD, average = 1000 mD and max. = 2000 mD

As can be noticed from Figure 54, there can be a large variation in outflow depending on the permeability. While it is difficult to predict how fast the pressure increases in the Solling Fm., the general trend is that the outflow decreases exponentially with an increasing distance. A summary of all situations can be found in Table 13.

Table 13 – Expected in-/outflows for the different pressure situations. The chosen cavern pressures are based on a depth of 450 m, whereas the pressures for the Solling Fm. have been chosen according to realistic values.

Situation	Length	P _{cavern}	P _{Solling}	250 mD	1000 mD	2000 mD
	m	bar	bar	(m³/day)	(m³/day)	(m³/day)
1	3	58	44,1	-5,8	-23,0	-46,0
2	30	58	47	-0,5	-1,8	-3,7
3	3	53	56	1,2	5,0	9,9
4	3	53	54	0,4	1,6	3,3
5	3	58	54	-1,7	-5,0	-13,2

When comparing the values of the outflow with the values from the individual mass balance tests (section 4.4) it can be concluded the theoretical outflow are possible, although the rates during the test were in some cases much higher.

Outflow rates:

- Average for all active caverns in the HBF: 14 to 20 m³/day
- Average for the caverns from the individual mass balance tests: 25 to 35 m³/day
- Theoretical rates: 5 to 46 m³/day

6.4 In-/Outflow test

It would be interesting to determine whether a cavern is closed or whether it has in-/outflow of fluids. When this has been established it could be proven that the cavern is losing fluids to the Solling Fm. or that it is connected to other caverns.

Different data is available:

- Theoretical volume to be recovered according to the geology
- Water inflow data, from which theoretical cavern volumes can be determined
- Cavern volumes by sonar measurements
- Volume/mass balance of individual caverns

With this data different ratios can be determined. Conclusions can't be drawn by only looking at 1 ratio. The different ratios have to be compared to each other in order to distinguish different situations. When combining these situations it is possible to determine the state of individual caverns. It is important to note that the loss and/or connections are not taken into account when determining the cavern volumes from injected water data. The most important ratio is data from individual mass/volume balance tests. The sonar ratio is then the most important, whereas the geological ratio is the least important ratio. However all three ratios are needed when drawing decisive conclusions. The different situations and respectively combinations which can occur are explained below.

6.4.1 Production vs. Geology

The volume created during the production can be compared to the theoretical volume which could have been produced according to the geology. Every 6.142m³ of injected water creates 1m³. Using this constant the amounts of injected water can be converted to cavern volumes which theoretically have been created. The following formula applies to this ratio:

$$\frac{\text{Production volume}}{\text{Geological volume}} \cdot 100\% = \text{geological ratio}$$

Two situations can be distinguished:

1. < 100%: Less water injected than theoretical geological volume.
Considerably less water injected, and therefore cavern volume created, when compared to the geological recoverable volume. *Production volume << Geological volume.*
2. > 100%: More water injected than theoretical geological volume.
More water injected than theoretical geological volume, water has most likely flowed out of the cavern. *Production volume >> Geological volume*

6.4.2 Production vs. Sonar

The volume of created cavern space from water injection data can also be compared to the measured sonar volume. The following formula applies:

$$\frac{\text{Production volume}}{\text{Sonar volume}} \cdot 100\% = \text{sonar ratio}$$

For this ratio three situations can be distinguished due to the uncertainty of neglected volumes of the sonar volume. Although a correction has been applied to the sonar volumes, there is still a grey area when comparing the production volumes 1:1 to the sonar volumes. The average ratio of the data is 116%, therefore a lower (-5%) and higher (+5%) value have been chosen to exclude doubts.

- a. <113%: Inflow of fluids into the cavern
Considerably less water injected, and therefore cavern volume created, however sonar shows large volume, water has flown into the cavern and leached salt. *Production volume << Sonar volume.*
- b. >120%: Outflow of fluids from the cavern
Considerably more water injected, and therefore cavern volume created than measured with the sonar, water has therefore disappeared. *Production volume >> Sonar volume*

- c. >113% - <120%: No clear distinction
Due to uncertainty in the sonar measurements and to some degree of the production data, no clear conclusion can be drawn about in- or outflow of fluids.

6.4.3 Brine out / Water in (Mass/Volume balance on individual caverns)

The mass/volume balance performed on individual caverns is an extra ratio which can be decisive whether a cavern has in- or outflow of fluids. At the moment this data is only available for 6 caverns (section 5.3). The following distinctions can be made:

- i. >97%: Inflow of fluids
- ii. <95%: Outflow of fluids
- iii. ≈96%: Neutral, ratio according to theoretical value

6.4.3 Possible combinations

When comparing the situations determined for individual caverns different combinations can occur. Certain combinations imply whether a cavern is experiencing in- or outflow of fluids. The possible outcomes and associated conclusions can be found in Table 14:

Table 14 – Possible combinations and conclusions

<u>Conclusion</u>	<u>Combination</u>	<u>Explanation</u>
A	1 / a	Inflow of fluids: Less water injected than geologically possible, less water injected than sonar volume shows; therefore fluids have to come from another location, possible connection between caverns.
B	1 / b	Outflow of fluids: Less water injected than geologically possible, more water injected than sonar shows; therefore fluids have flown out of the cavern, otherwise more volume was created.
C	1 / b / i	Unclear situation: Less water injected than geological possible, more water injected than sonar shows, however individual mass balance shows clear inflow of fluids.
D	1 / b / iii	Slight outflow of fluids: Less water injected than geologically possible, more water injected than sonar shows, mass balance approximately 96%, like 1 / b fluids are expected to flow out of the cavern
E	1 / c	Neutral: Less water injected than geologically possible, water injected compared with sonar is within error margin, cavern is possibly closed and developed as a 'theoretical cavern'
F	2 / b	Outflow of fluids: More water injected than theoretical possible (however still within the dimension limits), more water injected than sonar shows, fluids are flowing out of the cavern
G	2 / b / ii	Outflow of fluids: More water injected than theoretical possible (however still within the dimension limits), more water injected than sonar shows, mass balance smaller than 96%, no other explanation as outflow.

Other combinations are also possible, but did not occur in the current dataset. The results are discussed in the next subchapter.

6.4.4 Discussion

Only caverns which have finished the first leaching stage and are located in Usseleres have been checked to determine if in- or outflow occurs. However this test can also be performed on other caverns in the future, such as the new Ganzebos expansion. A summary of the results can be found in Table 15.

Table 15 - Summary of the results of the analytical in-/outflow test.

Cavern	Situations	Conclusion	
486	2 / b	F	Outflow
487	2 / b / II	E	Outflow
488	2 / b / II	E	Outflow
490	1 / b	B	Outflow
491	2 / b / II	F	Outflow
492	1 / c	D	Neutral
493	1 / a	A	Inflow
494	1 / c	D	Neutral
497	1 / a	A	Inflow
498	1 / a	A	Inflow
504	1 / b / III	C	Outflow
505	1 / a	A	Inflow
506	1 / b / III	C	Outflow
512	1 / a	A	Inflow

Cavern	Situations	Conclusion	
495*	1	-	
489*	1	-	
499*	2	-	Outflow?
501*	1	-	
502*	2	-	Outflow?
503*	1	-	
511*	1	-	
513*	1	-	

*Caverns where only the production data and theoretical geological volume are known, sonar determined with relationship from section 7.3.1

As can be seen in the Table 15, it is possible to determine at least 2 ratios for 14 caverns. Of these 14 caverns, 7 show outflow of fluids. This general trend corresponds with the results of the mass balance tests in chapter 4. When plotting the caverns (Figure 55), in combination with two large faults, inferred to be located on the northwestern and southwestern side of Usseleres, it can be seen that the outflowing caverns are located close to these faults. This could be coincidence, but a flowpath along these faults is not implausible.

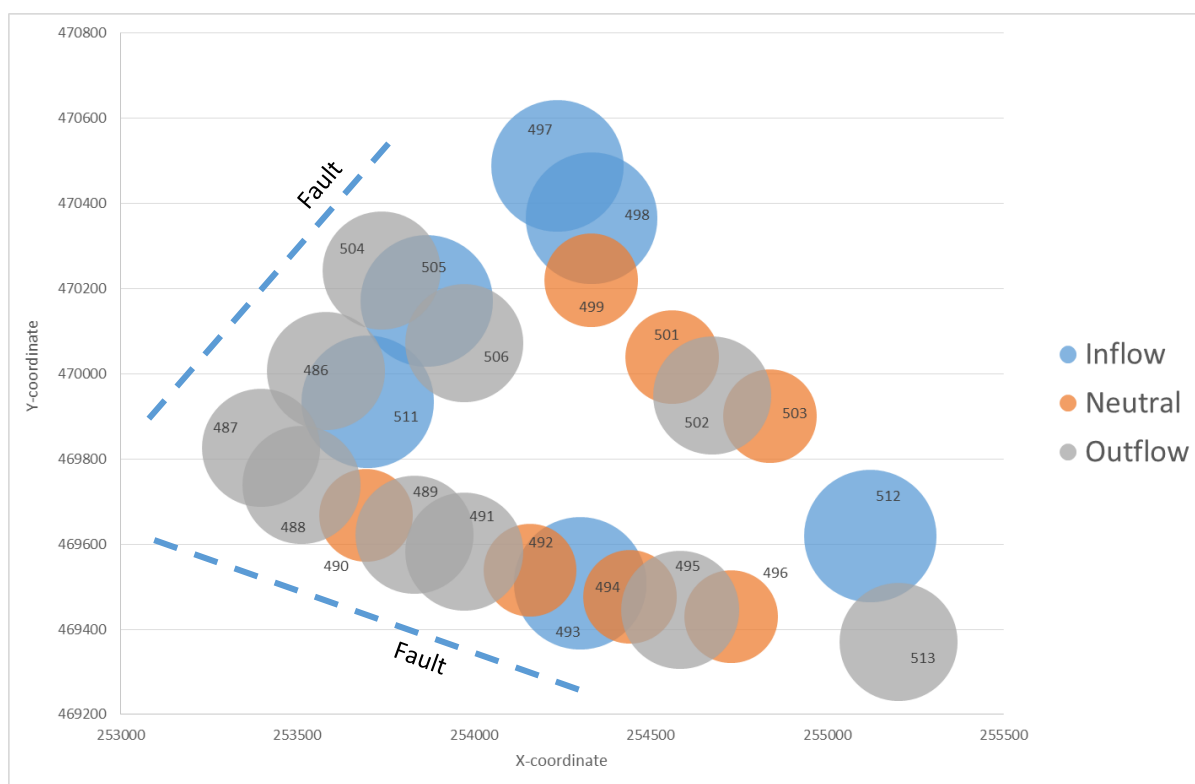


Figure 55 – Map showing the caverns of the analytical in-/outflow test, including two possible locations where faults might be located.

6.5 Where do the fluids go?

Due to the limited amount of flow meters the outflowing brine could only be measured at a few caverns (described in section 4.4). From the 'In-/Outflow test' it was concluded that of the 14 caverns analyzed in the test, 10 caverns showed fluid outflow, whereas at 6 caverns inflow was observed.

The overall amount of outflow is quite large. Assuming the conservative value regarding the plant data, i.e. comparing the flow measured at the producing caverns with the total brine flow measured at the plant (section 4.2.1), 3% of the injected water is lost per year. This results in a volume of $3.3 \cdot 10^5 \text{ m}^3$ of water per year. From previous sections it is known that the Solling Fm. allows flow. The most logical explanation is therefore that the network of fractures creates flow paths through which a large part of the Solling Fm. can be reached. A simple calculation shows the capacity of the Solling Fm., assuming that:

- the current area influenced by the SCC's is approximately 4 km^2 (area calculation),
- 40% of the Solling Fm. is reached over a height of 7 m (core observations),
- the average porosity is 30% (de Vlieg, 2015).

The total volume is in this case $3.36 \cdot 10^6 \text{ m}^3$, which means that the total volume created in the Solling can accommodate almost 11 years of fluid losses, assuming that the fluid losses remain at the $3.3 \cdot 10^5 \text{ m}^3/\text{yr}$.

Assuming that the caverns will lose less fluids in the 2nd main leaching stage, the estimated volume can hold all fluids losses.

It is important to note that the value of the total capacity of the Solling Fm. is highly dependent on the chosen input parameters (e.g. in case only 3 meters of Solling Fm. is influenced, only $1.5 \cdot 10^6 \text{ m}^3$ is available). Figure 56 shows a sensitivity plot with the possible volumes according to the different input parameters

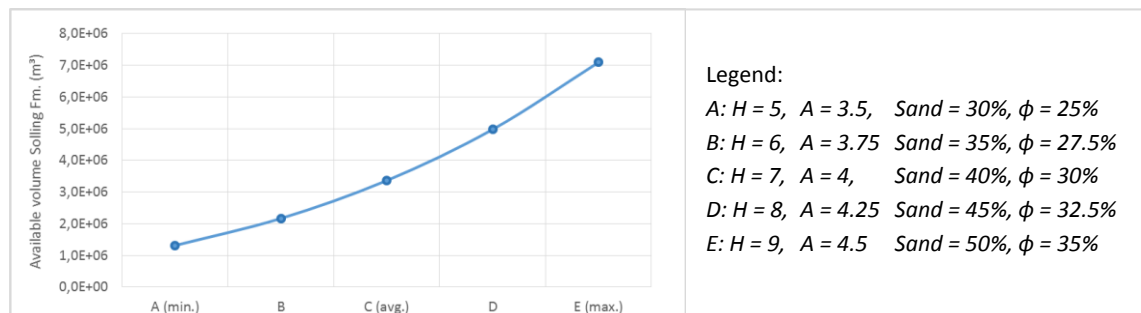


Figure 56 – Graph showing all possible available volumes in the Solling Fm. using different parameters, based on different scenarios (from minimum to maximum)

Another possibility is that the network of fractures creates flow paths to regions outside the concession. From the petroleum industry it is known that fractures can create perfect flow paths, being able to allow flow over 100's of meters. With the Boekelo fault zone (Figure 16) in the direct vicinity, which has a large throw (M. den Hartogh, personal communication, March 21th, 2015), this possibility should not be excluded.

6.6 Summary of key findings

The observations and results discussed in chapter 6 provide more insight into the Solling Fm. The total volume loss is larger than expected. This section summarizes the key findings of the Solling Fm.

- Core observations
 - Fractures filled with halite and anhydrite (structural history)
 - Veins filled with halite and anhydrite (burial phase)
 - Permeable sand layers/accumulations
 - Impermeable clay layers/accumulations
- Possibilities of fluid loss
 - Connection between caverns through the Solling Fm.
 - Fluid loss to the Solling
 - Direct connection between caverns
 - Connection probably created during the drilling procedure or development of the sump
- Interaction between caverns and the Solling Fm.
 - Favorable permeability and porosity
 - Pressure gradient between the caverns and the Solling Fm.
 - 5 different pressure phases identified between the caverns and Solling Fm.
 - Depending on the permeability, a broad variation of possible outflow is obtained (Figure 54)
 - Theoretical values in line with values obtained during experiments at caverns
- Is the calculated loss possible?
 - Using conservative assumptions 3% of the injected water is lost per year (section 4.2.1)
 - Based on various calculations the 'reservoir' in the Solling Fm. is large enough to hold

The data and observations clearly explain the relationship between the caverns and the Solling Fm. It becomes clear that this formation is an important factor influencing production of salt from the HBF. Fluids are lost, energy is lost in order to pressurize the formation constantly and operational delays are common.

7. Sonar measurements

The sonar tool is used to determine the shapes and volumes of the caverns. This is done after each leaching phase and after certain amounts of produced salt (every ~150.000 ton). A sonar device consists of a sound transmitter and receiver, which are located in the rotatable measuring head of the tool (Figure 57). The tool is lowered through the well into the cavern, where it takes its measurement.



Figure 57 – Sonar measurement. Left: Sonar tool hanging in the top part of the well. Middle: Rotatable head of the sonar tool which holds the sound transmitter and receiver. Right: Logging vehicle.

7.1 Methodology

The basic principle of sonar measurements is based on travel time measurements. An acoustic pulse is transmitted from the transmitter into the cavern and is reflected back from the cavern wall. After a certain time the pulse is measured at the receiver (Figure 58). The total travel can be measured and is described as the two-fold distance. When the total travel time is known, the time can be converted to a distance when the acoustic velocity of the medium is known. The sonar tool contains a short and long acoustic velocity calibration device. When a survey is started, the acoustic velocity of the brine is measured using this device. The acoustic velocity of a medium depends on various physical relationships, but in general the density and temperature of the medium are important parameters. In this case the brine density is the most important parameter.

In order to measure the whole cavern the sonar tool can be rotated and tilted. During a survey the sonar tool is rotated and takes a measurement every 5 degrees. This is repeated for different depths in the cavern. The roof is measured using the tilting option of the tool. The head of the tool can be tilted to every position between 0 and 90 degrees. This increases the measuring area drastically. Every measuring point is measured several times, checked, correlated, the energy adapted to the reflection conditions and then optimized.

The acoustic velocity and the measuring frequency determine the wavelength. The wavelength and the size of the survey sensor affect the angle of spread of the measuring beam. In general the following can be stated:

- the higher the measuring frequency, the smaller the angle of beam spread
- the lower the measuring frequency, the greater the range of the beam spread

Every medium has its own specific wavelengths or ranges of wavelength for which should be used during a measurement. Consequently, it is essential to appropriately adjust the sonar measuring device, and therefore the frequency, in order to obtain precise and reliable survey data (SOCON, 2015).

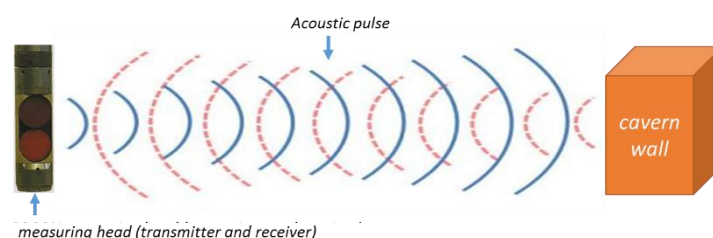


Figure 58 – Illustration of the sonar device when emitting acoustic pulses and the reflection from the wall.

7.2 Limitations & Neglected volumes

There are three main limitations which cause volumes to be neglected and therefore cause underestimation of the total cavern volume. These two limitations are: the geometry and shape of the caverns & the wavelength of the sonar tool.

The geometry and shape of the cavern limits the ability of the sonar tool to correctly measure the dimensions of the cavern. The acoustic pulses can propagate easily in fluids, however when 'hitting' a solid object, the signal is reflected. When measuring the top part of the cavern, the presence of stalactites hanging from the roof, as described in section 3.3 and Figure 59, prevents the sonar tool from measuring behind such objects, even though open volumes are present behind these objects. The result is that volumes are neglected.

The waves which are emitted by the sonar tool have a certain amplitude which is optimized to measure distances of about 60 m. The wavelength of the sonar tool limits the possibility to measure voids or openings smaller than 1 meter. This means that voids/openings which are less than 1 meter are not measured. This is mainly a problem in the sump, since its maximum height is only 2.5 meters. Although the walls of the cavern are assumed to be quite straight, narrow openings in the wall are neglected. These narrow openings in the wall of the cavern could possibly extend for several meters.

The third limitation is the functionality of the sonar tool itself. The head of the tool is tilted per 6 degrees. The measurement points at the edge of the roof at 60 meters distance are 6.31m apart (Figure 59). The current program which is used to create the 3-dimensional sonar volumes interpolates the cavern between these points using a perfect circle, whereas the edge of the roof should be close to 90 degrees because of the principles of the leaching process of salt.

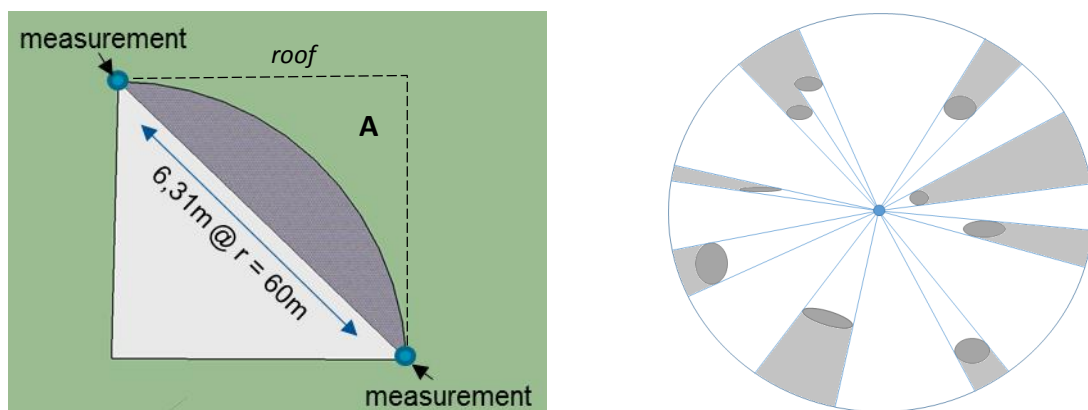


Figure 59 – Left: Illustration of the edge of the roof, the distance between the measuring points is 6.31m at 60m and 6°. Right: Illustration of the roof of the cavern; the grey marked areas indicate the areas which are neglected due to stalactites hanging from the roof.

A distinction can be made between the volumes which are neglected due to the limitations:

- 7.2.1 Sump
- 7.2.2 Roof
- 7.2.3 Wall

Using the Gemcom Surpac software, the neglected volumes for the sump, roof and wall were determined for 23 caverns in both the 1st as 2nd main leaching phase. The edge of the roof was however calculated by hand for each cavern, based on the radius of the cavern.

7.2.1 Sump

The sump is created according to the produced volume, i.e. 11,000 tons (HUT, 2012), which corresponds to a sump volume of approximately 6686 m³ (based on the dimensions and densities). The sonar volumes of the actual sumps of the caverns in the database have been compared to a theoretical sump. As expected all actual sonar volumes were smaller than the theoretical volume due to the limitation of the sonar tool. A large portion of the sump consists of 'wings' which are lower than 1 meter in height. After plotting the neglected volumes it appeared to be a normal distribution which is skewed to the right

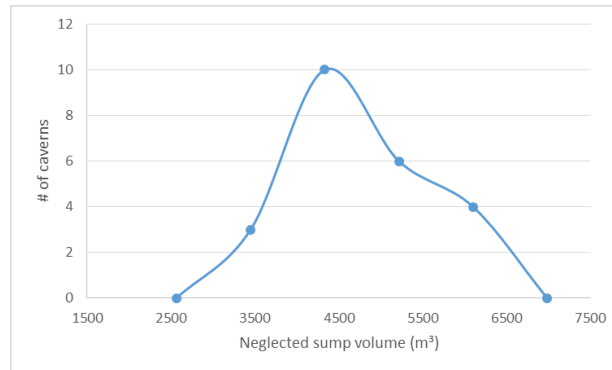


Figure 60 – Distribution of the neglected sump volumes

As described in the chapter 5 only inflowing water is measured. It should therefore be noted that when there is a strong connection with the underlying Solling Fm. fluids can disappear. Since only inflowing water is measured the actual sump can be much smaller than the theoretical sump.

7.2.2 Roof

Surpac was used to determine the neglected volumes caused by stalactites. Assuming that the stalactites have a maximum length of 2 meters (section 3.3) a cylinder was created and placed at the roof of the cavern, based on the borehole information. Subtracting the cavern from the theoretical cylinder resulted in the neglected volumes in the roof.

For the edge of the roof a different method was used. Based on the radius of the cavern the neglected volume was calculated using law of Pythagoras for the distance between the measuring points (Figure 59). When the circle segment is known, area A (i.e. the neglected surface, as shown in Figure 59) can be calculated. When this area is known it can be multiplied with the circumference of the cavern which results in the neglected volume for the edge of the roof.

When plotting the data according to the leaching phase it is clear that the caverns in the 1st main leaching stage contain more neglected volumes than those in the 2nd main leaching stage (Figure 61). This difference is mainly caused by the total size of the roof. The measurement for the 1st leaching stage is directly done after finishing this stage and can be considered as a fixed boundary with the roof leached over the total diameter. The measurement of the cavern during the 2nd leaching phase can however be considered a snap-shot of the cavern at that certain time. The roof doesn't necessarily have its maximum diameter yet. Therefore it is possible that less volume is neglected. Another reason is that the vertical height during MLS-2 is larger compared to MLS-1. The sonar will measure more accurately in this part. At this moment in time the 2nd MLS has not been finished yet in any single completion cavern (SCC). Therefore a good comparison can't be made.

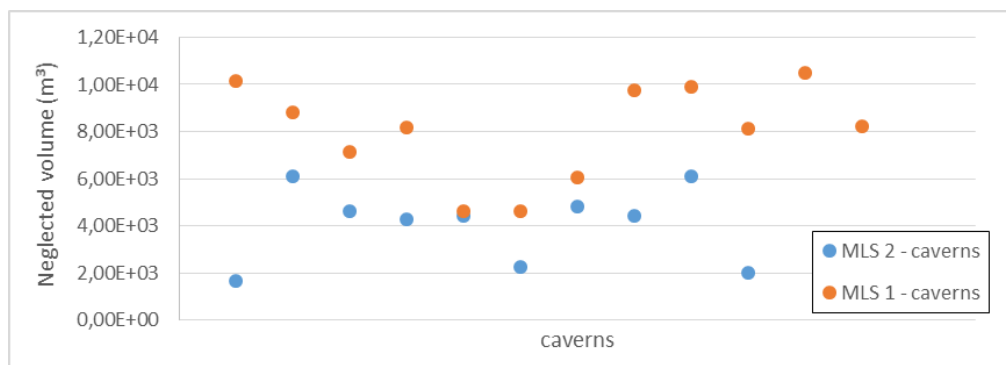


Figure 61 - Neglected roof volumes (i.e. neglected volumes due to stalactites and measuring inaccuracies of the edge of the roof) sorted on leaching phase.

7.2.3 Wall

The wall of the cavern was also checked with Surpac for consistency. 3-Dimensional modelling shows that the cavern wall oscillates along the average radius of a cavern, with an average deviation of 0.6m. This has been analyzed by plotting cross section on top of each other. The following calculation has therefore been made for each cavern:

$$\text{Neglected wall volume} = 2\pi r_{\text{cavern}} \cdot h_{\text{wall}} \cdot 0.6 \quad (1)$$

where the volume is calculated in m³ and the radius and height of the wall are known from the sonar measurements.

7.2.4 Combined neglected volumes

All neglected volumes can be added for each cavern from which a neglected volume distribution can be made. The average neglected volume is $13.9 \cdot 10^3 \text{ m}^3$ with a standard deviation of $2.2 \cdot 10^3 \text{ m}^3$. From this data a random dataset has been generated using the average and standard deviation of the measured cavern, to compare whether the calculation can be considered normal distributed or not. Figure 62 shows the results.

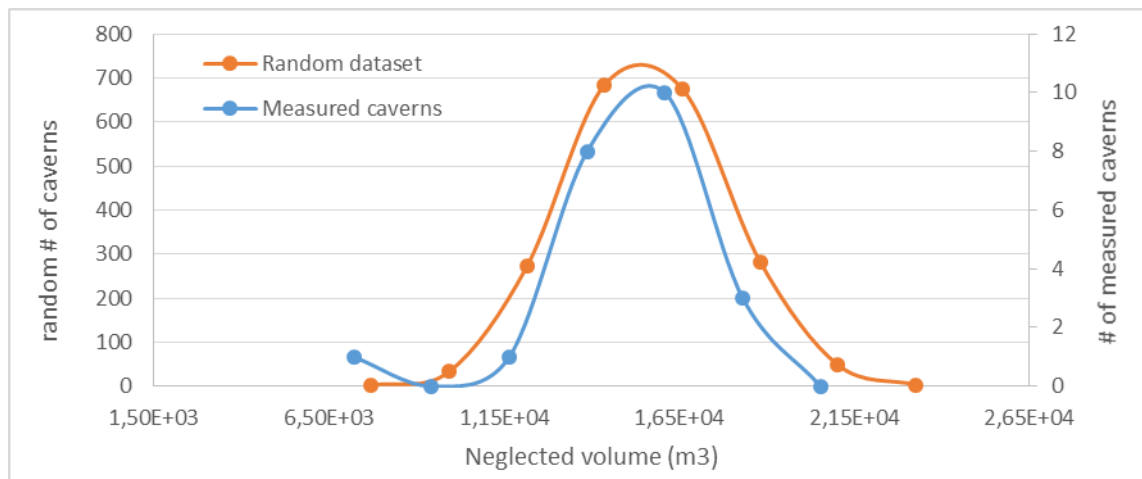


Figure 62 – Total neglected volumes for the measured caverns (i.e. the sum of the neglected volumes of the sump, roof and wall). The neglected volumes are clearly normal distributed.

The so-called 'Bell Curve' is clearly visible, indicating that the neglected volumes are normally distributed. When looking in more detail to the relevant leaching stages the following can be concluded:

- 1st MLS: average neglected volume: $13.4 \cdot 10^3 \text{ m}^3$ (+/- $2.7 \cdot 10^3 \text{ m}^3$)
- 2nd MLS: average neglected volume: $14.9 \cdot 10^3 \text{ m}^3$ (+/- $1.5 \cdot 10^3 \text{ m}^3$)

The differences of the average and standard deviations are mainly caused by the size of the neglected volume in the roof of the cavern.

The result of this neglected volume determination is that on average 23% of the cavern is neglected using the current sonar equipment. For the relevant leaching stages the following results apply:

- 1st MLS: average neglected volume compared to sonar measurement: 30% (+/- 6.6%)
- 2nd MLS: average neglected volume compared to sonar measurement: 14% (+/- 2.6%)

The large difference between these values can be attributed to the fact that the caverns are much smaller during 1st MLS, whereas the neglected sump volume is the same as for the 2nd MLS. Percentage-wise this has a huge impact on the average. In general it can be said that although the total amount of neglected volumes are similar for both leaching phases, although since the volume of the 1st MLS is much smaller, the impact of these volumes is greater for these caverns.

7.3 Sonar-/Production volume relationship

The term production volume refers to the volume created in the cavern (i.e. leached volume) based on production data. Correcting the sonar volumes with the neglected volumes, the 'new' sonar volumes can be compared to the volumes calculated from production data. From this comparison a relationship can be established between the sonar and production volumes.

The production volumes are determined from the injected amount of water. For this relationship the amount of injected water has been determined from the start of the 1st MLS until the last sonar measurement. The sump has been neglected, since the cavern is not yet saturated during this phase. The theoretical dissolution equation does therefore not apply. The theoretical sump volumes (i.e. 6086 m³) have therefore been subtracted from the corrected sonar volumes.

As described in section 5.1.3 96.1% of the injected water is theoretically produced. A similar calculation can be made for the amount of volume created in the cavern with respect to the injected water and produced brine. The density parameters are equal to those used in chapter 5.

Water needed to dissolve 1 m³ of halite:
$$\left[\frac{M_{\text{halite}} \cdot M_{\text{H}_2\text{O}}}{M_{\text{halite in brine}}} \right] = \frac{2165 \cdot 889}{312} = 6169 \text{ kg}$$

Brine volume after dissolving 1m³ of halite:
$$\left[\frac{\rho_{\text{halite}}}{M_{\text{halite in brine}}} \right] = \frac{2165}{312} = 6.9 \text{ m}^3$$

1 m³ remains in-situ, total volume produced: 5.9 m³

In order to produce this 5.9 m³ of brine, the following amount of water is injected:
$$\left[\frac{M_{\text{water}}}{\rho_{\text{water}}} \right] = \frac{6169}{998} = 6.181 \text{ m}^3$$

(This ratio produced/injected corresponds to the 96.1% from section 5.1, since $\frac{5.9}{6.181} = 96.1\%$)

Therefore it can be concluded that when injecting 6.181 m³ of water, 1 m³ of volume space is created. This conversion factor can be used to convert all production volumes to leached cavern volumes, after which the data can be compared to the corrected sonar volumes (i.e. actual sonar volume + neglected volume).

7.3.1 Relationship without taking loss of fluids into account

The sonar- & production volume relationship is shown in Figure 63. Fluid losses have not been taken into account when converting the raw production volumes to leached cavern volumes.

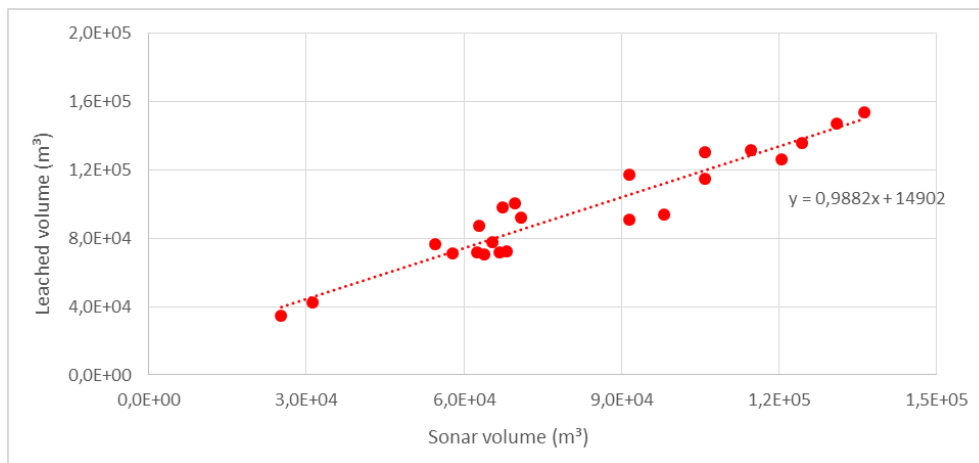


Figure 63 - Relationship between the leached volume and the sonar volume.

As expected a linear trend can be noticed between the leached volumes and corresponding cavern sonar volumes. The equation for the trendline shows however a systematic difference in both volumes, while it is

expected to be equal to each other. The calculated leached volume is consequently higher than the corresponding sonar volume. Indicating that either the injected water has disappeared, as described in chapter 5, or that the sonar volumes have even more unaccounted neglected volumes.

A distinction can be made between the 1st and 2nd main leaching stages regarding the relationship between the leached volume and sonar volumes. These relationships are shown in Figure 64.

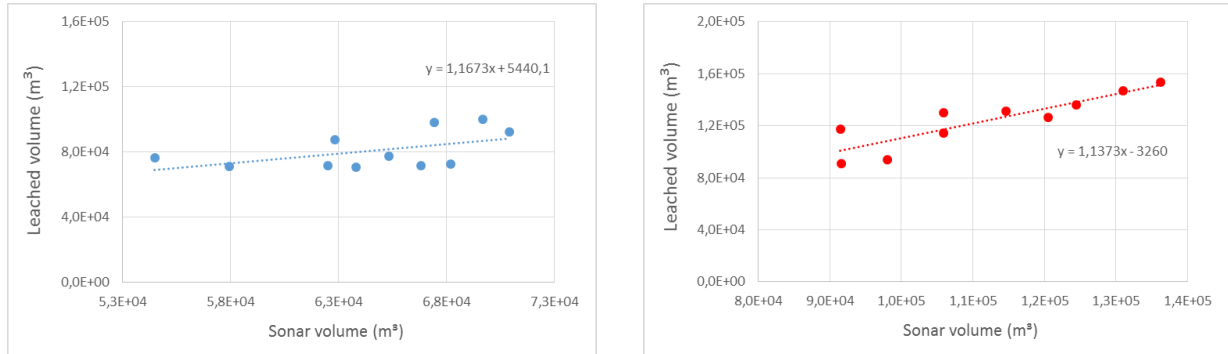


Figure 64 - Leached volume vs. sonar volume relationships. Left: Relationship for MLS-1 caverns. Right: Relationship for MLS-2 caverns.

From the equations for the trendlines the systematic deviation for both relationships is visible again, indicating that either less cavern volume is leached or the sonar measurement is still incorrect after correcting it for neglected volumes. For the MLS-1 caverns a deviation of 16.7% is observed, whereas for the MLS-2 caverns it is approximately 13.7%.

Although the trendlines show linear trends, the relative error can be calculated using the two relationships (i.e. the relationship of the combined caverns and the relationship for the specific leaching stage). Figure 65 shows the error calculation for the MLS-2 caverns. It can be noticed that for caverns larger than $1.1 \cdot 10^5 \text{ m}^3$ the error becomes smaller than 10%.

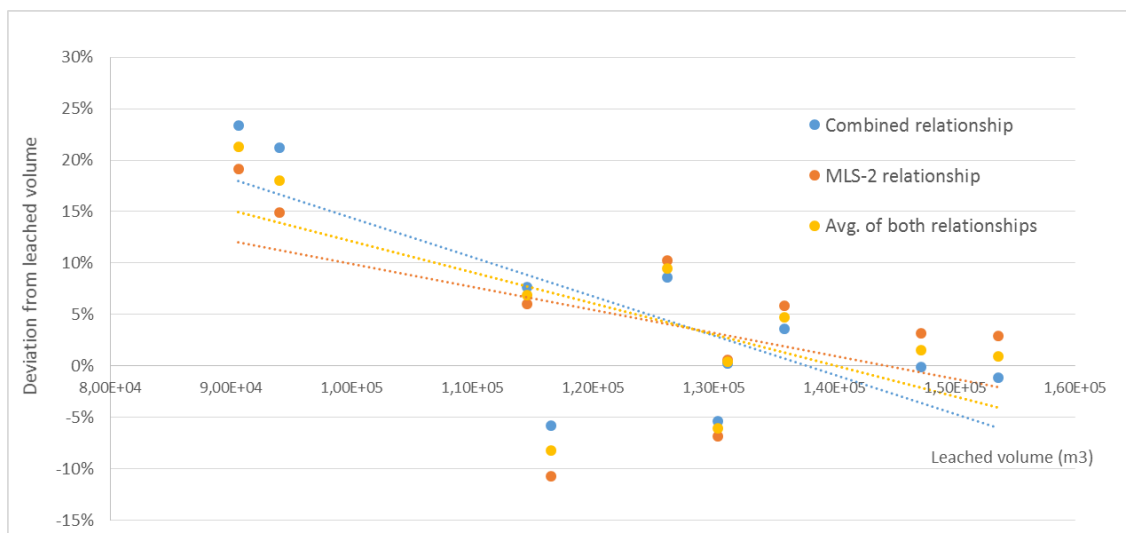


Figure 65 - Error when using the relationships to determine the cavern volume

7.3.2 Relationship when taking fluid losses in consideration

Assuming that the average fluids losses in the field are close to 3% of the total volume (chapter 5), the produced volumes can be corrected after which the leached volumes are updated to more realistic cavern volumes. Plotting the sonar data with these updated cavern volumes provides a more accurate relationship. Using this relationship after a sonar measurement has been conducted, will provide a good indicator for the leached amount of salt, which can be converted back into a certain production volume.

The relationships for MLS-1, MLS-2 and both types combined are shown in

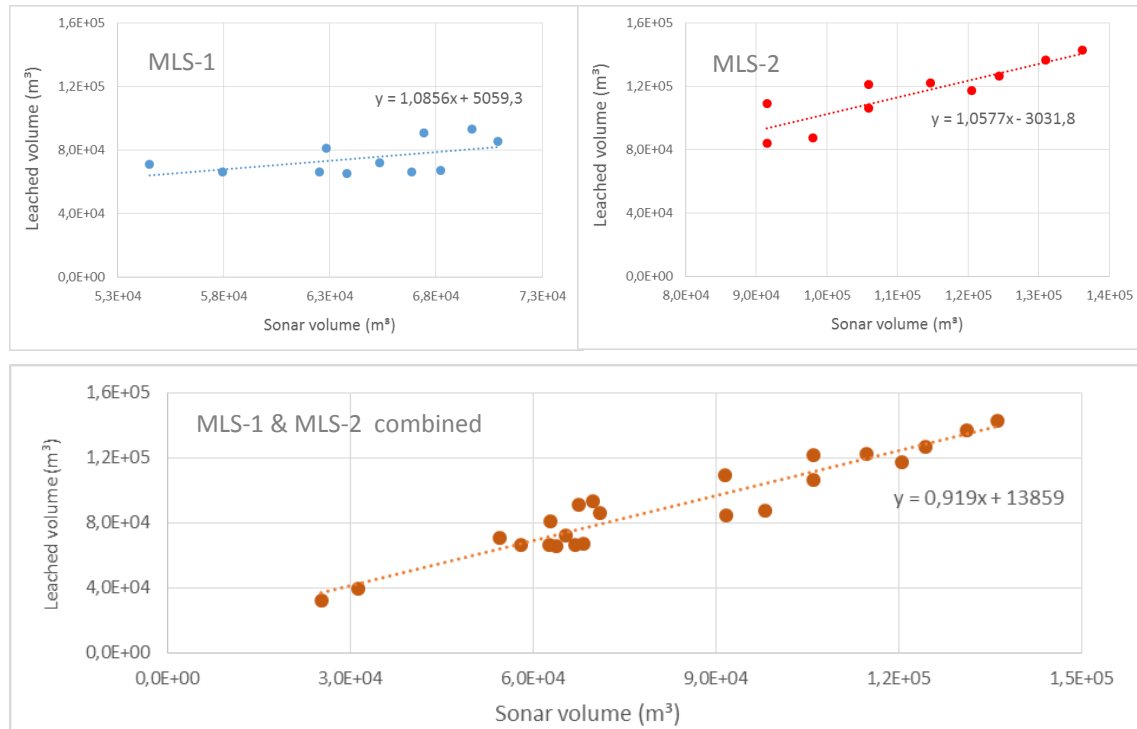


Figure 66 – Relationships between the leached volumes (calculated from the corrected production data) and volume from the sonar measurements (corrected for the neglected volumes) are shown in the three graphs. Top left: Relationship for MLS-1 caverns. Right top: Relationship for MLS-2 caverns. Bottom: relationship for the combined types of caverns.

7.4 Summary sonar measurements

The sonar tool is used in the HBF to determine the shapes and volumes of the caverns. In essence it is a monitoring tool which provides an 'image' of the cavern. The tool, which technique is based on transmitting and receiving acoustic pulses, has however some major limitations when used in salt caverns. The main limitation is the presence of stalactites. Another limitation is the resolution of the sonar tool.

These limitations translate into neglected volumes at different location in the cavern. The neglected volumes in the sump, roof and wall have been analyzed separately. According to the data it was concluded that the neglected volumes are normally distributed. The following averages were determined:

- Combined: average neglected volume: $13.9 \cdot 10^3 \text{ m}^3$ ($\pm 2.2 \cdot 10^3 \text{ m}^3$)
- 1st MLS: average neglected volume: $13.4 \cdot 10^3 \text{ m}^3$ ($\pm 2.7 \cdot 10^3 \text{ m}^3$)
- 2nd MLS: average neglected volume: $14.9 \cdot 10^3 \text{ m}^3$ ($\pm 1.5 \cdot 10^3 \text{ m}^3$)

As the cavern size increases, the standard deviation of the neglected volume decreases. Therefore it can be stated that the accuracy of measuring a cavern increases when the cavern becomes larger.

The data has been used to establish a relationship between the sonar- and produced volume. Although the exact production volume is unknown (sections 4 & 6), the relationship is linear and can be used in the reconciliation tool.

8. Insoluble material & Bulking factor

Before the volumes of the caverns can be determined accurately, the insoluble content of the caverns needs to be analyzed, since this will determine the total amount of halite to be produced. Closely related to the insoluble content is the bulking factor. This chapter will first discuss the bulking factor. The second part will describe the method used for determining the insoluble content, finally the results will be discussed.



8.1 Bulking factor

In general bulking occurs when soil or rock is excavated: volume-wise one cubic meter of soil or rock at the source does not translate into the same cubic meter when excavated. It is therefore necessary to use a *bulking factor* to determine the volume of material that will be created when leaching the salt. Bulking factor is defined as:

$$\text{Bulking Factor} = \frac{\text{Volume after dissolving}}{\text{Volume before dissolving}} \quad (1)$$

The bottom of the cavern is largely filled with insoluble inert material and secondary precipitates formed in the dissolution process. In case of the salt caverns the bulking factor of the insoluble material depends on the type of material that is present in and between the different salt layers. Therefore two bulking factors are applicable for the salt caverns:

- 8.1.1 *Bulking factor of the insoluble material in the halite*
- 8.1.2 *Bulking factor of the rock layers in between salt layers*

8.1.1 Bulking factor insoluble material in the halite

Most insoluble material in the halite consists of anhydrite and anhydritic claystone. When salt is washed out, these insolubles fall to the cavern bottom; with an insoluble bulking factor in the order of 1.5 (Bérest et al., 2006). This volume increase is partially caused by the swelling of clay. The nature of this reaction depends on the structure of the clays and their chemical state at the moment of contact. The other cause for the increase relative to the original volume is the settling of the angular anhydrite particles. The pieces typically do not fit together perfectly, which results in an increase in void space included with the anhydrite particles (Ofoegbu et al., 2008)

8.1.2 Bulking factor rock layers in between salt layers

The rock layers separating salt layers A, B and C, consist almost entirely of anhydrite and anhydritic claystone. When the cavern is leached up to the top of salt A, the rock layer between A and B normally collapses due to a loss in strength. It is however assumed that this layer breaks up in large sheets which float to the bottom of the cavern, resulting a low bulking factor. The bulking factor of these rock layer fragments can be assumed to be very low, in the order of 1.1. This is the same value as is determined by Bekendam (2011), who concluded that the bulking factor of the overlaying strata is approximately 1.11. Figure 67 shows a schematic representation of the bulking factors.

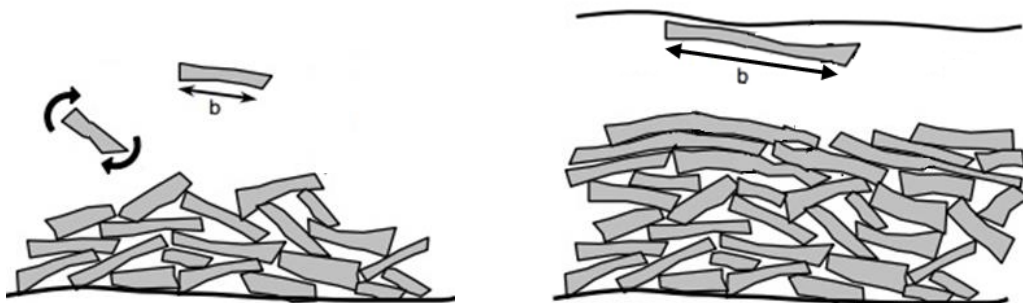


Figure 67 – Representation of the two bulking factors, the length of fragments is given by *b*. Left: Insoluble material present in the halite falls to the bottom of the cavern, the void space is quite high resulting in a high bulking factor. Right: When the cavern is leached out to the roof, i.e. the rock bench separating the salt layers, the roof can collapse, large fragments will float to the bottom and tend to pile up as layers, resulting in a low bulking factor.

8.1.3 Current bulking factor

A bulking factor of 1:1.55 is currently used for caverns around Hengelo. This value is based on reports and knowledge from other caverns in Europe. Accurate research regarding the specific bulking factor of the caverns of the Hengelo Brine Field has however never been carried out. It is important to determine the bulking factor as it is used to establish the safety height of the cavern and to compensate for the extra volume of the insoluble material. When the bulking factor increases the safety height of the cavern also increases. At the moment the insoluble material at the bottom of the cavern is calculated from the volume of the produced salt and multiplied by the bulking factor to determine the volume it occupies in the cavern.

With the large database it is possible to determine whether the current bulking factor is appropriate for the caverns in the Hengelo Brine Field or whether it should be changed.

8.1.4 Bulking factor vs. Void ratio

The bulking factor is closely related to the void ratio. The void ratio is the ratio of the volume of void space to the volume of solid substance in any material consisting of void space and solid material, such as the rock fragments on the bottom of the cavern. The total volume is therefore equal to the volume of the voids plus the volume of the solids. Furthermore the void ratio is closely related to the porosity. The following formulas show the relationships (Craig, 1974):

$$V_T = V_S + V_V \quad (2)$$

$$e = \frac{V_V}{V_S} = \frac{V_V}{V_T - V_V} = \frac{n}{1-n} \quad (3)$$

$$n = \frac{V_V}{V_T} = \frac{V_V}{V_S + V_V} = \frac{e}{1+e} \quad (4)$$

$$BF = \frac{V_T}{V_S} = \frac{V_T}{V_T - V_V} = 1 + e \quad (5)$$

Where V_V is the volume of void space, V_S is the volume of solids, V_T is the total volume, e is the void ratio, n is the porosity and BF is the bulking factor. From the formulas shown above it follows that the porosity can be determined using the bulking factor, this is shown in formula (6).

$$n = \frac{BF - 1}{BF} \quad or \quad BF = \frac{1}{1-n} \quad (6)$$

When the void space in the material on the bottom of the cavern is known, the porosity of this loose material can be determined. Eventually the relationship between the bulking factor and porosity can be used to determine a bulking factor which corresponds to the porosity / void space.

The current bulking factor of 1.55 implies that the insoluble material at the bottom of the cavern has void space of 35.5%. The insoluble material will be described before analysis will be done using three dimensional volumes from the sonar measurements,

8.2 Insoluble content background

Most of the insoluble impurities found in salt deposits around the world are anhydrite and traces of claystone (Bérest et al., 2006). The Röt salt deposit at the HBF is relatively thin, tabular and flat. Variations in the insoluble content are however identified and will be discussed in the next subchapters.

8.2.1 Insoluble content HBF

In the Röt salt the insolubles are formed during the evaporation cycles. During an evaporation cycle most insoluble material will precipitate first, whereas the soluble materials will precipitate at a later point during the cycle. Theoretically the top of the salt contains less insolubles. However, in the Röt salt certain sub-cycles have caused disturbance. During these sub-cycles the basin received more net water inflow, but not enough to induce a switch from evaporites to clays. These sub-cycles probably occurred during the formation of salt A (M. den Hartogh, personal communication, June 2, 2015), since an increase in insolubles is measured towards the top of salt A.

Furthermore the halite layers are separated by rock layers, mainly consisting of anhydrite and claystones. Salt A is normally the thickest (>25 meters) halite layer in the HBF.

In the drilled cores, the insolubles are clearly visible. The insolubles occur as continuous layers (A) but also smaller nodules (B) are observed.

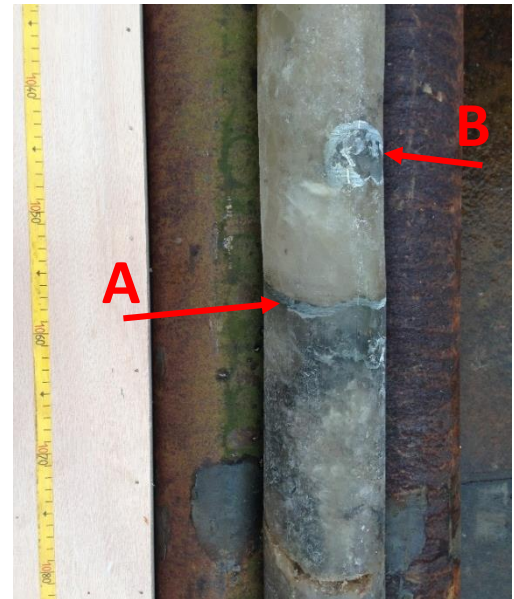


Figure 68 – Drilled core in salt A; showing insolubles in the clear salt. B; insoluble nodule present in the salt

The insolubles which sink to the bottom of the cavern vary in particle size. Figure 69 shows some examples of this insoluble material. It is clearly visible that there is a big variation in fragment size.

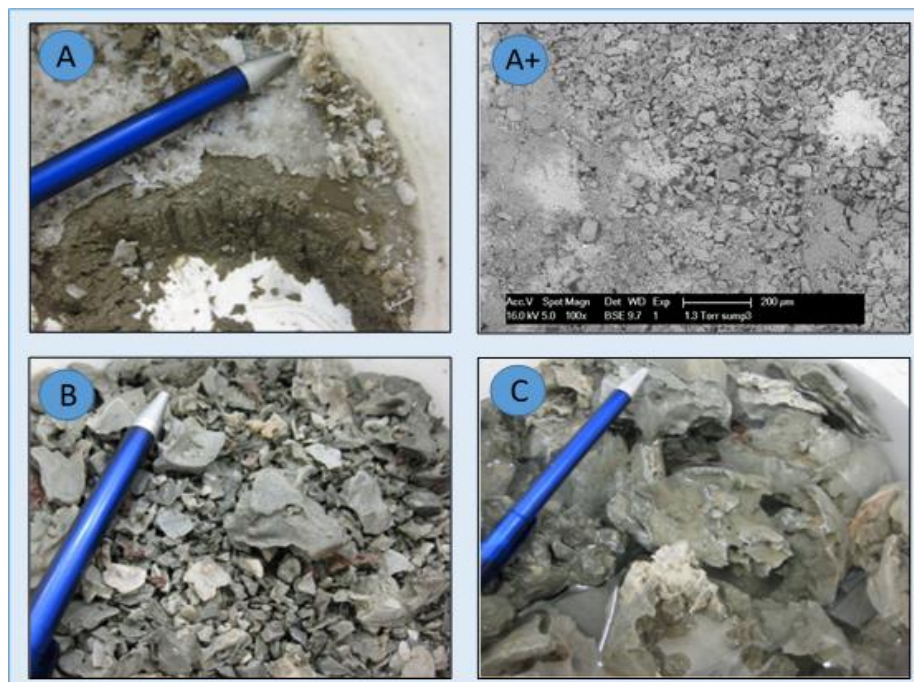


Figure 69 – Pictures from the fractions (Drost, 2012). A is the fraction with the smallest particles (< 2mm) and A+ shows the particles when zoomed in with an electron microscope, the particles of B range from 2mm to 6cm and C shows the particle fraction larger than 6 cm.

AkzoNobel is currently using an average value of 10% insolubles for its reserve calculations. This value is based on a report by Westendorp (1969). It should be noted that this report is based on 1 cavern (i.e. cavern 151). Although it is generally known that the insoluble percentage deviates over the field, 10% was believed to be accurate enough. However in order to increase the level of confidence when calculating the remaining and future reserves, a leaching-stage specific insoluble content should be determined.

8.3 Insoluble content determination

The insoluble content can be determined using the sonar measurements of the caverns. During the life of a cavern multiple sonar measurements are made. The total cavern can be visualized using the program Surpac. From these visualizations the insoluble content can be determined.

8.3.1 Method

In this section an overview is given of the steps involved when determining the insoluble content. The steps are shown in Figure 70. It consists of a general part (blue boxes) and Surpac modelling part (orange boxes). First of all, all sonar measurements of a particular cavern are saved in the BPB-database. From this database the 3-dimensional sonar files can be exported and imported into Surpac. In Surpac the sonar measurements are converted into so-called 'solids'. The entire cavern can be reconstructed by merging all solids. The last sonar measurement indicates the current cavern filled with brine. Eventually the insoluble content can be calculated by dividing the insoluble volume by the bulking factor and dividing it by the total, historic, volume. These steps are repeated for all caverns from the dataset (section 2.5).

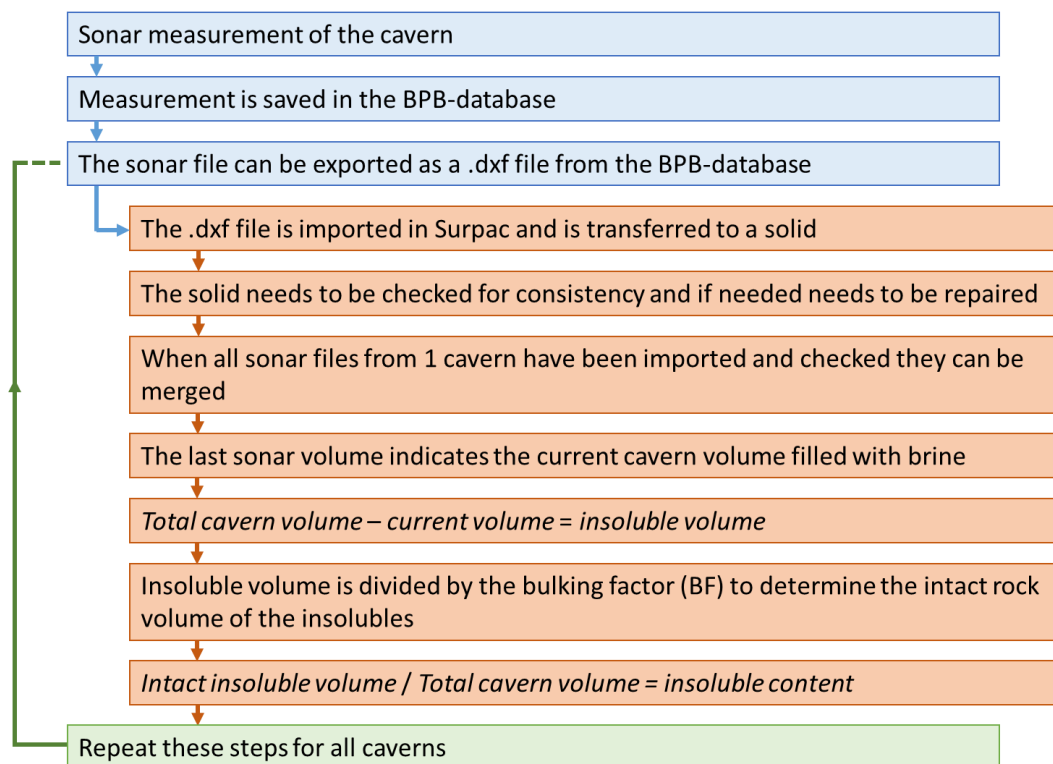


Figure 70 - Steps involved when determining the insoluble content

Figure 71 shows an example, using cavern 487. The green and white portions together form the entire cavern volume, whereas the white is the portion of the cavern which is currently filled with fluids. Subtracting the white (i.e. the current volume) from the total cavern volume results in the insoluble volume. The last two steps of the process are explained above.

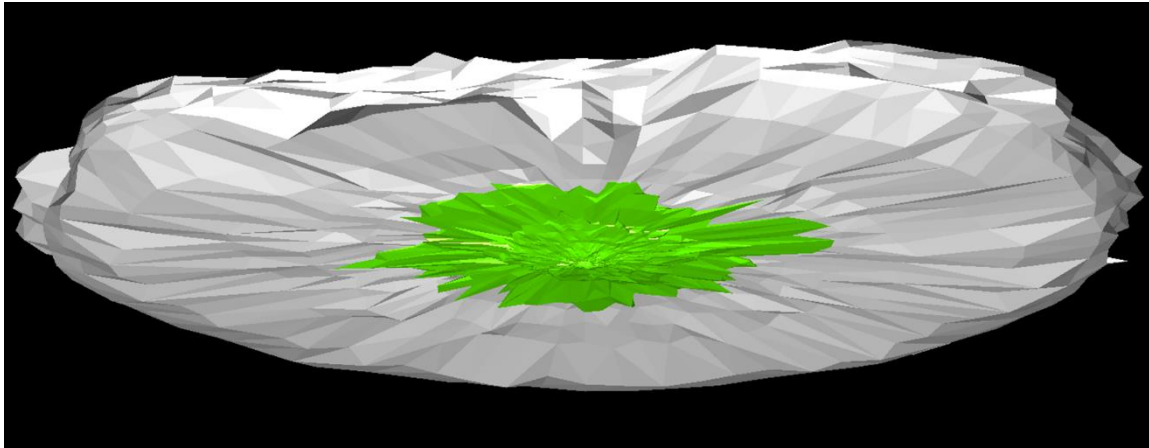


Figure 71 – Insoluble content analysis of cavern 487. The green portion indicates the volume measured during the first sonar measurements, whereas the white is the volume measured during the most recent measurement. Subtracting the white volume from the total volume gives the amount of insoluble material which lies currently at the bottom of the cavern.

8.3.2 Hypothesis

According to Westendorp (1969), the insoluble content is approximately 10%. The expectation is however that the insoluble content varies from leaching stage to leaching stage. Due to sub-cycles during the evaporation process of salt A, it is expected that the insoluble content varies in the salt layers, probably increasing towards the top. It is known (M. den Hartogh, personal communication, June 22, 2015) that there are three zones within salt A which contain with more insoluble material. Due to the fact that MLS-1 is much lower in height than MLS-2, there is the possibility that one of these bands is located in MLS-1 whereas the other two are located in MLS-2 (or even all three in MLS-2). This will cause a large variation in the insoluble content when comparing both stages.

8.3.3 Insoluble content from modified cavern volumes

The insoluble content was determined for 22 caverns (instead of the 23 from the dataset, cavern 504 was not taken into account due to some 3-dimensional validation issues). A distinction has been made between caverns in the 1st and 2nd main leaching stage. The results are given in Figure 72. The values shown have been calculated with the average bulking factor of 1.55. The average insoluble contents are:

- MLS 1: 4.8%
- MLS 2: 9.6%
- Combined: 7.1%

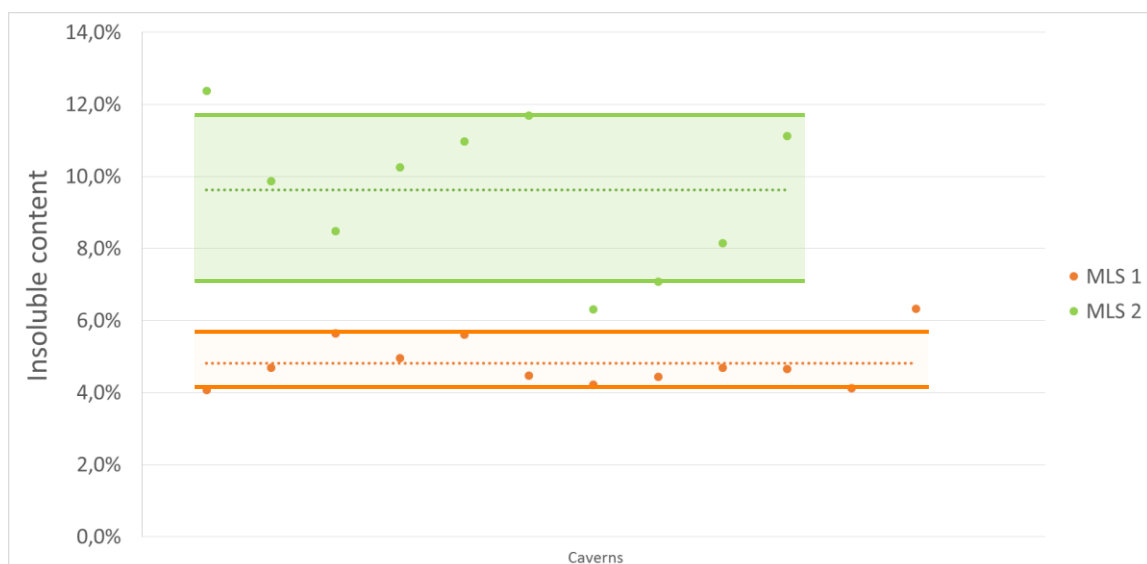


Figure 72 - Results of the insoluble content determination.

A clear distinction can be noticed between caverns in the 1st - vs. the 2nd main leaching stage. It can therefore be concluded that the insoluble content increases towards the 'top' of Salt A. This is in line with the hypothesis.

As a comparison the insoluble content has also been determined for 9 MCC's. In addition salt C has also been leached in 3 of these caverns, indicating that the insoluble interlayers plus salt B have collapsed. This is clearly visible in the insoluble content, i.e. on average 26% for these 3 caverns, whereas the insoluble content of the other 6 caverns, which were only developed in salt A show the same trend as the SCC's in Figure 73.

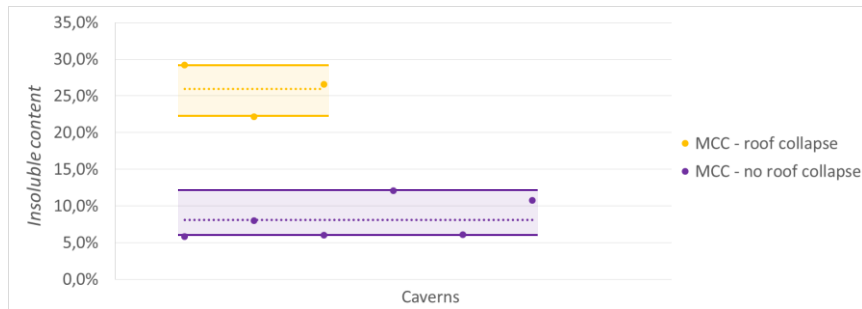


Figure 73 – Results of insoluble content determination for multiple completion caverns (MCC's), a bulking factor of 1.11 is used for the insoluble interlayers and salt B, as explained in Figure 67.

The results shown in Figure 72 are however determined with a bulking factor of 1.55. When varying the bulking factor from 1.4 to 1.7, a distribution of values is acquired from which both the average insoluble content can be determined as well as the standard deviation. The distribution for both leaching stages and the combined dataset are shown in Figure 74 below:

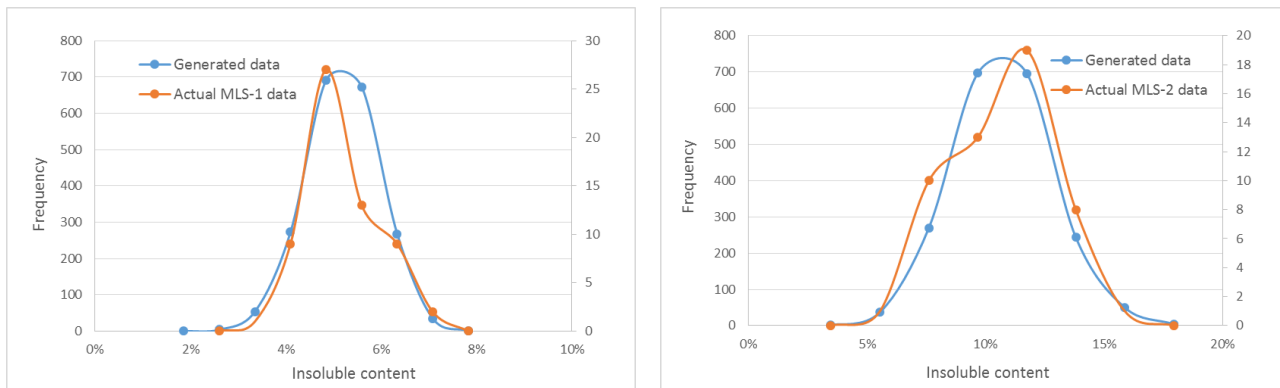


Figure 74 - Frequency distributions of the insoluble contents. Left: Distribution of MLS-1 caverns. Right: Distribution of MLS-2 caverns. The generated data shows the distribution of 2000 random numbers, determined with the average and standard deviation of the actual data.

Both graphs in the figure include two lines. The orange line shows the frequency of the actual data, whereas the blue line shows a distribution based on 2000 random number based on the average and standard deviation of the actual datasets. The following standard deviations have been determined:

- MLS-1: 0.75% (with an average of 4.8%)
- MLS-2: 2.1% (with an average of 9.6%)

Comparing the generated data with the actual data it can be concluded that the distribution of the insoluble content for the MLS 1 caverns is skewed to the right, whereas the distribution of MLS 2 data can be considered normally distributed. The chosen bulking factor of 1.55 seems appropriate, as it gives a good average of the insoluble contents in both leaching stages.

8.4 *Summary insoluble content*

The bulking factor and insoluble content are closely related. Most insoluble material in the halite consists of anhydrite and anhydritic claystone. When the salt is dissolved, these insolubles sink to the sump. There are two different bulking factors; one for insoluble material in the halite and one for the layers separating the different salt layers. For the insoluble material a bulking factor of 1.55 is used, whereas only 1.11 is used for the insoluble interlayers. The main reason for this difference is the size of the insoluble fragments. The regular insoluble material varies a lot in particle size, resulting in a high bulking factor. The fragments of the interlayers are generally much larger, resulting in a lower bulking factor (Figure 67).

Using the Gemcom Surpac software the amount of insoluble material has been determined for more than 20 caverns. By varying the bulking factor (with an average of 1.55) a distribution of insoluble contents was determined. For the entire dataset (i.e. a combination of MLS-1 and MLS-2 caverns was used) the average insoluble content is 7.1%. However, a distinction can be made between the two leaching stages:

- MLS-1 has an average of 4.8% insolubles, with a standard deviation of 0.75%
- MLS-2 has an average of 9.6% insolubles, with a standard deviation of 2.1%

Currently only one insoluble content (i.e. 10% (Westendorp, 1969)) is used for calculating the amount of salt in cavern. The results suggest however that AkzoNobel is currently overestimating the insoluble material, since the average insoluble content is only 7.1% instead of the assumed 10%. Furthermore the insoluble material can also be determined in greater detail because a distinction can be made between the different leaching stages.

9. Other uncertainties

In addition to the sonar measurement, bulking factor and insoluble content more uncertainties can be determined which are described in this chapter. First the Gamma Ray log will be discussed. The relation between the gamma ray & insoluble content and correlation between wells are analyzed. The seasonal effects on leaching and water volumes are discussed. The chapter concludes with the effects of salt creep.



9.1 Gamma Ray log

The natural radioactivity of rocks has been used for years to support derive lithologies. There are different naturally occurring radioactive elements such as uranium, thorium, potassium, radium and radon, along with the minerals that contain them. Gamma ray logging (i.e. GR logging) is a method of measuring naturally occurring gamma radiation to characterize the rock or sediment in a borehole.

The tool contains a sodium-iodide (NaI) scintillation detector. NaI detectors usually contain a NaI crystal coupled with a photomultiplier. When gamma ray from the formation enters the crystal, it undergoes multiple collisions with the atoms of the crystal, resulting in a short flashes of light when the gamma ray is absorbed. The light is detected by the photomultiplier, which converts the energy into an electric pulse (Ellis & Singer, 1987). The number of electric pulses is recorded in counts per seconds (i.e. c.p.s.). The higher the gamma-ray count rate, the larger the clay content and vice versa. After logging a borehole using this technique a Gamma Ray log (i.e. GR log) is acquired.

Every rock types has its own radiation level. Figure 75 shows the distribution of radiation levels for various rock types. Evaporites (halites, anhydrites) and coals typically have low levels. In other rocks, as the shale content increases, the radioactivity increases. The highest radioactivity is measured at organic-rich shales and potash.

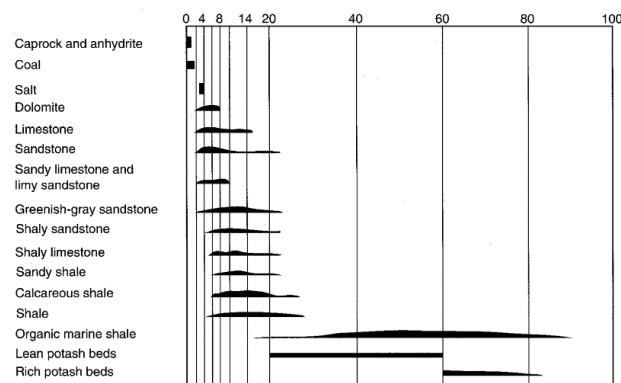


Figure 75 - Distribution of radiation levels (Russell, 1944).

The GR logging tool is mainly used in the Hengelo Brine Field to determine the boundaries of the top and the bottom of the salt. The transitions between the 4 salt layers (A, B, C & D) are also determined. These boundaries can easily be detected due to the high readings.

It would be useful to determine a relationship between the GR-log readings and the amount of insolubles present in the salt. However, it proves to be very difficult to determine such a relationship. This can be attributed to the following factor which affect the accuracy of the data:

- The resolution of the GR-logging tool
- Inclination of the borehole

9.1.1 Interpretation of Gamma Ray logs

Matlab has been used to interpret the GR-logs and determine the surface of the curve. The logs were loaded into Matlab and smoothed. The smoothing was done using the smooth-function. This MATLAB function smooths the data using a moving average filter. The result is for cavern 484 is shown in Figure 76.

The surfaces were determined with the trapz-function. This function performs numerical integration via the trapezoidal method. This method approximates the integration over an interval by breaking the area down into trapezoids with more easily computable areas. The GR-logging is done with a constant depth interval of 0,05m.

For an integration with N+1 evenly spaced points, the approximation is given by:

$$\int_a^b f(x) dx \approx \frac{b-a}{N} \sum_{n=1}^N (f(x_n) + f(x_{n+1}))$$

$$= \frac{b-a}{N} [f(x_1) + 2f(x_2) + \dots + 2f(x_N) + f(x_{N+1})]$$
(1)

where the spacing between each point is equal to the scalar value given by $\frac{b-a}{N}$.

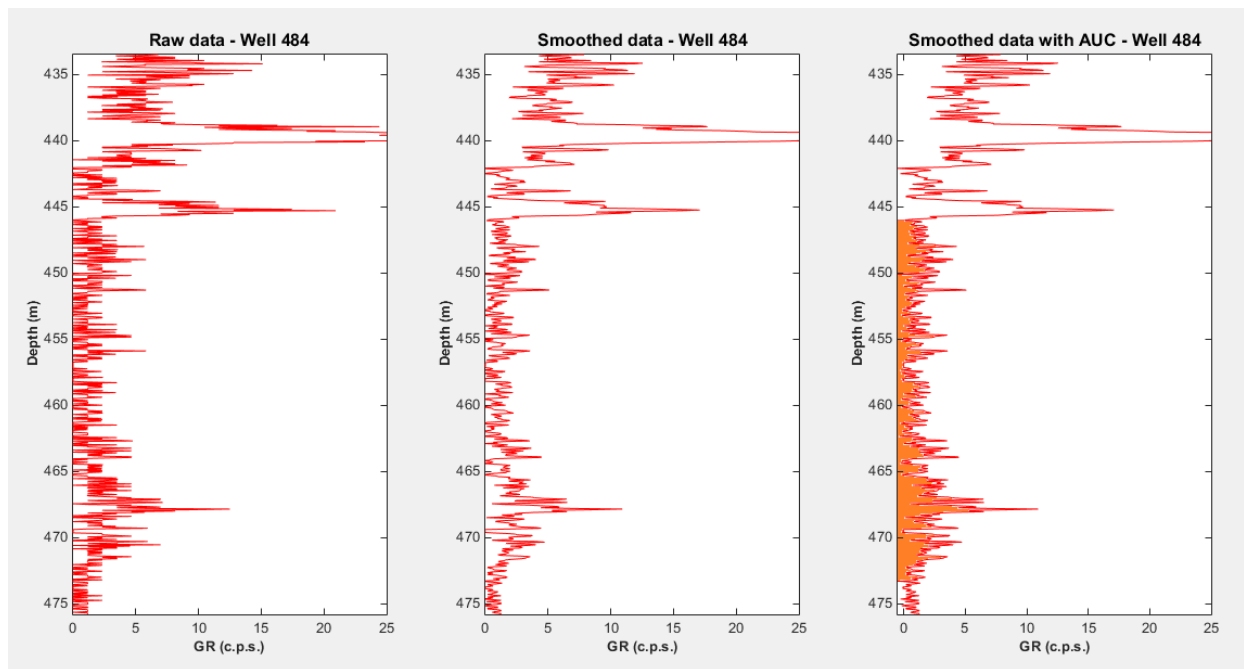


Figure 76 – GR-log data from well 484. Left: raw data. Middle: smoothed data. Right: Smoothed data, the orange coloured surface indicates the AUC (i.e. Area under Curve).

Three types of surfaces have been calculated for:

- The entire salt A, minus 1 meter from the top.
- The section which is mined in the first main leaching phase of salt A (MLS-1)
- The section which is mined in the second leaching phase of salt A (MLS-2), minus 1 m from the top.

The results are given in counts per second and are summarized in Table 16.

Table 16 - Properties of the surfaces, calculated for the 23 wells from the dataset.

c.p.s.	MLS-1	MLS-2	Salt A
Minimum	65	651	818
Maximum	205	2325	2600
Average c.p.s.	124	1197	1396
Average per m	24,9	59,9	46,5

The surfaces are then plotted versus the corresponding insoluble contents which are determined for the various caverns from the dataset. This has been done for the original insoluble data and the dataset which has been adapted to the neglected volumes in the sump and roof.

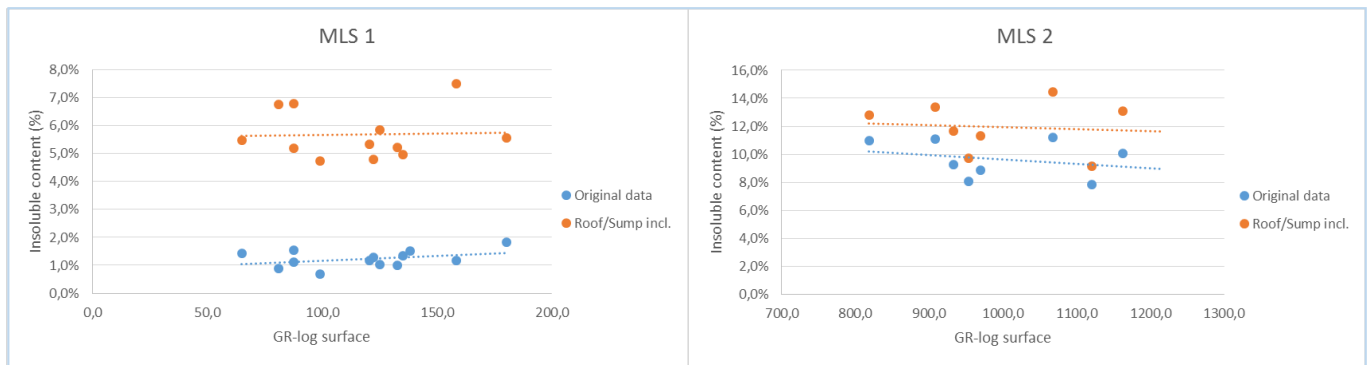


Figure 77 – Surfaces of the GR-logs plotted vs. the insoluble contents of the corresponding caverns. Left: showing the data from the first leaching phase (MLS-1). Right: data corresponding to the second leaching phases of salt A.

Figure 77 shows that there is not a clear relationship between the GR-log and the insoluble content. The relationship found from MLS-1 data indicates a very small increase in insoluble content with an increasing GR-log surface, whereas the MLS-2 data even show a slight decrease. The expectation was that with an increasing GR-log surface would correspond with a higher insoluble content, due to the anhydritic claystone, which is one of the main constituents of the insolubles present in the HBF salt.

The reason why a relationship can't be established is possibly caused by the resolution of the GR-logging tool and the inclination of the borehole. The salt in the HBF consists of very pure halite, it therefore has a very low natural radiation level. Insolubles consist of anhydritic claystones which only have a slightly higher radiation level. The levels between these lithologies do not exceed the 10 c.p.s. (counts per second). On average the readings of the GR-log vary by 4 c.p.s. Figure 78 shows a correlation between the gamma ray log of well 480 and its actual core. It can be noticed that large salt intervals (1 & 2) can be correlated to almost 0 readings on the GR-log. Small impurities, i.e. insoluble material, surrounded by pure salt, result in higher readings. It is however unknown if these impurities are continuous throughout the entire cavern.

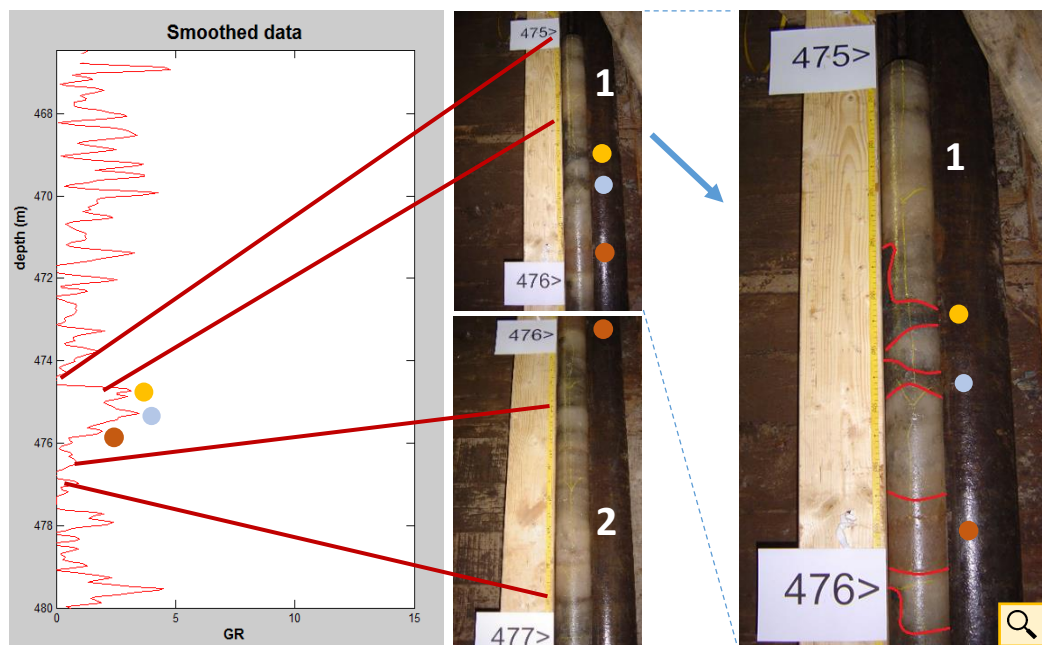


Figure 78 – Correlation between the gamma ray log and the actual core.

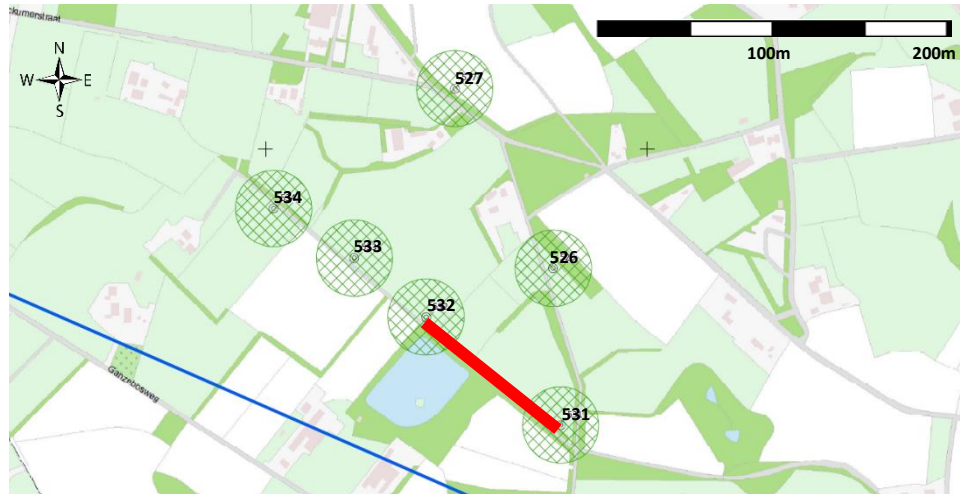


Figure 79 – Correlation between two adjacent caverns, indicated by the red line.

9.1.2 Correlating GR-logs

The boreholes are not drilled vertically. In case of an inclined borehole the GR-logging tool may lie against the borehole wall, resulting in relatively high gamma ray readings. Small impurities can cause high peaks in the data, while the impurity has a very local occurrence. In case the impurities form layers in the salt layer, it should theoretically be possible to interpret them on multiple logs. This has been done for wells 531 and 532, Figure 79 shows the location, whereas the correlation is shown in Figure 80. A clear correlation is observed for the rock layers separating the various salt layers. When looking closer also some smaller peaks show correlation. The combination of the inclined boreholes, background noise and resolution of the gamma ray readings make it however difficult to correlate all events.

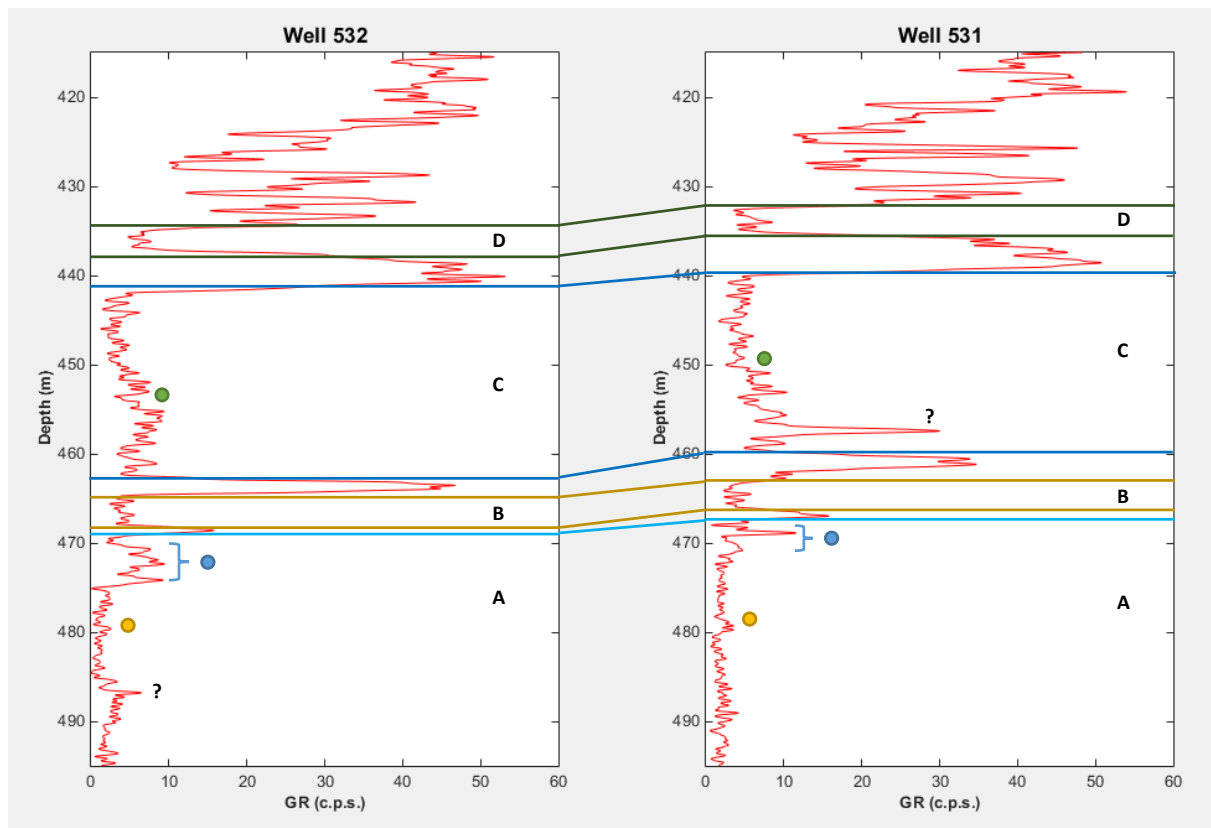


Figure 80 – Correlation of the GR-logs of wells 532 & 531. The 4 salt layers can easily be correlated, but the continuation of the individual smaller peaks are difficult to match on both GR-logs.

It can be concluded that the GR-logs are useful for defining the salt intervals, but that the information is insufficient to relate it to the insoluble material present in the salt. Due to the resolution and outliers caused by borehole inclination it is too difficult to determine continuous layers between caverns.

9.2 Seasonal effects

Two effects can be affected due to seasonal variation of the temperature:

- The leaching process might change due to temperature changes of the inflowing water
- The flow meters give lower readings due to thermal expansion of the water in the field

9.2.1 Effect on the leaching process

Due to the thermal gradient ($\sim 0,05 \text{ }^{\circ}\text{C/m}$) the temperature of the caverns is fairly constant at approximately $20\text{--}23 \text{ }^{\circ}\text{C}$. When assuming that the injection water is colder during the winter months, due to water intake from the canal, the temperature in the cavern might drop. The well can however be seen as a heat exchanger. The drop is therefore reduced to a minimum. When injecting this water into the cavern the difference in volumes can be compared to injecting water with a garden hose into an Olympic swimming pool. When injecting $25 \text{ m}^3/\text{h}$, only 0.35% is injected per hour. The temperature will therefore only change around the outlet of the water injection pipe.

The cold weather has however an effect on the wellhead. When the wellhead becomes too cold, the brine temperature also decreases, resulting in crystallization of salt minerals at the wellhead. When maintaining enough flow this issue can be addressed sufficiently.

Another effect of temperature changes could affect the solubility (Kunstman & Urbanczyk, 2008) of the salt. The solubility would decrease for a temperature decrease. A temperature decrease from $20\text{--}0 \text{ }^{\circ}\text{C}$ may cause a loss of 2.4 grams of salt to dissolve per liter of water, this will however never occur due to the heat exchange capacity of the borehole and the large cavern volume in relation to the flow.

9.2.2 Thermal expansion

Due to thermal expansion the volume of water measured at the flow meters is not equal to the volume of water which enters the cavern. The outside temperature changes throughout the year. This variation affects the temperature of the mixing water directly, because mixing water is a combination of run-off process water and water from the canal. Figure 113 in appendix G shows the average temperatures in Hengelo. Assuming that the canal water has the same temperature as the air, the temperature of the mixing water can be calculated with the following formula:

$$\text{mass} \cdot \Delta T_1 \cdot C_p = \text{mass} \cdot \Delta T_2 \cdot C_p \quad (2)$$

The temperature of the water from the processing plant is fairly constant at $20 \text{ }^{\circ}\text{C}$, whereas the ratio canal water/process water is on average $30\%/70\%$. The average temperature of the mixing water is shown in Figure 81.

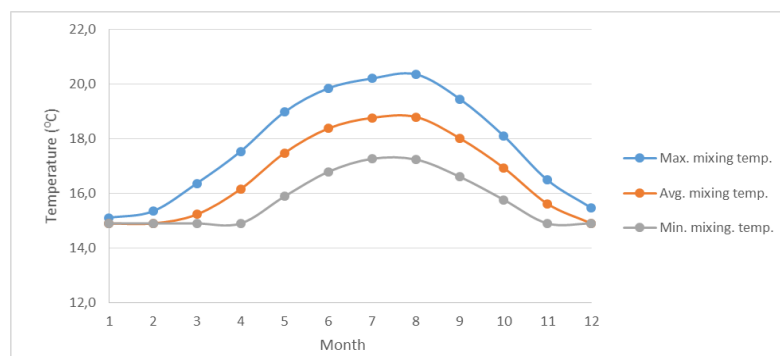


Figure 81 – Maximum, minimum and average temperatures of the mixing water.

When the water enters the cavern the temperature has increased to approximately 23 °C. Comparing the densities of the mixing water which is measured at the pump station with the density when it enters the cavern, a volume correction can be applied.

This correction is on a yearly average close to 1.0014 (1 m³ at the pump station is 1.0014 m³ at the cavern). This results in an underestimation of the total water volume which enters the caverns of 1.10·10⁴ m³ on average over the last 4 years. This is only 0.12% of the total water volume.

According to both effects explained above, the effect of seasonal temperature variation is negligible.

9.3 Salt Creep

Salt creep is a process that has the ability to decrease the volume of the cavern and therefore increase the pressure. The creep is usually subdivided into three phases: primary (strain-hardening, transient, decelerating), secondary (steady-state) and tertiary (accelerating, strain-softening) creep. The secondary phase is the most important one for salt creep. Secondary creep represents an equilibrium state between strain hardening and the recovery process. A general relation for deformation by creep is given by:

$$\frac{d\varepsilon}{dt} = A e^{\frac{-Q}{RT}} \sigma^n \quad (3)$$

where ε is the creep strain, A is the proportionality constant (MPa⁻ⁿ S⁻¹), Q the activation energy (J/mol), R the gas constant (J/mol/K), T the absolute temperature, σ the in-situ stress and n the stress exponent related to the micro-mechanism of deformation. According to research at 15 different salt types in the USA (van Sambeek et al., 2005) the creep is highly dependent on temperature, stress and type of material. Larger stress/higher temperature will induce higher creep rates. In the HBF the salt is only buried 500 m deep, which is considered shallow in the salt mining industry. In combination with a fairly constant temperature, the creep rate is very low in the HBF. Calculations conducted by Deltares (van Duijne, 2012) indicates a volumetric creep rate ranging from -0.014‰/year to -0.026 ‰/year, which corresponds to a volume loss of 3.6 m³ to 6.5 m³/year. After 15 years this results in a volume loss of 0.54‰ to 0.98‰, assuming a standard SCC cavern. These numbers are negligible.

Salt movement

When a viscous substrate is overlain by a frictional plastic overburden of laterally varying thickness the differential load of the overburden causes a pressure gradient and Poiseuille flow in the viscous material. In case of a sediments overlaying salt this phenomena is called 'salt mobilization' (Gemmer et al., 2005). For the HBF this effect is negligible due to the relatively shallow depth, and thin salt layer.

9.4 Summary of uncertainties in the field

As described in chapters 3, 4, 5, 7, 8 & 9, the operation is dealing with many uncertainties. Figure 82 shows the various subjects that cause uncertainties for the operation at the HBF. It can be concluded that currently the geological effects cause the most uncertainty for the production of salt in Hengelo.

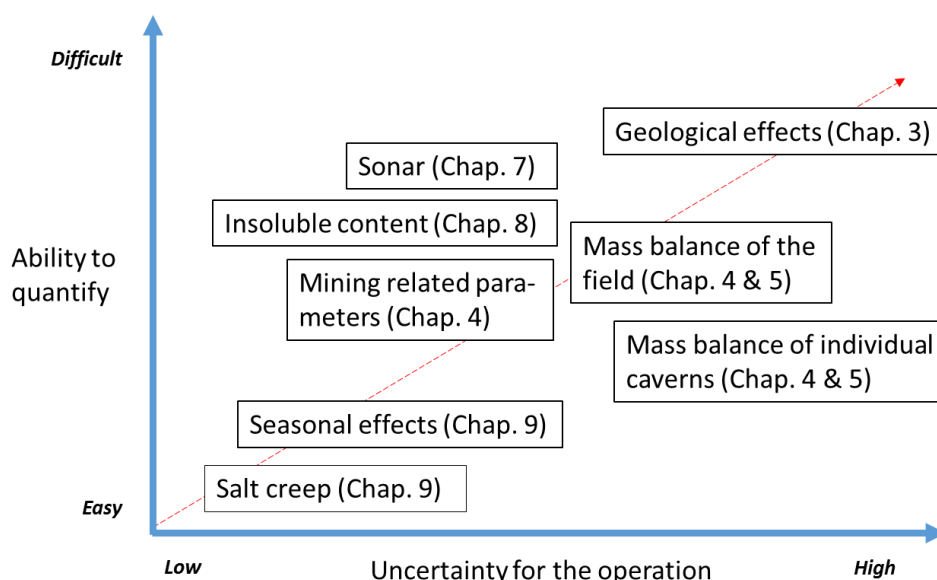


Figure 82 – Summary of the uncertainties in the HBF and the ability to be quantify each of them.

10. Reserve reconciliation tool & implementation

This chapter describes the proposed reserve reconciliation tool. First the current long term development plan (LT-plan) will be discussed, which will include a history matching analysis. A study regarding the recovery factor has been conducted, indicating two different recovery factors for a cavern.

Furthermore the reserve reconciliation tool has been implemented for 23 caverns in the Usse-leres area. The development of these reserves is discussed. This tool will include the relationship between the sonar- and produced volumes (chapter 7) and updated insoluble contents (chapter 8). Information from chapters 4, 5 and 6 can be very useful for certain caverns as well, as it is clear that the brine out/water in ratio is not 0.96 due to various reasons.



10.1 Current LT-plan

The Long Term plan (i.e. LT-plan) describes the production per month of the field. It is updated on a yearly basis and forms the basis for the planning of new caverns. The plan includes the following information (T. Pinkse, personal communication, June 2, 2015):

- Assumptions regarding the peak capacity of the plant
- The capacity utilization factor, based on field and plant data
- Assumptions regarding activities in the field (e.g. slack time for maintenance)
- The reserves for all caverns at the start of the year
- A production profile for the next 20 years

Peak capacity

When the plant is running at full capacity it is able to produce 8000 tons of salt per day. This means that the field must be able to produce enough brine to allow the plant to achieve its maximum capacity. A simple calculation of how much m³ brine equals 8000 tons can't be made, since the relationship is not one to one. A capacity utilization factor is for example used to make sure that the total amount of production always exceeds the minimum which is needed to allow the factory to reach full capacity.

Capacity utilization factor

The capacity utilization factor is established by using different data outputs from the field and plant. Figure 83 explains the calculation of this utilization factor. This factor is used when calculating the total amount of produced salt from field data.

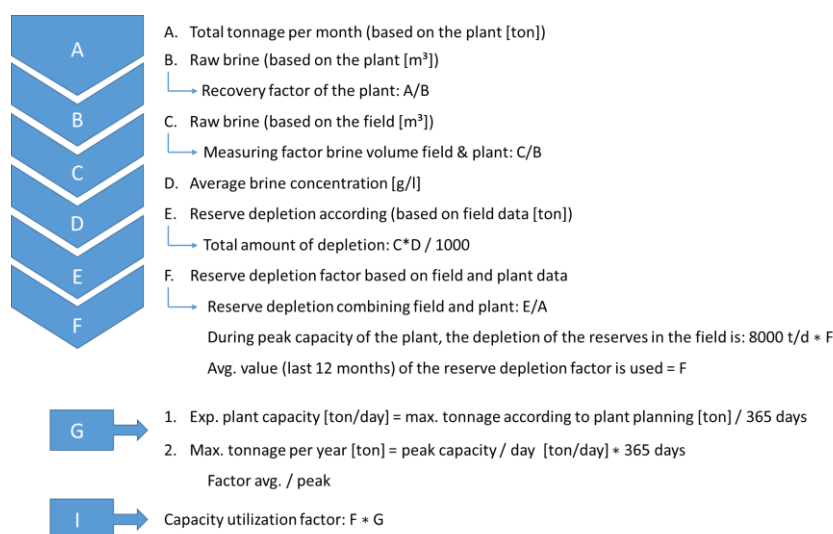


Figure 83 – Determining the capacity utilization factor

The last measured Reserve depletion factor (F) is 1.11, whereas the capacity utilization factor is 0.97 at the moment. These values have been constant over the last 2 years.

Production profile for the next 20 years

The predicted production profile for the next 20 years is shown in Figure 84. The profile is similar to production profiles from the oil and gas industry. Every time new wells come into production a peak can be noticed in the profile, after which the general decline trend is continued again. The red line indicates the level of the peak flow which results in the peak capacity of 8000 t/d. The purple line shows the average expected plant capacity for the coming years. The capacity of the all caverns combined should exceed this purple line in order to supply the plant with sufficient brine.

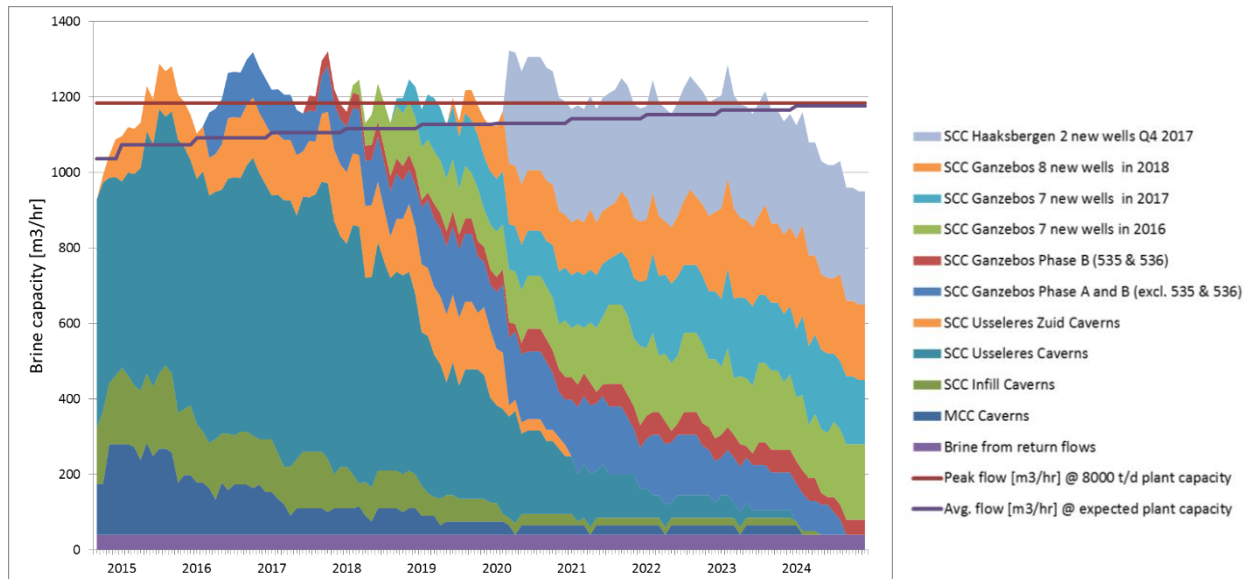


Figure 84 - LT production profile, showing the production for the next 10 years.

Based on the current development plan of the field, the processing plant will be supplied with sufficient brine until 2023. It should be noted that this production profile is a snapshot; the reserves of producing caverns are updated every year, whereas the amount of reserves of caverns which will be developed in the future predicted conservatively.

10.2 Analyzing predicted versus actual production data

Comparing the predicted- with the actual production is the first step in the reconciliation of the reserves. For this detailed reserve analysis only caverns from the Usseleres development was used (SCC Usseleres Caverns in Figure 84 & Location in Figure 120 in Appendix J). In total 28 caverns are active in this area, however for the analysis only 23 have been taken into account (500 & 507-510 have been excluded due to insufficient information). The predicted volumes are based on the LT-plan as is it used at the moment at AkzoNobel, whereas the actual production data is taken from the BPB-database. Comparing both datasets will show whether the production can be accurately predicted or not. The data used dates back to May 2008 which means that 7 years of data are available.

Different parameters can be compared:

- salt production in tonnes per month
- salt production in tonnes per year
- brine flow in m³/h

In Figure 85 the average flow is shown for the 23 caverns. The caverns are grouped according to the year in which the cavern was put into operation. The flows for these different groups are summed. The result can be seen on the next page.

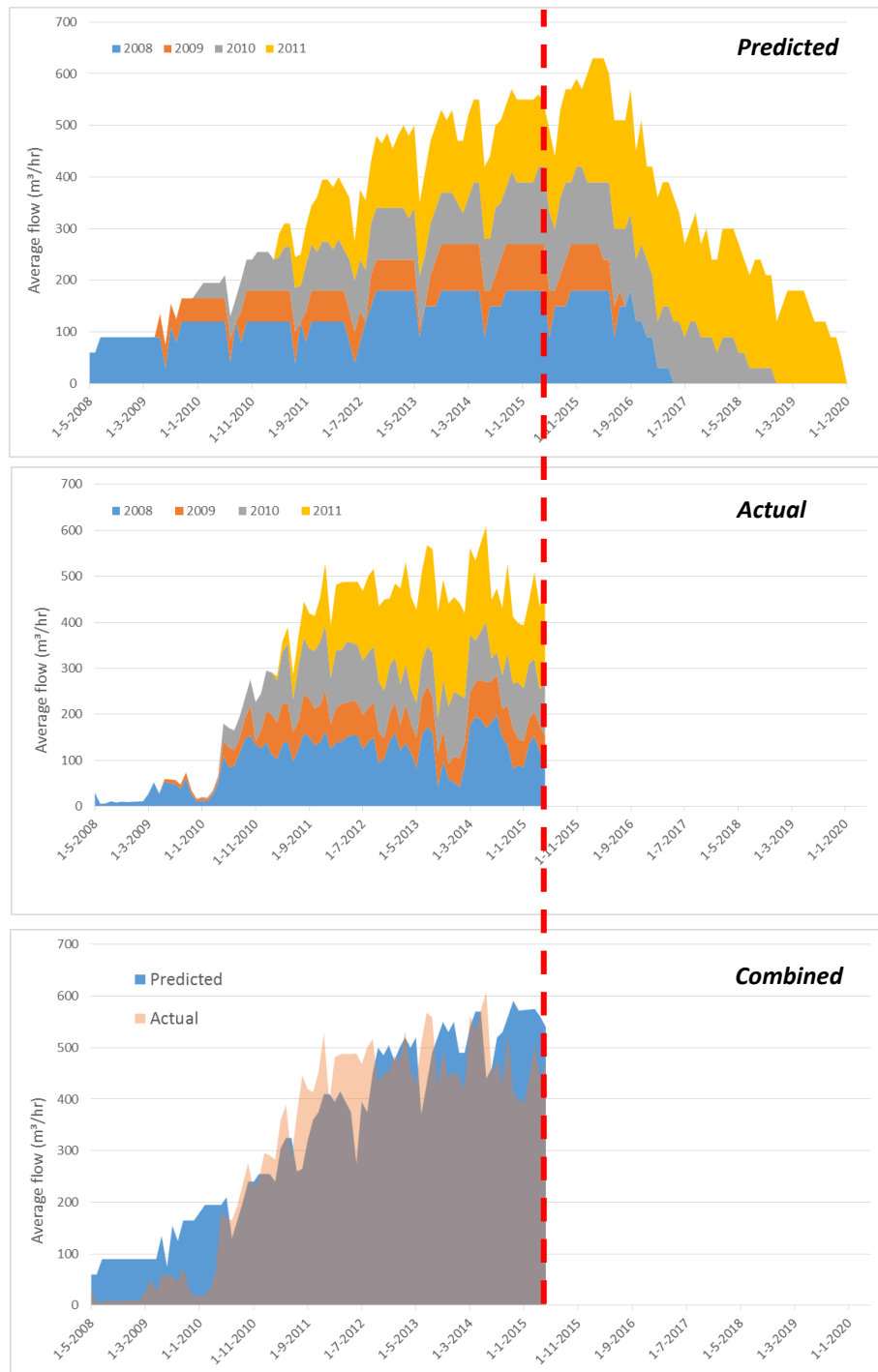


Figure 85 – Showing the average flow per hour for 23 of the 28 caverns in the Usseleres area
Top: Predicted flow for the different groups of caverns. Middle: Actual flow of the caverns. Bottom: Plotting the actual flow on top of the predicted in order to indicate deviations.

When comparing the predicted- with the actual production it can be noticed that the actual production follows the same trend as the predicted. The start-up period is only considerably longer. This can be explained by the time it takes to develop the sump, which are much significantly longer than anticipated. The following figures show a closer analysis of the differences between the predicted- and actual production.

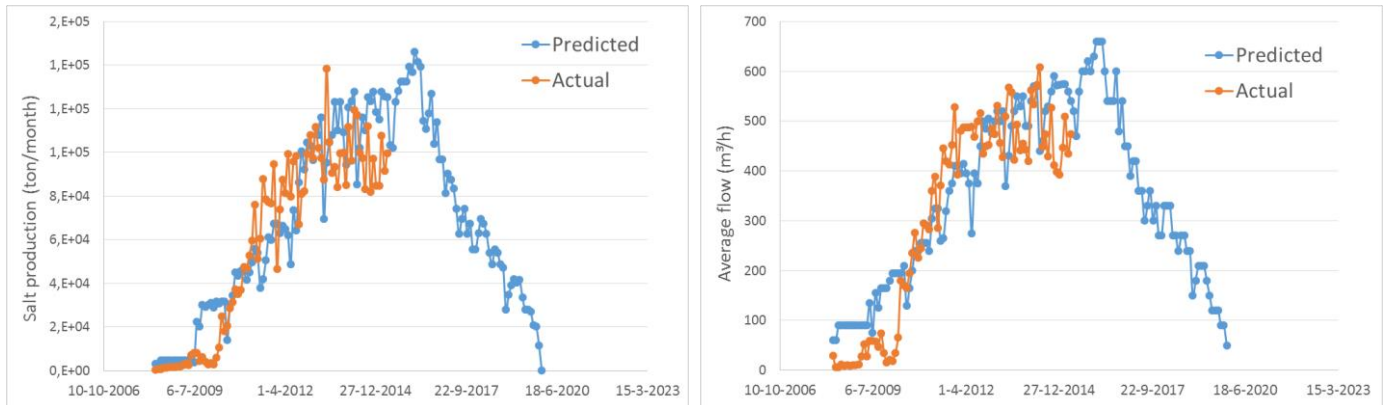


Figure 86 – Showing the raw data. Left: predicted and actual salt production in ton/month for the Usseleres caverns. Right: predicted and actual average flow per hour.

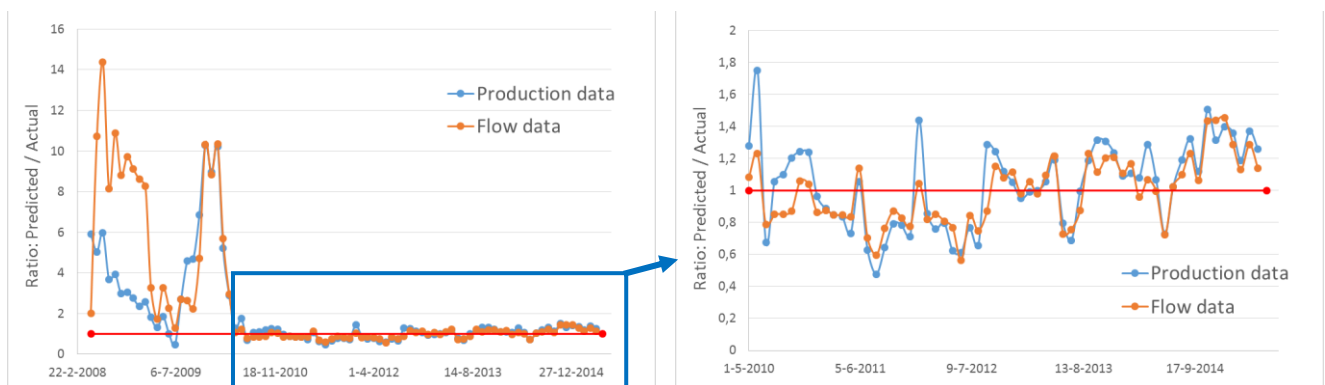


Figure 87 – The predicted/actual ratios are shown in the graphs for the period from 2008 until 2015. Left: the predicted/actual for the entire period, including the time during which the sumps are developed. Right: the ratio for the period in which all caverns are either in MLS-1 or 2.

In Figure 86 the raw data (tons per month and average flow per hour) are shown for the predicted- and for the actual production profile. When dividing the predicted data by the actual data two ratios can be obtained (for the tons per month and flow per hour). When this ratio exceeds 1, it implies that the predicted values are higher than the actual values and vice versa. This is shown in Figure 87. It is clearly visible in the figure that the ratio is quite high during the first two years, this is the period in which most of the sumps are active at the same time (they overlap each other). From June 2010 the ratio seems to stabilize around 1. When summing the amounts of produced salt, the total predicted and actual amounts can be compared on a yearly basis, as shown in Figure 88.

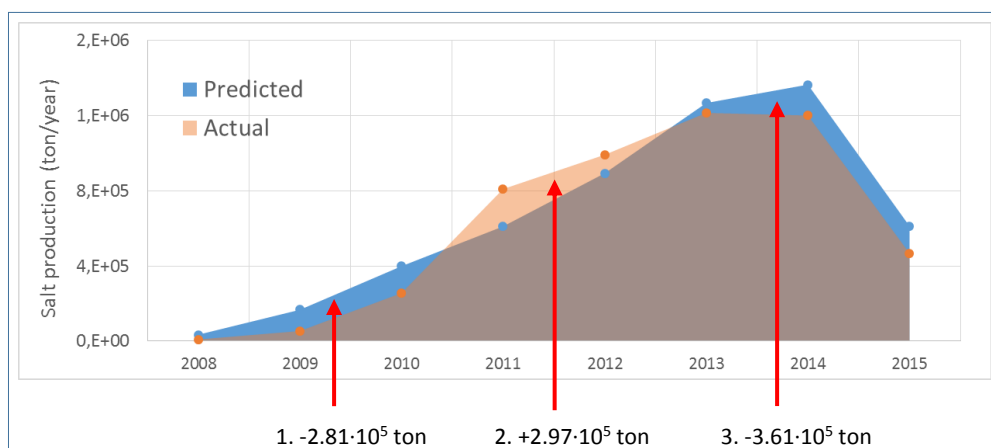


Figure 88 – Comparing the total amount of predicted and actual salt on a yearly basis.

Three periods can be distinguished in Figure 88:

1. 2008 until June 2010: $2.81 \cdot 10^5$ tons of salt were produced *less* than predicted
2. June 2010 until October 2012: $2.97 \cdot 10^5$ tons of salt *more* produced than predicted
3. October 2012 until present day (i.e. May 2015): $3.61 \cdot 10^5$ tons *less* produced

In the 1st period the actual production falls behind compared to the predicted production. This can be explained by the fact that many sumps are active at the same time. The duration of the development of the sump was highly variable during the early years of the single completion caverns (SCC's). Whereas it was expected that the sump would be developed in 14 months, the average time it took was 16.7 months. The production during the sump is much lower than during MLS-1, which explains why the total amount of produced salt is lower in this period.

During the 2nd period the total amount of produced salt was higher than the predicted amount. This can partly be explained by the average sump duration, which was 13.4 for the remaining caverns. Another reason is that the average flows were higher during this period. The average predicted flows for all caverns combined were estimated at 285 m³/hr, whereas the actual flow was on average 372 m³/hr.

The 3rd period lags behind again. In total $3.61 \cdot 10^5$ fewer tons were produced than expected. This can be explained by different events which could not have been predicted. The factory had some unscheduled maintenance stops and due to leakages in the pipe network in the field the capacity was considerably lower during some weeks.

After completing the calculation it can be concluded that during the first 7 years of production $3.45 \cdot 10^5$ less tons of salt were produced than predicted. This is only 3% of the total production during these years. It can therefore be concluded that the production can be estimated quite accurately (Figure 88).

10.3 Recovery factor analysis

Before the reserves can be reconciled an analysis of the recovery factor should be conducted. The radius of the cavern is related to the recovery factor. Different radii can be determined from the available data:

- When a sonar measurement is completed, the maxplot (in m²) will indicate the largest section through the cavern. Assuming that the maxplot is circular, the radius can be obtained.
- From production data the leached volume (m³) can be determined. After correcting the inflowing water for losses to the Solling Fm., the radius can be calculated when assuming that the leached volume is cylindrical.
- Another method is to use the relationship between the leached volume and sonar volumes from section 7.3.1 (Figure 64), to convert the sonar volume into a leached volume and calculate the radius accordingly.

Comparing the theoretical cavern with an actual cavern will however always result in deviations. In Figure 89 the shape of the theoretical cavern is shown, whereas an actual cavern (visualized during a sonar measurement) is also given.

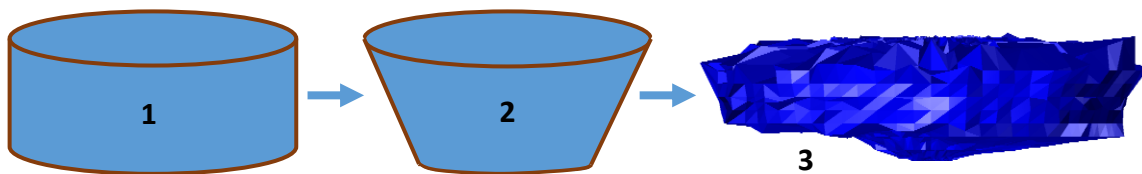


Figure 89 – Shape of the theoretical cavern at the far left (1) and a representation of an actual cavern at the far right (3). The shape in the middle (2) provides a better predicted shape.

These three radii have been determined for MLS-1 of 13 caverns (caverns: 486-499, excluding 495). As expected the radii from the maxplots are significantly lower than the radii from the production and sonar volume data. This difference is caused because the maxplots are not corrected for neglected parts in the cavern. When plotting the radii from the production data vs. the sonar volume measurements a fairly linear relationship is found, indicating that the radii from sonar volumes which have been corrected for neglected volumes are in line with the corrected production data. Another observation which can be made is that the radius never exceeds 58m whereas the assumed radius of a theoretical caverns is 60m, losing 2m of salt in all directions.

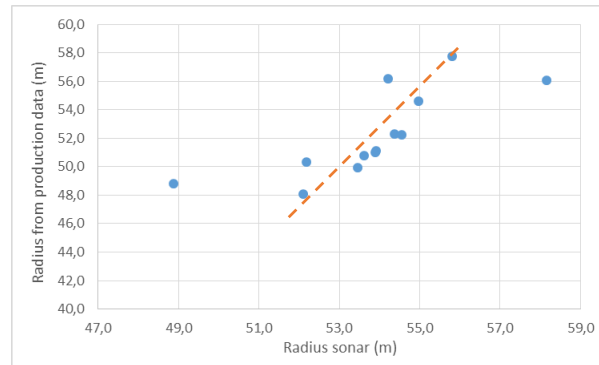


Figure 90 – Relationship between the radii from sonar measurements and production data.

Using the radius and the height of the cavern and the estimated produced tons of salt in combination with constant parameters (i.e. density halite, density salt in brine and the insoluble content) 2 recovery factors can be determined. One recovery factor for the actual radius and one for the theoretical radius of 60m. The following formula determines the recovery factor for the actual cavern radius:

$$\text{Recovery factor} = \frac{\text{Correction factor} \cdot \text{Produced tons}}{\left[h \cdot (\rho_{\text{halite}} \cdot \text{Ins. content} - \rho_{\text{salt in brine}}) \right] \pi r^2} \quad (1)$$

where h is the height of the cavern and the *correction factor* is the factor which corrects for the fluid losses and r is the measured radius of the cavern, $\rho_{\text{halite}} = 2.165 \text{ ton/m}^3$ and $\rho_{\text{salt in brine}} = 0.312 \text{ ton/m}^3$. When calculating the second recovery factor, the radius is constant at 60m.

Figure 91 shows the recovery factors versus the radii derived from the measured sonar volumes. The blue data points indicate the current recovery based on produced salt and the measured radius. The orange data points indicate the recovery factor when the production data is compared to the theoretical shape of a cavern. The amounts of produced salt are in general high, since these values are based on water inflow data.

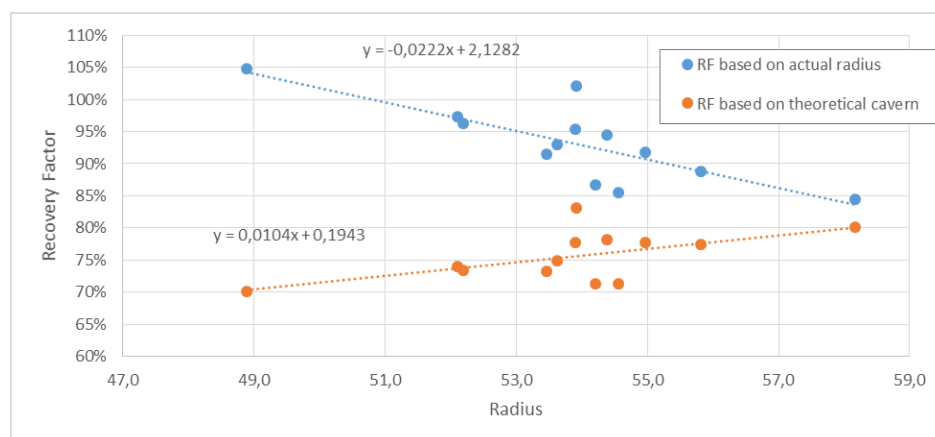


Figure 91 – Recovery factors as function of the measured radius

When the radius of the measured cavern is small, the recovery for that certain radius is high, because based on the production data everything is produced. However, when comparing this with the theoretical cavern the recovery value for such a particular cavern is very low, since it left many meters of salt in place in all directions, illustrated by (i) in Figure 92. The opposite is valid for caverns which have a large radius, the recovery factor of the actual radius approaches the recovery factor based on the theoretical radius. The difference in recovery factor decreases therefore, illustrated by (ii) in Figure 92.

Both cases can be seen in Figure 91, whereas the recovery factor for the cavern with a radius of 49 meters is quite high, the recovery in general is very low for this cavern. For the cavern with a radius of 58 meters, the recovery based on the theoretical cavern parameters increases, whereas the actual recovery decreases based on the actual radius.

From the trend in Figure 91 the recovery for a fully developed cavern can be determined. The following formula is used to calculate the recovery for a cavern with a radius of 60m:

$$\text{Recovery factor} = 0,0104x + 0,1943 \quad (2)$$

where x is the radius. This results in a recovery factor of 82%. This value is 2% higher than the theoretical 80% which is currently used. It is expected that the real recovery factor in the field is higher. However, the average recovery factor of the analyzed caverns is only 75%.

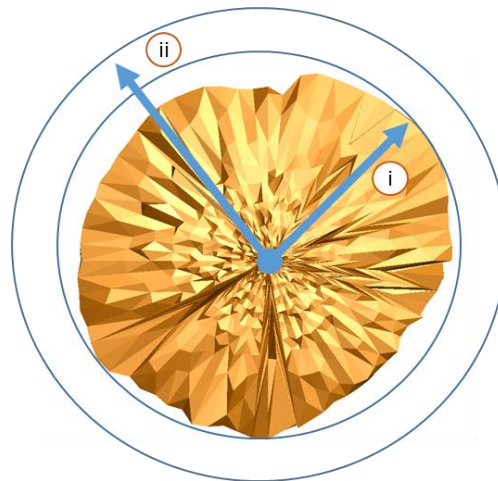


Figure 92 – Principle of the 2 recovery factors explained: (i) is based on the actual measured radius, whereas (ii) is based on the theoretical radius (i.e. 60 m)

10.4 Reserve reconciliation tool

The reserve reconciliation tool is a tool which accounts for the reserves systematically. It can therefore be described as an accounting tool as well. The tool can be described as a circle diagram with different input parameters. A representation of the tool is shown in Figure 93. The various parts of the tool, as listed in the figure, are explained accordingly:

- A. Hengelo Brine Field: All producing and planned salt caverns within the current concession.
 - Production profile: The production profile is a profile which can be divided into two parts; which is before and after today. The past shows the actual produced amounts of salt, whereas the future is based on predictions (as discussed in section 10.2).
 - Current reserves: All salt which can be produced from the current and planned caverns.
 - New caverns are based with an initial predicted recovery factor and insoluble content; this results in an expected cavern volume which is used for the reserve replacement.
- B. Cavern: The entire HBF consists of many individual caverns.
 - During a sonar measurement the actual radius, height and volume are determined (using the relationship from section 7.3)
 - The updated insoluble content values are used (as discussed in section 8.3.3).
 - In combination with the leaching phase the correct relationship between the production- and cavern volume can be chosen.

- The volume is compared with the production and geology data. From this information a quantitative prediction can be made whether fluids are flowing out or in to the cavern.
 - The production data are then compared to what the expected recovery/production should have been.
 - The remaining amount of salt production is determined and a prediction for the remaining lifespan is made, which is based on the predicted flow.
 - When a cavern has produced significantly less salt than initially predicted, a write-off of the reserve for that particular cavern will be executed.
 - Information from this part 'flows' back into part A and is used to update the production profile and current reserves figure.
- C. In case of deviation between the actual and predicted production, mitigation actions for the individual caverns can be implemented in order to increase production. Examples of actions are varying the flow speed or using a different height for the tubing in the cavern.
- D. Information from the plant is used in the reconciliation tool, since this is the demanding factor at the moment (the factory needs enough brine to meet its production goals)
- Capacity: The factory has production goals which require a certain brine input. The field must ensure that it will be able to provide the plant with this required amount of brine per hour.
 - Long term planning: The plant has a long term planning, in which the production numbers are planned for the current and next couple of years. These numbers are however slightly variable due to market conditions.

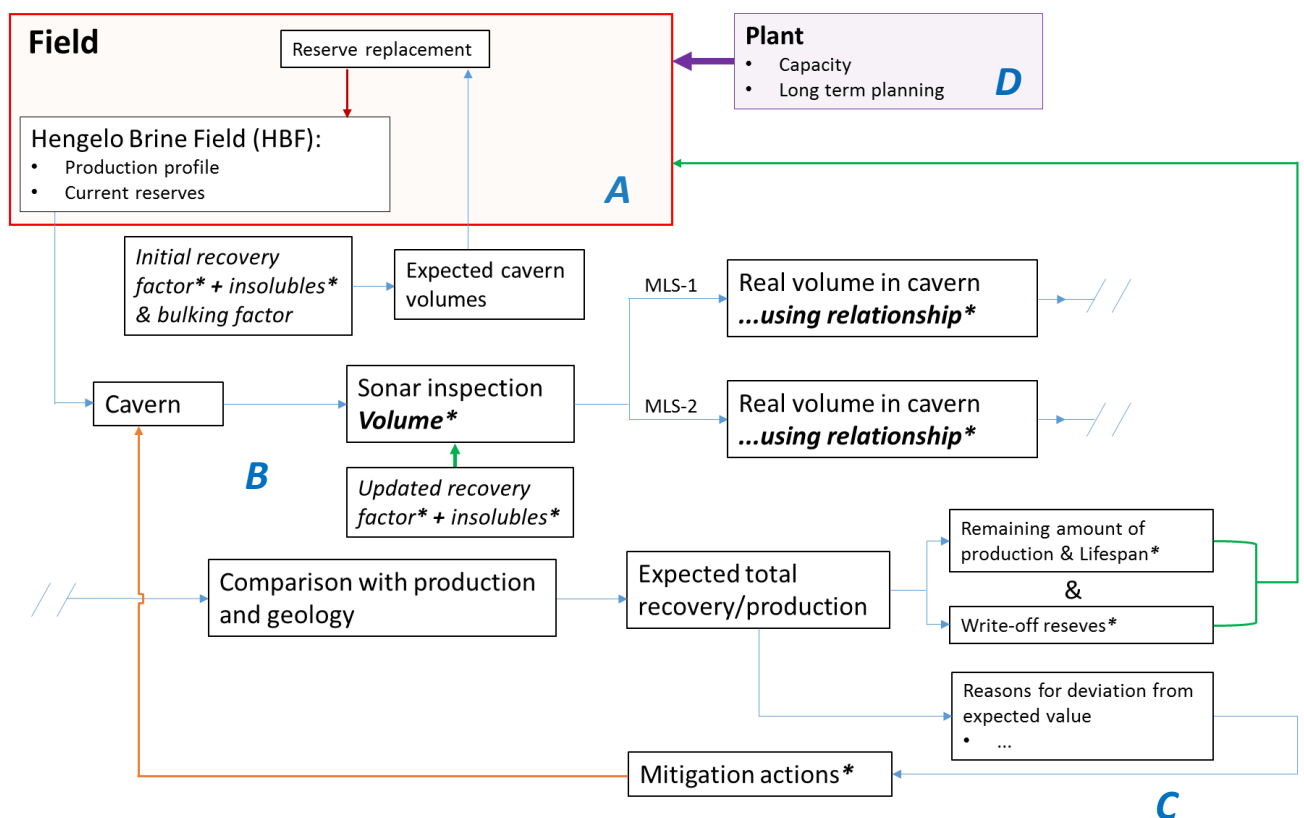


Figure 93 – Reserve reconciliation tool for the Hengelo Brine Field.

The entire model is built in Excel; this enables it to be used within the Mining Development & Compliance department of AkzoNobel Hengelo.

10.5 Validating the reserve reconciliation tool

The reserve reconciliation tool (section 10.4) was validated for 23 caverns located in the Usseleres area (Appendix J, Figure 120). When analyzing these caverns, the reserves were estimated at certain moments in time. The first reserve is entirely based on theoretical values with an estimated salt thickness. The quality of the information increases during the development and production of a cavern, which results in recalculations of the reserves.

Figure 94 indicates the stages during the development of the caverns at which the reserves will be estimated. The development has been divided into 5 parts; Pre-development, the sump-phase, MLS-1, MLS-2 & abandonment. The different reserve calculations include:

- Initial reserve: The reserve based on the initial assumptions (e.g. the anticipated height and recovery factor).
- Reserve with new insoluble contents & recovery factor: The estimation for the reserves using the insoluble content from section 8.3.
- Reserve based on flow data: The estimation for the reserve based on flow data from the individual caverns after MLS-1 has finished.
- Reserve based on sonar measurement MLS-1: Estimation of the reserve based on the sonar measurement after MLS-1 has been completed.
- Reserve corrected after sonar measurements: Current estimation of the remaining reserves.

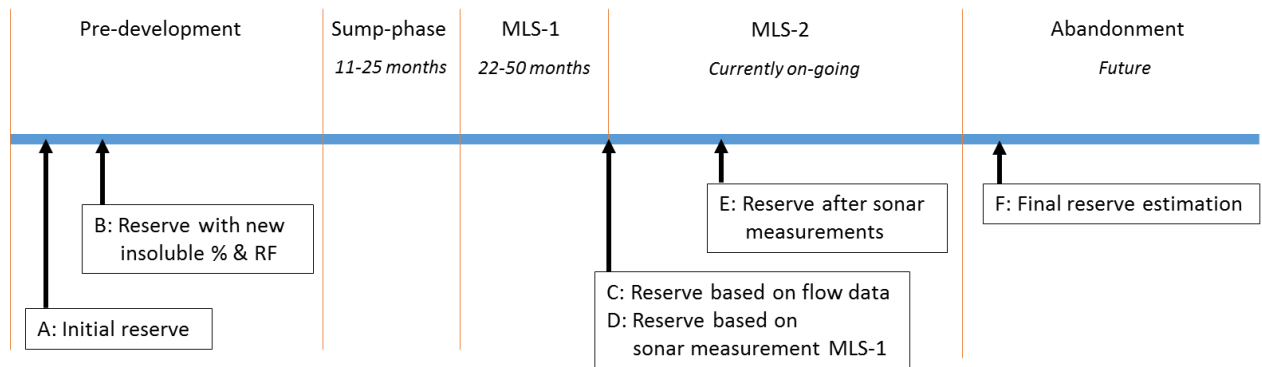


Figure 94 – Development phases of the 23 caverns in Usseleres. RF = recovery factor.

Figure 95 shows the reserves when combining all data from the 23 caverns in Usseleres. Based on the 5 categories, it can be noticed that between the initial estimation (A) and the first recalculation (B) there is an increase of $1.25 \cdot 10^6$ tons of salt, which implies 13% more reserves. This is equivalent to an additional 3 caverns. However, after completion of MLS-1 the total reserves decrease. Comparing (C) and (D) a difference is also noted. It should be noted that in Figure 95 time is neglected. Not all caverns are developed at the same moment. It is therefore an ongoing process.

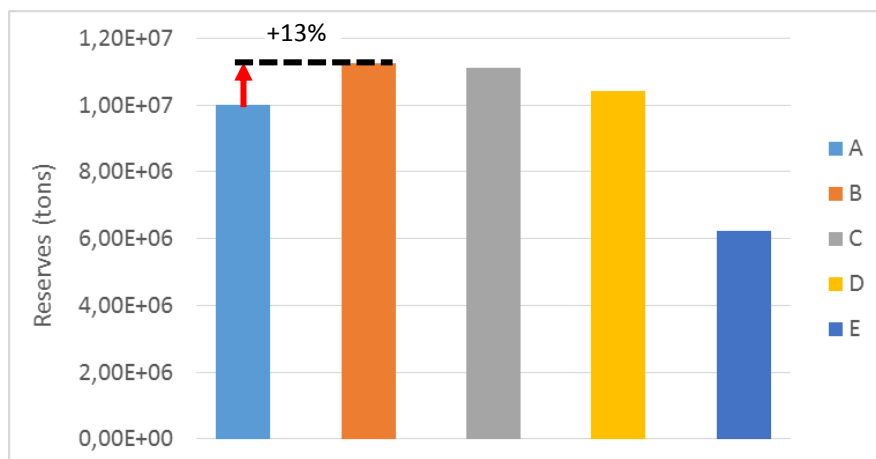


Figure 95 – The results of the different reserve estimations combined in 1 graph.

Analysis of the reserve development during MLS-1

Figure 96 shows the development of reserves for individual caverns. It can be seen that there is a gain in reserves. However, loss between the recalculated reserves (B) and the reserves after MLS-1 has finished (D) can also be seen.

- Between A and B an average reserve gain of 13% is observed (equal to 4 caverns)
- Between A and D an average reserve gain of only 5% is observed (equal to 1.5 caverns)
- The loss in reserves between B and D is 8% (equal to 2.5 caverns)

This loss in reserves can be explained by the fact that fluids are lost and the caverns are handled production controlled. Reserves C and D should be identical when no fluids are lost and the sonar measurement is performed correctly.

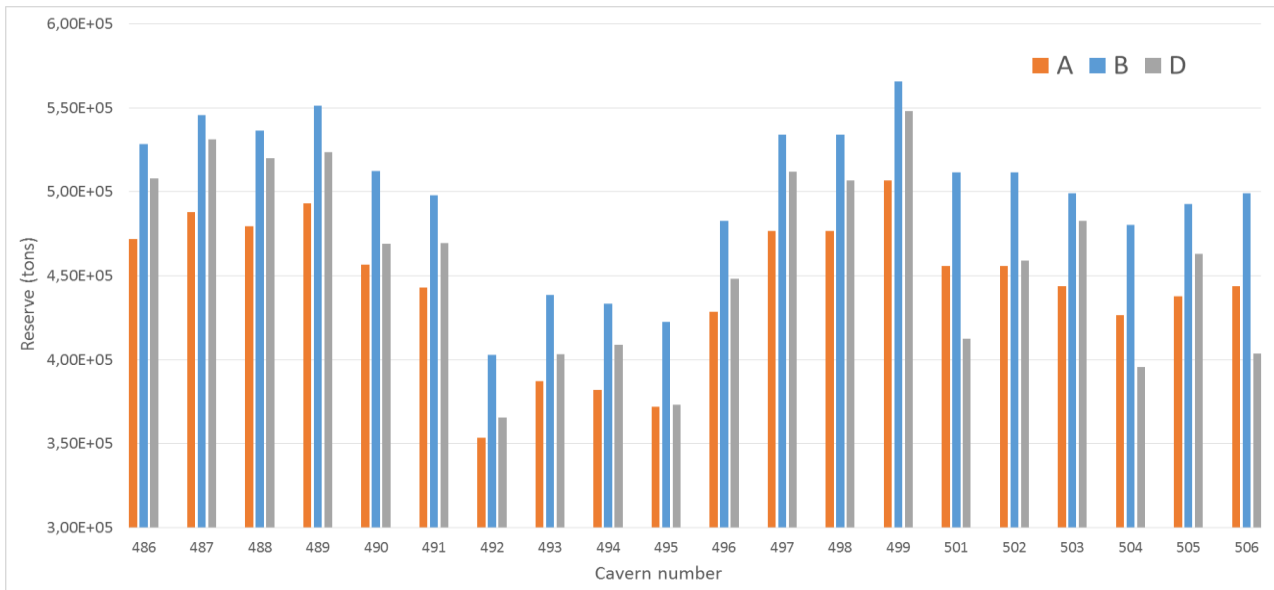


Figure 96 – Reserve development. The initial reserve (A), recalculated reserve based on the new insoluble contents (B) and reserves based on the sonar measurement after MLS-1 has finished are shown. A decrease in reserve from B to D can be noticed at every cavern.

According to procedure, after 150.000 tons have been produced during MLS-1, production is stopped and the cavern is converted to a MLS-2 cavern. However, as indicated in sections 4, 5 and 6, the caverns are connected with the Solling Fm. It has been described in these sections that fluids are lost. Losing fluids during the leaching process implies that the anticipated amount of salt can't be produced, although the flow meters suggest otherwise.

After the 150.000 ton 'marker' is reached the volume of the cavern is measured using the sonar tool. Because the sonar measurement has certain limitations (section 7.2) the sonar volume is corrected for neglected volumes using relationships from section 7.3. After this correction it can be noticed that the produced volume is considerably lower than the anticipated volume (associated with the 150.000 tons). This observation shows that fluids have been lost during MLS-1.

The difference between the actual and predicted volume can't be recovered after the cavern has been converted to MLS-2. The lost areas are probably located at a greater depth than the brine inlet, so the left salt can no longer be produced.

It can be concluded that although fluids are lost and the caverns are not completely produced, AkzoNobel still produces more salt than expected. The extraction process is however not optimal. This results in additional operational expenses. The initial reserve calculation is too conservative resulting in the extra tons of salt during production. Furthermore the reserve reconciliation tool works, although it has not yet been tested for caverns in MLS-2.

11. Discussion

The primary goal of this thesis is to identify whether a predictive methodology will be able to improve the long-term planning of the production and development of the Hengelo Brine Field. In order to approach this question, which combines the geological knowledge, cavern characteristics, hydrological properties and the mass balance of the field, the research was constrained by several assumptions.

Mass balance

Data from different sources (i.e. different departments) was used, while a proper measurement accuracy for all sources is unknown. When conducting the individual experiments the measurement error could be quantified by switching the meters. This resulted in a range of the measuring error of the flow meters of: 0.5 to 7.0%. The 7.0% was measured at a cavern which contained two different types of flow meters, indicating that the old meter has probably a large deviation with respect to the new type of flow meters.

Individual mass balance experiments are only performed on a handful of caverns. This can result in biased results. Using conservative values for the average fluid loss from caverns gives a broad range of total losses (i.e. $3.3 - 4.7 \cdot 10^5$ m³). Caverns with major inflow aren't measured. These caverns should be located using the *In-/Outflow test* (section 10.4) and be measured. This can give more clarification whether all fluids are lost to the Solling Fm. or not.

Pressure tests

The two series of pressure tests (i.e. carried out by AkzoNobel and DEEP/KBB) indicate two different average cavern compressibility values. For all tests a high and low compressibility value was calculated, by plotting trendlines the difference in compressibility factor can be noticed easily. A possible explanation can be the fact that the test of DEEP/KBB are performed on multiple completion caverns (MCC) whereas the tests carried out by AkzoNobel are performed on single completion caverns (SCC).

The proposed pressure tests were only tested on 2 caverns. Based on the results it is indicated that these tests can be performed on caverns when these are stopped for maintenance. The tests should however be repeated on caverns which are located in more active parts of the current field. Field observations at various caverns during this research do indicate pressure built up when caverns are stopped.

Solling Fm.

From the stratigraphy (and the observed cores) it is known that the Solling Fm. is overlain by an anhydrite layer, which acts as a boundary between the halite and the Solling Fm. This anhydrite forms an impermeable layer. In the case fluids are present in the Solling Fm., it could be discussed whether the regular hydrostatic pressure actually applies. Assuming that water will go up, due to the physical laws, it will be trapped under the anhydrite/halite. This will result in a higher pressure of the fluids, compared to the pressure calculated with the hydrostatic gradient, if there is enough inflow. It is however difficult to estimate the magnitude of this pressure.

Observations in the field (Quintessa, 2013) suggest in some cases an overpressure in the borehole of 1 to 3 bar after drilling into the Solling Fm. The maximum pressure drop, as described in Figure 53, is approximately 14 bars. In case the pressure in the Solling Fm. is a few bars higher, there will still be a positive pressure drop between the cavern and the Solling Fm. The amount of outflow will decrease but fluids will still flow into the Solling Fm.

Sonar measurements

The sonar measurements have a high limitation factor due to insoluble rock in the cavern and constraints of the tool itself. When comparing the sonar volumes with the production data large deviation are observed. Effort has been put into quantifying the neglected volumes, partly by comparing it to the production data. However, this production data has a high uncertainty, as it is proven in this report that (un)known amounts of injected fluids are lost in the Solling Fm.

Reserve reconciliation

The predicted and actual production profile have been compared, however the main limiting factor is the fact that the HBF is production controlled. With the lost fluids the actual production is just an estimation with a high degree of uncertainty. This is also indicated in section 10.5 where actual losses are indicated during MLS-1.

12. Conclusions

The goal of this study is to combine the geology, hydrological properties and mass balances of the field to determine the causes of volume discrepancies and to understand the mass balances in the Hengelo Brine Field in order to conduct reserve reconciliation. Throughout the project it became clear that the Solling Fm. plays an important role regarding volume and pressure losses in the field. Due to all uncertainties and the current influence of the Solling Fm. it proved to be difficult to create an accurate working model, however a basic model has been created, which can be built on in the future. This chapter provides and summarizes the most important conclusions.



12.1 Geology & Cavern shape

From the extensive geological background study the region has been exposed to two major structural geological events:

1. The Mesozoic rifting and breakup of Pangaea (260 to 220 million years ago)
2. Cenozoic subsidence and presence/absence of the Zechstein Fm. (65 million year ago until present day)

These events have resulted in various fault zones in the region, which must have had influence on the Solling Fm. (deposited 247 million years ago).

The video runs have given a detailed look of the cavern shape and geometry. It was confirmed that many stalactites hang from the roof, blocking the sonar signals. These stalactites are formed by insoluble material. The general assumption is that insoluble interlayers or accumulations are also present in the walls and cause notches smaller than 1 meter.

12.2 Mass balance

By accounting for material entering and leaving the caverns, mass flows can be identified and quantified. Hence different mass/volume balances were created for both the entire field as well as individual caverns. According to physical laws and formulas a theoretical ratio can be found for the amount of in- and outflowing fluids from a cavern. This value is 0.96 (for every m^3 of water 0.96 m^3 should be produced).

Plant and field data

The yearly averages shows a clear linear increase from 2010 to 2013, whereas from 2013 to 2014 the ratio seems to level off to a constant value of about 0.915. Comparing this value to the theoretical value gives a deviation of 4.5%. Which means that $3.7 \cdot 10^5 \text{ m}^3$ of fluids have been lost in the field.

When comparing the flow measured at the producing caverns with the recovered brine, the ratio is slightly higher with an average ratio of 0.93. This would suggest a deviation of 3%, which translates into an unaccounted volume of $2.5 \cdot 10^5 \text{ m}^3$.

Individual caverns

The data from the plant and field are however subjected to measuring errors which cannot be quantified properly. This issue is however less of a problem for the values measured at individual caverns. The real issue with performing tests on individual caverns was the clogging of the flow meters. Small insoluble particles are also produced, causing the flow meters to clog. Installing so called 'stone-catchers' proved to be successful to overcome this problem.

From the individual caverns it becomes clear that some caverns are losing significant amounts of fluids. Although differences exist, the average loss measured was approximately $30 \text{ m}^3/\text{day}$, which results in 3.0 to $4.0 \cdot 10^5 \text{ m}^3$ of losses each year. This value is in accordance with the values from the plant and field.

It can be concluded that a significant amount of fluid is lost every year. The only logical explanation would be that the fluids have flown from the caverns into the underlying Solling Fm.

12.3 Pressure tests

In 2013 and 2014 a series of pressure tests were performed. The results of these tests indicate that fluid pathways exist between caverns. By plotting the distance vs. the amount of inflow it can be concluded that pathways of up to 450m exist in the field.

From the data the main flow directions of the brine during the tests could be established. It is concluded that the flows either tend to follow isopachs to other caverns or pathways towards caverns which are located less deep, probably due to the pressure gradient. In some cases it was even noticed that fluids flowed towards caverns which were located deeper, indicating that due to the pressure gradient fluids could even flow downwards, which is under normal conditions not possible in the subsurface.

A pressure test to check whether a cavern was connected to other caverns was developed. The production was generally stopped at a cavern a couple of weeks prior to a workover. Measuring pressure responses at such stationary caverns could in theory indicate connectivity. Two isolated caverns were tested and no response was measured. This is in line with the hypothesis.

12.4 Solling Formation

The Solling Fm. is the formation which is located directly below the Rot salt, in which the caverns are developed. From the pressure tests in the field interactions between caverns were observed. Besides these connections, additional experiments and data, focused on the mass balances, indicated significant fluid losses in the field. The most obvious explanation for this fluid loss and/or connection between caverns, is to link the caverns with the underlying Solling Fm.

Observations from the drilled core (BKM-02) in combination with information gathered during a visit to the Core-house (TNO) not only confirmed the presence of permeable sand stone and impermeable claystone, but also the presence of fractures, and halite veins, which were formed during the burial phase of the Solling Fm.

Observations from the field indicate three possible flow paths, which are responsible for the loss/connections:

4. Connection between caverns through the Solling Fm.
5. Fluid loss to the Solling Fm.
6. Direct connection between caverns.

Allowing the fluids to leave the cavern, the following conditions were investigated and confirmed:

- the permeability is high enough to allow fluids to flow,
- a certain porosity is present, to provide the capacity in order to hold the fluids,
- a pressure gradient is in place.

The Solling Fm. can be seen as a giant sponge, which can absorb fluids but also release them. As part of the investigation 5 pressure situations (Figure 53) were determined and assessed. These 5 situations which can occur in the field indicate that the observed fluids losses can be explained and proven with the current information.

Calculations for the Usseleres region show that the capacity of the Solling Fm. is large enough to store 11 years of fluid losses, when 3% of the fluids are lost on a yearly basis.

Therefore it can be concluded that the Solling Fm. is an important factor in the HBF. The Solling Fm. has the following negative characteristics: Fluids are lost, unnecessary amounts of energy are wasted in order to pressurize the formation constantly, workovers are delayed due to interruptions when depressurizing the caverns resulting in inefficiency of the field crew and last but not least the real recovery factor of individual caverns can't be established due to varying in-/outflow ratios. Figure 97 shows a summary of this conclusion regarding the Solling Fm.

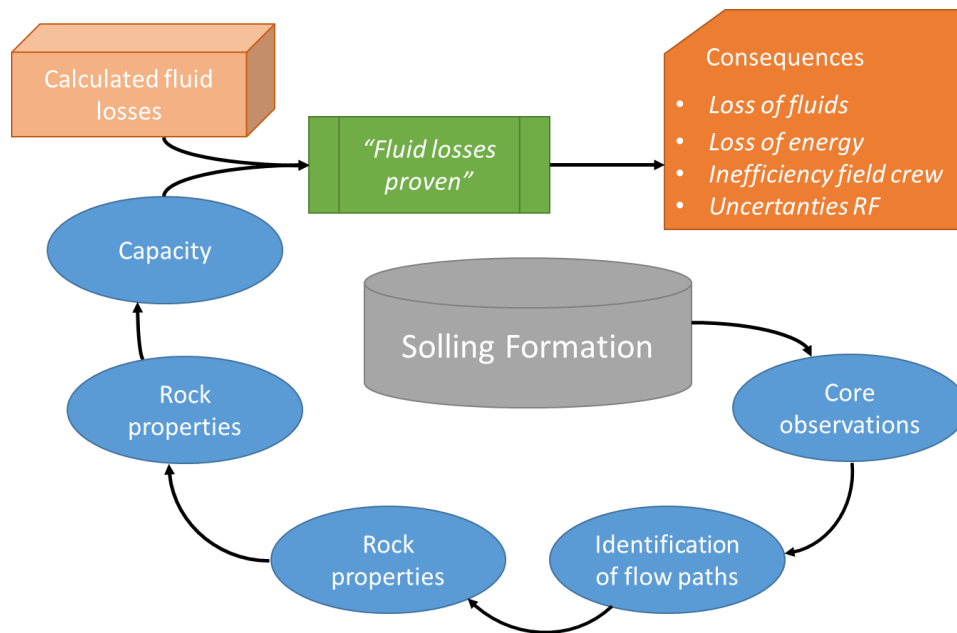


Figure 97 – Summary of the conclusions which are drawn with respect to the Solling Fm.

12.5 Sonar measurements

The sonar tool is used to determine the shapes and volumes of the caverns. The tool has however some limitations which cause major deviations in its results. Based on the video runs and the shapes of the 3-dimensional sonar volumes it can be concluded that stalactites cause the major neglected volumes in the roof. The resolution of the sonar tool (i.e. < 1m) causes neglected volumes in the sump and the irregular wall. All neglected volumes were added to the caverns in the given dataset and a distribution was made. The average neglected volume is $13.9 \cdot 10^3 \text{ m}^3$ with a standard deviation of $2.2 \cdot 10^3 \text{ m}^3$.

After correcting the sonar volumes with the neglected volumes, the 'new' sonar volumes were compared to the volumes which are theoretically created during the production (based on the amount of inflowing fluids). From this comparison a relationship was established. It can be concluded that there is still a deviation between the two values, even though the sonar volumes are corrected for their neglected volumes. This is not that remarkable since the theoretical value of 0.96 is probably overestimated. When the in-/outflow ratios from the field tests (chapter 4) are used to calculate the created volume from production data, a closer relationship is found. This indicates that the fluid losses cause the biggest deviation between the sonar- and production data after correcting the sonar data with their neglected volumes.

12.6 Insoluble material & Bulking Factor

During the life of a cavern multiple sonar measurements are made. The insoluble content is determined by using the information from the sonar measurements in combination with the program Surpac. 22 caverns are analyzed in total. A distinction was made between caverns in the 1st and 2nd main leaching stage (12 caverns for MLS-1 and 10 for MLS-2). By varying the bulking factor from 1.4 to 1.7, with an average of 1.55, a range of values is acquired from which it can be concluded that the insoluble content is normally distributed throughout the field:

- MLS-1: 4.8% (standard deviation of 0.75%)
- MLS-2: 9.6% (standard deviation of 2.1%)
- Combined: 7.1%

These values are lower than the assumed 10% according to Westendorp (1969), and indicate that the first 9.5 meters (2.5m sump and 7m MLS-1) of the salt formation contains approximately 50% less insolubles compared to the remaining salt which will be produced during the second main leaching stage. These updated insoluble content values were used when recalculating the remaining reserves.

12.7 Other uncertainties

Besides the Geology, Mass balances, Sonar measurements and Insoluble material contents, additional uncertainties were analyzed and quantified. The most important outcomes are discussed in this subchapter.

Gamma-Ray logs

Theoretically a relationship could be established between the gamma ray readings and the amount of insolubles. However, after analyzing and plotting the data from the gamma ray log and the insoluble content determination, no clear trend or relationship was found. This can be attributed to the following factors, which affect the accuracy of the gamma ray readings:

- The resolution of the GR-logging tool (and background noise)
- Inclination of the borehole

Furthermore it can be concluded that insoluble layers can be correlated between different wells in some cases. Looking at cores a difference can be made between insoluble interlayers and insoluble particles/nodules. The combination of both types of insolubles makes it difficult to correlate between wells, since the amount peaks on the GR-log differ. It can therefore be stated that the GR-logs are only useful for defining the salt intervals, because the information from these logs is insufficient to relate it to the insoluble material in detail.

Seasonal effects

Two effects were identified which can be affected by variation of temperature:

1. The leaching process might change due to temperature changes of the inflowing water
2. The flow meters give lower readings due to thermal expansion of the water in the field

The first effect can be neglected due to the large differences in magnitude. When injecting water with a rate of 25 m³/h, only 0.35‰ of fresh fluids is injected per hour taking the entire cavern into account. This will therefore not affect the dissolution process and production.

The second effect is negligible as well. A correction of 1.0014 is calculated (1 m³ at the pump station is 1.0014 m³ at the cavern). This results in an underestimation of only 0.12% of the total water volume.

Salt creep

Salt creep could also influence the volume of a cavern. Calculations indicate that the volumetric creep rates range from -0.014‰/year to -0.026 ‰/year, which corresponds to a volume loss of 3.6 m³ to 6.5 m³/year. After 15 years this results in a volume loss of 0.54‰ to 0.98‰ based on a fully developed single completion cavern. This effect can therefore be neglected as well.

12.8 Reconciliation of reserves

An analysis regarding the predicted and actual produced salt from 23 caverns in the Usseleres area indicate that the current LT-plan is followed quite closely. However when implementing the reserve reconciliation tool it is indicated that the initial reserves are too conservative. This can be attributed to the current recovery- and insoluble content factor. It can be concluded that the recovery factor during the first main leaching stage are only 75%, versus the currently assumed 80%. However due to the improved insoluble contents a surplus in reserves is calculated.

The updated insoluble contents & sonar volumes have been implemented in the reserve reconciliation tool. It can be stated that using the updated values, 13% extra reserves are added to each cavern. However, due to the production controlled handling of the caverns 9% of these gained reserves are lost during MLS-1.

The results from the mass balance tests and Solling Fm. analysis indicate major fluid losses. The losses during the reserve estimations are therefore in line with the observations from sections 4, 5, and 6. It can be concluded that the current production process is therefore not efficient.

The reserve reconciliation tool is working and is used to acquire the results shown in section 10.5.

12.9 Answer to the research questions

In order to answer the main research question: *“Is it feasible to develop a predictive methodology which is able to quantify the uncertainties properly, and is utilized in the long-term planning of the production and development of the Hengelo Brine Field?”* a short summary will be given of the answers to the secondary research questions.

During the production of salt from the HBF, the operation is affected by many uncertainties; both geological and mining related. Most of the uncertainties can be quantified globally, whereas for some this is impossible. The most important uncertainties discussed in this thesis which have an effect on the operation are:

- Cavern shape & geometry
- Fluid pathways
- Fluid loss from caverns, resulting in unbalanced mass balances for individual caverns and the field
- Insoluble material & Bulking factor

Whereas it was concluded that the seasonal effects and salt creep can be neglected.

The insoluble content was determined in detail, with the use of multiple sonar measurements for particular caverns. Varying the bulking factor, around the average of 1.55, resulted in a distribution of insoluble contents for a range of caverns. It is concluded that the insoluble content is much lower in MLS-1 than it is in MLS-2. A variation is therefore observed in the salt; the deeper part of salt A is more pure than the top part. Linking the GR-logs with the insoluble contents didn't result in a proper correlation. It is concluded that the resolution of the GR-tool is insufficient.

The theoretical brine in/water out ratio is determined to be 0.96. After analyzing the various mass- & volume balances in the field it was determined that fluids are missing, therefore the caverns are not closed systems. Different connections and or fluid pathways were identified. The caverns are either directly connected or connected through the Solling Fm. A third possibility for the fluid losses is that the fluids disappear in the Solling Fm. due to the pressure gradient. Core observations confirmed halite filled fractures and veins, which can act as fluid pathways.

Besides these mass balance tests pressure tests also indicated direct and indirect connections between caverns. The effects on the recovery factor of caverns is hard to determine, but it does have an effect. This is also indicated by the In-/Outflow test.

In order to determine the volume of caverns the sonar tool is used. This tool has however certain limitations which make it impossible to precisely determine the volume of a cavern. It was concluded that the main limitations are the wavelength and the inability to 'measure' behind stalactites (and to a lesser extent stalagmites). The neglected volumes were quantified and a relationship was established between sonar and production data. The different volumes, based on: production data, sonar measurement and theoretical geological assumptions, were quantified for a given group of caverns and used in the In-/Outflow test.

The capacity of the field is based on the demand of the plant. A huge overcapacity is currently in place in order to be able to supply the plant with peak capacity. After analyzing the current production profile it was concluded that the production can be predicted quite accurately. The main deviations occur in the initial phase, since the sump period takes longer than expected and when the plant is down or infrastructural issues occur. Implementing the reserve reconciliation tool indicates that the initial reserve estimation are too conservative, even though the recovery factor during the first leaching stage is calculated to be lower than the assumed 80%. Recalculation of the reserves indicates 13% more reserves, although due to the production controlled handling only a gain of 4% is eventually achieved.

Combining all of the above a predictive methodology can be developed and should be used in the long-term planning of the production and development of the HBF. Although the recovery factor is slightly lower than assumed, the lower insoluble contents (as determined in this thesis) increase the total amount of salt reserves, which will have an effect on the future development of the field.

13. Recommendation

The following recommendations are suggested to be implemented to both improve the control on the operation as increasing the knowledge for the reserve reconciliation tool.



13.1 General

- More emphasis should be placed on the in-situ leaching process. How does the leaching process take place?
- Research should be done regarding alternating the flow rate of the injected fluids, to see whether this changes the leaching process in some way.
- The resource reporting from AkzoNobel may have to be updated. The current resource reporting document is based on the JORC Code from 2004. However, in 2012 the JORC code was updated.

13.2 Mass balance

- The flow meters have a certain error which is a combination of the standard error of the flow meter (given by the manufacturer) plus the measuring error due to other field circumstances. The highest error is measured at cavern 487, whereas the error at the other caverns are much lower. At cavern 487 2 different meters are installed. In order to reduce the measuring error at this cavern it is recommended to replace the old flow meter by one of the newer flow meters.
- During this research it was only possible to perform measurements at caverns 486, 487, 488, 490, 491, 504 & 506. Due to certain events in the field and limited time the results at 486 and 492 are not sufficient. It is recommended to measure the outflowing brine at these caverns as well, since it will be interesting to see whether these caverns show a high ratio, explaining fluid flow from caverns 487/488 towards 486 or from 490/491 to 492.
- In general it is recommended to install rock catchers and flow meters at the outflowing brine to improve the entire mass balance of the field and measure the amount of fluid losses.

13.3 Pressure test

- It is recommended to perform pressure tests on stationary caverns (e.g. caverns which are waiting for a workover). By doing this the pressure regime in the Solling Fm. and the interaction between the Solling Fm. and the caverns can be better understood. Sufficient information regarding the interaction between caverns in combination with the Solling Fm. can eventually make the operation more efficient. Improved knowledge regarding which caverns need to be stopped will reduce both the time of workovers as will minimize the down time of other affected caverns.

13.3 Ganzebos expansion

Some recommendations are meant for the Ganzebos expansion, since they are impractical for implementation in the historic developed areas of the Hengelo Brine Field.

- Installing flow meters on the brine-side in order to measure the amount of outflowing brine. This is not the case in the field yet, but tests (chapter 5) showed that useful information regarding the mass balance can be acquired. This should be implemented at the caverns in the Ganzebos expansion, since these caverns will be developed in the next 8 year. The advantages of this action will be:
 - Accurate in-/outflow data from individual caverns
 - Proper volume- and mass balance information for these individual caverns and the whole Ganzebos expansion
 - An accurate recovery factor can be established
 - Operating conditions can be altered with more confidence
- When flow meters are installed on the outflowing pipe, rock catchers should be installed as well. The rock catcher have been used in during the tests (chapter 5) as well. The device is described in section

5.3.2, Figure 33. The main principle of this catcher is based gravity. This device will prevent the flow meter from being clogged.

- The drilling crew should not drill multiple meters into the underlying Solling Fm. As described in chapter 10, the Solling Fm. can be considered as a giant sponge. At the moment the direct connection between the sump and the Solling Fm., initiated by the wellbore and/or direct contacts between the sump and the Solling Fm. causes a considerable amount of fluid loss from the caverns. Therefore the drillers should stop drilling before hitting the Solling Fm. or they should plug the part that is drilled in this formation. The advantages of this action will be:
 - Reduction in fluids losses form the caverns
 - Less interaction between caverns; workovers can be finished faster, since it will be easier to depressurize the caverns
 - In combination with the flow meters, accurate statements can be made about the leaching process in the cavern and the volume-/mass balance should be equal to the theoretical value
 - Less energy will be lost by pumping water into the Solling Fm., this will result in a cost reduction.

13.4 Real time monitoring

In order to bring the development of the HBF to a higher standard, the current techniques should be modernized. The aim should be to implement real time monitoring and process control. Using real time monitoring & process control. When using real time monitoring & process control, real time optimization can be achieved.

13.5 Reserve reconciliation

- All caverns should be added to the current reserve reconciliation tool to in order to be able to use it as a long-term development and planning tool for current and future developments.
- All sonar measurements should be converted to real cavern volumes (chapter 7) and added to the reserve reconciliation tool. This will increase the understanding of reserve development throughout production of individual caverns and its effect on the entire field.
- It was concluded that due to the production controlled handling of caverns, salt is lost during the production process. Therefore it is recommended that the 150.000 ton marker is increased, in order to produce more salt during MLS-1 or flow meters are installed on the brine outlet.
- The reserve development during MLS-2 should be analyzed in detail using the reserve reconciliation tool. This can be done as soon as more sonar measurements are available.

References

	Personal communication:	Company
1	den Hartogh, M. Geologist and Project Manager Mining Development & Compliance	AkzoNobel
2	Leusink, H. Mining specialist Mining Development & Compliance	AkzoNobel
3	Keizer, J. Field crew member Drilling site AkzoNobel Hengelo	AkzoNobel
4	Pinkse, T. Manager Mining Development & Compliance	AkzoNobel
5	Robertus, S. Solution mining technologist Mining Development & Compliance	AkzoNobel

Bibliography

- Bachmann, G.H. & Kozur, H. (2004). The Germanic Triassic: correlations with the international chronostratigraphic scale, numerical ages and Milankovitch cyclicity, in *Hallesches Jahrbuch für Geowissenschaften, Band 26* (p. 17-62). Martin-Luther-Universität, Halle-Wittenberg.
- Bear, J. (1972). Dynamics of Fluids in Porous Media (p. 136). Courier Corporation, Dover.
- Bekendam, R.F. (2011). Toelichting op de waarde van de bulking factor. GeoControl, Maastricht.
- Bérest, P., Karimi-Jafari, M., Brouard, B., Bazargan, B. (2006). In situ mechanical tests in salt caverns. Solution Mining Research Institute, Spring 2006 Technical Meeting, Brussels.
- Callomon, J.H. (2003). The Middle Jurassic of western and northern Europe: its subdivisions, geochronology and correlations, in *Geological Survey of Denmark and Greenland Bulletin 1* (p. 61-73).
- Craig, R.F. (1974). Basic characteristics of Soil, in *Craig's soil mechanics* (p. 18). Spon press, London.
- Creative Safety Supply. (2015). DMAIC Cycle. Assessed on June 2nd 2015.
URL: <http://blog.creativesafetysupply.com/dmaic-cycle/>
- de Jager, J. (2007). Geological development, in *Geology of the Netherlands*, by Th.E., Batjes, D.A.J. & Jager, de, J. Wong, (p. 5-26). Royal Netherlands Academy of Arts and Sciences (KNAW), Amsterdam.
- de Vlieg, D. (2015). Research on potential hydrological connections between salt caverns in the upper part of the Solling Formation and its economic consequences. MSc. Thesis, University of Utrecht, Utrecht.
- Domenico, A.D. & Schwartz, F.W. (2008). Physical and Chemical Hydrology. John Wiley and Sons Inc., Hoboken. ISBN 0-471-59762-7.

- Doornenbal, H. & Stevenson, A. (2010). Petroleum Geological Atlas of the Southern Permian Basin. EAGE Publications B.V., Houten.
- Drost, G.I.A. (2012). Geomechanical properties of a backfill material suitable for stabilising salt caverns in Twente. MSc. Thesis, Department of Geotechnology, TU Delft, Delft, The Netherlands.
- Dufour, F.C. (1998). Grondwater in Nederland; Onzichtbaar water waarop wij lopen. NITG-TNO (Dutch research institute), Utrecht.
- Ellis, D.V. & Singer, J.M. (1987). Well Logging for Earth Scientists. Elsevier, Amsterdam
- Ensing, M.C. (2012). Salt Reserve Estimate for the Twenthe-Rijn concession. BSc. Thesis, TU Delft, Delft.
- Geluk, M.C. & Röhling, H.G. (1997). High-resolution sequence stratigraphy of the Lower Triassic Buntsandstein in the Netherlands and northwestern Germany, in *Geologie en Mijnbouw* 76 (p. 227-246). Netherlands Journal of Geosciences, Utrecht
- Gemmer, L., Ings, S. & Beaumont, C. (2005). Passive Margin Salt Tectonics - Dynamic Modelling of Sediment Progradation above a Viscous Salt Layer, in *Basin Research* (p. 383-402). EAGE Publications B.V., Houten.
- George, M. & Lawrence Jr., R. (2002). Lean Six Sigma: Combining Six Sigma with Lean Speed. McGraw Hill Professional.
- Geowulf Laboratories, (de Bruijn, P. & de Klerk, de, C.). (2011). Detailed Geology of the Hengelo Solution Mining Area, part 2 (report no GL11.901). Geowulf Laboratories, Voorburg.
- Geowulf Laboratories, (de Bruijn, P. & de Klerk, de, C.). (2014). Detailed Geology of the Usseler Es Area, Southern Part. Geowulf Laboratories, Voorburg.
- Herngreen, G.F.W., Kouwe, W.F.P. & Wong Th.E. (2003). The Jurassic of the Netherlands, in *The Jurassic of Denmark and Greenland. Geological Survey of Denmark and Greenland Bulletin 1*, by J.R. & Surlyk, F. Ineson, (p. 217–229). Geocenter, Copenhagen.
- Holentstein, N., Küchler, H. & Schaber, S. (2014). Pressure tests in cavern series 367, 372, 381 & 472. KBB, Hannover.
- HUT. (2012). Hengelo Uitloogtechniek 7e actualisering. Mining Technology Department AkzoNobel, Hengelo
- JORC Code. (2004). The JORC Code - 2004 Edition. AusIMM Publications Department, Melbourne, Australia
- JORC Code. (2014). The JORC Code – 2012 Edition. AusIMM Publications Department, Melbourne, Australia
- Klimaatinfo.nl (2015). Het klimaat van Twente. Assessed on April 4th 2015.
URL: <http://www.klimaatinfo.nl/nederland/twente.htm>
- Kozur, H.W. (1999). The correlation of the Germanic Buntsandstein and Muschelkalk with the Tethyan scale, in *The Epicontinental Triassic*, by G. Bachmann, (p. 701-725). Zentralblatt für Geologie und Paläontologie, Halle.
- Kunstman, A. & Urbanczyk, K. (2008). Designing of the storage caverns for liquid products, anticipating its size and shape changes during withdrawal operations with the use of unsaturated brine. SMRI 2008 Spring Meeting, Technical Conference, 28-29 April 2008. Porto, Portugal
- Li, Y.P., Yang, C.H., Qian, Q.H., Wei, D.H. & Qu, D.A. (2007). Experimental research on deformation and failure characteristics of laminated Salt Rock. In M. L. Wallner, *The Mechanical Behavior of Salt* –

- Understanding of THMC Processes in Salt* by M., Lux, K.H., Minkley, W. & Hardy Jr., H.R. Wallner (p. 69-74). Taylor & Francis Group, London.
- Maystrenko, Y., Bayer, U. & Scheck-Wenderoth, M. (2006). 3D reconstruction of salt movements within the deepest post-Permian structure of the Central European Basin System - the Glückstadt Graben, in *Geologie & Mijnbouw* 85 (p. 183-197). Netherlands Journal of Geosciences, Utrecht.
- McEwan, J. S. & Ramey, M. (2010). Solution mining - Mass balance calculations. *Mining Engineering Magazine* vol. 62, issue 9, (p. 65-68). Society of Mining Engineers, Englewood, CO.
- Mijnbouwwet. (2002). Dutch Government. Assessed on June 3rd 2015.
URL: http://wetten.overheid.nl/BWBR0014168/Aanhef/geldigheidsdatum_22-07-2015
- Mutterlose, J. & Bornemann, A. (2000). Distribution and facies patterns of Lower Cretaceous sediments in northern Germany: a review, in *Cretaceous Research* 21, (p. 733-759)
- MWH. (2010). Salt mining possibilities in areas adjacent to the Hengelo brine field (project nr. W09B0028). MWH Consultants, Arnhem
- MWH. (2011). Seismic survey and geological model update for Oele and Ganzebos areas, final report. MWH Consultants, Arnhem
- NITG-TNO. (1998). Geological Atlas of the Subsurface of The Netherlands, Sheet X: Almelo - Winterswijk. Nederlands Instituut voor Toegepaste Geowetenschappen, Haarlem
- Ofoegbu, G.I., Read, R.S., Ferrante, F. (2008). Bulking factor of rock for underground openings. Center for Nuclear Waste Regulatory Analyses, San Antonio, Texas
- Pharaoh, T. C., Dusa, M., Geluk, M.C., Kockel, F., Krawczyk, C.M., Krzywiec, P. & Van Wees, J.D. (2010). *Tectonic Evolution* in Petroleum Geological Atlas of the Southern Permian Basin (p. 25-57), by J.C. & Stevenson, A.G. Doornbal, 25-57. EAGE Publication B.V., Houten.
- Quintessa. (2013). Staged Risk Assessment of Salt cavern Stabilisation, Phase 1. Quintessa Ltd, Oxfordshire.
- Rasmussen, E.S., Vejbaek, O.V., Bidstrup, T., Piasecki, S. & Dybkjaer, K. 2005. Late Cenozoic depositional history of the Danish North Sea Basin: implications for the petroleum systems in the Kraka, Halfdan, Siri and Nini fields, in *Petroleum Geology: North-West Europe and Global Perspective, Proceedings of the 6th Petroleum Geology Conference* by A.G. & Vining, B.A. Doré, (p. 1347-1358). The Geological Society, London.
- Robinson, J.G. & Elliott, D. (2004). National Instrument 51-101 (NI 51-101) Reserves Reconciliation - Part 1. *Journal of Canadian Petroleum Technology - Volume 43 - Issue 11* (p. 6-12).
- Röhling, H.G. (1991). A lithostratigraphic subdivision of the Early Triassic in the Northwest German Lowlands and the German Sector of the North Sea, based on gamma-ray and sonic logs, in *Geologisches Jahrbuch Reihe A 119* (p. 3-23).
- Russell, W.L. (1944). The total gamma ray activity of sedimentary rocks as indicated by Geiger counter determinations. *Geophysics* 9 (p. 180-216).
- Schulz, R. & Röhling, H.G. (2000). Geothermische Ressourcen in Nordwestdeutschland, in *Zeitschrift für Angewandte Geologie* 46 (p. 122-129).
- Sharpe, R., Cork, G. (2006). Gypsum and Anhydrite, in *Industrial Minerals & Rocks* by J.E., Trivedi, N.C., Barker J.M., Krukowsk, S.T. Kogel, (p. 526). Society for Mining Metallurgy.

- SOCON. (2015). Acoustic velocity & Frequency. Retrieved at March 23rd 2015.
URL: <http://socon.info/80-2-acoustic-velocity.html> and <http://socon.info/77-2-measuring-head.html>
- SPE. (2007). *Petroleum Resources Management System*. Society of Petroleum Engineers.
URL: http://www.spe.org/industry/docs/Petroleum_Resources_Management_System_2007.pdf
- Stampfli, G.M., Borel, G.D., Marchant, R. & Mosar, J. (2002). Western Alps geological constraints on western Tethyan reconstructions. *Journal of the Virtual Explorer* (p. 77-106).
- TIME Magazine. (1982). A Brief History of Salt, in *TIME Magazine*. Published March 15th 1982.
URL: <http://time.com/3957460/a-brief-history-of-salt/>
- van Berkel, J.D.D. (2014). An insight in the mass balance and reserve reconciliation of salt caverns in the Hengelo brine field. MSc. Thesis, Delft University of Technology, Delft.
- van der Kroef, R.F.M. (2012). Fault pattern reconstruction of the Hengelo brine field, the Netherlands. MSc. Thesis, Utrecht University, Utrecht.
- van Duijne, H. (2012). Generic Technical Risk Assessment of Gas Oil Storage in Salt Caverns in the Twente Region based on the Second Use Containment Concept (2U-CC). Report number 1203390-000, Deltares, Delft.
- van Sambeek, L.L., Bérest, P. & Brouard, B. (2005). Improvements in mechanical integrity tests for solution-mined caverns used for mineral production or liquid-product storage. SMRI, Fall 2005 Technical Meeting, Nancy.
- Vasebi, A., Poulin, É. & Hodouin, D. (2014). Selecting proper uncertainty model for steady-state data reconciliation - Application to mineral and metal processing industries, in *Minerals Engineering* 65 (p. 130-144).
- Vinken, R. (1988). The Northwest European Tertiary Basin. Results of the International Geological Correlation Programme, Project No. 124, in *Geologisches Jahrbuch A 100*.
- Watson, T.L. & Bachu, S. (2009). Evaluation of the potential for gas and CO₂ leakage along wellbores, SPE Paper 106817. *SPE Drilling & Completion* 24 (1), (p. 115-126).
- Westendorp, J. (1969). *Onderzoek van boorkernen, afkomstig van Boring 151, te Hengelo (O)*. Koninklijke Nederlandse Zoutindustrie (KNZ), Hengelo.
- Wong, T.E. (2007). Jurassic, in *Geology of the Netherlands*, by Th.E., Batjes, D.A.J. & de Jager, J. Wong, (p. 107-125). Royal Netherlands Academy of Arts and Sciences (KNAW), Amsterdam.
- Ziegler, P.A. (1990). Tectonic and palaeogeographic development of the North Sea rift system, in *Tectonic evolution of the North Sea rifts*, by D.J. & Gibbs, A.D. Blundell, (p. 1-36). Oxford Science Publications, Oxford.
- Zulauf, G., Zulauf, J., Bornemann, O., Brenker, F.E., Höfer, H.E., Peinl, M. & Woodland, A.B. (2010). Experimental deformation of a single-layer anhydrite in halite matrix under bulk constriction. Part 2: Deformation mechanisms and the role of fluids. *Journal of Structural Geology Volume 32, Issue 3*, (p. 264-277). Elsevier.

Appendix A – Salt mining cavern types AkzoNobel

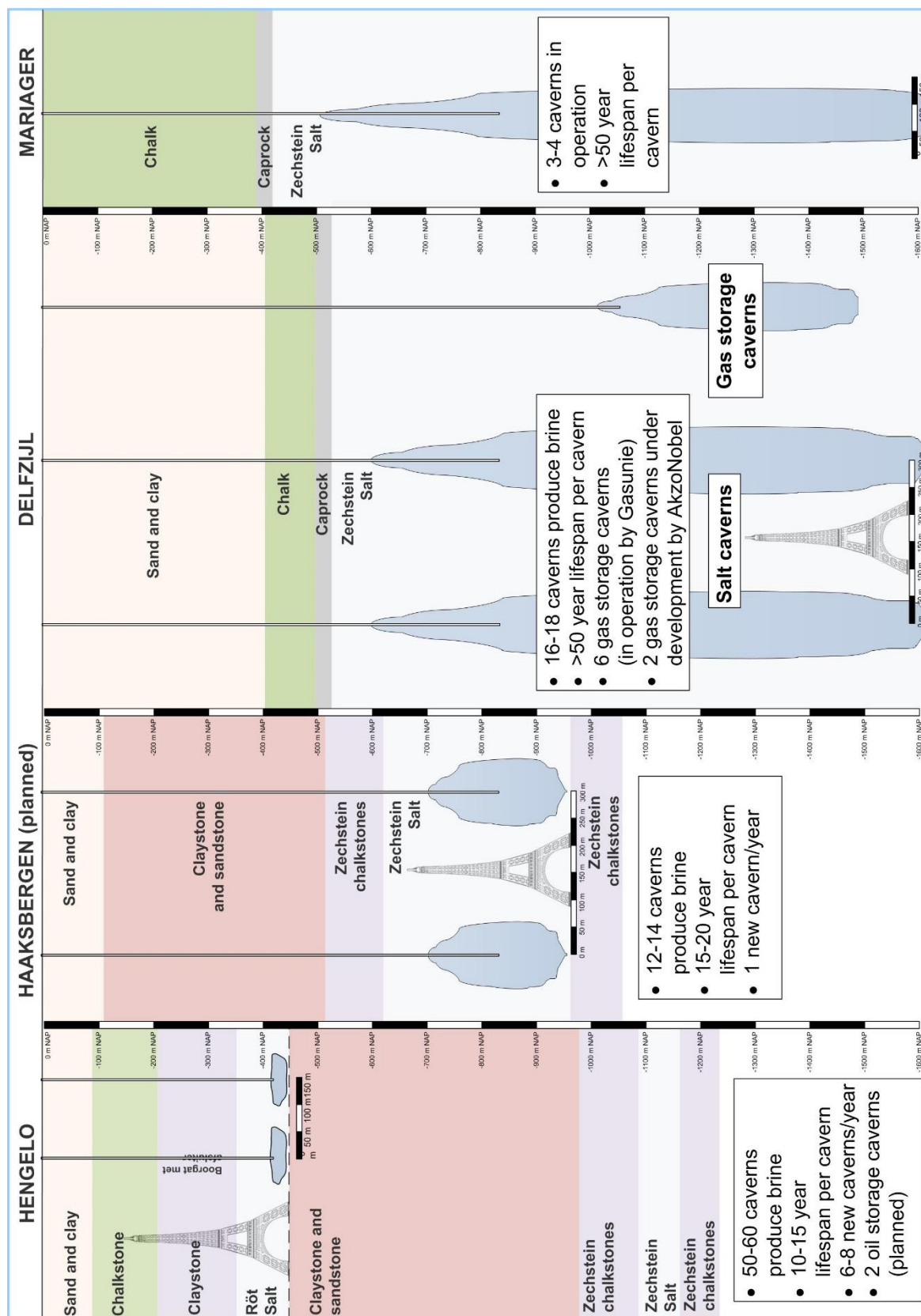


Figure 98 – Comparing the 3 salt mining operations of AkzoNobel. The typical shapes of the caverns and characteristics are given in the figure. Note that the cavern shape in Hengelo (i.e. the Hengelo Brine Field) is significantly different than the caverns at the other locations.

Appendix B – Caverns

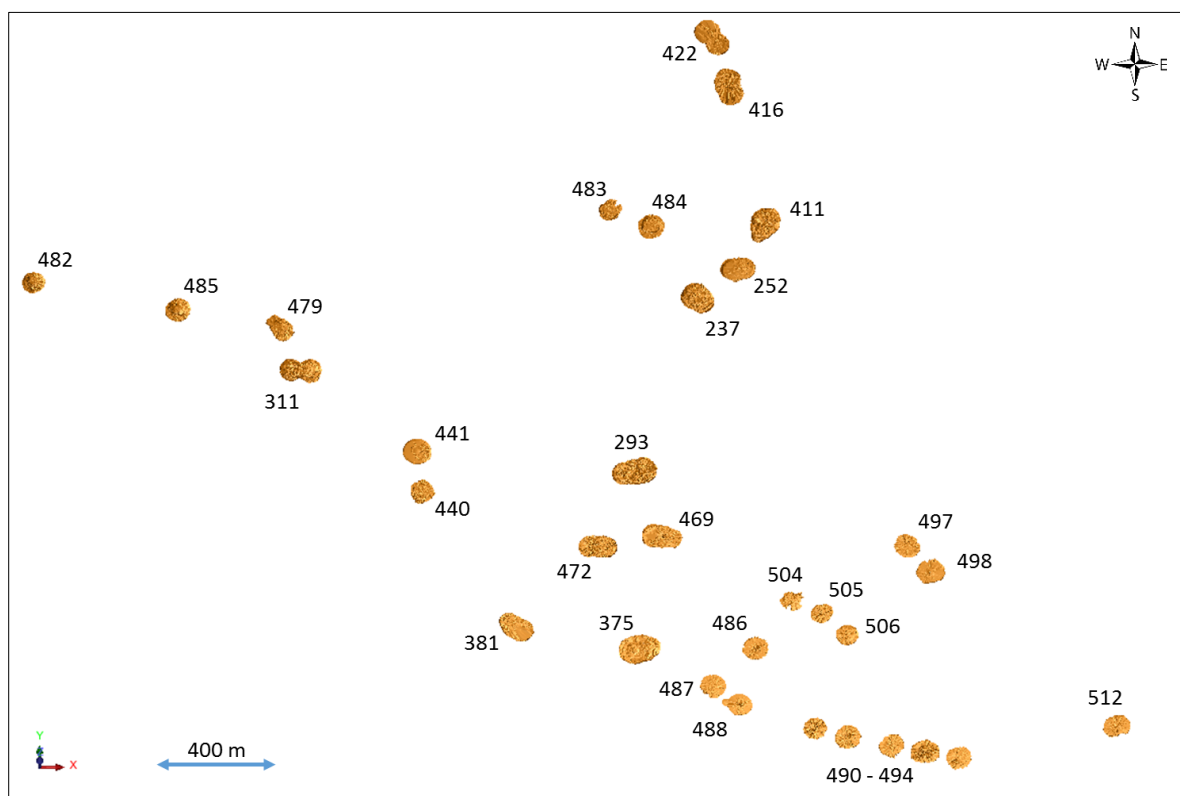


Figure 99 – Caverns used for determination of the insoluble content.

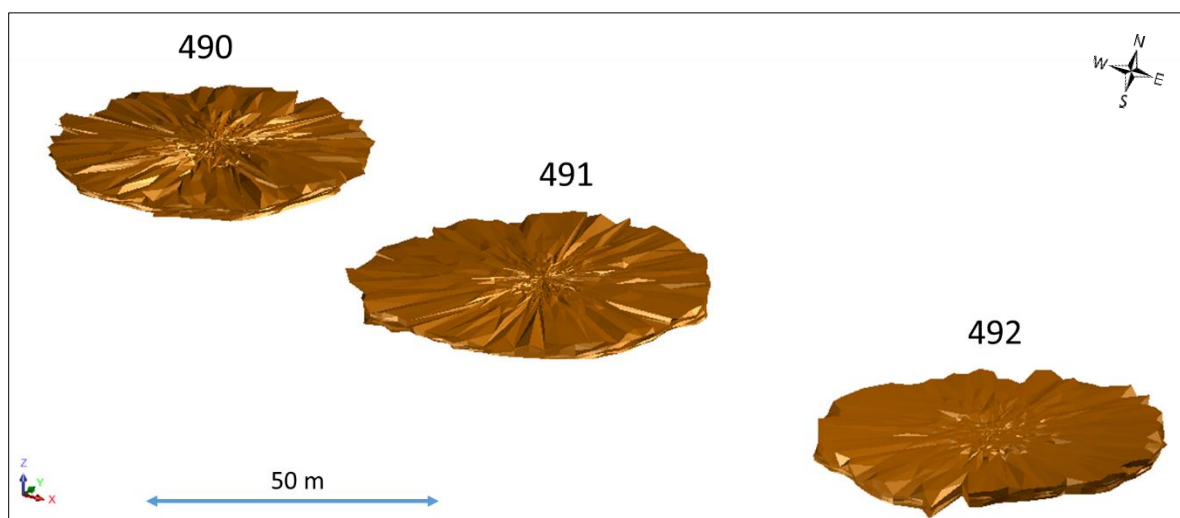


Figure 100 – Detailed representation of caverns 490, 491 and 492. The shape of the caverns is clearly visible. The general shape is circular with. It can be noticed that the top (i.e. roof) of the cavern is uneven, indicating that the roof is not flat. The emitted sonar pulses are reflected back from solid objects, insolubles hanging from the roof cause this uneven surface.

Appendix C – Cavern interior

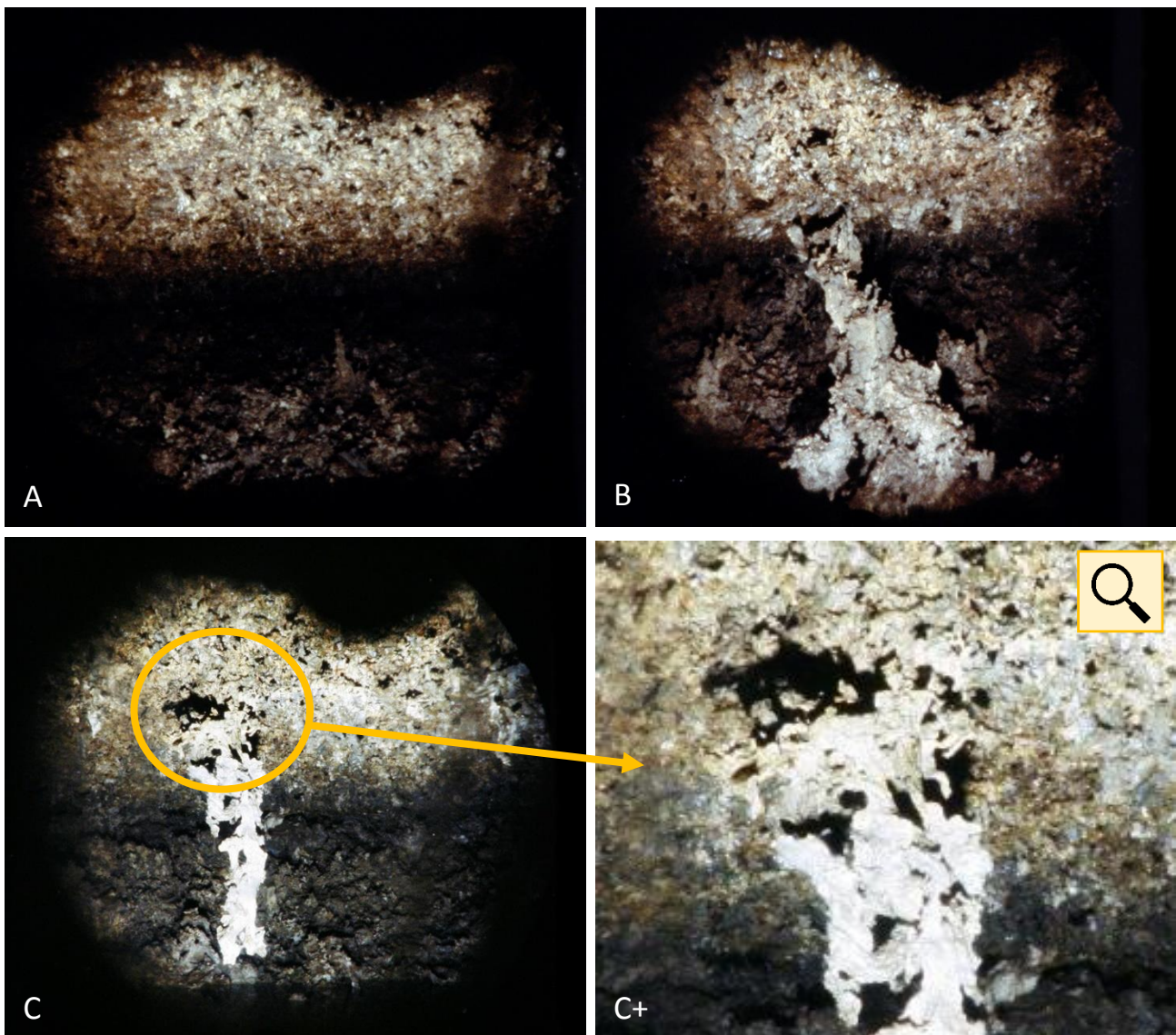


Figure 101 - The pictures above provide an inside look in the salt caverns around Hengelo. It is clearly visible how irregular the walls are and how big the rock fragments hanging from the roof are.

Appendix D – Resource Reporting (AkzoNobel)

The JORC Code (2004) was adapted to AkzoNobel's salt solution-mining operation, several definitions had to be tailored to this specific situation. The following definitions were formulated in cooperation with the AkzoNobel geologists (Ensing, 2012).

- **“Mineral Resource”** is used for estimates based on geological information only
- **“Salt Reserve”** is used for estimates in which the “modifying factors” have been taken into account.
- **“Modifying Factors”** includes the consideration of mining, metallurgical, economic, marketing, legal, environmental, social and governmental factors. In the context of salt mining it encompasses e.g. the technical criteria for stability as set by the good salt mining practice (i.e. GSMP), restrictions to mining due to surface infrastructure and environment, and economical considerations.
- **“Mineral Resource” vs. “Salt Reserve”**: estimates for an entire exploration license area based on regional geological information only vs. the sum of estimates on a cavern-by cavern basis. Cavern-specific considerations such as e.g. the technical guidelines for stability as set by the GSMP, restrictions to mining due to surface infrastructure and environment, and economical considerations have been taken into account.
- **“Inferred Mineral Resource”** is an initial estimate during the prospecting phase of a new salt deposit. It is based on already existing subsurface data such as e.g. wells, seismic that were not obtained in the context of the new prospecting.
- **“Indicated Mineral Resource”** is a fairly reliable estimate based on widely-spaced seismic lines acquired as part of the exploration phase of the new salt prospect and/or existing well data. Boundaries of the prospect are based on the exploration license.
- **“Measured Mineral Resource”** is a highly reliable estimate based on seismic lines and new well data acquired as part of the exploration phase of the new salt prospect. Well data include an accurate estimate of the grade (% insoluble) of the salt deposit. In practice, a zone is defined around a well or a seismic line for which the extrapolation of the actual data is considered to be so reliable that it can be said to be “measured”. A distance is used to define this zone, the value of which depends on the variation in the geology within the concession for which an estimate is made.
- **“Probable Salt Reserve”** is an estimate that is based on the indicated mineral resource, but with technical, infrastructural, environmental, and economical considerations taken into account.
- **“Proven Salt Reserve”** is an estimate that is based on the measured mineral resource, but with technical, infrastructural and economical considerations taken into account

Appendix E – Deviation in flow data caused by flow meter inaccuracies

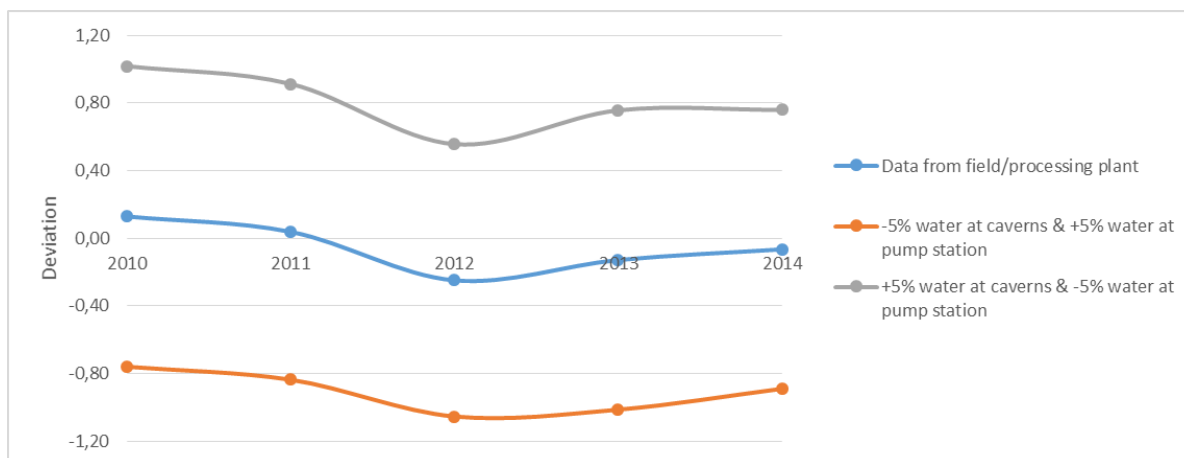


Figure 102 - Difference between volumes measured at the cavern and the volume at the pump station

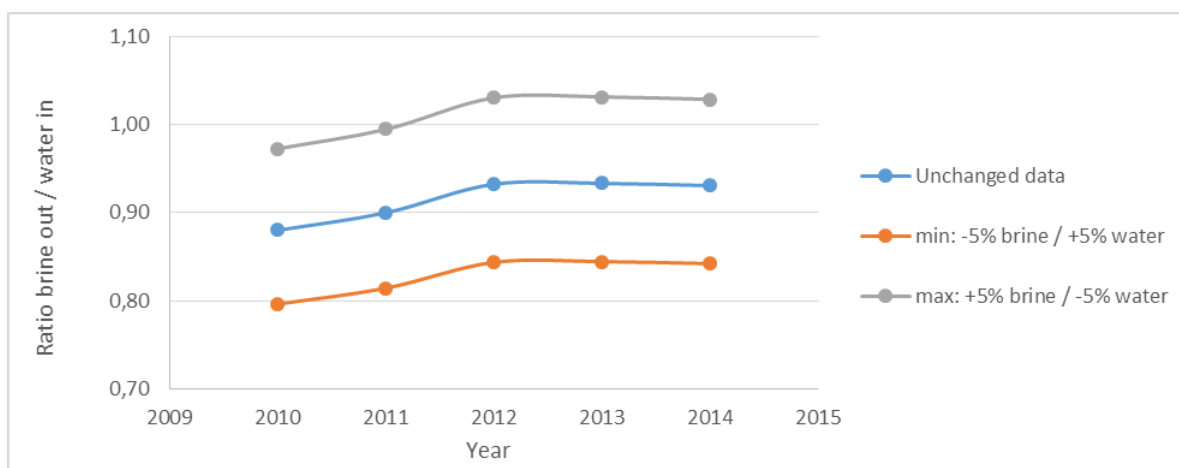


Figure 103 - Ratio between brine outflow and water inflow measured at the **caverns**.

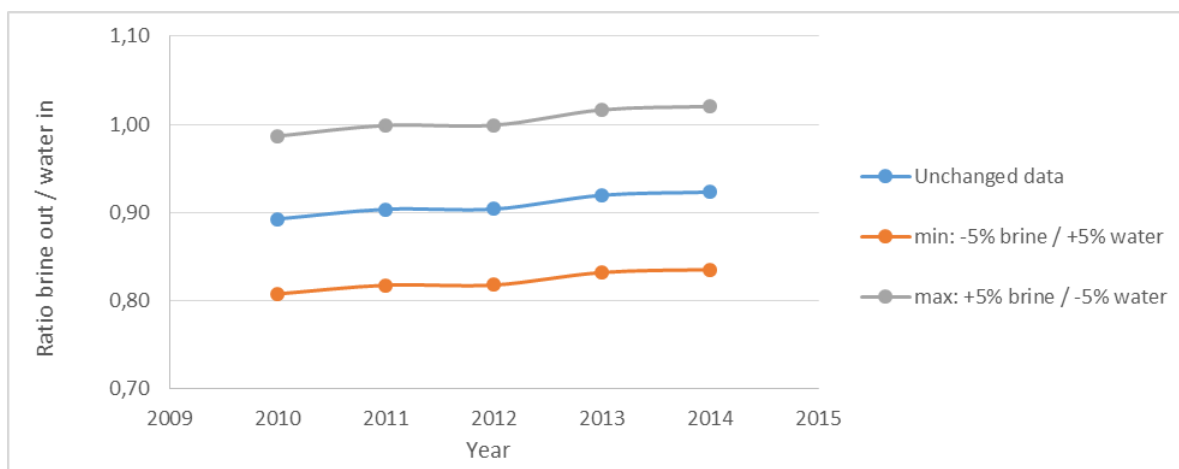


Figure 104 - Ratio between brine outflow and water inflow measured at the **pumpstation**

Appendix F – Graphs from pressure tests

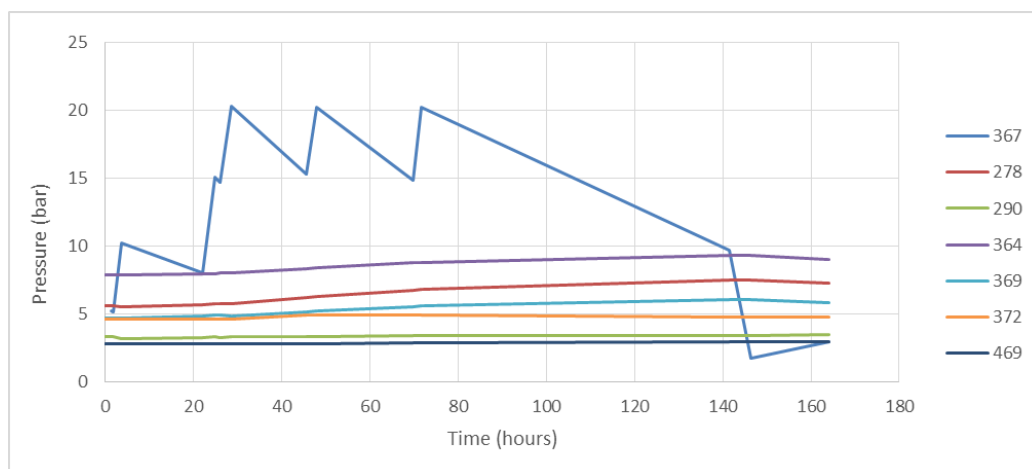


Figure 105 – Pressure test at cavern 367. The sharp increases to 20 bar indicate the moments of brine injection during the pressure test.

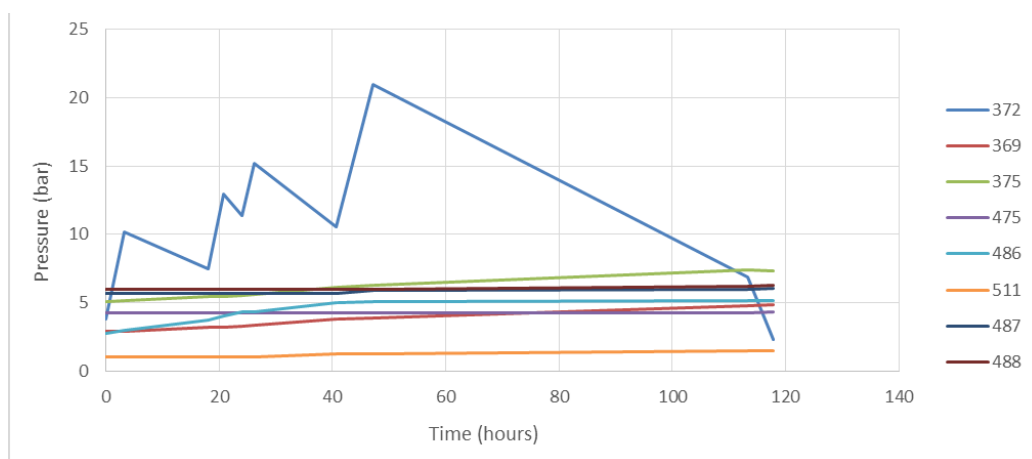


Figure 106 – Pressure test at cavern 372

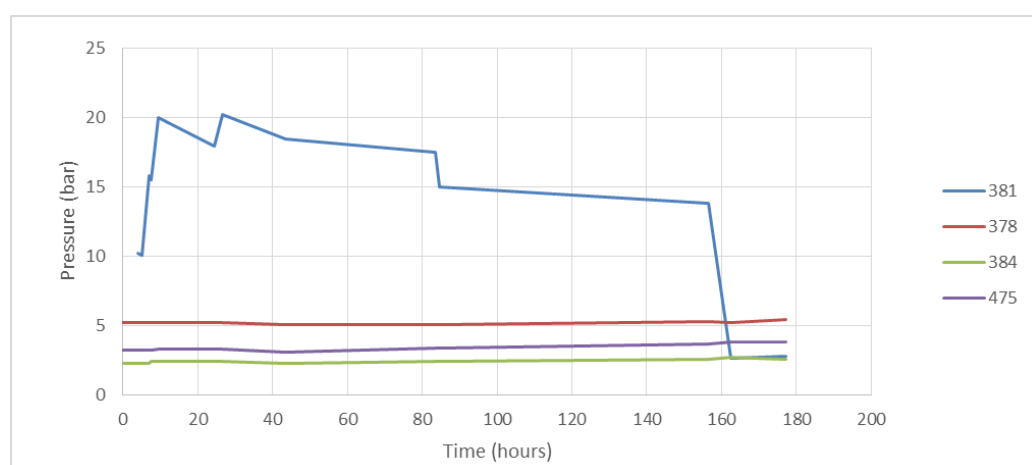


Figure 107 – Pressure test at cavern 381

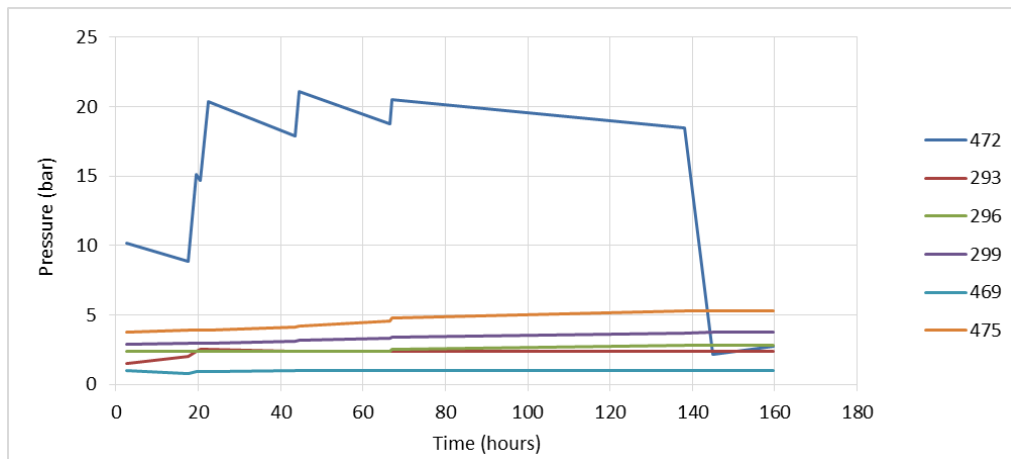


Figure 108 – Pressure test 472

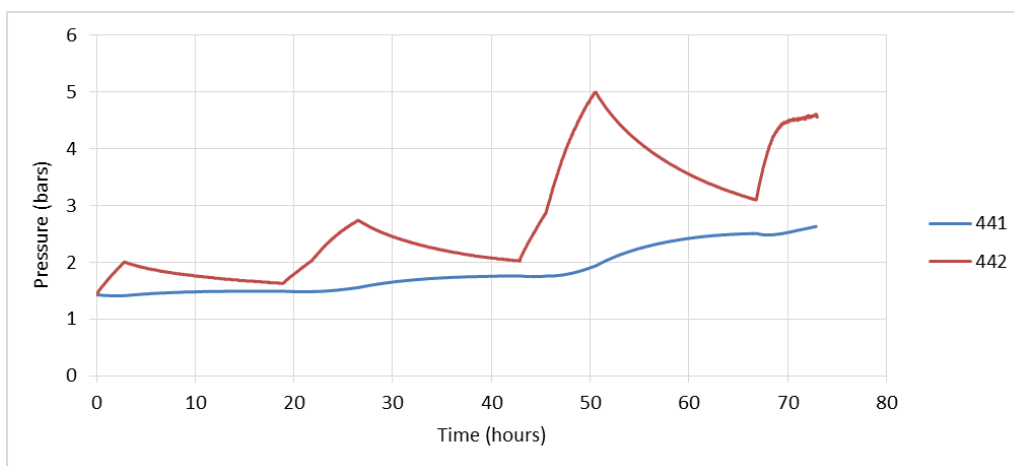


Figure 109 – Pressure test 441

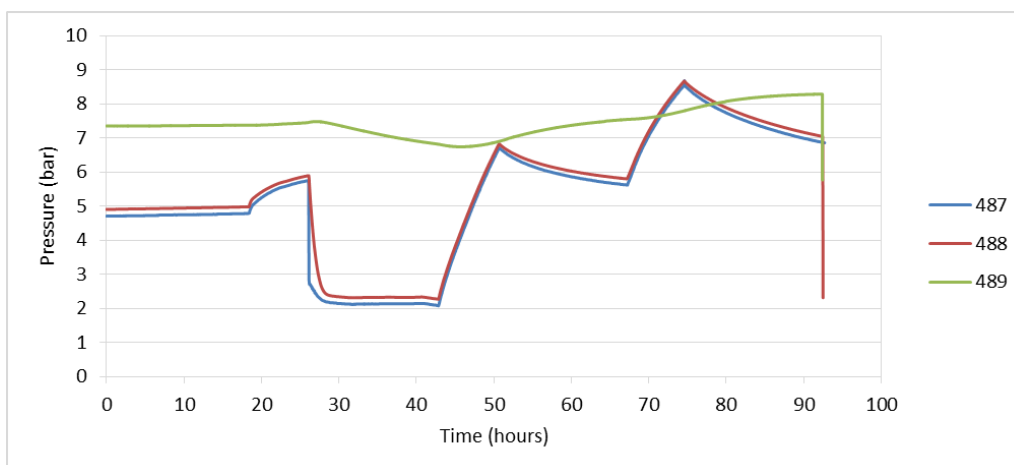


Figure 110 – Pressure test 487. The pressure in cavern 487 follows the trend of 488 closely, indicating a direct contact between both caverns.

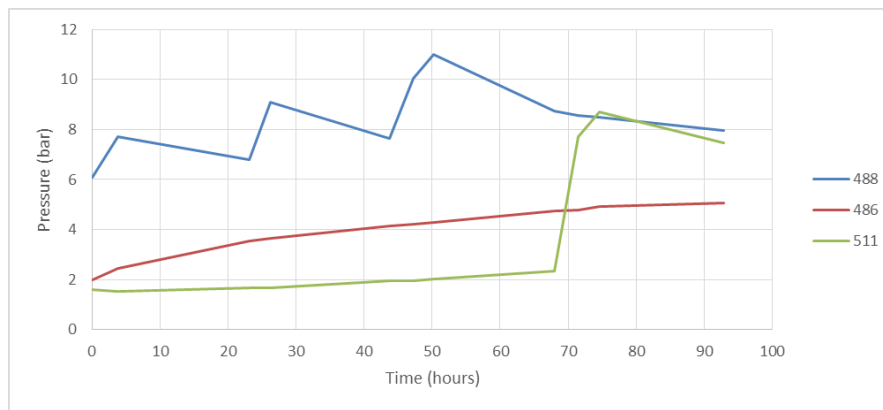


Figure 111 – Pressure test 488

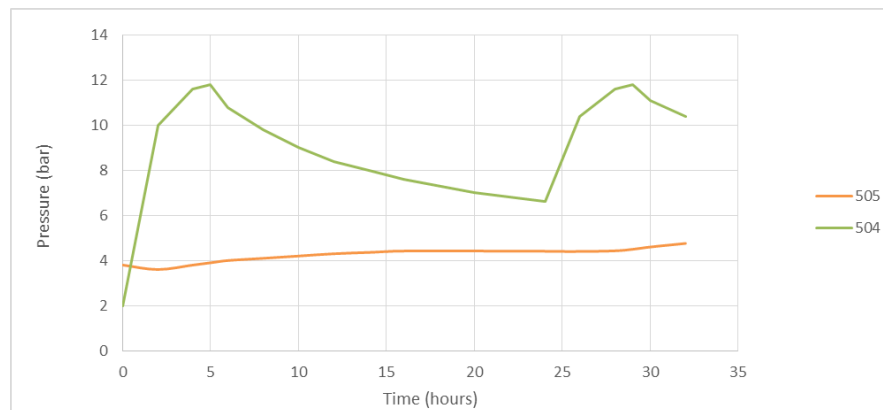


Figure 112 – Pressure test 505

Appendix G – Average temperatures and related water density

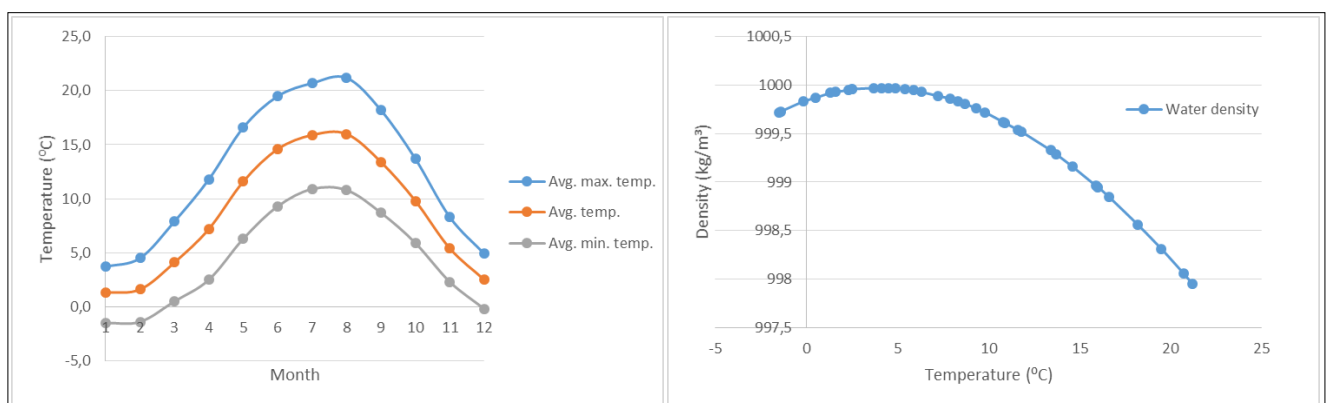


Figure 113 – Left: Average temperatures in Hengelo (Klimaatinfo.nl). Right: Density of water as function of temperature

Appendix H – Ratios for individual mass balance tests

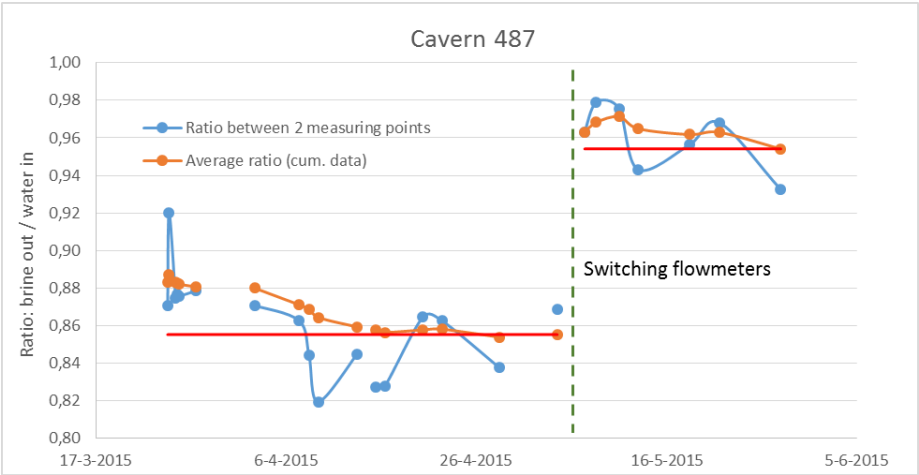


Figure 114 – Brine out / water in ratios of cavern 487 during tests 1 and 2.

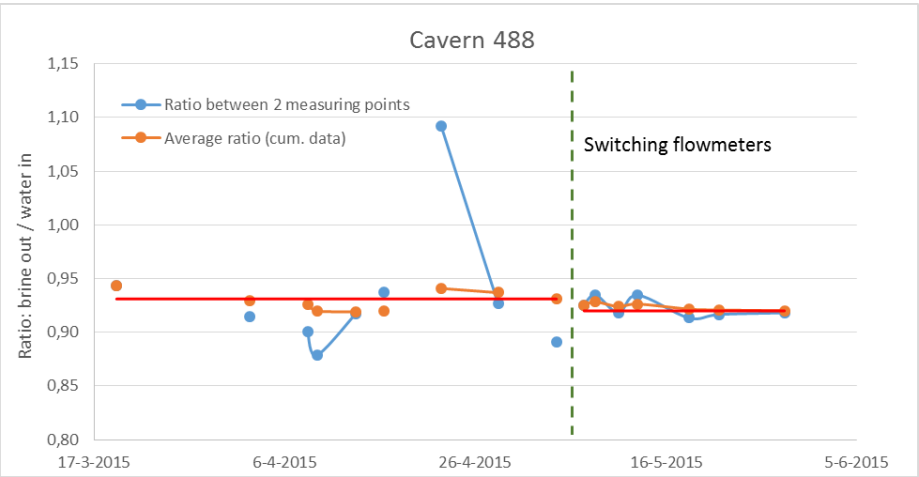


Figure 116 – Brine out / water in ratios of cavern 488 during tests 1 and 2.

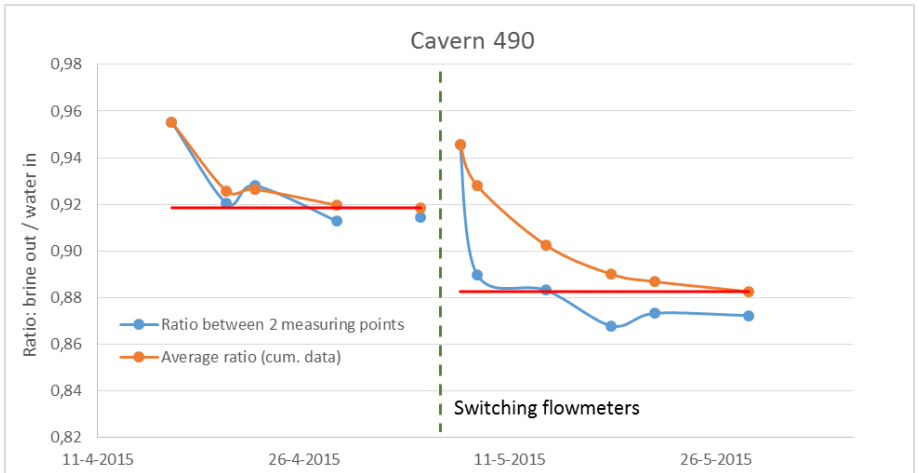


Figure 115 – Brine out / water in ratios of cavern 490 during tests 1 and 2.

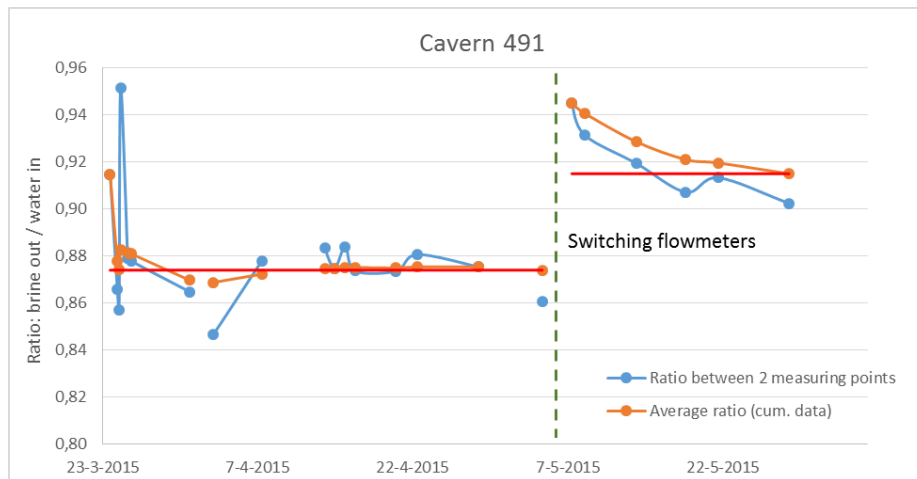


Figure 117 – Brine out / water in ratios of cavern 491 during tests 1 and 2.

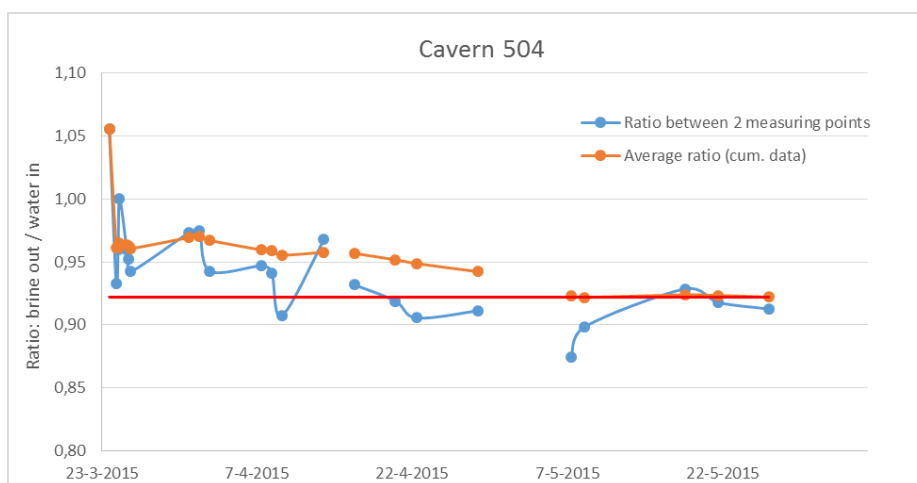


Figure 118 – Brine out / water in ratios of cavern 504 during tests 1 and 2.

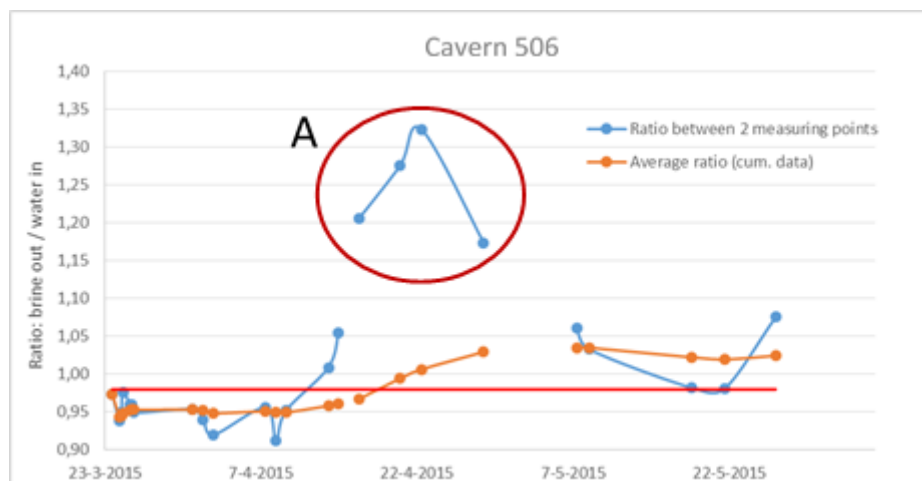



Figure 119 – Brine out / water in ratios of cavern 506 during tests 1 and 2. A large increase in ratio was noticed.

Appendix I – Solling Fm. core description

Table 17 – BKM-02 core description; core was drilled in the Solling Fm.

Well: BKM02 Core no. 3 date. 5-3-2015 From: 645.66 m-ground level To: 653.61 m-ground level Total core length: 8.95 m			
			
box no.	Top m-mv	Bottom m-mv	description
Box 1A	645.66	645.87	Fine siltstone, anhydritic parts (Halitic)
Box 1B	645.87	646.06	
Box 1C	646.06	646.16	
Box 2	646.16	646.98	Siltstone, less anhydritic parts (Halitic)
Box 3	646.98	647.63	Claystone/ Fine siltstone, more anhydritic parts (Halitic)
Box 4	647.63	648.59	Very fine sandstone (Halitic) (clear reduced and oxidized parts)
Box 5	648.59	649.58	Siltstone, more anhydritic (Halitic) (Oxidized)
Box 6A	649.58	649.77	Similar to Box 5
Box 6B	649.77	650.05	
Box 7	650.05	650.60	Fine sandstone (fractures, with halite cement 1mm) (Lots of halite veins) (Halitic)
Box 8	650.60	651.41	More sandy than Box 7 (Halitic) (reduced)
Box 9	651.41	652.20	Fine sandstone fracture filled with halite cement (1-3mm) (Halitic)
Box 10A	652.20	652.56	Siltstone, bit anhydritic Large halite veins (1-5 cm) veins coincide with fractures filled with halite (1mm) (Halitic) (Oxidized)
Box 10B	652.56	652.96	
Box 11A	652.96	653.15	Fine sandstone (Halitic) (Halitic) (Oxidized)
Box 11B	653.15	653.35	More sandy than A (large halite veins, few cm) (Halitic) (Oxidized)
Box 11C	653.35	653.45	More sandy than B (large halite veins, few cm) (fractures coincide with halite veins (1-3mm)) (Halitic) (Oxidized)
Box 11D	653.45	653.55	More sandy than C (large halite veins, few cm) (fractures coincide with halite veins (1-3mm)) (Halitic) (Reduced)
Box 11E	653.55	653.61	More sandy than D (fractures coincide with halite veins (1-3mm)) (Halitic) (Reduced)

144

Appendix K – Additional stratigraphic information

Muschelkalk formation

The Muschelkalk formation is subdivided into 4 geological units:

- *Lower Muschelkalk* - The Lower Muschelkalk Formation (RNMUL) contains grey thinly bedded calcareous clay- and limestones, which are interspersed by dolomites and some intercalations of red to brown colored calcareous claystones. Noteworthy is that the dolomites are rich in anhydrite nodules. The Lower Muschelkalk can be further subdivided into a lower (RNMU-A) and upper (RNMU-B) section (Geowulf Laboratories 2011). The thickness distribution of the lower section is quite uniform. The upper section varies in thickness, which can be explained by the upper boundary which is an unconformity throughout the entire HBF.
- *Middle Muschelkalk* - The Middle Muschelkalk (RNMUM) only occurs in the northeastern part of the HBF. It consists of two characteristic units. The lower part shows an alternation of anhydrite and dolomitic marl whereas the upper contains grey dolomitic marls, with increasing clay presence towards the top. The thickness of this member varies between 25 - 30m.
- *Upper Muschelkalk* - The Upper Muschelkalk (RNMUU) consists of an alternation of carbonate and claystone beds, and is only found at a few locations in the HBF (Dufour, 1998).

Altena Group

In the Netherlands the uppermost Triassic, and Lower and Middle Jurassic deposits comprise of a relatively thick succession of marine claystones, siltstones, marls and some sandstones, which have been placed in the Altena Group. In the HBF the Altena Group lies unconformably on top of the Muschelkalk Formation and is unconformably overlain by the Niedersachsen Group, or the North Sea Group (van Duijne, 2012). The group is subdivided into several formations: the Sleen Formation, the Aalburg Formation, the Posidonia Shale Formation, the Werkendam Formation and the Brabant Formation. Only the Sleen Formation and the Aalburg Formation are present in the HBF (Geowulf Laboratories, 2011)

- *Sleen Formation* - The Sleen Formation (ATRT) consists of black, claystone and clayey shale. Locally traces of pyrite, fossil remains and plant material have been found in the formation. The formation can easily be recognized by on GR-logs due to its uniform thickness and relative high gamma-ray readings. The formation is divided in an upper and lower part. The Sleen Formation has a thickness up to 19 m in the HBF (van der Kroef, 2012).
- *Aalburg Formation* - The Aalburg Formation (ATAL) consists of green-grey to black, sometimes calcareous, claystone with thin limestone layers. The lower parts of the formation contain some organic rich claystone layers (van Duijne, 2012)..

Niedersachsen Group

The Niedersachsen Group contains floodplain, lake and (hypo- to hypersaline) lagoonal deposits, locally with a high content of carbonates and evaporites. In the Twente area the Niedersachsen Group consists of the Weiteveen Formation and the Coevorden Formation. Within a graben to the west of the HBF a thickness of up to 200 m is encountered, whereas the group is only 13 to 65 m thick in the HBF (van der Kroef, 2012). The group is unconformably overlain by the Rijnland or North Sea Group.

- *Weiteveen Formation* - The Weiteveen Formation (SKWF) consists of an alternation of light grey to red colored fine grained clay stone, marl, fine grained sandstone and intercalations of anhydrite and limestone (van Duijne, 2012). The formation is quite irregular regarding its content, several units can be distinguished.
- *Coevorden Formation* - The Coevorden Formation (SKCF) can also be divided in different units. The lower comprises a sequence of claystones with in its lower part some limestones. In the middle unit an increase in silty and sandy claystones can be noticed. The upper part contains brown-gray, sometimes fine-grained sandy deposits that contain shell horizons as well as layers with iron oolites and bituminous deposits (van Duijne, 2012).

North Sea Group

The North Sea Group is the youngest group that occurs in the HBF and forms the boundary between the Niedersachsen group and the present land surface. It is of Tertiary to Quaternary age. The group has been divided into a lower and upper unit and mainly consists of clays and sands.

- *Lower North Sea Group* - The Lower part (N1) consists of a sequence of sandy clays with scattered occurrences of quartz pebbles. The unit has a relatively uniform thickness with slightly thinner occurrences in the southeast.
- *Upper North Sea Group* - The Upper part (N2) is of Middle Miocene to Quaternary age. Its lower units comprise a succession of black and green (due to the high content of glauconite) sands and brown to black clays (van Duijne, 2012). The remaining Quaternary formations consist of sand, clay and gravel, deposited in predominantly terrestrial and glacial conditions.